Bone Morphogenetic Proteins and zebrafish inner ear development.

Catriona Mowbray

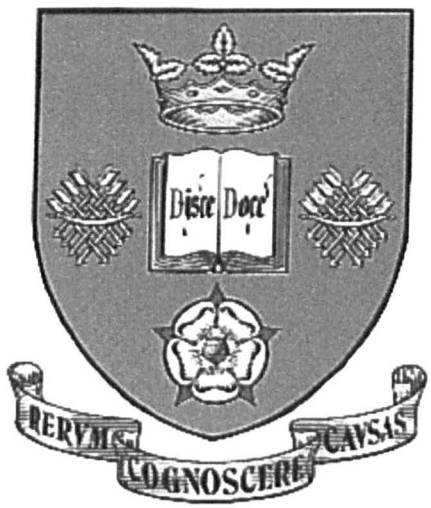

Centre for Developmental Genetics, Sheffield University

Submitted for the degree of Doctor of Philosophy

From the Centre for Developmental Genetics, Department of Biomedical Science
The University of Sheffield

May 2002

Declaration

I declare that this thesis is all my own work; any contribution by others has been acknowledged within the text.

Catriona Mowbray

I want to thank the many people who have helped me get this far, especially Tanya for patience beyond the call of duty and my parents for believing I could do it.

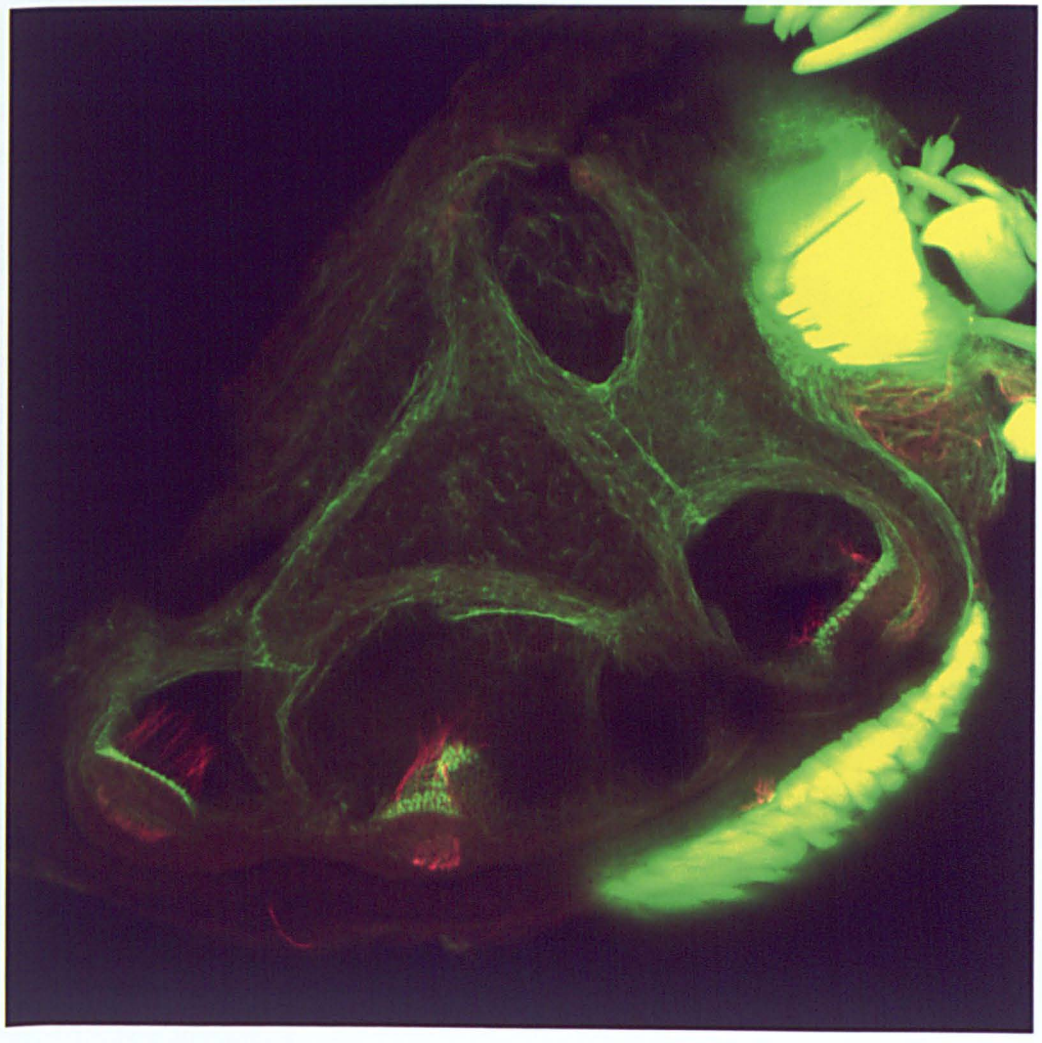

A lateral view of a 24 day old zebrafish inner ear showing the three semicircular canals and their sensory patches the cristae. The sample is labelled with a fluorescent marker of actin (green, FITC-phalloidin) which labels cell walls and stereocilia (projections from hair cells, which are found in the sensory patches of the inner ear) and an antibody against acetylated tubulin, which labels the kinocila (1 projects from each hair cell) and nerves (red).

Summary

This thesis describes the mRNA expression patterns of the Bone Morphogenetic Proteins (BMPs), downstream members of the BMP signal pathway, BMP antagonists and candidate target genes in the developing inner ear of wild type zebrafish. The crista Bmp expression pattern is conserved between four vertebrate species. However, unlike in chick, mouse and *Xenopus laevis* none of the *bmps* examined are macula markers in zebrafish.

This thesis identifies sources of Bmp signalling (the cristae, the endolymphatic duct (ED) and the semicircular canals (SCC)) and possible sites of Bmp action (the cristae, posterior macula, SCC and the mesenchyme around the ED). It also provides the first description of the early stages of ED development, a structure only recently described at later stages in the zebrafish (8dpf), and two mRNA markers of this structure (*bmp4* and *dachA*).

In analysis of zebrafish mutants with defective cristae, the presence of cristae correlated with the expression of the *bmps* and *msxc*, a putative Bmp target. This suggests the Bmps are required to form cristae and express *msxc*. Gain and loss of function studies have also supported a role for the Bmps in the development of the posterior macula and SCC.

Ectopic hBMP4 protein was applied to the otic vesicle via protein-coated beads. This inhibited the development of the posterior macula and SCC. However, these hBMP4 beads were not sufficient to induce the expression of ectopic *msxc*, generate ectopic cristae or rescue crista development in mutants. Beads coated in a BMP antagonist did not affect the development of endogenous cristae or the expression of endogenous *msxc*.

Rescued swirl (*bmp2b*) mutant adult zebrafish exhibit a balance defect. Early stages of inner ear development in rescued embryos were found to progress normally up until 7dpf. However, it is not clear when the rescuing mRNA or protein degrades, and work done by others in the lab has shown that Bmp2b is required at later stages to form adult SCC. The ectopic hBMP4 experiments suggest that moderating levels of Bmp signalling may be required for normal development of the SCC at early stages.

Contents

Chapter 1: Introduction

1.1 INTRODUCTION ---- 1
1.1.1 Advantages of using zebrafish ---- 3
1.1.2 Disadvantages of using zebrafish ---- 4
1.2 How a zebrafish inner ear develops
1.2.1 The otic vesicle and semicircular canals ---- 5
1.2.2 Sensory patches ---- 9
1.2.3 Otoliths ---- 10
1.2.4 Sensory patches consist of hair cells and support cells ---- 10
1.2.5 Later stages of inner ear development ---- 13
1.2.6 Sensory patches have an organised polarity ---- 13
1.2.7 Brief comparison with the development of other vertebrate inner ears ---- 15
1.2.8 How an inner ear works ---- 20
1.3 The Bone Morphogenetic Proteins
1.3.1 The BMP signal pathway ---- 23
1.3.2 There are two classes of BMP receptor ---- 25
1.3.3 Intracellular transduction of the BMP signal ---- 25
1.3.4 Intracellular inhibition of the BMP signal ---- 26
1.3.5 Extracellular antagonists inhibit BMP signal ---- 27
1.3.6 Zebrafish mutants found to be members of the BMP pathway ---- 29
1.4 Roles of BMP signalling
1.4.1 BMP activity gradient is required to pattern zebrafish dorsoventral axis ---- 30
1.4.2 BMPs are an example of subfunctionalisation ---- 30
1.4.3 Later roles during development ---- 32
1.4.4 Mechanisms of BMP signalling ---- 34
1.4.5 Targets of BMP signalling ---- 35
1.4.6 Possible BMP roles during inner ear development ---- 36

Chapter 2: Expression of the zebrafish *bmps* during inner ear development

2.1 INTRODUCTION
2.1.1 There are five BMP family members in zebrafish ---- 37
2.1.2 BMPs are expressed in conserved domains in the developing inner ears of chicks, mice, and *Xenopus* ---- 38
2.1.3 Differences in BMP expression are seen amongst these three species ---- 39
2.1.4 The lateral line system contains cell types similar to those in the inner ear ---- 39
2.2 RESULTS
2.2.1 *bmp2b* mRNA expression ---- 40
2.2.2 *bmp4* mRNA expression ---- 40
2.2.3 *bmp7* mRNA expression ---- 41
2.2.4 *bmp7-related* mRNA expression ---- 41
2.2.5 *bmp2b* and *bmp4* are expressed in hair cells and support cells ---- 41
2.2.6 *bmp* expression in the lateral line expression ---- 42
2.3 DISCUSSION

2.3.1 The BMPs have overlapping expression patterns----------47
2.3.2 The *bmps* have distinct expression patterns ----------48
2.3.3 *bmp7* expression is very different to that of the other *bmps* in the inner ear----------49
2.3.4 *bmp* expression prefigures the appearance of and subsequently labels cristae but is not found in the maculae ----------49
2.3.5 Comparison of inner ears between different species ----------50
2.3.6 Possible roles of *bmp* expression ----------52
2.3.7 The dorsal domain of *bmp4*expression marks the endolymphatic duct ----------52
2.3.8 *pax2.1*, *msxc*, and *brn3.1* are markers of different inner ear cell fates ----------53
Appendix
Tables 2.3 Chick *bmp* inner ear expression ----------55
Table 2.4 Mouse *bmp* inner ear expression ----------56
Table 2.5 *Xenopus bmp* inner ear expression ----------56

Chapter 3: Expression of downstream components of the BMP pathway, BMP antagonists and candidate target genes in the zebrafish inner ear.

3.1 INTRODUCTION
3.1.1 The BMP signal pathway----------57
3.1.2 Known and putative targets of BMP signalling----------57
3.1.3 Members of all levels of the BMP signal pathway have been cloned in zebrafish---58
3.2 RESULTS
3.2 mRNA expression of type I BMP receptors
3.2.1 *bmprIB*----------59
3.2.2 *tgfβrI*----------59
3.2.3 *thick veins* ----------59
3.3 mRNA expression of Bmp intracellular mediators
Receptor specific Smads
3.3.1 *smad1* ----------61
3.3.2 *smad5* ----------61
Inhibitory Smads
3.3.3 *smad6* ----------61
3.3.4 *smad7* ----------61
3.4 mRNA expression of BMP antagonists
3.4.1 *chordin*----------64
3.4.2 *noggin1*, *noggin2*, *noggin3*----------64
3.4.3 *follistatin* ----------64
3.5 mRNA expression patterns of putative targets of BMP signalling
3.5.1 *msxc*----------64
3.5.2 *spalt*----------64
3.5.3 *tbx2*----------66
3.6 DISCUSSION
3.6.1 All levels of the BMP signal pathway are expressed in the developing inner ear----------69
3.6.2 Controlling BMP action ----------70
3.6.3 The range of BMP signal----------71
3.6.4 Possible targets of BMP activity----------71
3.6.5 Differences between species ----------74
3.7 Possible roles for the Bmps during inner ear development

3.7.1 Role in cristae development ---- 75
3.7.2 Role in the development of the medial wall of the vesicle ---- 77
3.7.3 Role in semicircular canal development ---- 78
3.7.4 Development of a zebrafish endolymphatic duct ---- 78

Chapter 4: *bmps* expression in zebrafish inner ear mutants

4.1 INTRODUCTION
4.1.1 Inner ear mutants provide genetic tools to uncover the roles of BMPs ---- 80
4.1.2 *dog*, *vgo*, *cls*, and *val* mutant have specific cristae and SCC defects ---- 81
4.1.3 The inner ear phenotype of *valentino* mutants is not well characterised ---- 85
4.1.4 The function of the endolymphatic duct is not fully understood ---- 87
4.2 RESULTS
4.2.1 *bmp4* expression domain is not maintained in *dog* mutants ---- 89
4.2.2 *bmp2b* expression levels are reduced in *dog* mutants ---- 89
4.2.3 Ventrolateral *bmp4* expression levels are reduced in *vgo* mutants ---- 93
4.2.4 Dorsal *bmp4* expression is expanded in *vgo* mutants ---- 93
4.2.5 *bmp2b* expression domains are reduced in *vgo* mutants ---- 97
4.2.6 *cls* mutants do express *bmp4* and *bmp2b* although abnormally ---- 97
4.2.7 In *cls bmp* expression domains coincide with abnormal ventrolateral sensory patches ---- 97
4.2.8 *cls* mutants do not form epithelial projections or otoliths 103
4.3 Development of the dorsal domain of the otic vesicle
4.3.1 Live images show a dorsomedial extension from the otic vesicle 106
4.3.2 *bmp4* and *dachA* are markers of the early stages of ED development 106
4.3.3 The dorsal domain of *bmp4* expression is missing in *val* mutants 107
4.3.4 Dorsal *dachA* and *bmp4* expression, is abnormal in *vgo* and *cls* but is unaffected in *dog* mutants ---- 107
4.4 DISCUSSION
4.4.1 The initiation and maintenance of ventrolateral *bmp4* expression in the otic vesicle ---- 112
4.4.2 *eya1* is also required to regulate *bmp2b* expression ---- 117
4.4.3 *vgo* fails to initiate the proper expression of *bmp4* ---- 117
4.4.4 Are the *bmps* required for SCC development? ---- 119
4.4.5 *msxc* expression is associated with *bmp2b* and *bmp4* expression domains ---- 120
4.4.6 High levels of *bmp4* are associated with precocious ventrolateral sensory patches 121
4.5 The dorsal area of *bmp4* staining marks an endolymphatic duct
4.5.1 Zebrafish have an endolymphatic duct ---- 121
4.5.2 *bmp4* is an early marker of the zebrafish endolymphatic duct ---- 122
4.5.3 *vgo* develops an enlarged endolymphatic duct ---- 122
4.5.4 Is the ED required to regulate vesicle size? ---- 122

Appendix: Initial characterisation of the inner ear phenotype of the *colourless* mutant.

A1 INTRODUCTION ---- 126
A2 *cls* otic vesicles do not develop normal epithelial projections ---- 126
A3 *cls* develop abnormal sensory patches ---- 127
A4 *cls* otic vesicle have early patterning defects ---- 131
A5 *cls* have ectopic neuromasts ---- 137

Chapter 5: Implanting protein coated beads to disrupt BMP signalling within the developing zebrafish inner ear

5.1 INTRODUCTION
5.1.1 Aims ---------- 140
5.1.2 Beads are useful biological tools ---------- 141
5.1.3 What are beads? ---------- 141
5.1.4 hBMP4 has a specific effect on zebrafish development ---------- 141
5.1.5 The use of beads in studies of inner ear development ---------- 142
5.1.6 Adding BMP/antagonist coated beads to manipulate BMP signalling in zebrafish ---------- 147
5.2 RESULTS
5.2.1 Choice of Protein ---------- 147
5.2.2 Timing of implantation did not affect results ---------- 148
5.2.3 Beads could move away for otic vesicle during development ---------- 149
5.2.4 The effects of beads was assessed via live, in situ hybridisations and antibody analysis ---------- 150
5.2.5 Control beads did not affect the development of the otic vesicle ---------- 152
5.3 hBMP4 beads in wild type zebrafish
5.3.1 hBMP4 inhibits the development of the posterior macula ---------- 152
5.3.2 hBMP4 beads do not increase cell death ---------- 157
5.3.3 hBMP4 beads may not affect rate of cell division ---------- 157
5.3.4 Implanting hBMP4 beads around wild type ears did not affect cristae ---------- 160
5.3.5 hBMP4 beads affect the development of SCC ---------- 160
5.3.6 hBMP4 beads affect the development of otoliths ---------- 162
5.3.7 hBMP4 beads did not affect the expression of *bmp4* or *msxc* ---------- 162
5.4 hBMP4 beads in mutant zebrafish
5.4.1 hBMP4 beads affected development of part of *vgo's* single macula ---------- 165
5.4.2 hBMP4 beads do not rescue any aspect of the *vgo* phenotype ---------- 165
5.5 BMP antagonist coated beads
5.5.1 Noggin beads did not affect development of zebrafish inner ears ---------- 165
5.5.2 Chordin beads did not affect development of zebrafish inner ears ---------- 168
5.6 DISCUSSION
5.6.1 Ectopic hBMP4 has surprising effect on posterior macula development ---------- 172
5.6.2 What is happening to posterior macula cells? ---------- 172
5.6.3 Ectopic hBMP4 has a similar effect in *vgo* mutant embryos ---------- 174
5.6.4 Ectopic hBMP4 is not sufficient to form cristae ---------- 175
5.6.5 Ectopic BMP4 affects SCC development ---------- 176
5.6.6 Why were antagonist experiments inconclusive? ---------- 177

Chapter 6: Inner ear development in rescued zebrafish mutant swirl embryos

6.1 INTRODUCTION
6.1.2 Injection of mRNA rescues *swirl* mutants ---------- 179
6.1.3 Adult rescued *swirl* mutants have a balance defect ---------- 180
6.1.4 mRNAs from different organisms and levels of the BMP signal pathway can be used to rescue *swirl* mutants ---------- 181
6.2 RESULTS

6.2.1 *smad5* injections rescue *swirl* mutant embryos ---------- 182
6.2.2 Sensory patches appear normal in rescued embryos ---------- 183
6.2.3 Selected in situ hybridisation markers are expressed normally ---------- 183
6.3 DISCUSSION
6.3.1 Inner ear development progresses normally in rescued *swirl* embryos---------- 186
6.3.2 Studies on the adult rescued *swirl* mutants ---------- 188
6.3.3 Role for *bmp2b* in SCC development ---------- 190
6.3.4 Bmp signal may be required at semi-metamorphosis stage to form SCC---------- 191

Chapter 7: Conclusions & Future Prospects

7.1 Four possible sites of Bmp actions identified ---------- 192
7.1.1 The cristae---------- 192
7.1.2 The posterior macula---------- 193
7.1.3 The semicircular canals---------- 194
7.1.4 The endolymphatic duct ---------- 195
7.2 Future Prospects ---------- 197

Chapter 8: Materials and Methods

8.1 Fish Handling
8.1.1 Zebrafish stocks ---------- 199
8.2 In situ hybridisation I---------- 200
8.3 In situ hybridisation II---------- 202
8.4 Rescuing injection of *smad5* mRNA ---------- 203
8.5 Genotyping protocol---------- 205
8.6 Beading ---------- 207
8.7 TUNEL in situ assay of apoptosis ---------- 209
8.8 Mitosis marker ---------- 210
8.9 Phalloidin labelled actin stains ---------- 211
8.10 Microscopy ---------- 211

Bibliography

Chapter 1

1.1 INTRODUCTION

I am interested in how the otic vesicle is patterned in zebrafish and how this simple hollowed out ball of cells becomes the elegantly complex inner ear (Fig. 1.1). The morphological changes that take place during the development of vertebrate inner ears have been well documented (reviewed in Torres and Giraldez (1998) see also Nieuwkoop and Faber (1994); Bissonnette and Fekete (1996); Haddon and Lewis (1996); Morsli et al., (1998)) and the molecular interactions behind these changes are beginning to be uncovered (reviewed in Fekete et al., (1997); Torres and Giraldez (1998); Whitfield et al., (in press)). This thesis investigated the role of one family of signalling molecules during the development of the zebrafish inner ear.

Members of the Bone Morphogenetic Protein (BMP) family of signalling molecules are expressed during the development of chick, mouse, *Xenopus*, and zebrafish inner ears (Oh et al., (1996); Wu and Oh (1996); Morsli et al., (1998); Kil and Collazo (2001); Knochel et al., (2001); Mowbray et al., (2001)). Some aspects of this inner ear expression pattern (crista expression, see Chapter 2, Table 2.2) are conserved between these species.

The BMPs are required in many different developmental pathways. They have been shown to regulate cell death and proliferation, as well as specifying cell fate (Hogan, 1996). These roles will be explained in more detail below (section 1.3). Functional studies in the chick have suggested roles for these signalling molecules in the development of the semicircular canals while this work suggests other possible sites of action in zebrafish inner ears. Both chick and mouse are very useful models for studying inner ear development. However, the zebrafish provides certain advantages over each of these species.

This chapter introduces the zebrafish as a model system and describes how a zebrafish inner ear develops. It also introduces the BMPs, explaining how their signal is transduced and some of the roles they play during development.

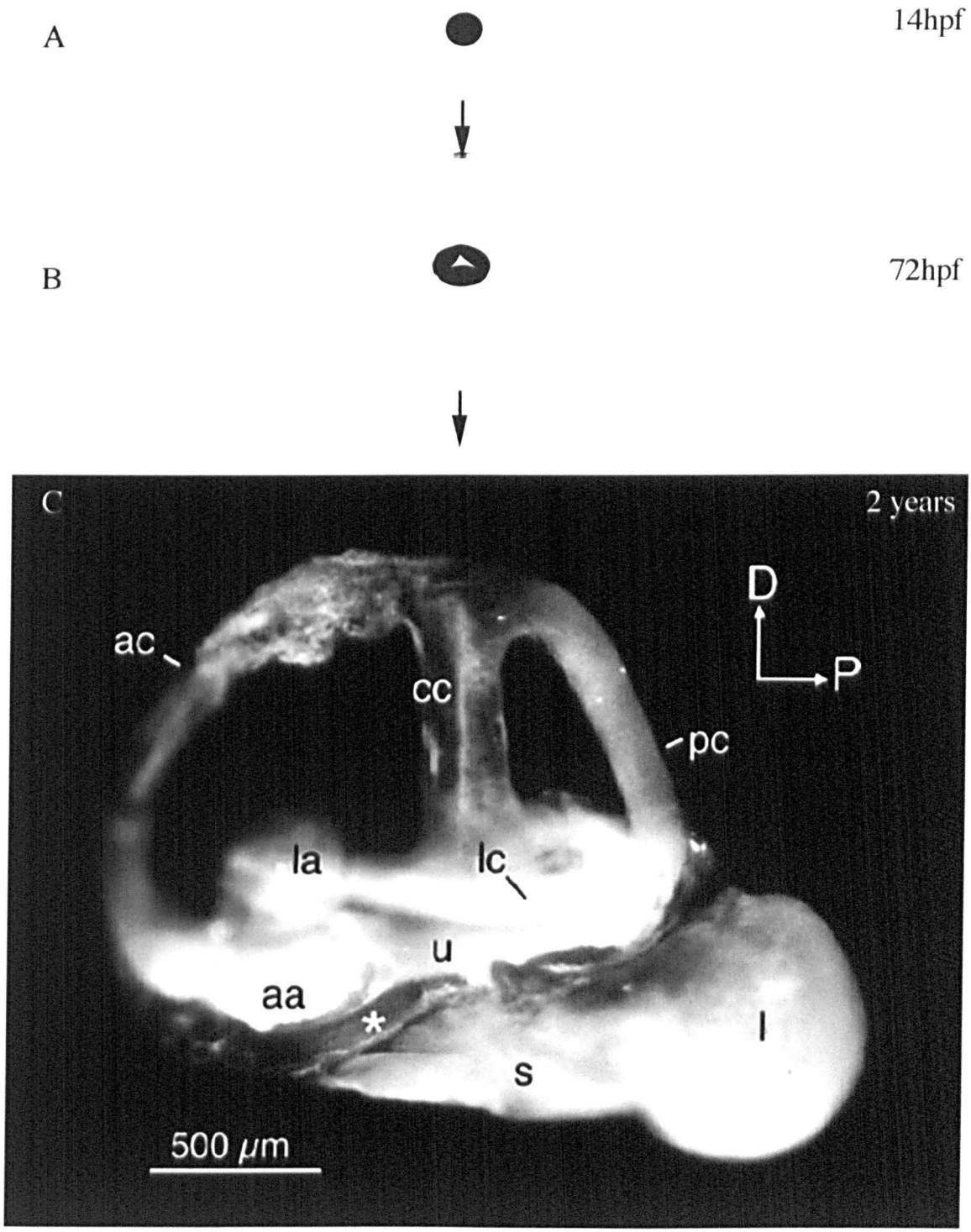

Figure 1.1 The inner ear increases dramatically in size and complexity.
(A+B) sketch of otic placode and vesicle respectively, (C) paint fill of adult zebrafish, all are lateral views anterior to left dorsal to top. Scale bar = 500 μm.

(A) An epithelial thickening is visible from 14hpf either side on the zebrafish hindbrain. (B) This cavitates and undergoes many morphological and molecular changes so that by 72hpf most of the structures seen in the adult inner ear have formed. (C) These structures then expand out during the rest of embryogenesis to form the adult structure shown in this paint fill. This last image was kindly provided by M. Bever and shows all the interconnected chambers of the inner ear. A more detailed description of inner ear development is given in the following figure.
Abbreviations: aa, anterior ampulla; ac, anterior semicircular canal (SCC), cc, common crus; l, lagena; la, lateral ampulla; lc, lateral SCC; pc, posterior SCC; s, saccule; u, utricle.

1.1.1 Advantages of using zebrafish embryos.

Two of the main advantages zebrafish have over both chick and mouse, are its external development of an optically transparent early embryo. This means the developing inner ear can be viewed, using a microscope, from the earliest stages of development (placode stages ~14hpf (hours post fertilisation)) through to 7 days, when almost all the structures seen in the adult inner ear have formed (see 1.2 for stages of development, Fig. 1.2). This degree of visual clarity and accessibility makes it easier to manipulate the embryos and to follow the effects of mutations or physical disruptions.

There are also numerous inner ear mutants identified in two large-scale ethyl-nitrosourea (ENU) screens (Malicki et al., 1996; Whitfield et al., 1996) as well as other mutagenesis screens (Moens et al., 1996). Some of these mutants have now been cloned and so are improving understanding of the molecular interactions behind the development of the inner ear (Whitfield et al., in press). Four mutants from these screens have been described in Chapter 4, where the expression patterns of the *bmps* are analysed in mutants with defects in inner ear development.

The zebrafish offers other genetic advantages as well as the availability of mutants. One of the major obstacles in studying the functions of BMPs is the early requirement for BMP signalling during development. This is common to many species and means that BMP mutants tend to be early embryonic lethal (see section 1.3). However, in zebrafish it is possible to inject BMP mRNA into early embryos (1-2 cell stage), rescuing the early requirement and generating fertile adult zebrafish. This technique has suggested a later role for *bmp2b* in inner ear development as rescued *bmp2b* mutants display a balance defect. This will be explored in more detail in Chapter 6.

As mentioned above the clarity of the zebrafish embryo and its external development means physical manipulations are easier. The implantation of protein coated beads (Chapter 5) takes advantage of this and allows BMP signalling within the otic vesicle to be manipulated at stages when the otic vesicle is developing.

Homologous recombination in ES cells, which in mice can be used to generate knock-outs, is not yet possible in zebrafish (although it is being developed (Ma et al., 2001)). However, it is possible to reduce translation of specific genes. This "knocking down" uses antisense morpholinos designed against specific mRNAs (Nasevicius and Ekker, 2000). This technique has proved useful in studying the role of Fgfs in inner ear induction (Phillips et al., 2001). It may, if coupled to electroporation techniques, enable

the local effect of the lack of certain genes to be analysed during later stages of inner ear development. This technique may prove useful in future studies (see Chapter 8).

1.1.2 Disadvantages of using zebrafish.

There are two disadvantages to using zebrafish. Zebrafish do not develop a specialised hearing organ like the cochlea found in mammals. This could limit the usefulness of zebrafish as models for all forms of human deafness. However, the vestibular part of the inner ear is highly conserved containing similar cell types and undergoing similar developmental processes (see section 1.2.7 and Fig. 1.6). The simpler inner ear of the zebrafish may help improve understanding of the more complex higher vertebrate inner ear. For example the zebrafish is opening up new interpretations of old defects in aspects of cochlear development. The zebrafish *colourless* mutation is in the gene *sox10*, and results in a lack of pigment cells and abnormal inner ear development (Chapter 4 and Appendix). In humans, mutations in *SOX10* result in Waardenburg Shah syndrome, in which patients are deaf, it was thought due to the lack of pigment cells in the cochlea (Pingault et al., 1998). However, the abnormalities seen in the zebrafish may reveal other roles for Sox10 during inner ear development overlooked in other studies.

The other difficulty in using zebrafish is the fact that its multigene families contain more functional members than in mammals, e.g. Bmps or Hedgehogs. This can cause complications when determining whether proteins are orthologues i.e. direct functional counterparts or paralogues i.e. members of the same family. The Bmps will be discussed in more detail in section 1.3.

1.2 Development of the zebrafish inner ear.

This section provides a brief summary of how the inner ear forms in zebrafish, concentrating on the stages between 18hpf (hours post fertilisation) and 5dpf (days post fertilisation). To simplify the explanation different aspects of otic vesicle development have been described separately, taking in turn the morphology of the vesicles including the semicircular canals, the sensory patches and the otoliths. For details on neurogenesis, the induction of inner ear development and later aspects of inner ear development refer to (Waterman and Bell, (1984); Platt, (1993); Haddon and Lewis, (1996); Bang et al., (2001); Bever and Fekete, (in press); Whitfield et al., (in press)).

1.2.1 The otic vesicle and semicircular canals.

The zebrafish inner ear develops from an ectodermal thickening that is present on either side of the hindbrain from around 14hpf. This is known as the otic placode (Fig. 1.2A), which then cavitates to form the otic vesicle (Fig. 1.2B), from which all the cells of the inner ear are thought to develop, including the neurons of the statoacoustic ganglion (Haddon and Lewis, 1996). The vesicle then increases in size, mainly due to the expansion of the vesicle lumen, rather than a dramatic increase in cell number (Haddon, 1997). The vesicle is then divided up by projections that push in from the anterior, posterior, lateral, and ventral walls of the vesicle (Fig. 1.2C outlines show lateral projections, M shows anterior and posterior projections). These projections consist of a thin layer of otic epithelium covering a core of acellular matrix. It has been shown in *Xenopus* that as the volume of this matrix increases, due to the production of Hyaluronic acid, the projection elongates (Haddon and Lewis, 1991). Evidence for a similar mechanism in zebrafish comes from the mutant *jekyll* in which the epithelial projections fail to elongate and fuse (Neuhauss et al., 1996). This mutation is in an enzyme required to produce the extracellular matrix, including Hyaluronic acid (Walsh and Stainier, 2001).

In wild type embryos from 72hpf the projections meet and fuse together in a hub of tissue known as the fusion plate. A dorsolateral septum grows ventrally to join the fusion plate. The pillars of tissue now resemble a cross-like structure dividing the lateral part of the lumen of the otic vesicle (Fig. 1.2D outline). The spaces around the projections, not the projections themselves, will go on to form the lumen of the semicircular canals (SCC) (Fig. 1.2D arrows). The dorsolateral septum separates the future anterior and posterior SCC.

There are three SCC, each in a different plane, which is important given their function to detect angular acceleration. At 72hpf, the remaining otic vesicle contains two areas of specialised epithelia known as the anterior and posterior maculae, which are described below. The maculae containing chamber and the SCC remain connected throughout development and life and are described as the membranous labyrinth (see Fig. 4.3+4). By 4dpf the SCC have the adult pattern but they need to expand out to achieve their adult proportions. Later in development the chamber containing the maculae undergoes further morphological changes to form three connected chambers, the utricle, the saccule and the lagena (see below + Fig. 1.1C + Bever and Fekete, (in press)).

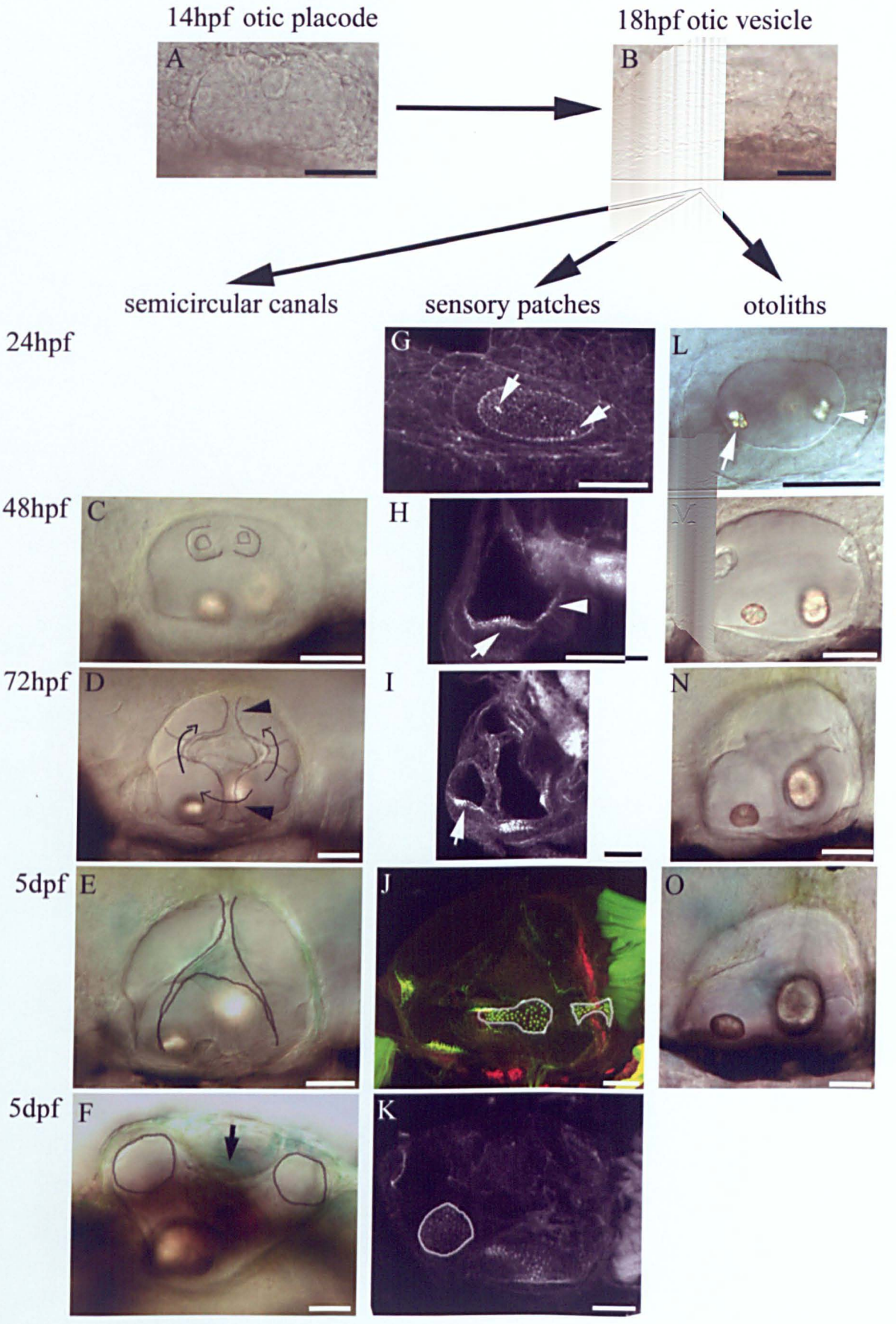

Figure 1.2 Stages in zebrafish inner ear development
(see legend overleaf)

Figure 1.2 Stages of development in the inner ear.

In this figure the development of the inner ear is divided into three parts: the morphology of the vesicle including the semicircular canals (SCC), the sensory patches, and the otoliths. Scale bar in all images = 50μm.

Placode cavitation

(A+B) DIC images of live embryos, anterior to left, dorsal to top.

(A) The otic placode is visible from 14hpf. (B) At 18hpf there is a concentration of actin in the middle of the placode that marks the beginning of the cavitation, which turns the placode into the otic vesicle.

Semicircular canals

(C-F) DIC images of live zebrafish, all lateral views with anterior to left, and dorsal to top except F, which is a dorsal view with anterior to left, lateral to top.

The first stages of SCC formation are the finger like projections, which invaginate from the anterior, posterior and lateral walls of the vesicle. (C) The lateral projections are shown here (outlined). The anterior and posterior projections are shown in M. (D) These projections meet and fuse within the otic vesicle, being joined by a ventral projection and a dorsal septum (a thin layer of cells, rather than a projection) (arrowheads). At this stage the fused projections form a pillar of tissue in the shape of a cross which divides up the lateral lumen of the vesicle (outline). The lumens of the SCC are the spaces around this cross of tissue (arrows). (E) By 5dpf the vesicle has expanded in size. The SCC have started to bulge out which results in the appearance of a three pronged star laterally (outline). This star shows the deeper surface layer of the vesicle surrounded by the bulging projections; this is clearer in the dorsal view (F arrow). (F) The dorsal view shows the anterior and posterior SCC in cross section (circles).

Sensory patches

(G-K) samples are labelled with a fluorescent marker of actin (FITC-phalloidin) that labels stereocilia and cell boundaries. One case (J) is also labelled with an antibody against acetylated tubulin, which labels the kinocilia and nerves. The stereocilia are found at the apical surface of mature hair cells. These images are compressed confocal Z sections, allowing the entire vesicle to be visualised at once but with clear detail of all the different levels.

G+K dorsal views anterior to left, H+I, transverse section lateral to left dorsal to top, J lateral views anterior to left dorsal to top.

(G) At 24hpf the first mature hair cells are seen at the anterior and posterior ends of the vesicle. Only a couple of hair cells have formed in each macula at this stage (arrows). (H) At 48hpf there are around 18 hair cells in the anterior and 10 in the posterior macula. The anterior macula is now on the ventral floor of the vesicle (arrow) and the posterior macula is on the medial wall (arrowhead). (I) At 72hpf the SCC have fused and three ventrolateral sensory patches have formed, one of which is shown in this transverse section (arrow). These ventrolateral sensory patches are called cristae; each is associated with a SCC, and so is called the anterior, lateral and posterior crista respectively. (J) By 5 days the maculae and cristae have increased in size each containing around 50-60 and ~20 hair cells respectively. The distinctive shape of the posterior macula still on the medial wall of the vesicle, is clear, a round posterior 'pan' with a slim anterior extension or 'handle' (outline). The cristae are bow tie shaped (outline). (K) In a dorsal view the anterior macula is roughly round (outline).

Otoliths

(L-O) DIC images of live embryos taken medial to those showing SCC development. All are lateral views anterior to left, dorsal top.

(L) At 24hpf two bright reflective otoliths can be seen at the anterior and posterior ends of the vesicle (arrows). (M-O) At later stages the otoliths have distinct shapes. The anterior otolith is smaller than the posterior otolith. Both still overlie their respective macula. In the adult the posterior otolith will become the sagitta and the anterior the lapillus.

This complicated morphology is easier to appreciate when looking at a whole otic vesicle, or a paint fill. Paint fills have been used to great effect in both chick and mouse studies into inner ear development (Bissonnette and Fekete, 1996; Morsli et al., 1998). Gloss paint is injected into the membranous labyrinth and, as all the chambers and canals are connected, they all fill with paint (Fig. 1.1C). This is now possible in zebrafish and is particularly useful when studying the state of SCC development and later stages of zebrafish inner ear development, as the embryos are no longer transparent. It is important to ensure that all the chambers of the inner ear are filled in order to generate a reliable image (Bever and Fekete, in press).

1.2.2 Sensory patches

The inner ear responds to various stimuli: angular and linear (gravity) acceleration and sound. It does this through the stimulation of specialised cells (hair cells) within thickened areas of epithelium known as sensory patches. There are two types of sensory patch, maculae and cristae. Each of the sensory patches consist of an area of stratified epithelium containing two types of cells, hair cells and support cells, which are described in more detail below. Each sensory patch has a characteristic shape, location and polarity, which are thought to be important for their function. The development of sensory patches is assessed using markers for the differentiated hair cells.

The two maculae are the first sensory patches to form, at the anterior and posterior ends of the otic vesicle. These maculae are visible from around 24hpf and hair cells are added until at least 30dpf, and probably throughout life (Bang et al., 2001) (Fig. 1.2G). As development proceeds the anterior macula is positioned on the anteroventral floor of the vesicle while the posterior macula is on the medial wall. The anterior macula is roughly round (Fig. 1.2K outline, dorsal view shown at 5dpf) whereas the posterior macula appears more like a frying pan. It has a fat, round posterior area and a thin, long anterior "handle" (Fig. 1.2J outline shown at 5dpf). The three cristae develop later; three areas of thickened epithelium are visible ventrolaterally from 48hpf. Differentiated hair cells in each of these ventrolateral regions are visible from 60hpf and each is associated with a SCC (Fig. 1.2I arrow, shown at 72hpf). At much later stages another two maculae develop, the lagena (21dpf)(Bang et al., 2001), and the macula neglecta (17dpf) (Bever and Fekete, in press). At these later stages the anterior macula is known as the utricular macula, and the posterior macula as the saccular macula.

The cristae detect angular acceleration (Haddon and Lewis, 1996). The roles of the maculae are not as distinct. They detect linear and acoustic stimuli. The utricular macula is thought to be more associated with vestibular (balance) stimuli while the saccular macula is more associated with acoustic responses (Whitfield et al., in press). The zebrafish has no specialised hearing sensory patch like our organ of Corti. The inner ear is functioning by 72hpf as newly hatched larvae can orientate themselves correctly, showing they can detect gravity and can respond to vibrational stimuli (Nicolson et al., 1998).

1.2.3 Otoliths

The anterior and posterior maculae are each overlain by an otolith. These are aggregations of calcium carbonate that are analogous to the otoconia seen in mammalian ears. The otoliths are visible from around 19hpf at either end of the vesicle (Fig. 1.2L arrows, shown at 24hpf). Their development depends on the presence of primary hair cells or tether cells. These are the first hair cells, which form around 18hpf just as the vesicle is cavitating. The granules of calcium carbonate, which are visible floating around the otic vesicle, stick to the apical projections of the tether cells eventually forming the large otoliths. These tether cells are subsequently incorporated into the developing anterior and posterior maculae as mature hair cells (Riley et al., 1997).

The otoliths sit in a gelatinous matrix (otolithic membrane) on top of the hair cells in the maculae. They are responsible for transmitting acceleration forces and sound vibrations to the hair cells of the macula they are in contact with. At later stages a third otolith develops over the lagenar macula.

The otoliths have distinctive shapes, which are similar to those found in goldfish. These shapes may be important in responding to underwater sound (Platt, 1993).

1.2.4 Sensory patches consist of hair cells and support cells.

The hair cells and support cells make up the sensory patches. Cell labelling studies have shown that hair cells and support cells can share a common progenitor in zebrafish (Haddon et al., 1998) and chick (Fekete et al., 1998). Lateral inhibition is thought to be responsible for the pattern of their differentiation, ensuring a single hair cell is surrounded by a ring of support cells (reviewed in Lewis, (1998)). Within the differentiated sensory patch, hair cell nuclei are positioned apically to those of support

cells giving the sensory patch epithelium a stratified appearance (Fig. 1.3 A see also Fig. 2.5H).

Hair cells have a hair bundle projecting from their apical surface. This bundle is made up of many stereocilia (~300) arranged to one side of a single kinocilium. The stereocilia consist of actin filaments (labelled using FITC-phalloidin) while the kinocilum consists of microtubules (labelled with an antibody against tubulin). There is variety in the length of kinocilia and in the number and lengths of stereocilia between the different sensory patches and even across the same sensory patch (Platt, 1993; Bang et al., 2001). This may relate to different sensitivities of these patches. A simplified explanation of how a hair cell is activated is given in section 1.2.8.

The function of support cells is not as clear. They are required to maintain the integrity of the otic epithelium. *mindbomb* is a zebrafish mutant that produces too many hair cells at the expense of support cells due to a failure in the lateral inhibition. In *mindbomb* mutants the hair cells differentiate normally. However, they can not form proper connections to neighbouring nonsensory cells or form a basal lamina and so fail to separate themselves from underlying mesenchymal cells. This eventually leads to them becoming extruded from the otic epithelium (Haddon et al., 1999). The hair cells in *mindbomb* mutants also show increased levels of apoptosis and it is suggested that the support cells are required to secrete a survival factor (Haddon et al., 1999).

Support cells are also required for the correct formation of otoliths. In *mindbomb* mutants otoliths do form, although they are smaller than normal. In mammals, it is thought cells outside the sensory patches secrete the major protein of otoconia (e.g. otoconin-95, (Verpy et al., 1999)).

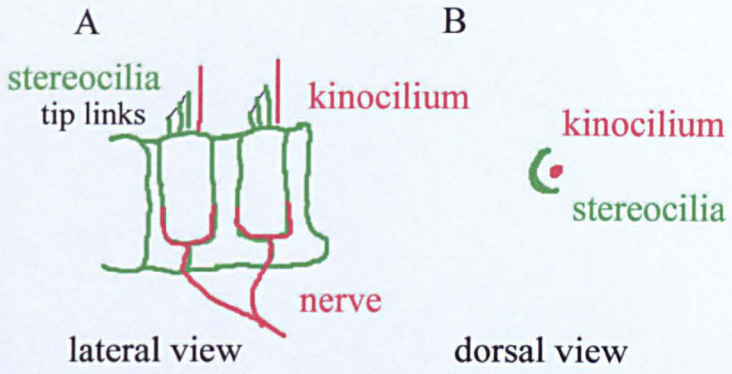

Figure 1.3 A cartoon showing the arrangement of hair cells and support cells and the hair bundle.

(A) The sensory patches are areas of stratified epithelium. The hair cells are positioned more apically than the support cells. The hair cells have hair bundles projecting from their apical surface and nerves connecting to the statoacoustic ganglion at their basal end.
(B) These bundles consist of numerous stereocilia arranged in a horseshoe around the single kinocilium. This arrangement gives the hair cells a polarity within the plane of the epithelium. Tip-links connect the stereocilia and are thought to act as gates for the transduction channels.

1.2.5 Later stages of inner ear development.

In the adult zebrafish inner ear the single chamber which contained the anterior and posterior maculae at 4dpf has undergone further morphological changes. There are now three connected chambers each with its own macula; the utricle, the saccule and the lagena. The anterior macula forms the utricular macula and the posterior macula forms the saccular macula (Bang et al., 2001). Between 15 and 21dpf the lagenar macula become distinguishable (Bever and Fekete, in press and Bang et al., 2001). Each of these maculae is associated with its own distinctive otolith (Platt, 1993). A fourth macula, the macula neglecta, does not have an associated otolith, is much smaller than the other three and consists of two patches of hair cells that differentiate form 17dpf. It may form from the posterior macula (Fig. 1.4 and Bever and Fekete, (in press)).

1.2.6 Sensory patches have an organised polarity.

Each sensory patch has an organised planar polarity. This is in addition to the apicobasal polarity seen in each hair cell. The planar polarity depends on the relative orientation of the kinocilium of each hair cell within the sensory patch (Fig. 1.5A) and is thought to be functionally significant. The differing polarities of the hair cells are thought to be important in providing directional information about where a signal is coming from (Lu, 2001). In adult inner ears this polarity has been described by Platt, (1993). Each crista has uniform orientation. The anterior and posterior crista hair cells face away from the utricular macula and those of the lateral crista face towards it. Each macula shows bi-directional opposition. In the utricular macula and lagenar macula the hair cell polarities face towards a dividing line. In the saccular macula the polarities face away from the dividing line which runs around longitudinally near the middle of the macula. The dividing line is closer to the midline in the lagenar macula and saccular macula; however, in the utricular macula it is much closer to the anterior side. The thin strip of hair cells facing back into the anterior macula is called the striola. Each of the two patches that constitute the macula neglecta are arranged in opposition to each other (Fig. 1.5B (Platt, 1993)).

This work demonstrates that these polarity patterns are already obvious in the embryo (Haddon et al., 1999). At 5dpf the anterior and posterior maculae each contain around 60 hair cells. In the anterior macula the region of reversed polarity is clearly visible (Fig. 1.5C+D). The posterior macula is shaped like a frying pan (Fig. 1.5E) and has a

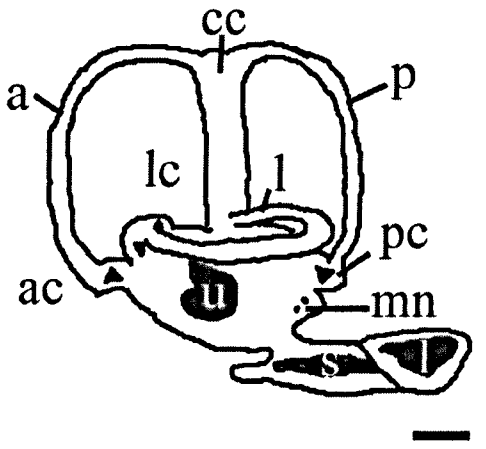

Figure 1.4 Sketch of an adult zebrafish inner ear adapted from Haddon and Lewis (1996).
A lateral view of the adult inner ear, anterior to the left, dorsal to the top. Scale bar=500 μm.
There are three cristae each with its associated SCC, anterior (ac, a), lateral (lc, l) and posterior (pc, p). The anterior and posterior SCC both connect to the common crus (cc). All three SCC are connected to the utricle, which contains the utricular macula (u) and the macula neglecta. Unlike the utricular macula, the macula neglecta does not have an otolith. Two further chambers develop posterior and medial to the utricle, the saccule and the lagena. Each of these contains a sensory patch, the saccular macula (s) and the lagenar macula (l) respectively, and an otolith.

dividing line running anterior to posterior through the middle of the patch. At the posterior, larger pan end, the hair cells point away from the midline. In the thinner anterior handle the hair cells are arranged in an antiparallel manner (Fig. 1.5F). The posterior macula's antiparallel region is not seen in the adult sacculus, which is the sensory patch thought to develop from the posterior macula (Platt, 1993; Bang et al., 2001). However, the medial wall of the otic vesicle and the posterior macula undergo some dramatic morphological changes between these early stages and the adult (Bang et al., 2001). It is possible this antiparrallel part of the patch may represent the beginning of the macula neglecta. Other studies have suggested that as in other fish, part of the posterior macula goes on to form the macula neglecta (see Bever and Fekete, (in press) and references therein).

1.2.7 Brief comparison with other vertebrate inner ears.

There are two major differences between the development of the mouse, chick and *Xenopus* inner ear and that of the zebrafish. Zebrafish do not have a specialised hearing organ like the mouse or chick cochlea and zebrafish do not form an otic cup.

Mouse and Chick

In both these species the inner ear develops in similar manner. The otic placode invaginates forming the otic cup, which then pinches off to form the hollow otic vesicle. The SCC develop from bilateral outpocketings of otic vesicle epithelium. The central regions of these pockets fuse forming a single layer, which is then resorbed. The resorption process is not fully understood; however, it results in these cells disappearing, either retracting into the canal epithelium, or undergoing programmed cell death (Martin and Swanson, 1993; Fekete et al., 1997).

There is also a neural crest contribution to the hearing organ of chick and mouse. The cochlea contains a specialised epithelium, the tegmentum vasculosum (chick) and the stria vascularis (mammals). This epithelium contains melanocytes, which are of neural crest origin and may be important in regulating the ionic concentration of endolymph (Wangemann, 1995; Vetter et al., 1996; Masuda et al., 2001). Endolymph is the fluid that fills the membranous labyrinth. Its ionic concentration is important for the function of hair cells (see 1.2.8).

A Polarity

B Adult sensory patches

C Anterior macula

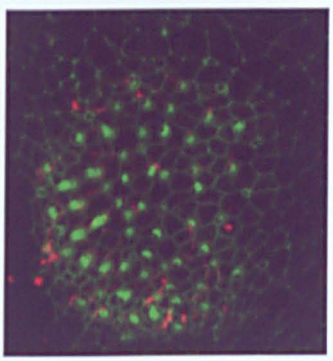

D Polarity of patch hair cells

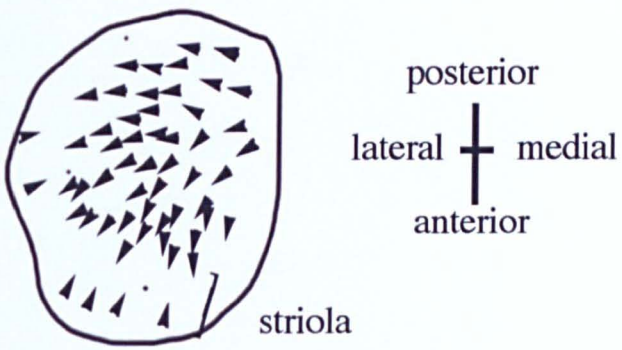

E Posterior macula

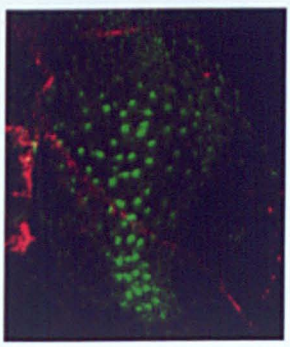

F Polarity of patch hair cells

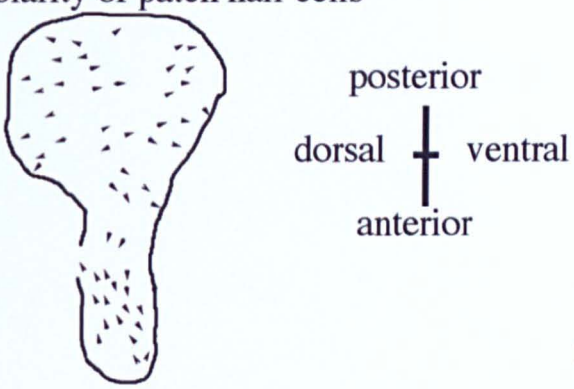

Figure 1.5 Polarity of hair cells

(C+E) compressed confocal images of the anterior macula and posterior macula stained with FITC-phalloidin (green) and rhodamine anti tubulin (red). (A, D+F) Sketches detailing the polarity of the hair cells throughout the individual patches, (B) sketch adapted from Platt, (1993) which shows the polarity of adult sensory patches.

(A) The polarity was taken as the direction towards the kinocilium within each hair bundle if that was distinguishable. (B) In the adult utricular macula, the polarity of the majority of its hair cells is to point anterolaterally, with hair cells in a striolar region pointing back into the patch. The other two maculae have a dividing line through the middle. In the lagena the polarities face towards the line; in the saccule the majority of polarities face away. A small group of saccular macula hair cells extend over the dividing line.

Hair cells in the anterior and posterior cristae point away from the utricular macula and those in the lateral crista point towards it. Hair cells in the two patches of the macula neglecta show the opposite polarity to each other. (C+D) At 5dpf the anterior macula is well developed with the majority of hair cells pointing anterolaterally. As in the adult, a rim of hair cells at the anterior edge of the patch points back into it, posteromedially, corresponding to the striola. (E+F) At 5dpf the posterior macula has distinct polarities around a dividing anteroposterior line. In the round posterior part all the dorsal hair cells point dorsally and the ventral hair cells point ventrally from a midline. In the thin handle the dorsal cells point posteriorly and the ventral cells anteriorly.

Xenopus

Xenopus also develops an otic cup. It also forms its SCC by generating bilateral outpocketings that fuse. However, these areas of fusion are less broad than in the chick and mouse, although they do undergo similar processes of resorption (Haddon and Lewis, 1991; Bever and Fekete, 1999). *Xenopus* have two unique acoustic organs, the basilar papilla and the amphibian papilla, which are not thought to be homologous to the cochlea or basilar papilla (Bever and Fekete, 1999). However, it also develops a saccular and lagenar macula and its vestibular sense organs are thought to be highly conserved in position and structure to those of other vertebrates (Kil and Collazo, 2001).

The relative timings of the different events during inner ear development of the species described above are displayed in Table 1.1. It is interesting to note that unlike zebrafish and *Xenopus*, in chick and mouse SCC development is initiated before the first hair cells differentiate. The inner ears of the four species described in the table are shown in Fig. 1.6. This figure is intended to demonstrate the similarities in overall shape between species, especially with respect to SCC.

Table 1.1 Comparison of inner ear development in four vertebrate species.

Developmental event	zebrafish hpf	Chicken som/days(E) (stage)	Mouse days	*Xenopus* hours (stages)
Placode visible	14	4-5 som (s8)	8.5	22 (s21)
otic cup	na	13 som(s11-17)	9	(s23)
otic vesicle	18	E2.5 (s17)	9.5	27-28 (s28)
delamination of neurons	22-42	22 som (st14)	9	~36 (s31-35)
first hair cells differentiate	24	E4	10	44 (s33/34)
endolymphatic duct visible	46	E3-3.5	10.75	42 (s32)
SCC development initiated	44	E3.5-4	11.5	76 (s41)
SCC complete	72	E6.5	13	120h (s46.5)
cochlear anlage			10.75	(s47)

Adapted from Bever and Fekete (1999), Baker and Bronner-Fraser (2001), (Nieuwkoop and Fabre (1994), Denman-Johnson and Forge (1999), Haddon and Lewis (1991).

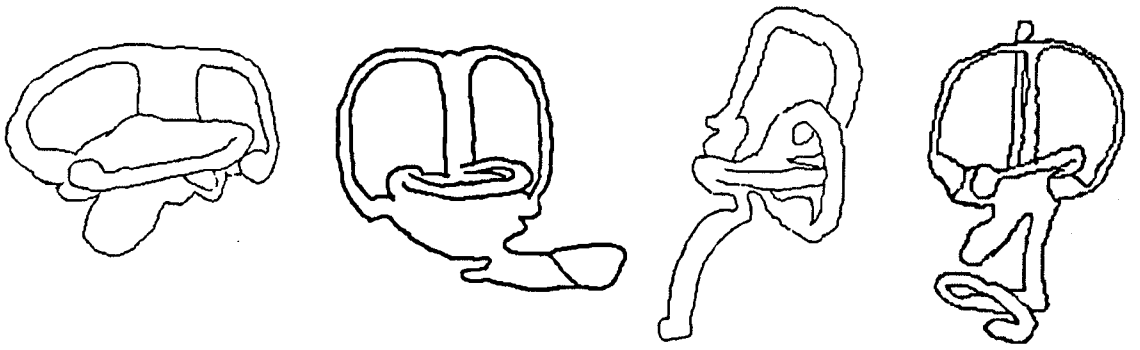

Figure 1.6 Comparison of adult inner ears.
Sketches of the inner ears of the various species described in this chapter highlighting the similarity of structure between them.
Adapted from Bissonnette and Fekete (1996), Haddon and Lewis (1996), Kil and Collazo (2001) and Fekete (1999).

1.2.8 How an inner ear works.

In order to put all these processes in context the following section provides a simplified explanation of how the inner ear works. This is not meant to be comprehensive and indeed many of the details are not understood. This description is of an adult inner ear and so some of the sensory patches have different names than those described in the embryos (anterior macula = utricular macula, posterior macula = saccular macula)(see Fig. 1.4).

The adult inner ear is a collection of interconnected chambers, the membranous labyrinth, surrounded by bone. For the sake of description it is divided into two, the pars superior and the pars inferior. The pars superior consists of the utricle and the SCC and is highly conserved amongst vertebrates. The pars inferior contains the saccule, the lagena, and in some cases a specialised hearing organ such as the cochlea (Bever and Fekete, 1999). There is another structure, the endolymphatic duct, which projects dorsomedially from the saccule. It is not clear what the function of this structure is although it may be important in regulating the volume of endolymph (Rask-Andersen et al., 1999). The membranous labyrinth is filled with endolymph, a potassium rich fluid. This fluid provides the K^+ ions required for hair cells to depolarise.

The hair cells are the mechanoreceptors of the inner ear. Their hair bundles consist of stereocilia arranged in rows of increasing height around a single kinocilium. The stereocilia are all connected by tip links (Pickles et al., 1984). When the stereocilia are displaced towards the kinocilium the tip links are stretched and they open channels which allow the influx of K^+ (Denk et al., 1995). This depolarises the cell, opening Ca^{2+} channels resulting in the release of neurotransmitter onto the afferent nerve around the base of the hair cell (see Nicolson et al., (1998) and references therein). Various stimuli - linear (gravity) and angular acceleration, and sound - cause the initial displacement of the hair bundle.

The inner ear is divided up functionally into vestibular (balance) and acoustic (hearing) areas. The species with cochlea type organs have the most specialised hearing sensitivity, with the responses of the hair cells tuned depending on the position within the cochlea. The cochlea is connected to the outer world via the middle ear (small bones and membranes) and outer ear (tube and funnel) which transfer the sound vibrations to the hair cells in the cochlea.

In other species the distinction between acoustic and vestibular function is not as clear and there is no clear evidence for a similar hearing only sensory patch. In the zebrafish it is thought that the saccular macula is more involved in hearing as it communicates with the Weberian ossicles. These are thought to have a similar function to the middle ear bones in higher vertebrates, amplifying sound vibrations. However, they have a different developmental origin and communicate with the swim bladder not the outer ear.

1.3 The Bone Morphogenetic Proteins (BMPs).

This thesis concentrates on the role played by members of one family of signalling molecules, the Bone Morphogenetic Proteins (BMPs), during the patterning of the inner ear. This family regulate many diverse biological processes throughout development, some of which are conserved in different species. This section is intended to introduce the family and discuss some of the processes the BMPs are involved in.

The BMPs are members of the TGFβ (Transforming Growth Factor) superfamily of signalling molecules. The BMPs were originally identified due to their ability to generate ectopic cartilage and bone in rats (see Hogan, (1996) and references therein). Members of the BMP family are found in many different organisms from *Drosophila* to man and based on sequence comparisons of the mature carboxy terminus of the protein they can be organised into sub groups (Fig. 1.7). There are two main subgroups, the Decapentaplegic (DPP)/BMP4 subfamily and the Glass bottom boat-60A (GBB-60A)/BMP7 subfamily. The DPP/BMP4 subfamily includes DPP from *Drosophila* and its functional orthologues BMP2 and BMP4 in vertebrates. The BMP4 ligand domain sequence can substitute for the DPP ligand sequence in *Drosophila* (Padgett et al., 1993) and DPP can induce endochondrial bone formation in mammals (Sampath et al., 1993). The other subfamily contains the *Drosophila* ligands GBB-60A and the vertebrate ligands BMP5, 6, 7, and 8. The *Drosophila* ligand Screw is also more distantly related to this subfamily. It is not known if the members of this subfamily are functional orthologues.

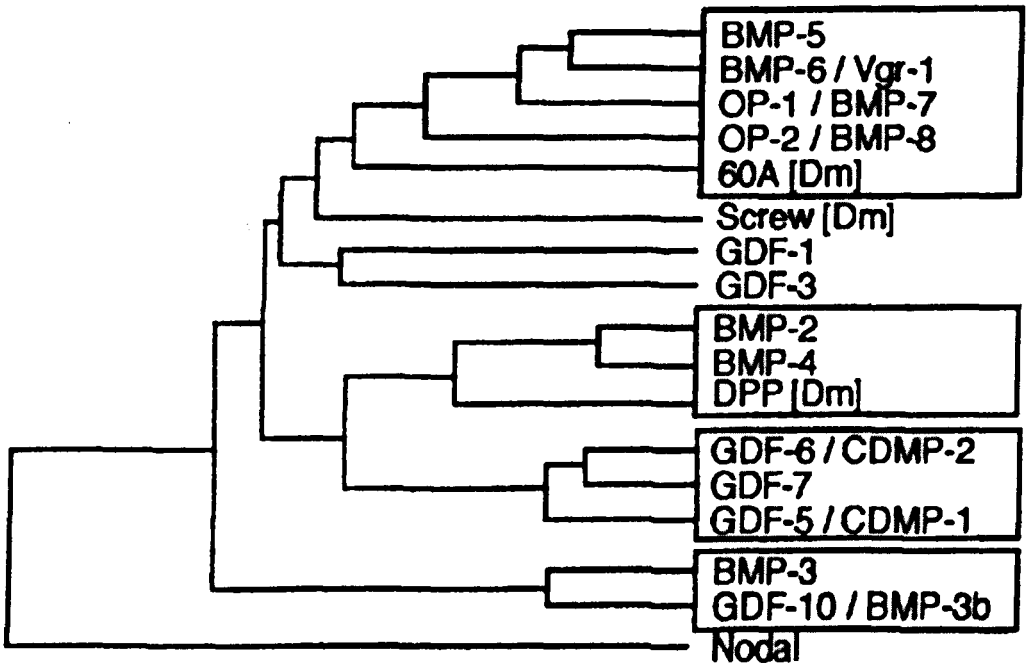

Figure 1.7 Members of the BMP family. Adapted from Yamashita et al., (1996)

Mammalian and *Drosophila* members of the BMP family are listed. The phylogenetic tree was made based on the amino acid sequence similarities between the mature BMPs.
Dm: Drosophila melanogaster

1.3.1 The BMP signalling pathway

BMPs are synthesised as large precursors that are proteolytically cleaved to generate a carboxy-terminal mature protein. These precursors form dimers before being cleaved and secreted (Hazama et al., 1995). BMPs can form heterodimers in vitro (Hazama et al., 1995), and different types of dimer have different activities. BMP2-BMP7 and BMP4-BMP7 heterodimers have been shown to be more potent at inducing ventral mesoderm than their homodimer forms in *Xenopus* animal cap experiments (Suzuki et al., 1997; Nishimatsu and Thomsen, 1998). It has been suggested that Bmp2b and Bmp7 heterodimers are required in early zebrafish dorsoventral patterning (Schmid et al., 2000).

As TGFβ family members, BMP dimers signal via two transmembrane serine-threonine kinase receptors, which activate a SMAD (defined in more detail below) intracellular transduction chain. This leads to the upregulation of target genes (Fig. 1.8). As well as the ligands, the intracellular parts of the signal transduction pathway are highly conserved from *Drosophila* to man (see Table 1.2 and (Baker and Harland, 1997).

Table 1.2 Vertebrate and *Drosophila* BMP homologues in their signalling pathway pathway. Adapted from Massague and Chen, (2000).

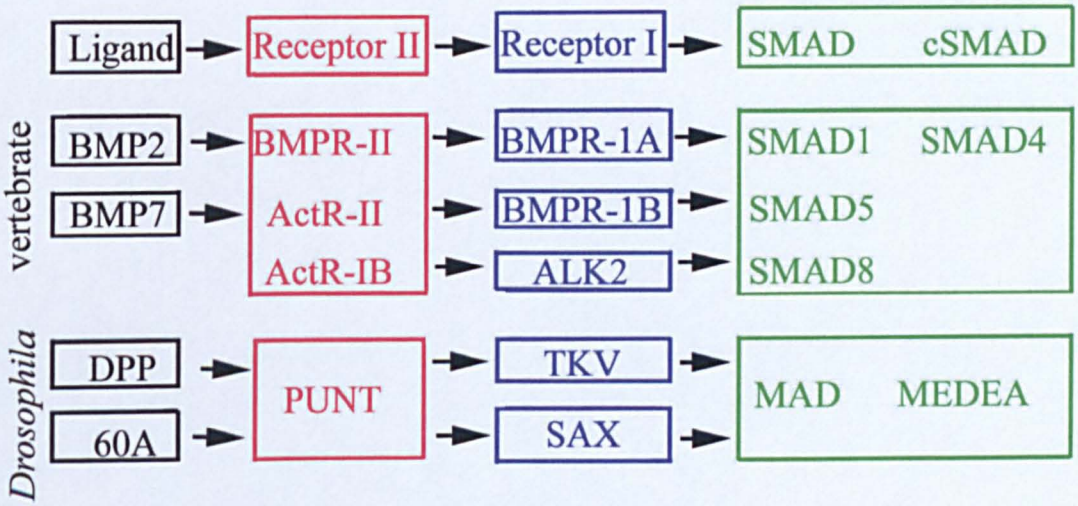

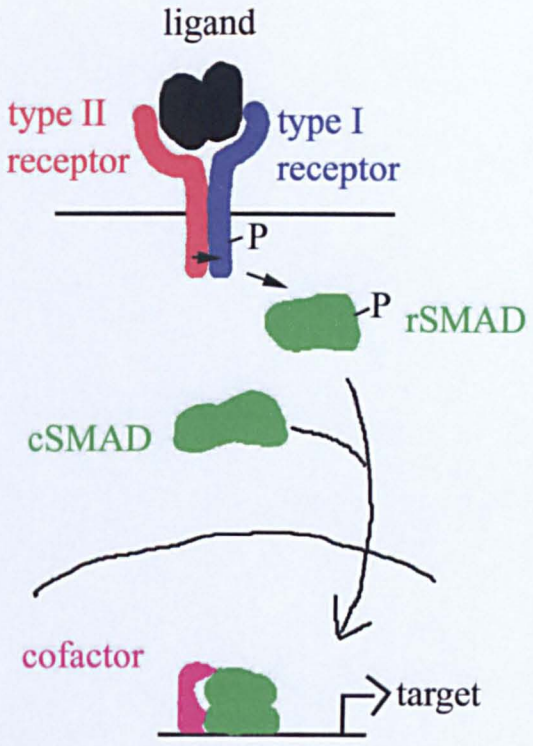

Figure 1.8 Simplified BMP signalling pathway.

The ligand dimer induces the association of two type I and two type II receptors. The type II receptor then phosphorylates the type I receptor. The type I receptor then catalyses rSMAD phosphorylation. This increases the rSMAD's affinity for cSMAD and the resultant complex moves into the nucleus where it can associate with other cofactors and bind to DNA.

1.3.2 There are two classes of BMP receptors.

There are two types of BMP receptor, type I and type II. Within these types there are various members, which have different affinities for particular ligands (Table 1.3). BMP4 binds to ALK3 and 6 whereas BMP7 (OP1) binds to ALK 2 and 6 (ten Dijke et al., 1994). ALK3 and ALK 6 are now designated BMPR1A and 1B respectively (see Table 1.2 (Reddi, 1994)). BMPs ligands bind both of the receptors at low affinity individually but at high affinity when both types are expressed together. When the ligand is bound by both receptors, the type II receptor phosphorylates the type I receptor. The type I receptor then phosphorylates a SMAD protein (Fig. 1.8).

In zebrafish the following receptors have been identified: three type I receptors, Bmpr-1A (Nikaido et al., 1999), Bmpr-1B (Nikaido et al., 1999), and Alk8 (*lost-a-fin*) (Bauer et al., 2001; Mintzer et al., 2001); two type II receptors ActRIIa and ActRIIb (Nagaso et al., 1999) and a fourth type I receptor, *thick veins* (*tkv*)(M. Hammerschmidt pers. comm.).

Table 1.3 BMP receptors

Receptor	Other names	Ligands
Type I		
BMPR1A	ALK3, BRK1 TFR11	BMP7, BMP2, BMP4
BMPR1B	ALK6, BRK2	BMP7, BMP2, BMP4
ActR1	ALK2, R1, Tsk7L	Activin, BMP7, BMP2
Drosophila melanogaster		
Sax		DPP (BMP2[a])
Tkv		DPP (BMP2[a])
Type II		
ActRII		Activin, BMP7, BMP2
ActRIIB		Activin, BMP7, BMP2
BMPR-II	BRK3, T-ALK	BMP7, BMP2, BMP4
Drosophila melanogaster		
Punt	AtrII	DPP (BMP2, activin[a])

[a] nonphysiological ligands, binding shown in vitro
Adapted from (Yamashita et al., 1995)

1.3.3 Intracellular transduction of the BMP signal.

The SMADs are the vertebrate homologues of MAD, MEDEA, and DAD found in *Drosophila* and the *sma* proteins in *C. elegans*. There are three families of SMADs, the receptor-regulated SMADs (rSMADs), the co-SMADs (cSMADs) and the inhibitory SMADs (iSMADs). The rSMADs are phosphorylated by the activated type I receptor and are specific to certain pathways, SMAD 1, 5, and 8 being specific to BMP

signalling. The phosphorylated rSMAD is then able to form a complex with a cSMAD due to its conformational change. There is only one vertebrate cSMAD known, SMAD4, which is common to all TGFβ signal pathways. This is a homologue of MEDEA in *Drosophila.*

The uninhibited rSMAD-cSMAD complex is then translocated into the nucleus. This complex is capable of binding DNA. However, in *Xenopus* OAZ, has been shown to be a cofactor that aids binding of the SMAD1-SMAD4 complex to upregulate the expression of *Xvent* (Hata et al., 2000). No cofactors specific to SMAD5 or BMP signalling have been reported. The ability to regulate gene expression with or without these cofactors provides another level of regulation to BMP signalling. Other signalling pathways (Fig. 1.9, reviewed in Massague, (2000) may regulate these cofactors. The cocktail of signals from the different pathways is probably important in determining the different responses generated by the BMP pathway. There is also growing evidence for BMP signals being transduced by another pathway not involving the SMADs (MAPK, reviewed in Bubnoff, (2001)).

Smad1, *5*, and *4* have been cloned in zebrafish (Dick et al., 1999; Dick et al., 2000).

1.3.4 Intracellular inhibition of Bmp signalling.

The third class of SMADs, which inhibit the transduction of the signal, are the inhibitory SMADs (iSMADs) Smad6 and Smad7. These two SMAD proteins can both inhibit BMP signalling by binding to the type I receptor (Imamura et al., 1997; reviewed in Massague, (1998)). However, when *smad6* is expressed at lower levels it competes with the cSMAD, Smad4 for binding to the activated rSMAD, Smad1, generating inactive Smad6-Smad1 complexes (Hata et al., 1998; Ishisaki et al., 1999). Both *smad6* and *smad7* are also expressed in response to Bmp signalling in mouse cell lines, suggesting negative feedback is moderating the levels of Bmp signalling (reviewed in Massague and Chen, (2000)).

Another form of negative feedback inhibition is provided through BAMBI (BMP and Activin membrane bound inhibitor), a transmembrane protein that is similar to TGFβ receptors except that it lacks an intracellular kinase domain. It can act as a dominant negative receptor binding to normal receptors and preventing them forming a functional complex. It requires Bmp signalling to be expressed and so acts as a negative feedback on BMP signalling (Fig. 1.9). As it binds to other TGFβ receptors it also affects other TGFβ superfamily signals (reviewed in Bubnoff, (2001)).

Signalling via rSMAD proteins in other organisms can also be inhibited by their ubiquitination via Smurf1, an E3 ubiquitin ligase (Zhu et al., 1999). This protein has been shown to regulate the competence of cells to respond to BMP by regulating the levels of Smad1 in *Xenopus* (Wrana, 2000).

smad6, *smad7* and *BAMBI* have been cloned in zebrafish (M. Hammerschmidt pers. comm.; Tsang et al., 2000).

1.3.5 Extracellular antagonists inhibit BMP pathway signalling.

As well as the intracellular regulation of the Bmp signal transduction pathway there are extracellular inhibitors. These antagonists bind to the Bmp dimers and prevent them binding to the receptor (Fig. 1.9). These include Chordin (Hammerschmidt et al., 1996), and Noggin 1-3 (Bauer et al., 1998; Fürthauer et al., 1999). Another secreted antagonist Follistatin (Bauer et al., 1998) may act in a slightly different manner. Follistatin-bound Bmp dimers can still bind to the receptors but not activate it (Iemura et al., 1998). There is another zebrafish Follistatin, however, no details are available on this gene yet (B. Thisse pers. comm.). However, all these antagonists have been shown to bind to the BMPs through immunoprecipitations, in culture and in over expression studies in *Xenopus* and zebrafish (Follistatin (Iemura et al., 1998; Fürthauer et al., 1999), Chordin (Piccolo et al., 1996; Miller-Bertoglio et al., 1997), and Noggins (Zimmerman et al., 1996; Fürthauer et al., 1999)).

The relationship between the antagonists and the BMPs is important in the regulation of active BMP signal which patterns the dorsoventral axis of developing zebrafish embryos (see below). The metalloprotease Tolloid cleaves Chordin-Bmp complexes releasing active Bmp dimers (Blader et al., 1997). This modification of the Bmp activity gradient is required to pattern the ventral tail, ventroposterior somites and vasculature (Connors et al., 1999).

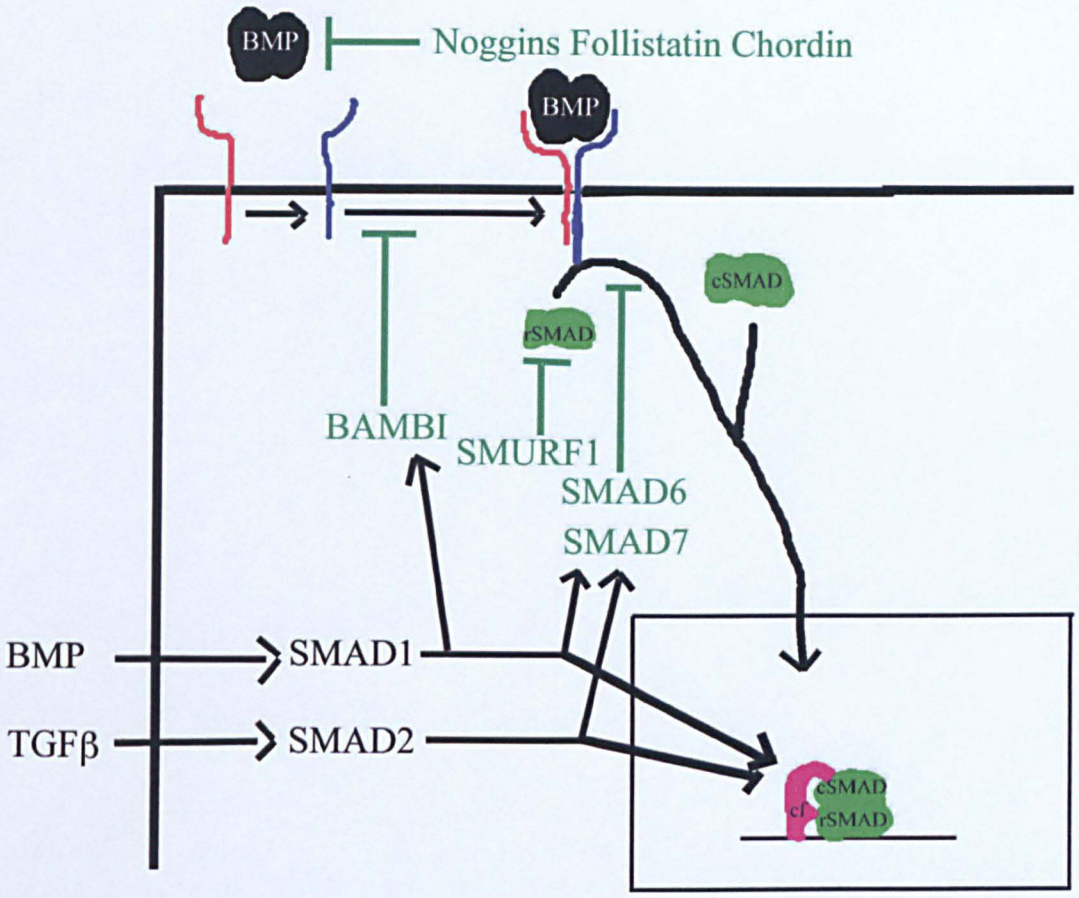

Figure 1.9 More complex BMP signalling pathway.

There are different levels of regulation to the simple pathway mentioned in previous figure. Extracellular antagonists (Noggin, Follistatin, Chordin) bind to the BMP dimers preventing them from activating their receptors. Intracellular antagonists inhibit the formation of active receptor complexes (BAMBI) or prevent the formation of rSMAD-cSMAD complexes (SMURF1, Smad6, Smad7). The availability of the different cofactors (cf) is regulated by other signal pathways, as are some of the intracellular inhibitors (iSMADs, BAMBI). More detail can be found in the text.

1.3.6 Zebrafish mutants found to be members of the BMP pathway.

In 1996 two large-scale mutagenesis screens isolated around 400 zebrafish genes (Driever et al., 1996; Haffter et al., 1996) classified according to their phenotype. One class of mutants, which have a dorsalised phenotype, were analysed and found to be required for specifying the ventral regions of the early zebrafish embryo (Mullins et al., 1996). Subsequent analysis of these mutants has identified them as members of the BMP pathway (Table 1.4). No Bmp4 mutant has been identified in zebrafish. Another class of mutants which showed a ventralised phenotype were also described (Hammerschmidt, 1996). One of these was shown to carry a mutation in the gene encoding a BMP inhibitor, *chordin* (Table 1.4). This early role in patterning the dorsoventral axis is the main focus of research into Bmp signalling in zebrafish. However, in other species, later roles for the BMPs have been investigated such as chick limb and mouse tooth and lung development (see below).

Table 1.4 Members of the BMP pathway identified from the 1996 mutant screens

Mutation	Gene	Molecular role	Phenotype	Reference
swirl	*bmp2b*	Bmp signal	severely dorsalised	(Kishimoto et al., 1997; Lee et al., 1998; Nguyen et al., 1998)
snailhouse	*bmp7*	Bmp signal	not as severely dorsalised	(Dick et al., 2000; Schmid et al., 2000)
lost-a-fin	*alk8*	type I Bmp receptor	dorsalised	(Bauer et al., 2001; Mintzer et al., 2001)
somitabun	*smad5*	Transcription factor	severely dorsalised	(Dick et al., 1999)
mini fin	*tolloid*	Metalloprotease for Chordin	slightly dorsalised	(Connors et al., 1999)
piggy tail	?	?	slightly dorsalised	(Mullins et al., 1996)
chordino	*chordin*	extracellular BMP inhibitor	slightly ventralised	(Schulte Merker et al., 1997)
ogon (mercedes)	?	in/direct BMP antagonist?	ventralised	(Miller-Bertoglio et al., 1999)

The phenotype described is that of the most severe allele.
All the dorsalised mutants were originally described in (Mullins et al., 1996). All the ventralised mutants were described in (Hammerschmidt et al., 1996).

1.4.1 A BMP activity gradient of is required to pattern the zebrafish dorsoventral axis.

Loss of Bmp signalling in both zebrafish and *Xenopus* affects the development of the dorsoventral axis of the embryo. This leads to dorsalised embryos, which lack ventral cell types (epidermis, ventral and lateral mesoderm) and have expanded dorsal tissues (somites and anterior neural ectoderm). The simple model is that a graded activity of Bmp patterns the dorsoventral axis. The restricted expression of Chordin in the shield (analogous to the Spemann-Mangold organiser in *Xenopus*) is responsible for the concentration gradient of activity of the widely expressed *bmps*. Chordin protein binds to Bmp dimers inhibiting Bmp signalling strongly dorsally and less so ventrally (Fig. 1.10) (Neave et al., 1997; Schier, 2001). Studies into this patterning process have revealed that after the initial induction of *bmp2b*, *bmp4*, and *bmp7* expression, the maintenance and induction of their new expression domains requires Bmp2b, Bmp7 and Smad5 in zebrafish (Kishimoto et al., 1997; Nguyen et al., 1998; Schmid et al., 2000).

There are complications to this simple model such as other inhibitors that regulate Bmp transcription (Bozozok and *bmp2b* (Solnica-Krezel, 2001)) or act extracellularly (Noggin 1 (Fürthauer et al., 1999) and Twisted gastrulation (Ross, 2001)). The different *bmps* are not thought to be redundant each being responsible for the patterning of a different area of the embryo together with a related protein, ADMP (anti dorsalisation morphogenetic protien) (Willot et al., 2001). The BMPs may also be signalling as homodimers and heterodimers to specify these different fates (e.g. Bmp2b and Bmp7 (Dick et al., 2000; Schmid et al., 2000)). There is also some debate as to whether the Bmps signal via Smad5 or not during this early stage (Dick et al., 1999, M. Mullins pers. comm.). However, the basic pathway is generally accepted and is similar to that seen in other vertebrates (with exceptions, see 1.4.2).

1.4.2 BMPs are an example of subfunctionalisation.

As mentioned above, each BMP is thought to be responsible for the specification of certain ventral fates. This is an example of the preservation of duplicate genes through the complementary loss of subfunctions (Force et al., 1999). The function of a common

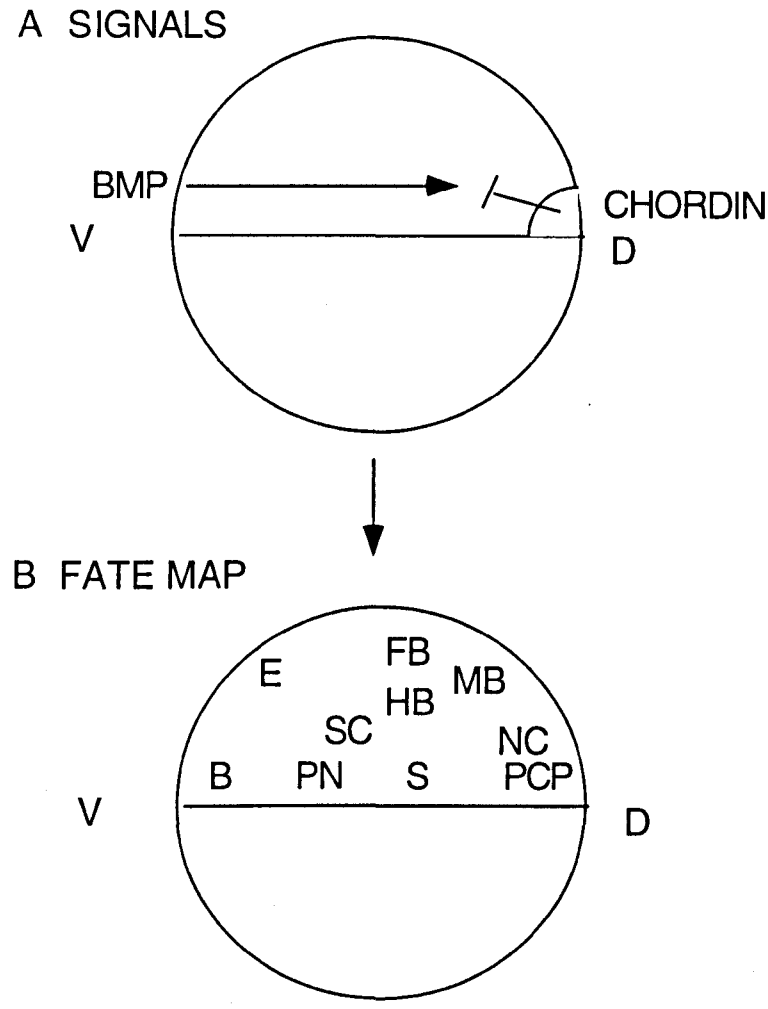

Figure 1.10 Dorsoventral patterning of the early zebrafish embryo. Adapted from Schier, (2001)
(A) A concentration gradient of active Bmp signals is required for early dorsoventral patterning. (B) A fate map of the cell types that form along the dorsoventral axis.
Abbreviations: B, blood; D, dorsal; E, epidermis; FB, forebrain; HB, hindbrain; MB, midbrain; NC, notochord; PCP, prechordal plate; PN, pronephros; S, somites; SC, spinal cord; V, ventral.

ancestor (Dpp) is split between its duplicated descendants, and these similar proteins are expressed in domains that together recapitulate that of the ancestor.

The interesting part is that during early zebrafish development Bmp2b is believed to be performing the same function as *Xenopus* and murine BMP4, although there is a zebrafish Bmp4, which has a slightly higher sequence homology to the *Xenopus* and murine BMP4 (Kishimoto et al., 1997; Nikaido et al., 1997). Therefore different homologues can perform the same function in different species. It has also been shown that these homologues can perform the same tasks when expressed in different organisms e.g. *Xenopus BMP4* can ventralise zebrafish embryos (Kishimoto et al.. 1997).

These gene duplications are thought to be due to a genome duplication event that occurred between 300-450 million years ago (prior to teleost radiation (Amores et al., 1998; Taylor et al., 2001)). This duplication provides the opportunity for dissecting the role played by these genes. This is of limited use when studying Bmp2b and Bmp7 in later stages of zebrafish development, due to their requirements during early dorsoventral patterning (Mullins et al., 1998). However, rescue techniques mentioned in section 1.1.1 have allowed the study of later roles of these Bmps by satisfying these early requirements in the mutants (see Chapter 6).

1.4.3 Later roles of Bmp signalling.

As well as being expressed at early stages, the Bmps and their inhibitors have dynamic expression patterns later in zebrafish development. Work in other species has shown that the BMPS are required in the development of many tissues. A limited number of examples are described here, which provide information that is useful in understanding possible roles for the BMPs during inner ear development.

Neural development

The dorsoventral axis of the spinal cord is thought to be patterned by two signalling centres, the BMPs from a dorsal source and Sonic Hedgehog from the ventral midline. Sonic hedgehog (Shh) has been shown in recent functional analysis, to act as a morphogen along the dorsoventral axis of the neural tube to specify ventral cell fates (Briscoe et al., (2001) and references therein). The BMPs have been shown to specify dorsal neural cell fates (e.g. trunk neural crest (Nguyen et al., 1998)). They are also thought to act over longer distances to restrict more ventral cell fates (Nguyen et al.,

1998; Barth et al., 1999) and in the chick they may act at an early stage over greater distances. It is thought the BMPs are required to form a floor plate competent region, the most ventral neural tube tissue, which then responds to Shh signalling (Patten and Placzek, 2002).

Tooth development

BMP signalling is required throughout tooth development (Jernvall and Thesleff, 2000). At early stages BMP4 is required to specify the type of tooth that will form in a competent area of dental mesenchyme. BMP4 signals from thickened areas of epithelium to the underlying mesenchyme in an antagonistic relationship with FGF8. BMP4 induces and maintains the expression of *Msx1* and *BMP4* in these mesenchymal cells, which will form incisors (Vainio et al., 1993; Tucker et al., 1998). BMP signals are also important to ensure the correct progression through tooth development. Together with other signals from a signal centre, BMP4 is thought to regulate apoptosis while BMP2 inhibits proliferation. At later stages *BMP4* expression is associated with a certain dental cell type and it may regulate the proliferation or differentiation of these cells (reviewed in Hogan, (1996)).

Limb development

The limbs develop from small buds of undifferentiated mesenchyme encased in ectoderm. A recent paper has shown that the BMPs may have a role in both the dorsoventral patterning of the limb and the induction of the AER (Apical Ectodermal Ridge) (Pizette et al., 2001). BMP signalling from the ventral ectoderm limits the expression of certain genes to the dorsal aspect of the limb. These genes then go on to pattern the dorsal side of the limb. BMP signals in the ectoderm are required to control *Fgf8* expression and induce the AER. The AER is required for the proximal-distal elongation of the limb.

Digit development

Different digit identities are thought to be generated through a morphogen gradient of BMP (Dahn and Fallon, 2000; Drossopoulou et al., 2000). As part of patterning which type of digit will form, the BMPs are also thought to be involved in regulating the fate of cells in the limb bud. Cells at the distal end of the limb bud have two alternative fates, chondrogenesis or apoptic cell death, depending on whether they are incorporated into digital rays or interdigital regions respectively. BMP2, 4 and 7 are expressed in the interdigital regions. Blocking BMP signalling inhibits cell death in the limb and

reduces levels of *msx2* expression (Zou, 1996) while adding ectopic BMP induces cell death (Macias et al., 1997). Interactions between FGFs, BMPs, TGFβs and Noggin are thought to control *Bmpr1B* expression in digit forming mesenchyme and so regulate size and position of digits. However, it is not clear if this receptor is involved in cell death (Merino et al., 1998).

1.4.4 Mechanisms of BMP action.

The mechanism of BMP action is not clear in all cases. However, BMPs are associated with specific cell fates (tooth identity). They act as morphogens specifying certain cell fates at different concentrations (neural, dorsoventral patterning). They also control proliferation (tooth, lung) and apoptosis (digits) through the expression of *Msx1* and *Msx2* (Davidson, 1995; Bendall and Abate-Shen, 2000).

In order to be a morphogen, a signal has to be able to act at long distances without using a relay system involving intermediate signals. Squint, another TGFβ superfamily member, has been shown to have long range concentration-dependent effects, without the need of secondary signals, in the induction of mesoderm in zebrafish (Chen, 2001). The morphogen activity of BMP4 has been shown in *Xenopus* (Dosch et al., 1997).

It is also not clear how these signals (including Squint) travel across tissues. Do they diffuse freely through the extracellular matrix? Do they go through cells via planar transcytosis, where proteins are endocytosed at one side of a cell and then transported across and released at the other (as for Wingless, reviewed in Christian, (2000))? Or do they interact with components of the extracellular matrix such as heparan sulphate proteoglycans (Paine-Saunders et al., 2001)? The diffusion of another signalling molecule Hedgehog is thought to be mediated via a heparan sulphate proteoglycan-related molecule, Tout velu (The et al., 1999). It has also been suggested that filopodia-like extensions (cytonemes) of cells extend towards the source of the morphogen (Ramirez-Weber, 1999). This suggests that all the cells receive the same amount of signal which is then diluted depending how long the cytoneme is i.e. the concentration of the secondary signal transducer becomes the regulating factor.

The regulation of *Msx* expression usually seems to involve epithelial-mesenchymal interactions. In the tooth BMPs signal from the epithelium at one stage and then from the mesenchyme at a later stage, showing that the BMPs can have multiple roles throughout the development of one structure. This is also true in the limb where the BMPs act to establish anterior-posterior patterning and then later control proximal-distal

growth and cell death between the digits. These studies into later roles have also established that there is complex interplay between the different signalling pathways to achieve the desired tissue.

1.4.5 Targets of Bmp signalling

As well as *smad6*, *smad7* and the *bmps* themselves, other targets of BMP signalling have been identified. *Msx1* and *2* are thought to be one target and as mentioned above they are induced during tooth, limb and digit development where they are thought to regulate cell death and division. The programmed cell death of rhombocephalic neural crest cells is dependent on the expression of *BMP4* and *Msx2* in chick (Graham et al., 1994). In vitro and over-expression studies have also shown that *Msx1* can inhibit the differentiation of cells preventing them leaving the cell cycle (by maintaining elevated levels of cyclin D1). *Msx1* may be performing this function in the limb bud and myogenic precursors (Hu et al., 2001). In cell lines, adding BMP4 induces expression of *Msx2* and programmed cell death (Marazzi, 1997).

Spalt is a nuclear *Drosophila* protein, a transcription factor with a double zinc-finger domain. It is required to form specific structures in the wing and thorax. In the wing, it is regulated by Decapentaplegic (Dpp) and regulates the positioning of wing veins (de Celis et al., 1996; Lecuit et al., 1996; Nellen et al., 1996). It is regulated by Hh, Dpp and Wg in the thorax where it is required to specify a particular sense organ. Two types of sensory organ, macrochaetae and microchaetae, cover the *Drosophila* thorax. They form from sensory organ precursor (sop) cells that are specified from within a cluster of potential precursors by proneural genes (*achaete* and *scute*, (Campuzano, 1992)). *Spalt* is required (together with *spalt-related*) to form a subset of machrochaetae and is thought to be one of a group of transcription factors required to regulate where proneural genes are activated (de Celis et al., 1999). It is expressed in the region where most of the proneural clusters form but in order to differentiate *spalt* must not be expressed in the sensory organ precursor cell. Failure to express *sal* or *salr* results in the loss of that type of macrochaete (de Celis et al., 1999).

Another *Drosophila* homologue *eyes absent1* may be a target of Bmp signalling during zebrafish inner ear development as part of a regulatory feedback loop. This is explored in Chapter 4 (4.4.1).

In chick and *Drosophila* Bmp homologues have been shown to induce the expression of Tbx genes. BMP2 is thought to induce *Tbx2* in chick heart development (Yamada et al.,

2000) while in the chick limb beads soaked in BMP2 induced the expression of *Tbx5* (Rodriguez-Esteban et al., 1999). In *Drosophila* the Dpp target gene *optomotorblind* encodes a Tbox gene, similar in amino acid sequence to the founding member of the Tbox family, *Brachyury* (Kopp, 1997; Yamada et al., 2000). These Tbx genes have been shown to be required for specifying cardiac, limb and abdomen fates respectively (reviewed in Smith, (1999)).

1.4.6 Possible BMP roles during inner ear development.

Section 1.2 described the morphological changes the zebrafish inner ear goes through during its dramatic change from a simple ball of cells to the complex adult structure. These changes require the specification and maintenance of different cell fates, cell death and division and the rearrangement of cells within the epithelia, as well as communications with the surrounding mesenchyme.

All the cell types found within the inner ear come from the otic vesicle. Fate mapping studies have shown that there are broad areas of cells competent to form related cell types early in development (17hpf). These cells have to be specified and possibly maintained in those fates.

There are scattered areas of apoptosis and cell division during inner ear development (Haddon, 1997; Bever and Fekete, 1999; Cole and Ross, 2001). During SCC development there may be an increase in cell death in areas where the projections fuse similar to that seen in chick and mouse, also in the area where cells delaminate to form the statoacoustic ganglion (Cole and Ross, 2001). The developing SCC will also probably need to communicate with the surrounding mesenchyme to enable their growth.

As described above the BMPs have been shown to specify cell types, control cell number and signal between cell layers. They may be involved in these roles in during inner ear development. They may have multiple roles at different stages of development. The following chapters provide a detailed analysis of where and when the BMPs are expressed in both wild type and mutants. These results, together with functional studies, have provided evidence for sites of BMP action during zebrafish inner ear development.

Chapter 2

Expression of the zebrafish *bmps* during inner ear development.

2.1 INTRODUCTION

Members of the BMP family are expressed in the developing inner ear of chicks, mice and *Xenopus*. There is a level of conservation between these three species, all of which express BMP4 in their cristae (see 2.1.2). This chapter documents the expression of the BMP homologues during zebrafish inner ear development, to determine if the conserved crista expression continues in a species that offers certain advantages over the three species mentioned above.

As described in the previous chapter the structure of the zebrafish inner ear is very similar to those of other vertebrates. The pars superior of the inner ear, including the cristae, is conserved. Zebrafish also provide a method of studying BMP mutants and the affect of increasing or decreasing BMP protein levels.

To take advantage of the zebrafish as a model organism the expression patterns of its Bmp homologues during normal development have to be described in detail. This chapter provides the backbone on which all the later work is built. It reveals that there is conservation of the crista expression seen in other species and compares other aspects of the expression patterns of the different *bmps* and their homologues. Together with Chapter 3, which details the expression patterns of members of the Bmp signal pathway, it provides clues as to where and when the BMPs are acting.

2.1.1 There are five BMP family members in zebrafish.

Five BMP family members have been cloned in the zebrafish: *bmp2a* (Martinez-Barbera et al., 1997), *bmp2b* (Martinez-Barbera et al., 1997; Nikaido et al., 1997) (bmp2b=zbmp2 in Nikaido et al., (1997), *bmp4* (Chin et al., 1997; Nikaido et al., 1997), *bmp7* (Dick et al., 2000; Schmid et al., 2000), and *bmp7-related* (*bmp7r*)(T. Schilling, unpublished). *bmp2a* is reported to be expressed strongly at 11 and 36hpf in the posterior tail tip and then in the distal tip of the fin bud mesenchyme respectively (Martinez-Barbera et al., 1997). Studies on *bmp2b* mutant zebrafish suggest *bmp2a* is

not functionally redundant to *bmp2b* at early developmental stages (Nguyen et al., 1998). *bmp2a* is not reported to be expressed in or near the otic vesicle and so was not examined in this study. Inner ear expression was briefly mentioned for each of the other homologues in the original cloning papers. However, it was not described in any detail.

The Bmps are divided into subfamilies based on the sequence homology of the carboxy-terminal mature region (See Table 2.1 and Hogan, (1996). The different homologues have been named according to their sequence similarities to each other; Bmp2a, Bmp2b, Bmp4 show high sequence homology to *Drosophila* Dpp, as well as mouse, *Xenopus* and human BMP2 and BMP4. Bmp7 belongs to a different subgroup of the Bmps and is closely related to *Xenopus*, mouse and human BMP7. There is a *Xenopus* BMP7-related to which Bmp7 is less closely related (Nishimatsu et al., 1992) and as yet there is no information on where zebrafish Bmp7-related fits into the family.

Table 2.1

Mammalian (mouse)	Frog (*Xenopus laevis*)	Zebrafish (*Danio rerio*)	Fly (*Drosophila melanogaster*)
BMP2 BMP4	BMP2 BMP4	Bmp2b (*swirl*) Bmp2a Bmp 4	Decapentaplegic (DPP)
BMP5 BMP6 BMP7 BMP8	BMP7 BMP7r	Bmp7 (*snailhouse*)	Glass bottom boat (GBB)
		Bmp7r	

Summary table showing members of the different subfamilies of BMP proteins in different species adapted from Hogan, (1996).

2.1.2 BMPs are expressed in conserved domains in the developing inner ears of chicks, mice and *Xenopus*.

Homologues of the *bmps* have been analysed during the development of inner ears of different species. They have been found to be expressed in chick (Oh et al., 1996; Wu and Oh, 1996), mouse (Morsli et al., 1998), and *Xenopus* (Hemmati-Brivanlou and Thomsen, 1995; Kil and Collazo, 2001; Knochel et al., 2001) inner ear sensory patches. These studies described conservation of expression between species, each initially expressing *BMP4* in areas thought to be the presumptive cristae and then subsequently in all sensory patches. Different cell types within the patches express *BMP4* depending on the species (see Table 2.2). In the chick, for example, *BMP4* is expressed in the hair

cells of the basilar papilla, whereas in the mouse, it is expressed in the support cells (Hensen's and/or Claudius' cells) of the cochlea, the analogous mouse structure (Oh et al., 1996; Morsli et al., 1998). In the chick and mouse *BMP4* is expressed in the supporting cells of the cristae (Oh et al., 1996; Morsli et al., 1998). In *Xenopus BMP4* is seen in both the hair cells and support cells of the lateral and posterior cristae. Expression was too weak to determine if both cell types were labelled in the anterior cristae (Kil and Collazo, 2001).

2.1.3 Differences in BMP expression are seen amongst these three species.

In the chick and mouse broad anterior domains of *BMP4* are thought to mark a possible common origin for the anterior and lateral cristae. This is not reported in *Xenopus*. In the chick, *BMP7* and *BMP5* are also expressed in similar domains to *BMP4*. *BMP7* is expressed more widely than *BMP4* and *BMP5* is more transient than *BMP4*. *BMP2* is not expressed in the chick otocyst (Oh et al., 1996; Wu and Oh, 1996). Table 2.3 in the appendix describes the chick BMP expression patterns in more detail.

In the mouse only *BMP4* has been described (Jones et al., 1991; Takemura et al., 1996; Morsli et al., 1998). Unlike chick *BMP4*, murine *BMP4* is not a marker for all the presumptive sense organs. However, it is reported to be expressed in the supporting cells of all the maculae at later stages (Morsli et al., 1998) (see Appendix Table 2.4).

In *Xenopus* both *BMP2* and *BMP4* were analysed, but only *BMP4* is reported to be in the inner ear (Hemmati-Brivanlou and Thomsen, 1995). A broad *BMP7* domain, larger than the *BMP4* domain at placode and otocyst stages, and similar to that seen in the chick, is mentioned in Kil and Collazo, (2000), but no details are provided (see appendix Table 2.5).

2.1.4 The lateral line system contains cell types similar to those in the inner ear.

The lateral line is a mechanosensory system arranged in lines along the body of the zebrafish. This system of connected groups of cells, known as neuromasts, contain hair cells and support cell types similar to those found within the inner ear. These cells allow the zebrafish to detect water movement. Lateral line organs develop from migrating placodes that are formed around the otic placode and move, either anteriorly

or posteriorly, along the zebrafish leaving clusters of cells, which mature to form the neuromasts (Metcalfe et al., 1985).

2.2 RESULTS

To detect the target mRNA digoxigenin-UTP labelled mRNA probes were used on whole embryos. In some cases the whole embryos were sectioned by hand to provide clearer images of internal staining. All stages are given as hours post fertilisation (hpf) or as primordia stages (P) based on the level reached by the migrating posterior lateral line primordium as in (Kimmel et al., 1995). All the zebrafish used in this study were raised at 27.8°C.

2.2.1 *bmp2b* mRNA expression.

bmp2b is one of the earliest *bmps* to be expressed in the inner ear. It is expressed at 20hpf, when the otic placode has just cavitated to form a vesicle, concentrated dorsolaterally (Fig. 2.1A+B). By 24hpf expression is still concentrated laterally, but at the anterior and posterior ends of the vesicle (Fig. 2.1C and 2.5C). It is not clear if the broad dorsal stripe resolves into these two domains or if they arise *de novo*. At 27hpf the anterior area expression is expanded ventrally (Fig. 2.1D). This is clearly seen as a separate third ventrolateral domain by 34hpf (Fig. 2.1E arrow), and by 48hpf it is clear that the three domains, marking thickened epithelium, correspond to the developing cristae (Fig. 2.1F and Fig. 2.5G). This staining persists as crista hair cells differentiate (at 60hpf (Haddon and Lewis, 1996)). At 72hpf *bmp2b* also stains the epithelial projections (Fig. 2.5K white arrow). The stain in the cristae is present but at a reduced level, spanning the epithelium (Fig. 2.5K bracket). This *bmp2b* stain is not seen at later stages.

2.2.2 *bmp4* mRNA expression.

bmp4 is expressed weakly in the otic vesicle from 24hpf. It is expressed laterally at its anterior and posterior ends (Fig. 2.2A and Fig. 2.5D). This pattern is stronger by 25hpf (P6) (Fig. 2.2B) and by 27hpf, a third ventrolateral domain, and a fourth non-sensory dorsal domain are present (Fig. 2.2C, arrow and arrowhead). The dorsal domain appears initially as a horizontal stain in a single layer of cells. At later stages this layer of cells forms a hairpin extending dorsally. The nature of this domain of *bmp4* expression is explored more fully in Chapter 4 (see 4.5.1). At 48hpf strong expression

is seen in the three ventrolateral crista thickenings and the dorsal stain has a more pinched appearance (Fig. 2.2D and Fig. 2.5H). This pattern persists until 72hpf when the dorsal area of expression fades (Fig. 2.2E and Fig. 2.5L). The cristae continue to stain faintly at 7dpf (Fig. 2.2G).

2.2.3 *bmp7* mRNA expression.

bmp7 is expressed in a single posterior ventromedial domain from 24hpf until 42hpf (Fig. 2.3 arrow). This expression domain does not correspond to the posterior ventrolateral crista thickening or the posterior macula. This expression domain spans the epithelium.

2.2.4 *bmp7-related* mRNA expression.

bmp7-related (*bmp7r*) is the earliest *bmp* to be expressed, found in the otic placode at 16hpf (14 somites)(Fig. 2.4A). It is expressed in a posterior domain that extends anteroventrally. This pattern persists until cavitation at 24hpf when it becomes more concentrated laterally, at the anterior and posterior ends of the vesicle (Fig. 2.4C, arrowheads). It does not appear as discrete as *bmp2b* or *bmp4*. At 27hpf (P11) it has become more discrete, with a broad anterior domain and a posterior domain more reminiscent of *bmp2b* and *bmp4* (Fig. 2.4D). At 48hpf it is expressed in the three ventrolateral thickenings (Fig. 2.4E arrowheads). It is still faintly expressed in the cristae at 5dpf (Fig. 2.4F).

2.2.5 *bmp2b* and *bmp4* are expressed in hair cells and support cells.

At 24hpf both *bmp2b* and *bmp4* are expressed in lateral domains at the anterior and posterior of the vesicle (Fig. 2.5C+D arrows). These domains appear to abut the medial expression domains of *pax2.1* (Fig. 2.5B). The primary hair cells develop within this *pax2.1* domain and continue to express *pax2.1* (Fig. 2.5A-D arrows and brackets (Riley et al., 1999)). The zebrafish *Delta* homologues, *deltaA*, *deltaB*, and *deltaD*, are also expressed in this area at early stages (18hpf) in cells thought to be hair cell precursors (Haddon et al., 1998).

At later stages *bmp2b* and *bmp4* are expressed in the developing cristae (Fig. 2.5G+H). At 48hpf they are both expressed throughout the thickened epithelium in the same area

as *msxc*, a crista marker ((Ekker et al., 1992), Fig. 2.5F). These sections also reveal that the thickening of the developing lateral crista is contiguous with that of the anterior macula (Fig. 2.5H). Neither macula expresses any of the *bmps* (Fig. 2.5G+H arrows).

At 72hpf, when the cristae have differentiated, the thickened epithelium is pseudostratified with the hair cells positioned apically and the support cells basally. At this stage the *bmps* are still expressed throughout the epithelium although at lower levels (Fig. 2.5K+L brackets). However, *brn3.1*, a marker of differentiated hair cells, is expressed apically in the macula and cristae (Fig. 2.5J brackets). It is therefore concluded that *bmp2b* and *bmp4* are marking both hair and support cells.

2.2.6 *bmp* expression in the lateral line.

At early stages *bmp2b* and *bmp7r* are expressed in the migrating posterior lateral line primordium (Fig. 2.6A arrows, F). At 72hpf there is weak *bmp4* staining in the neuromasts along the tail (Fig. 2.6D). At 7dpf strong stain is still seen in the neuromasts of the head as well as the tail (Fig. 2.6E and data not shown). The mature neuromasts also express *bmp7r* and *bmp2b*, at least until 5dpf (Fig. 2.6C+G). This pattern of early *bmp2b* and *bmp7r* expression followed by later *bmp4* expression is reminiscent of that seen during inner ear development.

Figure 2.1

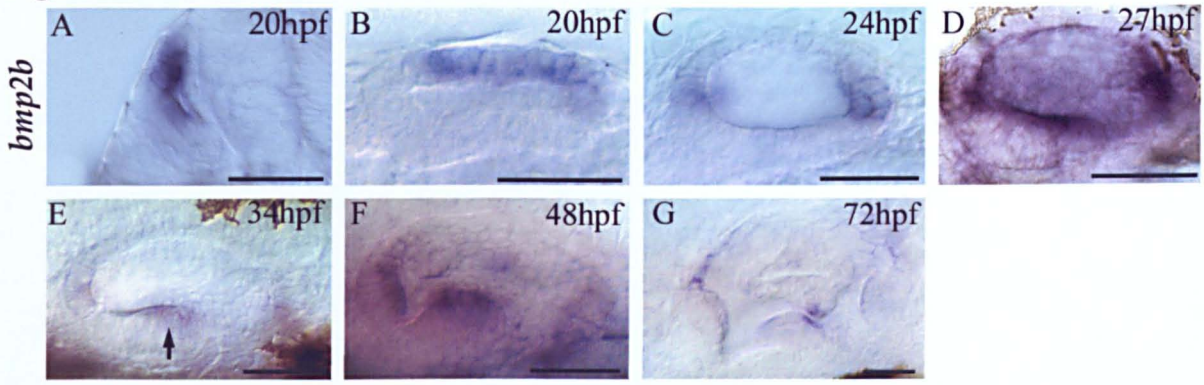

Figure2.2

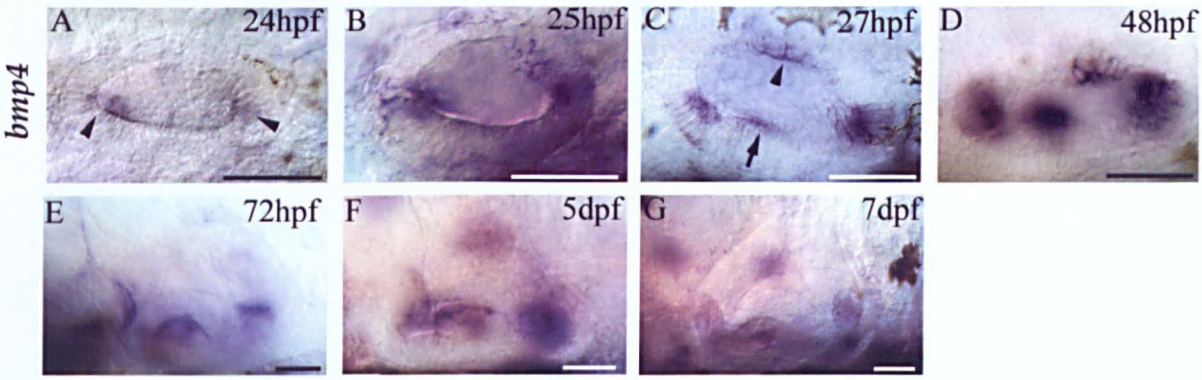

Figure 2.3

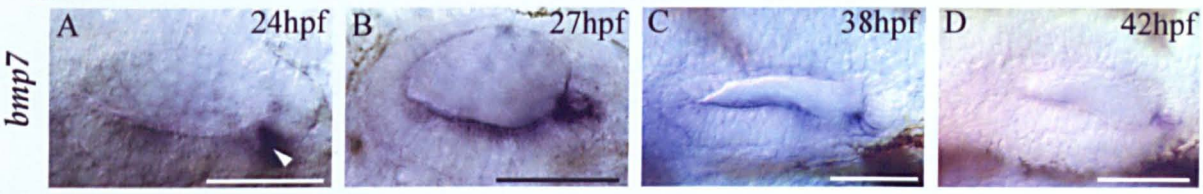

Figure 2.4

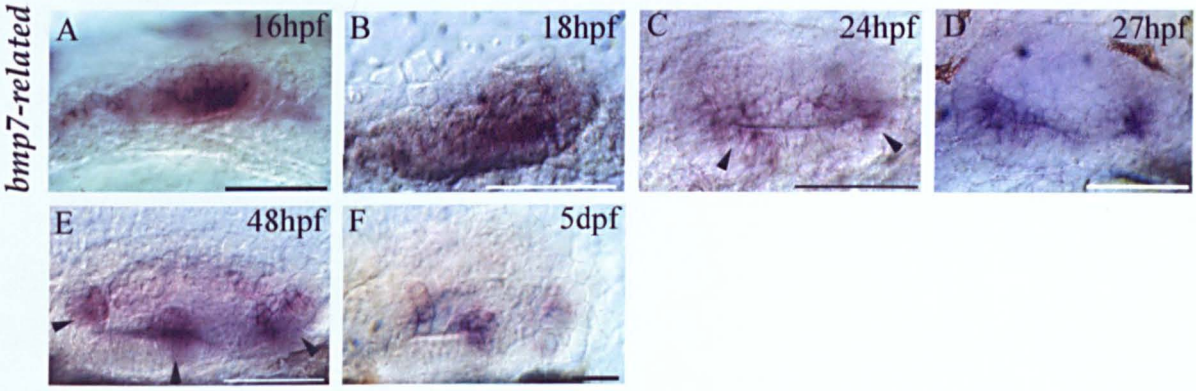

Expression patterns of the *bmps* during inner ear development.

Figure 2.1 *bmp2b* mRNA expression

DIC images of whole mount in situ hybridisations. (A) transverse section, dorsal to top; (B-K) lateral views, anterior to left, dorsal to top. Scale bar=50μm

(A, B) *bmp2b* is expressed dorsolaterally at 20hpf. (C) *bmp2b* expression is concentrated at the anterior and posterior ends of the vesicle at 24hpf (see also dorsal view, Fig. 2.5C). (D) A third ventrolateral domain of *bmp2b* expression appears at 27hpf. (E) At 34hpf (P22) can see three separate ventrolateral domains (arrow). (F) Cristae thickenings become more obvious at 48hpf. (G) *bmp2b* is still expressed in the cristae and is now expressed in the epithelia of SCC projections at 72hpf.

Figure. 2.2 *bmp4* mRNA expression.

All lateral views, anterior to left, dorsal top. Scale bar = 50μm.

(A) *bmp4* is expressed weakly at the anterior and posterior ends of the vesicle at 24hpf (arrowheads; see also dorsal view, Fig. 2.5D). (B) This expression pattern is stronger by 25hpf (P6). (C) Two additional areas of *bmp4* expression appear at 27hpf, ventrolaterally (arrow) and dorsally (arrowhead). (D) The dorsal *bmp4* expression domain begins to thicken and extend dorsally at 48hpf. Three strong ventrolateral domains now mark thickened areas of epithelium (the cristae). (E) At 3dpf the levels of dorsal expression decreases; staining persists in the cristae, and is still seen at 5dpf (F) and 7dpf (G). The shadow of neuromast staining, lateral to the optical section photographed in F+G is showing through.

Figure. 2.3 *bmp7*mRNA expression.

All are lateral views, anterior to left, dorsal to top. Scale bar = 50μm.

(A-D) *bmp7* expression is concentrated in a single posteroventral domain from 24-42hpf (arrowhead), with weak expression elsewhere in the ventral epithelium at 24 and 27hpf.

Figure. 2.4 *bmp7r* mRNA expression.

All are lateral views, anterior to left, dorsal to top. Scale bar = 50μm.

(A) *bmp7r* is expressed in a posteroventral domain at 16hpf (14 somites) and 18hpf (B). (C) Expression is more localised laterally to anterior and posterior ends of vesicle at 24hpf (arrowheads). (D) At 27hpf there is a broad anterior domain and a more narrow posterior domain. (E) At 48hpf *bmp7r* is expressed in the three ventrolateral crista thickenings (arrowheads). (F) Staining is still present at 5dpf.

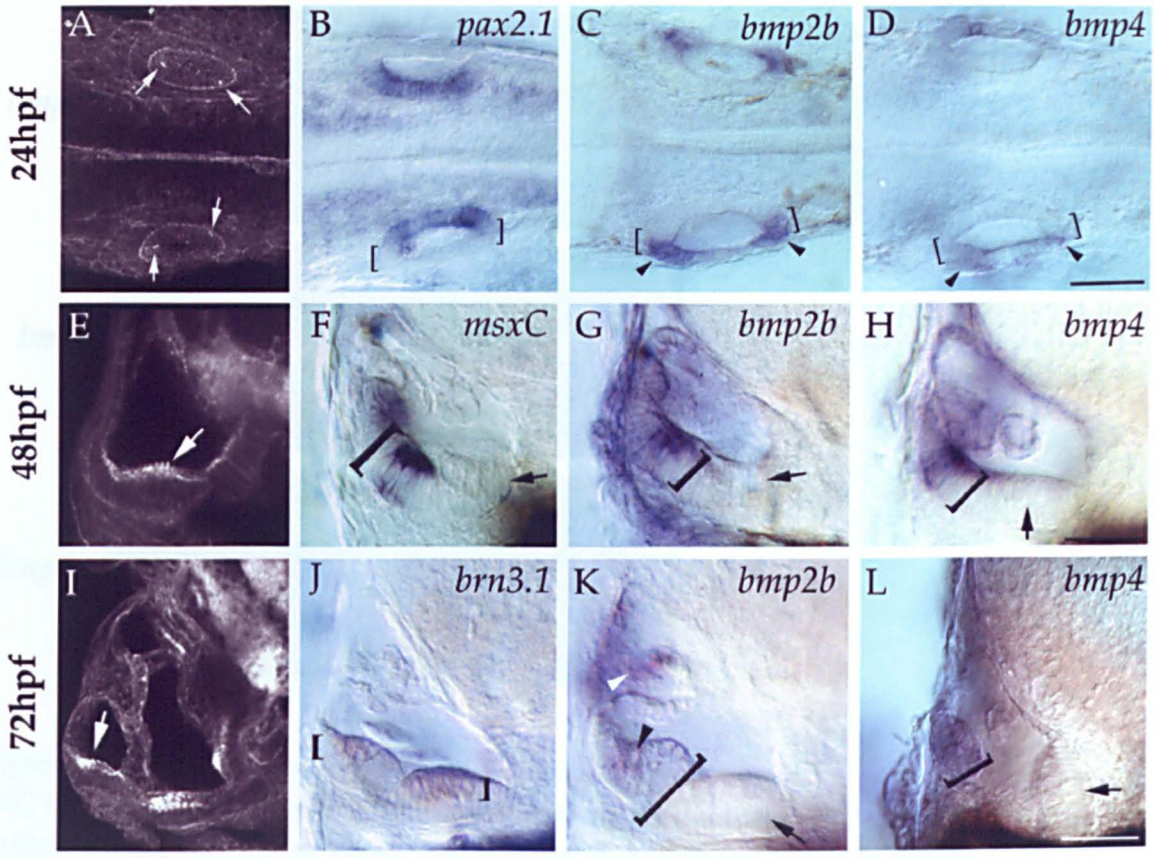

Figure 2.5 Expression of *bmps* during sensory patch differentiation.
(A, E, I) Confocal optical sections of zebrafish ears stained with FITC-phalloidin, labelling stereociliary bundles of differentiated hair cells (bright dots, arrows) and cell boundaries. (B-D, F-H, J-L) DIC images of whole mount in situ hybridisations. (A-D) Dorsal views, anterior to left; (E-L), transverse sections at the level of the developing lateral crista; dorsal up, lateral to left. Scale bar=50μm.

(A) At 24hpf the first macular hair cells (arrows) form at the anterior and posterior limits of the medial *pax2.1* domain (B, brackets in B-D). (C, D) Lateral expression of *bmp2b* and *bmp4*,at the anterior and posterior ends of the vesicle (arrowheads). (E) At 48hpf differentiated hair cells are present in the anterior macula (arrow), but the prospective lateral crista is not yet a separate thickening. (F-H) *msxc*, *bmp2b*, and *bmp4*, are expressed in the presumptive lateral crista. Expression of all three markers spans the epithelium at this stage (brackets). This domain is lateral to the unlabelled anterior macula, with its apically-positioned hair cell nuclei (arrows). (I) At 72hpf differentiated hair cells are found in the lateral crista (arrow; SCC tissue is also now seen dividing the lumen of the ear). (J) Apically-positioned hair cells in the lateral crista and anterior macula, labelled with *brn3.1*, a hair cell marker (brackets). (K, L) *bmp2b* and *bmp4* expression in the lateral crista is less discrete, still spanning the epithelium at this stage, apparently marking both hair cells (K, black arrowhead) and supporting cells (brackets). Arrows indicate the unlabelled anterior (K) and posterior (L) maculae. *bmp2b* is also weakly expressed in the epithelial projections (K, white arrowhead).

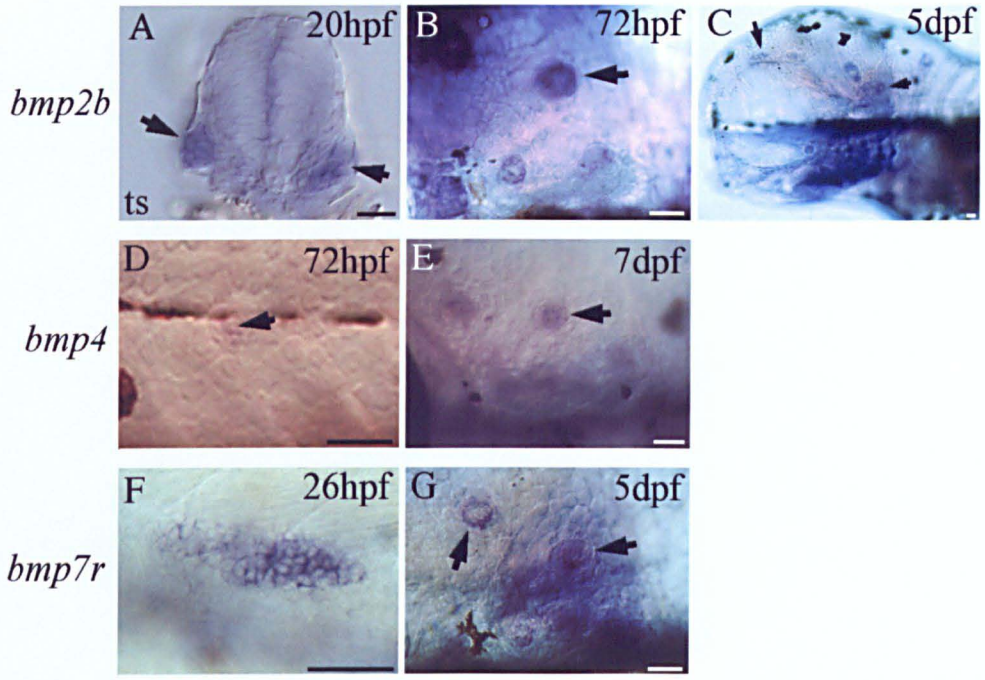

Figure 2.6 Expression of *bmps* during lateral line development.
DIC images of wholemount in situ hybridisations. A is a transverse sections with dorsal to the top. B-G are lateral views with anterior to the left and dorsal to the top.
Scale bar=50μm

(A) *bmp2b* is expressed in the posterior lateral line primordium shown at 20hpf. (B) At 72hpf *bmp2b* is expressed in the neuromasts in the head (arrow), and tail (data not shown). (C) Mature neuromasts in the head still express *bmp2b* at 5dpf (arrows). (D) At 72hpf *bmp4* is expressed weakly in the tail neuromasts. (E) At 7dpf *bmp4* is still expressed strongly in the neuromasts of the tail (arrows) and head (data not shown see Fig. 2.2F+G). (F) *bmp7r* is expressed strongly in the posterior migrating lateral line primordium. (G) *bmp7r* is expressed in the mature neuromasts (arrows).

2.3 DISCUSSION

This chapter documents the mRNA expression patterns of four zebrafish Bmp homologues during inner ear development and the development of the lateral line. They have similar, yet distinct patterns that share the conserved crista expression seen in other species. Both *bmp4* and *bmp2b* appear to mark both cell types in the cristae. *bmp4* is also expressed in a novel dorsal domain, which is discussed in more detail in Chapter 4, that is believed to mark the developing endolymphatic duct.

The coexpression of *bmp4*, *bmp2b*, and *bmp7r* is maintained to some extent in the developing lateral line, in a pattern similar to that seen in the inner ear. At early stages in both the inner ear and lateral line *bmp2b* and *bmp7r* are expressed before *bmp4* and *bmp7*. Also as in the inner ear *bmp7* is not coexpressed with the other *bmps* in the developing lateral line system.

2.3.1 The *bmp*s have overlapping expression patterns.

bmp2b, *bmp4*, and *bmp7r* have similar expression patterns between the stages of 24hpf and 72hpf. Each of these three genes is expressed in two ventrolateral domains at early stages and in three ventrolateral domains by 48hpf. By 48hpf these domains coincide with epithelial thickenings which go on to form the cristae, the sensory patches associated with the SCC (Haddon and Lewis, 1996).

BMPs form dimers; therefore as these genes appear to be expressed in the same cells these cells could be secreting heterodimers as well as homodimers. This is also possible in the chick where early in development *Bmp7*, *Bmp4*, and *Bmp5* share domains (Oh et al., 1996). Heterodimers have been shown to provoke different responses compared to homodimers. In vitro experiments with *Xenopus* have shown heterodimers to be more potent than homodimers in provoking osteogenic differentiation (Hazama et al., 1995) or mesoderm induction (Suzuki et al., 1997). There is also in vivo evidence from zebrafish that suggests the BMPs could act as heterodimers early in development to specify ventral cell fate. Embryos with both *bmp2b* and *bmp7* mutations do not have a stronger dorsal phenotype than that seen in either single mutant. This suggests these genes do not function redundantly during development. Coinjection of *bmp2b* and *bmp7* mRNA into the same blastomeres produced a stronger ventralised reaction than that seen with injections of each into adjacent blastomeres (Schmid et al., 2000). Together these results suggest Bmp2b and Bmp4 are working as heterodimers.

It is possible therefore that these lateral domains of *bmp* expression in the zebrafish are acting as signalling centres, secreting heterodimers (in six possible combinations) or homodimers.

2.3.2 The *bmps* have distinct expression patterns.

Importantly, there are also differences in the expression patterns of the *bmps*. *bmp2b* is initially expressed in a broad dorsolateral domain while *bmp7r* has an even larger early expression domain. This is perhaps reminiscent of the broad domains of *Bmp4* and *Bmp7* seen in the early stages of inner ear development in chick, mouse, and *Xenopus* (Tables 2.2-5).

These broad expression patterns could represent large domains of competent cells, which become restricted as development progresses. Early fate maps have shown that at 17hpf the anterolateral area of the placode can contribute to the anterior macula, anterior and lateral cristae as well as nonsensory, SCC fates (Haddon, 1997). By 24hpf the reduced *bmp* domains may represent cells that can contribute to only a sensory fate. Given that the *bmp* domains appear to exclude macula markers (*pax2.1* see Fig. 2.5B-D) this fate could be further restricted to cristae. The association of *bmp* expression and cell fate does not appear to follow further fate restrictions, as both hair cells and support cells appear to express *bmp*s once differentiated. However, factors downstream of BMP signalling may be differentially expressed following the integration of different signals allowing further restriction.

At later stages *bmp2b*, unlike the other *bmps*, is expressed in the SCC epithelium. This pattern does not persist for long and could either represent movement of cells from the previous areas of *bmp2b* expression, or the upregulation of *bmp2b* expression in cells that did not previously express it.

It will be interesting to learn how similar *bmp7r* is to *bmp2b* and *bmp4*, in sequence and function, compared to *bmp7*, given the disparity in expression domains. Its expression pattern appears similar to the widespread domains of chick BMP7.

2.3.3 *bmp7* expression is very different to that of the other *bmps* in the inner ear.

The single domain of *bmp7* expression is unlike the expression of other *bmps* in zebrafish, chick, mouse or *Xenopus*. It is not associated with any sensory region or with delaminating neurons or epithelial projections.

In the zebrafish *bmp7* is required early in dorsoventral patterning, possibly working with *bmp2b* and forming heterodimers (Dick et al., 2000; Schmid et al., 2000). However, in the inner ear *bmp7* does not appear to be coexpressed with any of the other *bmps* and so would not form heterodimers, but the resultant homodimers could trigger a different set of BMP targets in the posterior of the vesicle. This is possible as the different BMPs have different affinities for their receptors (see 1.3.2).

BMP7 is a member of the *bmp5, 6, 7, Gbb-60A* subfamily rather than the *bmp4, 2, Dpp* subfamily (reviewed in Massague, (2000)). However, in the chick inner ear *Bmp5* and *Bmp7* share similar expression pattern to members of the *bmp4, bmp2* subfamily (mouse *BMP5* is not expressed in the inner ear (King et al., 1994)).

It is not clear whether different BMPs have different roles during development as often their expression patterns overlap and methods used to manipulate BMP signalling such as the addition of antagonists or dominant negative receptors could affect multiple BMPs. The analysis of mutations in single BMPs have revealed dramatic phenotypes as is shown in the Mullins paper (Mullins et al., 1996). However, there are difficulties in interpreting them due to redundancy and early lethality.

The rescue mRNA injections possible in zebrafish will be useful in uncovering unique later roles for mutant genes. This technique will be discussed in Chapter 6. The rescued *bmp7* mutant (*snailhouse*) is not reported to have any balance or hearing defects which argues against Bmp7 having a unique role during inner ear development (Mullins pers. comm.). However, this has not been extensively examined and it is not clear when the rescuing mRNA is active. This will be explored more fully in Chapter 6.

2.3.4 *bmp* expression prefigures the appearance of and subsequently labels cristae but is not found in the maculae.

As in chick, mouse, and *Xenopus*, in zebrafish the *bmps* (except for *bmp7* and *bmp2a*) are expressed in ventrolateral domains that prefigure the formation of the ventrolateral

thickenings, which are the first signs of future crista development. This pattern precedes the expression of the crista marker, *msxc*. However, unlike the chick there does not appear to be a restriction of subsequent expression as the hair cells and support cells differentiate. Wax or cryosection methods may provide more conclusive results.

In the chick *BMP4* and *BMP7* are expressed in the developing and differentiating maculae. In mouse and *Xenopus BMP4* is not the first marker to be expressed in all the differenting maculae, although at later stages *BMP4* is expressed in all the maculae of both species. However, in the zebrafish, expression was not detected in the maculae at any of the stages examined. These expression patterns could mean that the BMPs are involved in a subset of the functions they perform in chick or mouse. This may represent the adoption of the BMPs to function in the maculae of higher vertebrates. Indeed, the difference in expression seen in the developing cochlea and basilar papilla in chick and mouse is suggested to be due to the relative differences in complexity (Morsli et al., 1998). Alternatively this may be due to the subdivision of functions in the zebrafish because there are generally more members of the gene families in zebrafish. In this case other members of the *bmp* family, as yet unknown, may be expressed in the developing zebrafish maculae.

2.3.5 Comparison of inner ears between different species.

As mentioned previously there are some differences in *bmp* expression between chick, mouse, and zebrafish. These data are summarised in Table 2.2. This table suggests greater similarity between zebrafish *bmp2b* and *BMP4* expression in chick and mouse. It also highlights the ability to ascribe *BMP*s to particular cell types in chick and mouse sensory patches unlike in zebrafish. *BMP* expression in chick, mice and *Xenopus* is described in more detail in Tables 2.3-5.

Table 2.2

Comparison of *bmp* expression in the inner ears of chick, mouse, *Xenopus laevis* and zebrafish.

The expression pattern of *bmp4*, *bmp7*, and *bmp7-related* are described in inner ears at similar developmental stages in the different organisms.

Domain of expression	Chick		Mouse	*Xenopus*	Zebrafish			
	BMP4	*BMP7*	*BMP4*	*BMP4*	*bmp4*	*bmp7*	*bmp7r*	*bmp2b*
Otic placode	+	+	+	+	-	-	+	+
Otic vesicle anterior + posterior	+	+[a]	+	+	+	+[b]	+	+
Cristae	+ sc	+[b] hc	+ sc	+	+	-	+	+
Maculae	+ sc	+[t]	+ sc	+	-	-	-	-
Basilar papilla/ cochlea	+ hc	+ sc	+ sc	?	na	na	na	na
Non sensory								
Canals	+[m]	+[e]	?	?	-	-	-	+
Ampullae	+	+	?	?	-	-	-	+

+ expression seen as structure differentiates
- no expression seen
sc support cells
hc hair cells
+[a] expressed throughout vesicle
+[b] expressed in subregion
+[t] transiently expressed
+[m] expressed in mesenchyme around canals
+[e] expressed in epithelium around canals
? expression not described
na structure not found in organism

2.3.6 Possible roles of *bmp* expression.

The BMPs are signalling molecules and as such could be acting in an autocrine way on the cells that secrete them, or in a paracrine fashion on other cells within the vesicle. If working in an autocrine manner, the BMPs could have positive or negative regulatory roles on the cristae. They could be important in initiating, or maintaining crista cell fate. During tooth development BMP4 has been shown to be required in generating mesenchyme competent to form teeth (St Amand et al., 2000). Alternatively they could be involved in inhibiting these cells from differentiation at all maintaining a population of hair and support cell progenitors, or preventing them from following a non-sensory or macula cell fate.

However, if they are working in a paracrine fashion, the relative concentration of a BMP signal as well as the distinct species of dimer could act as a lateromedial or anteroposterior axis determining concentration gradient. The BMPs have been shown to function in a concentration dependent manner in the patterning of the dorsoventral axis of different species including zebrafish (reviewed in Schier, (2001)).

The presence or absence of other essential members of the signal pathway will be important in regulating where the BMP signal can be interpreted. This and possible function of BMPs will be explored in more detail in Chapter 3.

2.3.7 The dorsal domain of *bmp4* expression marks the endolymphatic duct.

Until recently the existence of an endolymphatic duct in zebrafish had not been documented. However, the expression patterns of *bmp4* (this work), *dachA* (Hammond et al., in press) and histological studies (sections, and in paint fills (Bever and Fekete, in press) have demonstrated that this structure is present in zebrafish. This dorsal domain of *bmp4* expression will be described in more detail in Chapter 4 (4.3.2), documenting the early development of the endolymphatic duct.

2.3.8 *pax2.1*, *msxc*, and *brn3.1* are markers of different inner ear cell types.

Markers were used to identify what structures the *bmps* were expressed in. These markers are genes that have clear expression patterns in specific cells at specific times. In this case *pax2.1*, *msxc* and *brn3.1* mRNA probes were used.

pax2.1 is a member of the *pax2/5/8* subfamily of transcription factors (Pfeffer et al., 1998). Like the other members of this subfamily it is expressed in the developing inner ear and is the second member to be induced, expressed from 11hpf. Its initial domain of expression is wide. It is then restricted to and is maintained in hair cells at 24hpf and is induced in newly specified hair cells (Riley et al., 1999; Whitfield et al., in press). The *pax2.1* mutant *no isthmus* develops ectopic hair cells and it is thought that normal *pax2.1* is required to maintain normal levels of Delta-mediated lateral inhibition (Riley et al., 1999).

There are at least five *msx* genes in the zebrafish. The *msx* genes are the vertebrate homologues of the *Drosophila muscle segment homeobox* (*msh*) gene. *msxc* is expressed in the inner ear from 38hpf, just as the ventrolateral thickenings are visible, and is localised to these thickenings. Its expression can be followed in the cristae through their development (see Chapter 3 and Fig. 2.5F). Its expression is ablated in mutants known not to form cristae (Whitfield et al., 1996). It is therefore used as a marker of the cristae where it may be a transcriptional target of BMP signalling (see 3.6.4).

brn3.1 codes for a POU domain transcription factor expressed in hair cells in mouse and zebrafish (Erkman et al., 1996; Mowbray et al., 2001). Mutant mice with a deletion in the coding region of *Brn3.1* do not develop functioning hair cells (Erkman et al., 1996) but they do express at least one molecular marker, *Myosin VIIa*, and so hair cells do differentiate to some extent (Steel, 1998). In humans, mutations in *Brn3.1* (POU4F3) have been implicated in progressive sensorineural hearing loss (Vahava et al., 1998). Brn3.1 is therefore required in the differentiation of hair cells and their maintenance during life in mice and humans. It acts as a marker of differentiated hair cells in the inner ear and the lateral line of zebrafish (Mowbray et al., (2001), and data not shown) suggesting it may carry out a similar role in zebrafish. Interestingly other members of the Brn3 family are involved in the pathfinding of inner ear neurons (Brn3a (Huang et al., 2001)).

The following chapter describes where the other parts of the BMP signal pathway are expressed, and discusses where the BMP signal may be acting.

APPENDIX

Table 2.3 Chick *BMP* expression as in Oh et al., (1996); Wu et al., (1998)).

Gene	Age	Description of expression patterns
BMP7	E1.5 (8.5s)	expressed in otic placode
	E2 (21som)	dorsal+posterior of otic cup as invaginates
	E2.5 (st 16)	most of otic cup except ventral
	E4 (st 24)	all 7 presumptive sensory patches (BMP4+ve) within BMP7 domain except anteromedial part of mu.
	E5	entire bp positive sensory and nonsensory cells.
	E6.5	in bp restricted to similar domain as *BMP4*
	E8	bmp7 in periphery + in side wall of ampulla
	E12	expressed through entire bp epithelium (*BMP4* just in hc.)
	E16	bmp7 in bp restricted to sc remained at least until hatching. weak bmp7possibly in cristae (results not consistent.)
BMP5	E2 (st 13)	dorsal + posterior margins of otic cup
	E2.5 (st16)	expression on posterior rim of cup restricted to one focus (like *Bmp4*) also concentration on anterodorsal rim which disappears when otocyst formed.
	E3.5 (st22)	st22 E3.5 posterior stain goes (p.c,c,l,mn) strong exp in 1st branchial furrow until st24. This furrow will form external auditory meatus.
BMP4	st10	expressed in hindbrain rh3 +5
	st11 (E1.5)	as otic placode invaginates BMP4 broad posterior and dorsal domains in rim of cup and small ventral in ectoderm outwith otic epithelium rim of cup.
	E2.5 (st16)	a posterior focus and anterior streak
	st19	two foci at anterior and posterior, anterior streak replaced with single focus not sure streak becomes focus
	st20	medial domain that is presumptive sm posterior domain expands ventromedially
	st22/23	presumptive lateral cristae ampulla
	st24 (E4)	presumptive um appeared + broad domain btw sm + lc ampulla 7/8 presumptive sense organs identifiable
	E5	bmp4 in um very discrete
	E6	bmp4 discrete in m.neglecta in sc E7 gone byE12
	E7 (st27)	lc, um and sm, discrete areas of bmp4 presumptive bp + lagena continuous also in mesenchyme around ant +post canals. *BMP4* in cristae sc and in sc of sm + um
	E8	*BMP4* conc in sc except at periphery where span epithelium. Signal in ampulla weak E12 gone E16.
	st29	m.neglecta identifiable by *bmp4*
	st30	Above organs + bp and lagena are discrete entities now. Also in roof of ampulla, probably separate to pc staining
	E9	In bp hc concentrated by E12 still there E16 (BMP7 in sc) BMP4 gone from sm by E9 gone from um by E12.

Abbreviations: bp, basilar papilla; c, cristae; hc, hair cells; lc, lateral crista; pc, posterior crista; sc, support cells; sm, saccular macula; um, utricular macula

Table 2.4 *BMP* expression in Mice adapted from Morsli et al., (1998).

Gene	Age	Description
Bmp4	9dpc	placode invaginating bmp4 in posterior margin of otic cup.
	9.5	diffuse remains in posterior
	10.25	posterior signal becomes focus + anterolateral streak, independent of posterior
	11dpc	anterior stain the same, post expanded
	11.5dpc	posterior stain splits into dorsal spot + ventral streak = pc + lateral cochlea hybridisation signal (lco).
	12	ant streak splits into anterior and lateral focus = ac + lc. Still in pc. lco becomes complex around greater curviture of cochlea um appears marker by *Fng* not *BMP4*
	13dpc –15	Expression maintained in ac lc, pc and greater curve of cochlea
	16dpc	In support cells of cristae + um and sm (data not shown)
	P1	*BMP4* probably in presumptive Hensen's and/or Claudius' cells lateral to outer hair cells also exp in mesenchyme surrounding cochlea (previously reported in Takemura)

Abbreviations: ac, anterior cristae (superior cristae); lc, lateral cristae; pc, posterior cristae; sm, saccular macula; um, utircular macula.

Table 2.5 *BMP* expression in *Xenopus laevis* adapted from Kil and Collazo, (2001).

Gene	Age	Description
Bmp4	st25	posterior of placode
	st27/8	posterior stronger now in otocyst ventral stain too
	st28	first A stain now broad ventroposterior stain replaced with A and a smaller P foci. Cross sections show *BMP4* mainly lateral. A+P stain throughout otocyst stages (looked until st 35/36)
	st33	possibly in lateral line (just figure no detail in text)
	st45	all sense organs formed and exp *BMP4*. lc + pc strongest in both hc +sc. Weak in ac, um, and sm, couldn't say if in hc or sc.
Bmp7		domain larger than *bmp4* at placode and otocyst stages as in chick (data, not shown)

BMP4 but not *BMP2* also reported in otic vesicle of *Xenopus tropicalis* (Knochel et al., 2001).

Abbreviations: A, anterior, ac, anterior crista; hc, hair cells; lc, lateral crista; pc, posterior crista, sc, support cells; sm, saccular macula; um, utricular macula.

Chapter 3

Expression of downstream components of the Bmp pathway, Bmp antagonists and candidate target genes in the zebrafish inner ear.

3.1 INTRODUCTION

3.1.1 The BMP signalling pathway.

The BMPs are signalling molecules and as such require receptors and intracellular mediators to transduce their signal. The BMPs are members of the TGFβ superfamily and as mentioned in Chapter 1 they signal via type I and II serine threonine kinase receptors and members of the SMAD family (see Table 1.2, Fig. 1.8).

There are multiple levels of regulation of Bmp signalling. At the level of Bmp transcription, as shown in Chapter 2, these genes have dynamic expression patterns throughout development. Extracellular antagonists such as Chordin, Noggin and Follistatin bind to the Bmp dimers preventing them activating the receptors. At the level of entering the cell, the availability of receptors and differences in their affinities for the ligands controls how the dimers bind (ten Dijke et al., 1994). Intracellularly, inhibitory SMADs (iSmads) act to prevent transduction of the signal through the cell.

3.1.2 Known and putative targets of BMP signalling.

As described in Chapter 1, genes that are target of Bmp signalling have been described in other species. The iSmads have been shown to be targets of BMP signalling in murine cell lines (reviewed in Massague, (2000)). In the *Drosophila* wing disc, *spalt* is a direct target of the Bmp homologue Dpp (de Celis et al., 1996; Lecuit et al., 1996; Nellen et al., 1996). In mouse tooth and chick limb development *Msx1* and 2 are thought to be targets (Vainio et al., 1993; Pizette et al., 2001). During cardiogenesis BMP2 has been shown to regulate the expression of *cTbx2* and *cTbx3* (Yamada et al., 2000) and there is thought to be a regulatory

feedback loop between cTbx5 and BMP2 during the proximal distal outgrowth of the chick limb (Rodriguez-Esteban et al., 1999).

This chapter describes the otic expression patterns of members of this signalling pathway, including type I receptors, intracellular mediators (Smads), and antagonists. It also analyses the expression patterns of putative targets of Bmp signalling, *msxc*, *spalt* and *tbx2*. These data reveal sites where the Bmp signal could be received during inner ear development and suggest other sites of action.

3.1.3 Members of all levels of the Bmp pathway have been cloned in zebrafish.

In zebrafish seven Bmp receptors have been cloned. Five of these are type1 receptors; Alk8 (Yelick et al., 1998 and Mintzer et al., 2001); Thick veins and Tgfβr1 (M.Hammerschmidt unpublished); and Bmpr1A and 1B (Nikaido et al., 1999 and Nikaido et al., 1999). Two are type II receptors; ActIIa and b (Nagaso et al., 1999). Five members of the SMAD family have been cloned: two rSmads, Smad1 and 5 (Müller et al., 1999); two iSMADs, Smad 6 and 7; and the cSMAD Smad4 (M. Hammerschmidt unpublished and Dick et al., 2000).

In zebrafish three Noggin homologues (Nog1-3;Fürthauer et al., (1999)), one Chordin (Schulte Merker et al., 1997) and two Follistatin homologues (Bauer et al., (1998) and B. Thisse pers. comm.) have been described. One Spalt homolog (J.Wittbrodt pers. comm.) and five *msx* genes have been described in zebrafish (Akimenko et al., 1995; Ekker et al., 1997). *tbx2* was originally called *tbxc* (Dheen et al., 1999) and is one of six zebrafish Tbx genes that have been published (Ahn et al., 2000; Begemann and Ingham, 2000; Ruvinsky et al., 2000).

There may be more homologues of these genes yet to be discovered. However, all levels of the BMP signalling pathway are represented in the list above.

3.2 mRNA expression of Bmp type I receptors.

3.2.1 *bmprIB*

bmpr1B is expressed in the inner ear, initially widely at low levels from 18hpf (Fig. 3.1A bracket). It appears to be concentrated anteroventrally (Fig. 3.B arrow). At 27hpf this domain has become more distinct in the anterior and along the medioventral floor of the vesicle (Fig. 3.1C+D). The size of the domain is more restricted by 38hpf, and includes the anterior macula (Fig. 3.1E arrow). The domain extends up the medial wall of the vesicle including the posterior macula by 46hpf (Fig. 3.1F). The posterior macula staining is clearly seen in transverse sections of 48hpf embryos (Fig. 3.1G bracket). Its not clear if staining is restricted to the hair cells. The epithelial projections also express *bmpr1B* (Fig. 3.1G+H arrow). The posteromedial edge of the anterior macula continues to express *bmprIB* at 48hpf (Fig. 3.1 H white arrow).

3.2.2 *tgfβrI*

This is not expressed in the inner ear at 24 or 48hpf (Fig. 3.2). *tgfβrI* is one of the type one receptors associated with TGFβ signalling, not normally associated with BMP signalling.

3.2.3 *tkv*

thick veins (*tkv*) is expressed in the anterior and weakly in the posterior of the otic vesicle at 24hpf (Fig. 3.3A+B arrows). By 28hpf the posterior stain has been down regulated, but *tkv* is still expressed in the anterior (Fig. 3.3C arrow). At 48hpf the small anterior domain marks the anterior edge of the anterior macula (Fig. 3.3D arrow).

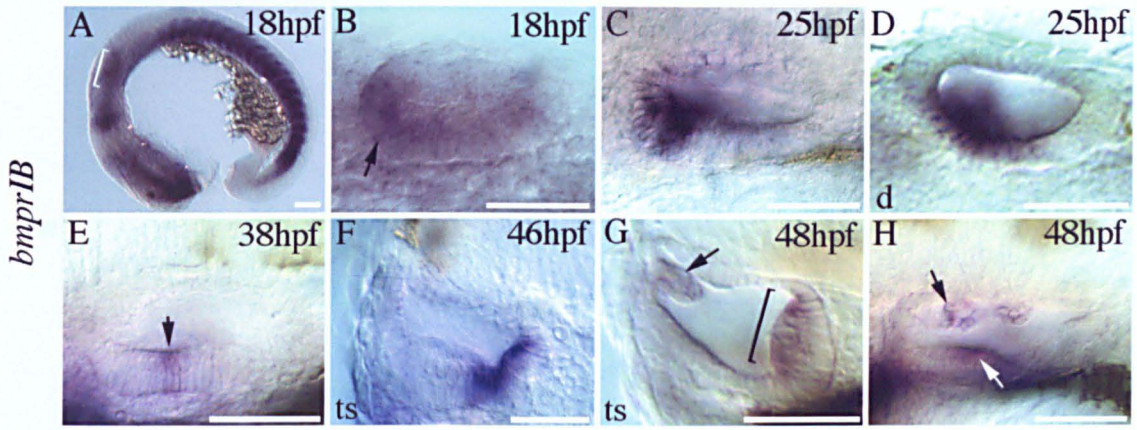

Figure 3.1 *bmprIB*

DIC images of whole mount in situ hybridisations. (A-C, E+H) lateral views, anterior to left dorsal to top; (D) dorsal view (d) anterior to left lateral to top; (F+G) transverse sections (ts), lateral to left. Scale bar =50 μm.

(A+B) *bmprIB* is expressed throughout the otic placode at 18hpf but is concentrated anteroventrally (bracket denotes placode in A). (C+D) At 24hpf expression is restricted anteroventrally and medially as shown in dorsal view (D). (E) At 38hpf in lateral views there is staining of 2-3 cells in the anterior macula, spanning the epithelium (arrow). (F) At 46hpf the staining stretches medially and dorsally up the posterior macula. Staining is still seen in the medial edge of the anterior macula. (G+H) At 48hpf it is expressed in the epithelial projections (black arrow), the medial edge of the anterior macula (white arrow) and the posterior macula (bracket). Its not clear if it is restricted to just the hair cells in the posterior macula.

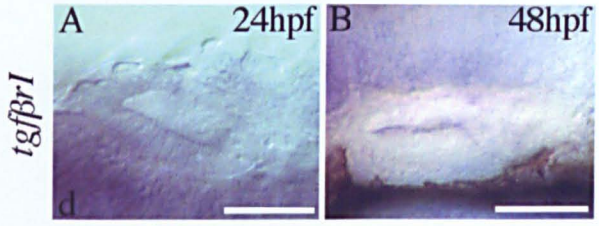

Figure 3.2 *tgfβrI*

(A) dorsal view, anterior to left, lateral to top; (B) lateral views, anterior to left, dorsal to top. Scale bar = 50 μm

(A+B) *tgfβrI* is not expressed within the otic vesicle at 24hpf or 48hpf.

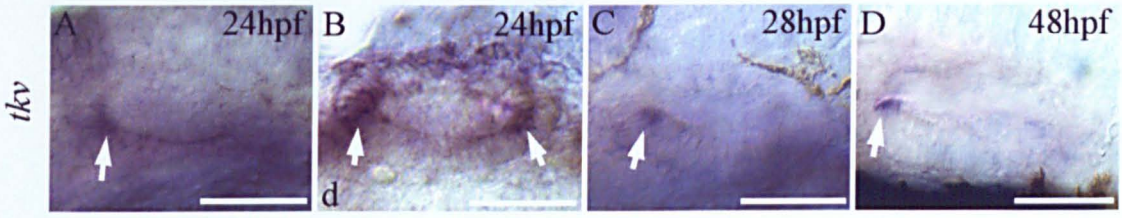

Figure 3.3 *thick veins*

(A, C-D) lateral view, anterior to left; (B) dorsal view, anterior to left, lateral to top. Scale bar =50 μm.

(A) *tkv* is expressed in the brain behind the otic vesicle. It is expressed strongly in the anterior (A, arrow) of the vesicle and weakly in the posterior (B, arrow). (C) At 28hpf the posterior stain has gone but staining persists in the anterior (arrow). (D) At 48hpf staining is restricted to the apical surface of a few anterior cells in the anterior macula (arrow).

3.2 The mRNA expression pattern of Bmp intracellular mediators.

Receptor specific Smads

3.3.1 *smad1*

From 24 to 48hpf, *smad1* expression is concentrated in the statoacoustic and lateral line ganglia (Fig. 3.4A-D white and black arrows respectively).

3.3.2 *smad5*

smad5 is not expressed in the otic placode at 18hpf (Fig. 3.5A bracket, B). It is weakly expressed throughout the head, including the otic vesicle at 24 and 48hpf (Fig. 3.5C+D, F-H). As with *smad1*, *smad5* is expressed strongly in the statoacoustic and lateral line ganglia (Fig. 3.5 C-I white and black arrows respectively). At 72hpf the ganglion expression persists as does low level expression in the otic vesicle, labelling cristae and SCC epithelium. The overall staining levels in the embryo head have dropped (Fig. 3.5I). Sense control in situ hybridisations did not show any staining (Fig. 3.5E).

Inhibitory Smads

3.3.3 *smad6*

smad6 is expressed laterally within the otic vesicle at 24hpf (Fig. 3.6A+B). It is expressed in the lateral edge of the vesicle until at least 72hpf being expressed in the cristae and SCC (Fig. 3.5E-J). At 72hpf it also appears to be expressed in the hair cells of the anterior macula (Fig. 3.6H arrow).

3.3.4 *smad7*

smad7 is not expressed at 24hpf in the otic vesicle (Fig. 3.7A). At 48hpf it is expressed in the dorsal roof of the vesicle and the epithelial projections (Fig. 3.7B+C).

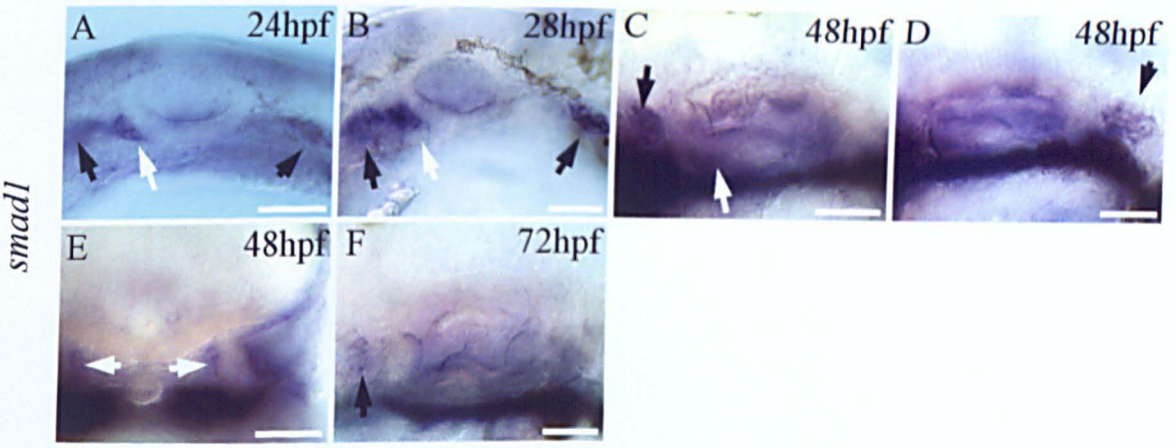

Figure 3.4 *smad1*
(A-D+F) lateral views, anterior to the left, dorsal to the top. (E) transverse section, dorsal to top. Scale bar=50 μm
(A-F) *smad1* is expressed in the statoacoustic ganglion (white arrows) and the anterior and posterior lateral line ganglion (black arrows) from 24hpf to 48hpf.

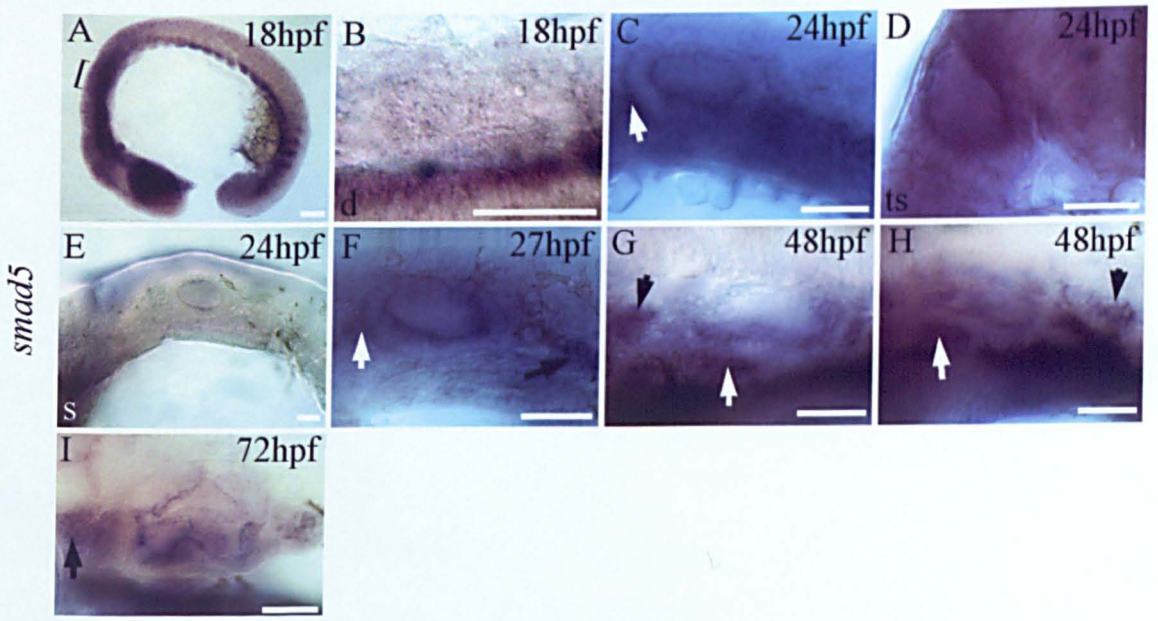

Figure 3.5 *smad5*
(A, C, E-I) lateral views, anterior to left dorsal to top; (B) dorsal view anterior to left, lateral to top; (D) transverse section, dorsal to top. Scale bar=50 μm.
(A+B) *smad5* is expressed through the brain at 18hpf but not in the otic placode.
(C+D, F-I) At 24hpf it is expressed at low levels throughout the otic vesicle. It is also concentrated in the statoacoustic ganglion (white arrows) and the anterior and posterior lateral line ganglion (black arrows). This pattern persists until at least 72hpf although ubiquitous staining levels drop. (E) sense *smad5* in situ hybridisations show no staining.

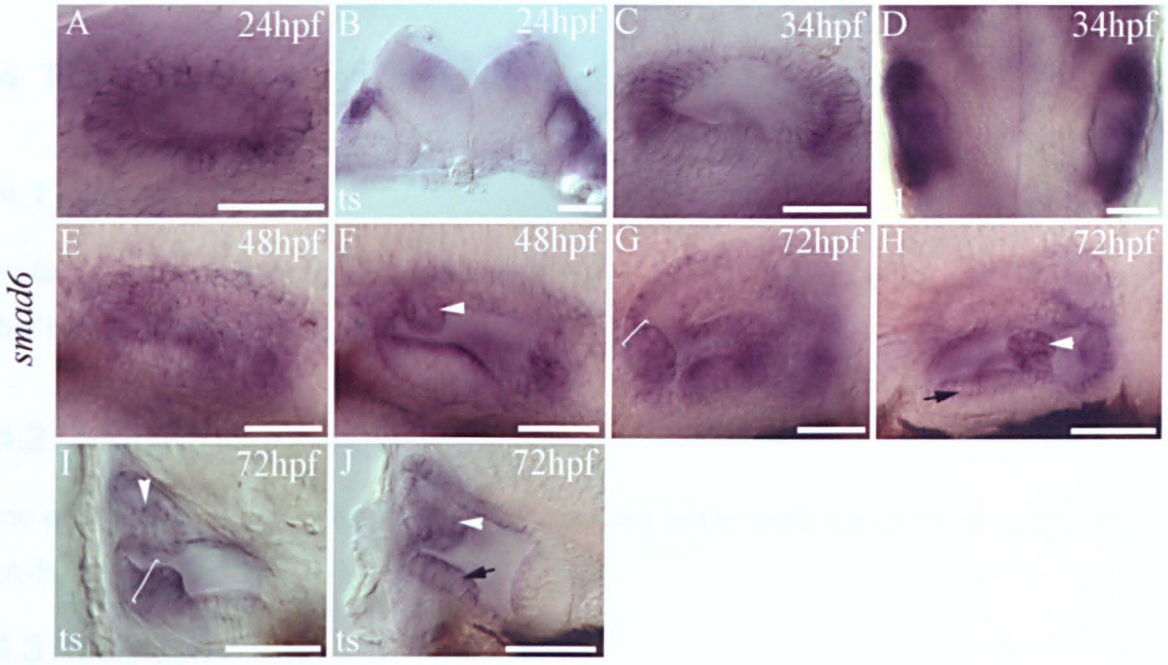

Figure 3.6 *smad6*
(A, C, E-H) lateral views, anterior to left; (B, I, J) transverse sections dorsal to top; (D) dorsal view, anterior to top. Scale bar=50 μm.
(A+B) *smad6* is expressed over the lateral surface of the otic vesicle. (C+D) At 34hpf this lateral stain is concentrated at the anterior and posterior ends of the vesicle. (E+F) At 48hpf the epithelial projections express *smad6* (arrowhead). (G, I+J) At 72hpf cristae *smad6* expression spans the epithelium (brackets). J= lateral crista. (H+I) The anterior macula expresses *smad6* weakly possibly just in the hair cells (arrow). (H-J) The epithelial projections still maintain strong expression (arrowhead), as does the dorsolateral roof of the vesicle although its not clear if this domain includes the putative ED.

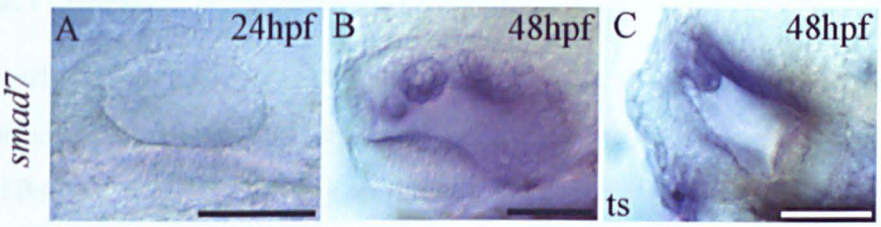

Figure 3.7 *smad7*
(A+B) lateral views, anterior to left; (C) transverse section, dorsal to top.
Scale bar=50 μm.
(A) *smad7* is not expressed in the otic vesicle at 24hpf. (B+C) It is expressed in the epithelial projections and the dorsal roof of the vesicle at 48hpf.

3.4 The mRNA expression patterns of Bmp antagonists.

3.4.1 *chordin*

chordin is not expressed in the inner ear at any of the time points examined: 18, 24 and 48hpf (Fig. 3.8A-C).

3.4.2 *noggin 1-3*

None of the three *noggins* examined are expressed in the inner ear at 24 or 48hpf (Fig. 3.9A-H).

3.4.3 *follistatin*

follistatin is expressed in mesenchyme surrounding the otic vesicle at 22hpf (Fig. 3.10A), and in a discrete posterior region of the inner ear epithelium from 24hpf until at least 48hpf (Fig. 3.10B+C, arrow).

3.5 The mRNA expression patterns of putative Bmp signalling target genes.

3.5.1 *msxc*

At early stages *msxc* is not expressed in the otic vesicle (Fig. 3.11A). At 38hpf *msxc* is expressed in three ventrolateral domains in the thickenings that will form the cristae (Fig. 3.11B+C). At 48hpf the cristae thickenings are more obvious and still express *msxc* (Fig. 3.11D). The stain spans the epithelium and shows the same expression pattern at 59hpf (Fig. 3.11E). At 72hpf a fourth domain of expression is seen dorsally. This domain of expression appears to be in the mesenchyme around the putative endolymphatic duct (Fig. 3.11F arrow).

3.5.2 *spalt*

spalt is not expressed in the otic vesicle at 24hpf (Fig. 3.12A). At 48hpf it is weakly expressed apically within the posterior macula in cells that appear to be hair cells

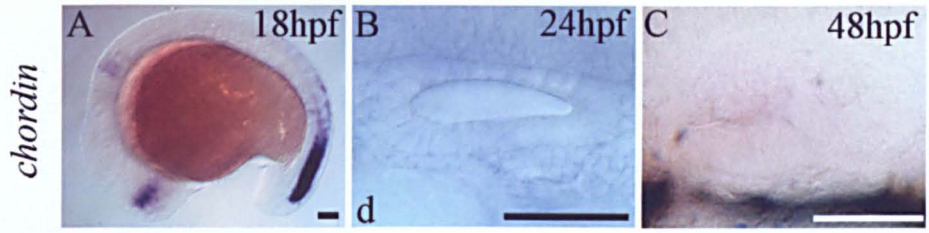

Figure 3.8 *chordin*
(A+C) lateral views, anterior to left; (B) dorsal view (d) anterior to left. Scale bar=50 μm.
(A) At 18hpf *chordin* is expressed in the tail and brain but not in the otic placode.
(B+C) *chordin* is not expressed in the otic vesicle at 24hpf or 48hpf.

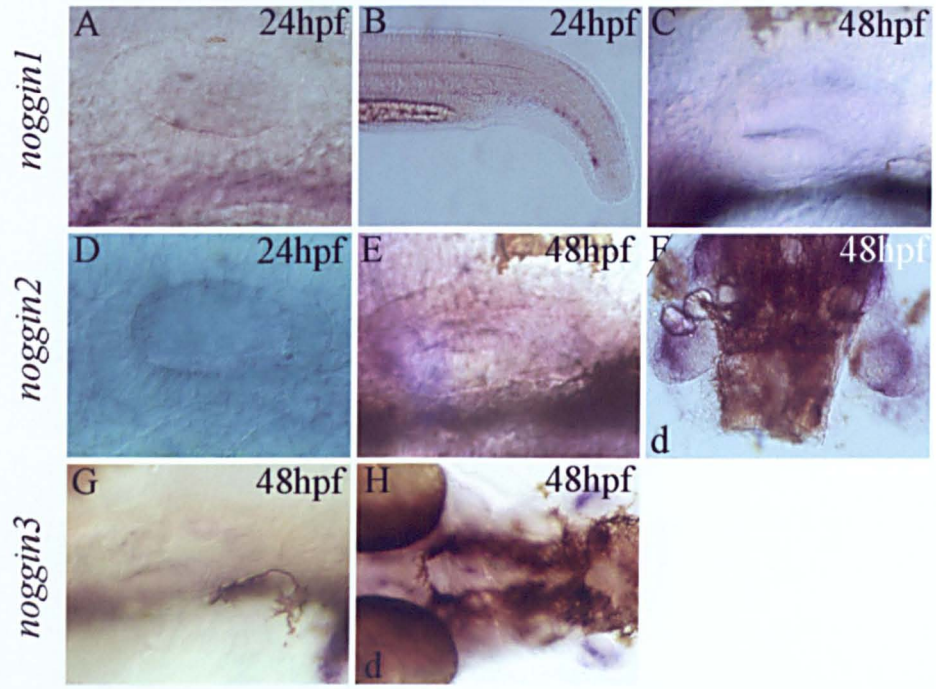

Figure 3.9 *noggins*
(A-E, G) lateral views, anterior to left; (F+H) dorsal views, (d) anterior to top in F, to left in H. Scale bar=50 μm
(A, C) *noggin1* is not expressed in the otic vesicle at 24hpf or 48hpf. (B) It is expressed in ventral aspect of caudal somites at 24hpf as previously reported (Fürthauer et al., 1999).
(D+E) *noggin2* is not expressed in the otic vesicle at 24hpf or 48hpf. (F) It is expressed in the pectoral fins as is *noggin3* (H). (G) *noggin3* is not expressed in the otic vesicle at 48hpf, the earliest any *nog3* stain has been reported (Fürthauer et al., 1999).

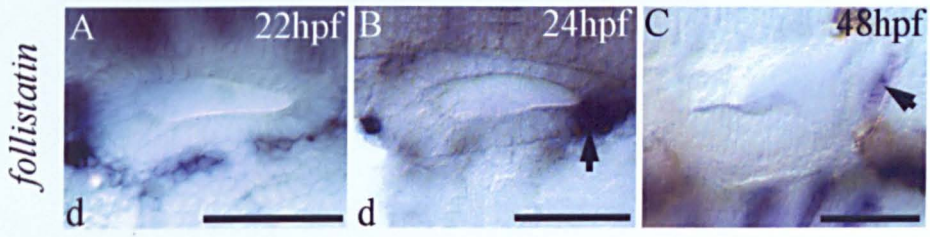

Figure 3.10 *follistatin*
(A+B) dorsal views, anterior to left; (C) lateral view, anterior to left. Scale bar=50 μm.
(A) *follistatin* is expressed in the mesenchyme around the otic vesicle at 22hpf. (B) At 24hpf it is expressed within the otic vesicle at the posterior end (arrow). (C) At 48hpf it is expressed in a small region of posterior otic epithelium (arrow). It does not localise to any thickenings.

(Fig. 3.12C bracket). It is also expressed in a group of cells medial to the otic vesicle, adjacent to the posterior macula (Fig. 3.12C+D arrow). These cells may be the statoacoustic ganglion, which is positioned medially at this stage (Haddon and Lewis, 1996). *spalt* is still expressed in these areas at 72hpf (Fig. 3.12F+G, bracket and arrow).

3.5.3 *tbx2*

tbx2 is expressed throughout the otic placode at 18hpf (Fig. 3.13A+B) and the early otic vesicle (Fig. 3.13C+D). At 48hpf it is expressed in the epithelial projections, the dorsal roof of the vesicle and the hair cells of all the sensory patches (Fig. 3.13E-H). At 72hpf levels of expression have dropped dramatically. Low level expression in the hair cells may remain (Fig. 3.13I-K).

Figure 3.11

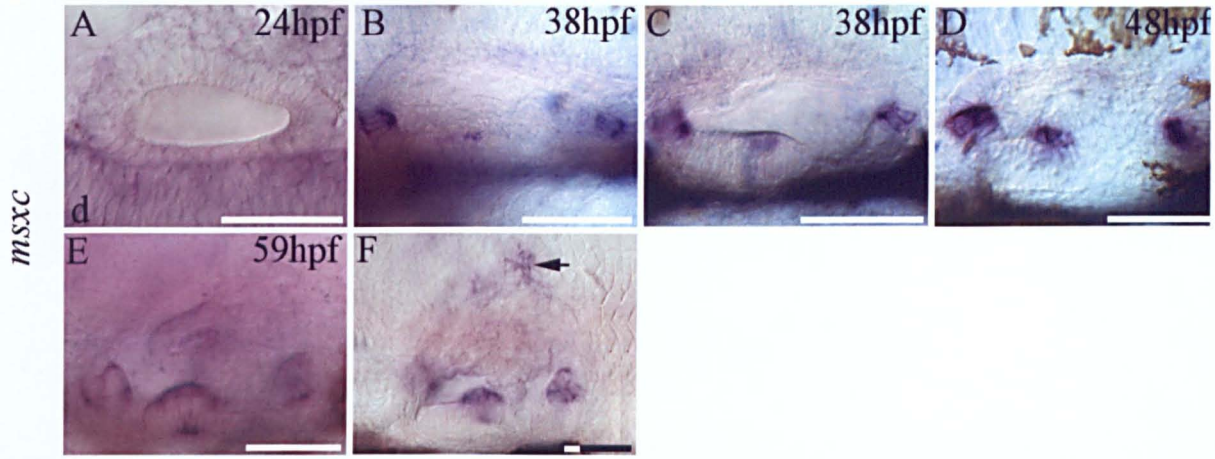

Figure 3.12

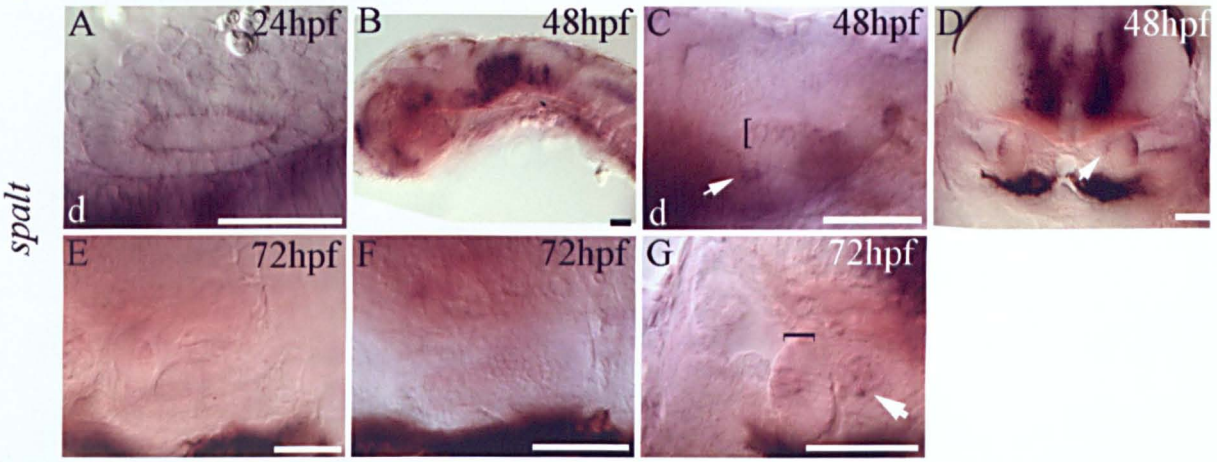

Figure 3.13

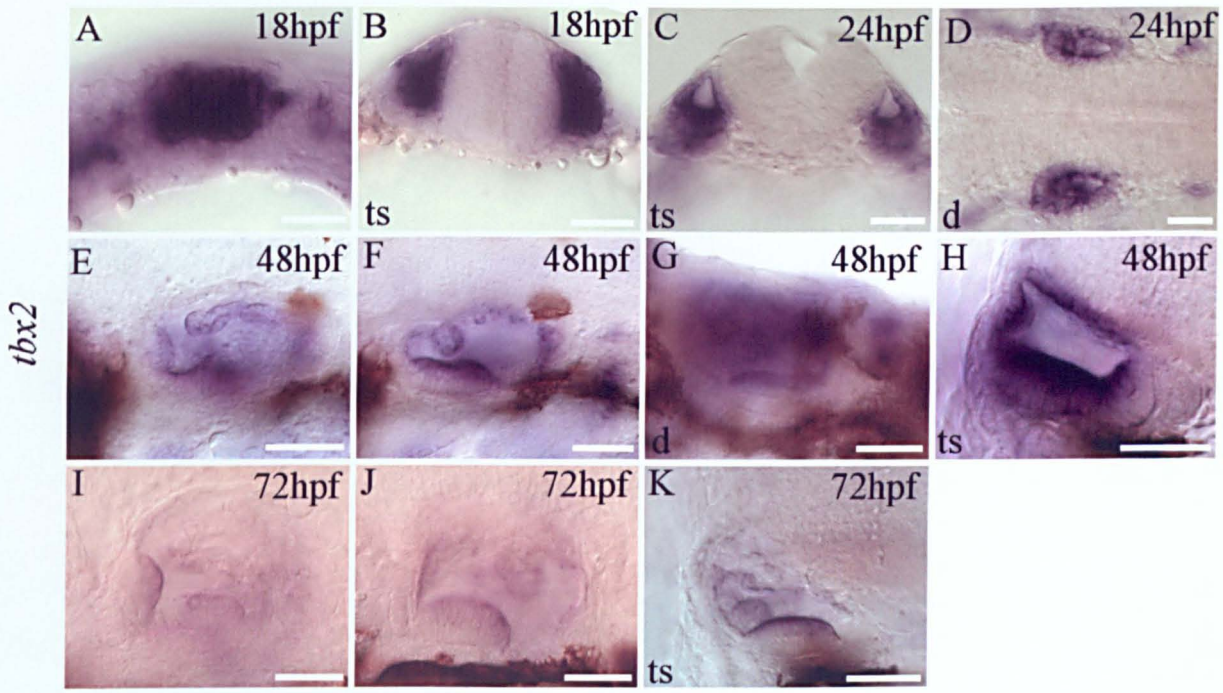

Figure 3.11 *msxc*

(A) dorsal view, anterior to left; (B-F) lateral views, anterior to left. Scale bar=50μm.

(A) *msxc* is not expressed in the otic vesicle at 24hpf. (B+C) At 38hpf it is expressed in three ventrolateral domains; these domains span the epithelium and prefigure the appearance of crista thickenings. (D+G) This staining persists at 48 and 59hpf as the crista thickenings differentiate. (H) At 72hpf a new dorsal area of expression appears (arrow). This domain appears to be in the mesenchyme around the structure labelled by *bmp4* (see Chapter 4 section 4.5.1).

Figure 3.12 *spalt*

(A+C) dorsal views, anterior to the left; (B, E, F) lateral views, anterior to left; (D, G, H) transverse sections, dorsal to top. Scale bar=50μm.

(A) *spalt* is not expressed in the otic vesicle at 24hpf. (B-C) At 48hpf it is expressed strongly in the brain and weakly in the posterior macula hair cells (bracket) and the statoacoustic ganglion (arrow). (E-H) This pattern is still seen at 72hpf.

Figure 3.13 *tbx2*

(A, E, F, I+J) lateral views, anterior to left; (B, C, H+K) transverse sections, dorsal to top; (D+G) dorsal views, anterior to left. Scale bar=50μm.

(A-D) *tbx2* is expressed strongly throughout the otic placode at 18hpf and the otic vesicle at 24hpf. (E-H) At 48hpf it is expressed in the epithelial projections and the hair cells of the anterior and posterior macula. (I-K) At 72hpf expression levels have dropped; faint stain is still seen in the anterior macula.

3.6 DISCUSSION

This chapter documents the expression of all the known members of the Bmp signalling pathway during inner ear development. Together with other published expression patterns, this work demonstrates that all levels of the signalling pathway are represented during inner ear development and reveals possible sites of Bmp action. The expression of the Bmp type 1 receptor suggests a medial role, while the expression of putative targets also suggests the cristae and posterior macula as sites of action. The expression of *spalt* in the posterior macula suggests it could be downstream of *bmpr1B* activation by the Bmps (see Table 3.1).

However, the main caveat to this work is that it only describes where these genes are expressed and can only provide clues as to where they may be acting. It is not clear how far the BMPs can signal, or whether the right receptors are expressed to receive these signals in the cristae or more dorsal areas.

Table 3.1 Summary of inner ear expression of members of Bmp pathway.

Region of inner ear where expressed	Gene expressed
Whole otic placode	*smad5*, *ActIIa* and *b* (type II receptors), *tbx2*
Anterior and posterior of otic vesicle	*bmp2b*, *bmp4*, *bmp7r* *bmprIB* *tkv* (possibly overlaps with Bmps)
Posteroventral otic vesicle	*bmp7* *follistatin* (possibly overlaps for some stages)
Lateral line and statoacoustic ganglia	*smad1*, *smad5*, *spalt* (statoacoustic)
Medial wall of otic vesicle	*bmprIB*, *tbx2*, *spalt* (hair cells of posterior macula)
Ventrolateral otic vesicle	*bmp2b*, *bmp4*, *bmp7r*, *msxc*, *tbx2*, *smad5*, *smad6*
Epithelial projections	*bmp2b*, *bmprIB*, *smad5*, *smad6+7*, *tbx2*.
Dorsal projection (putative Endolymphatic duct)	*bmp4* (epithelium), *msxc* (mesenchyme) (*dachA*, epithelium)

For details of the expression data see results sections of Chapters 2+3.

3.6.1 All levels of the Bmp signalling pathway are expressed in the inner ear during its development.

In order to function, if the current model for BMP signalling is correct, the BMPs require a type I +II receptor and the presence of members of the SMAD family. This chapter shows that two type I receptors and one of the rSMADs, Smad5 is expressed widely within the

developing inner ear. Previous work has shown that cSmad4 and two activin type II receptors are expressed ubiquitously in the embryo at 24hpf, the latest stage examined in these reports (Nagaso et al., 1999; Dick et al., 2000). It is possible that there are other receptors expressed in the otic vesicle. The distinct domains of putative BMP targets genes suggests other sites of BMP action which would require the expression of receptors in patterns not described here.

3.6.2 Controlling Bmp action.

The low-level widespread expression of *smad5* from 24hpf suggests that all the cells within the otic vesicle are capable of responding to Bmp signals. Therefore control of Smad5 activation is occurring at different levels within the pathway.

The expression of receptors.

The type I receptors have distinct restricted domains of expression. *bmpr1B* is initially widely expressed but is then restricted to the medial wall of the vesicle including the posterior macula. This expression domain does not appear to match that of the *bmps* at similar stages. However, at early stages *tkv* is expressed in similar domains to those of the *bmps*, the anterior and posterior ends of the vesicle. This matching expression pattern is not seen at later stages when *tkv* is restricted to only the anterior edge of the anterior macula. The Bmps are secreted ligands and therefore their receptors do not have to be coexpressed with them to be activated (see 3.6.3).

It is not known if *bmprIB* has a greater affinity for a particular Bmp in zebrafish. However, in vitro BMP7 has been shown to bind to a BMPRIB homologue with higher affinity than BMPRIA (ten Dijke et al., 1994). The affinities of the different receptors are affected by different combinations of type I and type II receptors (Yamashita et al., 1996). The affinities of the other type I receptor, *thick veins*, are also not clear.

The presence of inhibitors

The expression of inhibitors of Bmp signalling within the vesicle is dynamic, suggesting that the control of Bmp signalling is important to ensure the correct development of the inner ear, not just in specific regions, but at specific times. Both extracellular (Follistatin) and intracellular (Smad6 + Smad7) controls are present. Follistatin has a very restricted

pattern in the posterior of the vesicle. This could reduce Bmp signalling within that area, depending on how far Follistatin can diffuse.

The two iSmad proteins can both inhibit Bmp signalling by binding to the type I receptor (Imamura et al., 1997; reviewed in Massague, (1998)). Both of these iSMADs are also expressed in response to Bmp signalling suggesting a negative feedback pathway is moderating levels of Bmp signalling (reviewed in Massague and Chen, (2000)). This feedback loop could be responsible for the late expression of *smad7*, which is not seen in the otic vesicle at 24hpf, when *bmp* expression is already established but is expressed at 48hpf. *smad6*, on the other hand, is expressed strongly from 24hpf and so could be regulating early responses to Bmp signals.

3.6.3 The range of Bmp signalling.

The surprising result obtained in this chapter was the strong expression of *bmpr1B* in the medial wall of the otic vesicle. This suggests the Bmps could be acting at some distance from their strong ventrolateral sources of expression. The Bmps are signalling molecules and have been shown to work as long range signals. In *Xenopus*, studies have tracked Bmp signalling over 10-20 cells (Dosch et al., 1997; Cui et al., 2001). However, how this signal moves is not understood (see 1.4.4). At early stages the *bmprIB* expression domain is close to that of the *bmps*. However, by 42hpf, the vesicle has expanded. If the Bmps are secreted into the extracellular matrix they could diffuse through the fluid in the lumen of the vesicle rather than being passing over the ventral floor. Antibody stains for the Bmp protein would be useful in tracing the path of these proteins.

The lack of a type I receptor expressed within the cristae does not rule out the possibility of Bmps acting in the crista cells they are expressed in. Given the general trend in zebrafish to have multiple members of the same family it is possible that more receptors will be cloned. They may be expressed in the otic vesicle, possibly in domains including the cristae.

3.6.4 Possible targets of Bmp activity.

The direct targets of Bmp signalling are not conclusively known in zebrafish. However, as discussed above (3.1.2), they have been identified in other species (1.4.5). This section

considers four possibilities: the Bmps themselves, *msxc*, the zebrafish *spalt* homologue and *tbx2*.

Bmps

Early in development, studies using *swirl* (*bmp2b*) mutants have shown that the initiation and maintenance of early *bmp4* and regions of *bmp2b* expression require functional Bmp2b (Kishimoto et al., 1997). As described in Chapter 2, *bmp2b* and *bmp7r* are expressed before *bmp4* within the otic vesicle and then from 24hpf *bmp2b*, *bmp4*, and *bmp7r* are expressed in very similar domains. Therefore an early function of *bmp2b* could be to initiate *bmp4* expression within the vesicle, with a later autocrine role maintaining its expression. However, the normal expression of *bmp4* in the inner ears of rescued *swirl* embryos suggests that at later stages *bmp4* expression is not reliant on Bmp2b (see Chapter 6).

tkv is expressed at the anterior and posterior ends of the vesicle at 24hpf in a pattern reminiscent of *bmp2b*, *bmp4*, and *bmp7r*; therefore it is possible that one of these *bmps* is responsible for initiating or maintaining the expression of the others using this receptor.

Studies in the chick have provided evidence for a feedback loop regulating BMP expression in the inner ear. Noggin (Bmp antagonist) coated beads implanted around the developing inner ear lead to the upregulation of BMP4 expression in the mesenchyme around the bead and in the SCC epithelium (Chang et al., 1999; see 5.1.5). This loop has also been found in other structures. In the chick limb it is suggested that BMP4 protein normally reduces the levels of *bmp4* expression (Capdevila and Johnson, 1998; Pathi et al., 1999). However, in the mouse BMP4 protein is thought to upregulate *Bmp4* expression via *Msx1*, as part of the epithelial-mesenchymal interactions that occur during tooth development (Vainio et al., 1993; Chen et al., 1996). None of the zebrafish Bmps are expressed in the mesenchyme; however, *bmp2b* is expressed in the SCC. Therefore it is possible that aspects of this loop are found in zebrafish and Bmp2b regulates its own expression in the SCC.

Msxc

In the mouse application of ectopic BMP4 protein can induce the expression of *Msx1* and *2* in dental mesenchyme (Vainio et al., 1993). There is also evidence from chick work that inhibiting BMP4 signalling by implanting *X*Noggin coated beads leads to the down regulation of *Msx1* expression in SCC epithelium (Chang et al., 1999).

Msx1 is expressed in the developing chick inner ear (in the 3 cristae, lagena, macula neglecta, posterior part of the papilla, some portions of the SCC and a dorsal area that gives rise to endolymphatic duct (Wu and Oh, 1996)) suggesting it is important during inner ear development. However, there appears to be conflicting evidence from mutant studies about the role of *Msx* in inner ear development. *Msx1* mutant mice have an abnormality in their middle ear, not their inner ear (Satokata and Maas, 1994), due to problems in branchial arch development. In contrast Goldenhar's syndrome in humans, which may be due to a defect in Msx (Scholtz et al., 2001), results in deafness due to both conductive and sensorineural defects i.e. both the middle and inner ear are malformed. In the inner ear of Goldenhar's syndrome patients, the SCC are affected, which are normally sites of *Msx* expression in chick (Wu and Oh, 1996).

The zebrafish have 5 *msx* genes (*A-E*), three of which have previously been described as being expressed in the developing inner ear (*msxc* and *d* (Ekker et al., 1992) and *msxe* (Ekker et al., 1997). These genes are not thought to be orthologues of the mouse and chick Msx1 and 2. They are more closely related to murine *Msx3*, which appears to be the common ancestor related to *muscle segment homeobox* gene (*msh*) in *Drosophila*, that has been duplicated independently in zebrafish compared to mouse and chick (Ekker et al., 1997). Although these proteins are not orthologues they may have similar functions through subfunctionalisation (Force et al., 1999). Here, the functions of an ancestral gene are divided up amongst different members of the orthologous gene following genome duplication.

Both *msxd* and *msxe* are reported to be expressed in the inner ear dorsally at 24hpf and *msxd* is expressed in the cristae at 48hpf (Ekker et al., 1992; Ekker et al., 1997). *msxc* is also expressed in the cristae (Ekker et al., 1992) and the work described in this chapter characterises its inner ear expression pattern in more detail. *msxc* is expressed after the *bmps* in a ventrolateral pattern. This is as expected if *msxc* is a target of Bmp signalling. If *msxc* is a target, it suggests that the Bmps have an autocrine role, affecting the development of the cells in which they are expressed. At later stages *msxc* is also expressed around the dorsal *bmp4* domain although it is coming on at a time when *bmp4* expression is fading from this area (see 3.7.4).

However, other results obtained during this thesis argue against Bmp4 directly inducing the expression of *msxc*. The implantation of hBMP4 beads around the developing inner ear did not induce the ectopic expression of *msxc*. This result is discussed in detail in 5.6.4.

Spalt

The murine homologue of the *Drosophila* gene *spalt*, *msal*, is expressed during inner ear development. It is expressed ventromedially within the otic vesicle from 11dpc (Ott et al., 1996). This area gives rise to the neurons of the inner ear, the organ of Corti and the utricular and saccular maculae (see Ott et al., (1996) and references therein). The statoacoustic ganglion also expresses *msal* from 11dpc. At 14dpc it is expressed in the cochlea but no longer in branches of the acoustic ganglion. In the newborn mouse it is detected in the organ of Corti in the epithelial ridge that forms hair cells and in the cristae (Ott et al., 1996). The zebrafish homologue is not as widely expressed at early stages, although at later stages it is expressed in a subset of the domains seen in the mouse, the hair cells of the posterior (future saccular) macula, and the statoacoustic ganglion. It is not expressed in these structures during their earliest stages i.e. when the neurons are delaminating to form the ganglion or when the first hair cells are forming in the posterior macula (around 24hpf). The time scale of expression matches the medial expression of *bmprIB*, and so provided the Bmp signal can reach this receptor, *spalt* may be a target of Bmp signalling via BmprIB.

Tbx2

As mentioned in the introduction to this chapter, in other systems Tbx genes have been induced by Bmps. However, the expression pattern of *tbx2* during zebrafish inner ear development argues against a similar relationship in the inner ear. It is strongly expressed at a stage before the majority of Bmps are expressed. It remains strongly expressed until 72hpf when the expression of the Bmps is also starting to fade. Unless the Bmps are required to maintain its expression it seems unlikely that there is any direct relationship between Tbx2 and the Bmps.

3.6.5 Differences between species.

In the chick, *Noggin* is expressed in tissue around the otic cup for a short period and then it is expressed weakly in the ventral tip of the cochlear duct (Chang et al., 1999). In

zebrafish, no *noggin* is expressed in the developing vesicle, but *follistatin* is expressed around the vesicle and then in a restricted posteroventral domain. Both of these antagonists are capable of binding all the Bmps and so could both act as sinks for Bmp signalling.

The murine *BmprIB* homologue is also expressed in the developing otic vesicle. *BmprIB* is expressed in cells lining the saccule, cochlea, and the SCC (12.5dpc)(*alk6=Bmpr-IB* (Dewulf et al., 1995)). No hair cell expression is mentioned; however, this paper does not present a detailed examination of otic expression. Both the mouse and zebrafish homologues are expressed in the SCC.

These two examples may reveal how different proteins can perform the same function in different species (Noggin+Follistatin) and that homologues can perform conserved functions between species (BmprIB).

3.7 Possible roles for the Bmps during inner ear development.

3.7.1 Role in crista development.

Early roles – induction/maintenance of cristae fate

As briefly mentioned in the previous chapter, the Bmps could have a role in establishing crista cell fate. BMP signals may be required to specify crista fate. The data in this chapter do not rule out such a role. There is a type I receptor which appears to be expressed initially in the correct domains (*tkv*, anterior and posterior of vesicle). However, this receptor is then expressed in the anterior macula, one of the other possible fates for cells in the anterior quadrant of the vesicle, and its posterior expression is transient. This may just mean another receptor not yet examined could be expressed correctly (e.g. *bmprIA*), or that the requirement for Bmp signalling is transient. Alternatively the Bmps are not associated with establishing a crista fate.

Later role-crista differentiation

The expression of *msxc* within the ventrolateral thickenings appears just after that of *bmp2b*, *bmp4*, and *bmp7r*. At subsequent stages all four genes are strongly expressed in the differentiating cristae. Again, although there is no receptor reportedly expressed in the cristae it is still possible that these *bmps* are inducing *msxc* expression here.

The *msx* genes are homeobox-containing transcription factors and as such control cell fate by regulating the expression of other genes. As with the Bmps, direct transcriptional targets are not known; however, Msx homologues have been implicated in controlling proliferation and cell death in limb and neural crest, regulating epithelial-mesenchymal interactions during tooth and limb development and in preventing differentiation by maintaining proliferation (reviewed in Davidson, (1995); Bendall and Abate-Shen, (2000)). The cells in the cristae have to form a thickened epithelium, which then gives rise to two cell types to form a pseudostratified epithelium containing hair cells and support cells. Therefore cell divisions and cellular rearrangements are required. However, there is no evidence for interactions between the epithelium and underlying mesenchyme or for *msxc* areas to be associated with concentrated areas of cell death or proliferation.

Does the presence of inhibitors rule out a role in crista development?

The strong lateral expression of *smad6* in the developing vesicle including the cristae does not rule out a role for the Bmps in crista development. As mentioned above, *smad6* is induced by Bmp signal. Perhaps the Bmps themselves induce *smad6* expression to moderate rather than completely inhibit the strong lateral signal from the cristae. The broad lateral expression of the *ismads* may allow the refining of the Bmp signal to a narrower region see Fig 3.14 below. Therefore high levels of Bmp signal are required to specify cristae and express *msxc*.

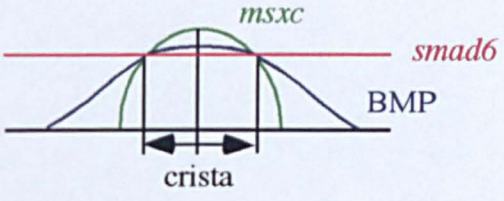

Figure. 3.14 Model of crista specification
The uniform level of *smad6* expression ensures that *msxc* is only induced at the highest level of Bmp signalling.

Conclusion- cristae role

The putative Bmp targets *msxc* and *smad6* are expressed in the presumptive cristae. The timing and position of *msxc* expression corroborates with it being a target of BMP signals. Results discussed in Chapter 4, in which mutants lacking *bmp* expression lack *msxc* expression, support this conclusion. However, the addition of ectopic hBMP4 did

not induce ectopic *msxc* expression or rescue it in mutants (Chapter 5). This is discussed further in Chapters 4 and 5.

3.7.2 Role in the development of the medial wall of the otic vesicle.

Early role-medial wall

Another area of possible Bmp signal action is the anterior ventromedial wall of the otic vesicle. From early stages the expression domain of the *bmprIB* receptor is expressed adjacent to the expression domains of *bmp2b*, *bmp4*, and *bmp7r*. So it is possible that these *bmprIB* expressing cells could be receiving Bmp signals. These signals could be important for specifying the fate these cells will follow. Cells from the ventral region of the otic vesicle, which may include the *bmprIB* domain, delaminate to form the statoacoustic ganglion between 22-30hpf (Haddon, 1997).

Later role - medial wall

At later stages the vesicle has expanded and it is not clear how the laterally expressed Bmps reach the medially expressed *bmprIB* as discussed above. However, the expression of *spalt* in the posterior macula and ganglion could be a result of the Bmp activated BmprIB receptor. The ganglion expression of *spalt* may also be due to an early Bmp signal received when the cells are delaminating.

In *Drosophila, spalt* and *spalt-related* are required to form a particular subset of macrochaetae (mechanoreceptor sense organs, consisting of a hair, socket, nerve and sheath) and to position veins in the wing. No downstream targets are known; however, they appear to be involved in specifying cell types (de Celis et al., 1999; Elstob et al., 2001). The human Spalt homologue, SAL1, is mutated in patients with Townes-Brocks Syndrome. One of the defects associated with this syndrome is malformation of the external ear and sensorineural deafness. The cause of the sensorineural deafness is not understood (Kohlhase, 2000).

None of the inhibitors of Bmp signalling are expressed medially. The lateral position of the source of Bmp signal suggests any signal will be weaker medially compared to laterally during normal development. This reduced level of signal may be sufficient to induce *spalt*. Interestingly, in *Drosophila*, Hedgehog (Hh) signalling induces *spalt*, in both Dpp independent and dependent pathways in the thorax. The midline is a strong source of Sonic

Hedgehog (Shh) (a Hh homologue) in the zebrafish and this signal may also be important in activating *spalt* that is expressed medially i.e. the part of the otic vesicle closest to the midline.

Conclusion- medial wall

The putative Bmp target *spalt* is expressed in the developing otic vesicle. It appears to label differentiated hair cells and delaminated neurons in the statoacoustic ganglion. *spalt* may be induced by low level Bmp signalling via the BmprIB receptor. Activation of *spalt* may also require Shh. It would be interesting to monitor *spalt* expression in mutants lacking *bmp* expression or with reduced Shh signalling. The addition of ectopic BMP4 did affect the development of the medial wall (see Chapter 5).

3.7.3 Role in semicircular canal development.

The *smad6* expression pattern at 72hpf is similar to that of *bmp2b* (compare Fig. 3.6I and Fig. 2.5K). *smad7* is also expressed in the epithelial projections although it preferentially inhibits Activin and TGFβ over Bmp signalling and it is normally not active unless stimulated by TGFβ signalling (reviewed in Massague and Chen, (2000)). The expression domains of these iSmads suggest control of the Bmp signal is required in forming the SCC. None of the putative targets analysed here are expressed in the SCC suggesting there is no need for Bmp2b in forming the SCC. However, work described in Chapter 6 demonstrates that *bmp2b* is required to form adult SCC.

3.7.4 Development of a zebrafish endolymphatic duct.

As well as the cristae domains *msxc* is also expressed dorsally within the otic vesicle. This dorsal domain is where the putative endolymphatic duct is thought to develop in zebrafish (see 4.5.1). This domain of expression is further support of an association between *bmp4* and *msxc* expression.

As with the ventrolateral domains *bmp4* is expressed well before *msxc* in dorsal regions. The third ventrolateral domain of *bmp4* appears at around the same time as the dorsal domain (~27hpf). However, *msxc* is not expressed dorsally until 72hpf, when *bmp4* expression levels are starting to fall. This could be due to the levels of Bmp signalling being less compared to the ventrolateral domains, where three Bmp homologues are

expressed together. It could therefore take longer for a threshold of Bmp signal to be reached. The iSmads may also be expressed in this dorsal domain, and therefore *msxc* induction may require high levels of Bmp signal to accumulate. Alternatively the relationship is not direct or it is inhibitory requiring a lack of Bmp signals to allow *msxc* induction.

In the chick, *Msx1* is reported to be expressed in the dorsal portion of the otocyst which gives rise to the endolymphatic duct (Wu and Oh, 1996). This expression is possibly under the control of *BMP7* (Oh et al., 1996) as it remains unresponsive to reduced endogenous BMP4 signalling through the application of antagonist-coated beads (Chang et al., 1999).

Conclusion- endolymphatic duct.

In the cristae both *bmp4* and *msxc* are coexpressed in the epithelium. However, in the dorsal domain *bmp4* is expressed in the duct epithelium while *msxc* appears to be in the surrounding mesenchyme. The pattern of *bmp4* in one tissue and *msxc* in another is what is normally seen in other systems, e.g. tooth development (see 1.4.3).

CHAPTER 4

BMP expression in inner ear mutants.

4.1 INTRODUCTION

4.1.1 Inner ear mutants provide genetic tools to uncover the role of BMPs.

The previous two chapters documented the expression of *bmps* and members of their signalling pathway during inner ear development. These data suggest the *bmps* may act on the cristae, the semicircular canals (SCC), and the medial wall of the otic vesicle. Work in the chick, discussed in more detail later, has led to speculation that the BMPs are involved in SCC development ((Chang et al., 1999; Gerlach et al., 2000) and see Chapter 5). It seemed reasonable, therefore, to investigate what happens to *bmp* expression in zebrafish which have abnormal cristae and SCC.

As mentioned previously (Chapter 1) numerous mutants with inner ear defects were identified based on morphology (examining SCC development, the presence of otoliths and general size of the otic vesicle) (Malicki et al., 1996; Whitfield et al., 1996). Other mutants in these large-scale screens where found to have inner ear defects, although they had originally been described through other defects, e.g. *colourless* (a pigmentation mutant (Kelsh et al., 1996)) and *swirl* (a mutant affecting dorsoventral patterning (Mullins et al., 1996)). From these screens three mutants were chosen (*dog-eared*, *van gogh*, and *colourless*) which have obvious inner ear phenotypes in specific structures thought to arise from *bmp* expression domains (cristae and SCC). Examining *bmp* expression in these mutants would reveal if *bmp* signalling is also abnormal. If the expression is normal, *bmps* are not sufficient to form cristae and SCC; if expression is absent, *bmps* may be required for the correct development of these structures.

A fourth mutant, *valentino* (*val*), was chosen from another ENU screen (Moens et al., 1996), to investigate the dorsal domain of *bmp4* expression specifically. This domain is thought to mark the endolymphatic duct (ED). The *val* mutant is the zebrafish equivalent

of a mouse mutant, *kreisler*. The *kreisler* mutant has hindbrain defects that disrupt the signalling required to pattern a normal inner ear including the ED (Moens et al., 1998). The absence of the dorsal domain of *bmp4* would indicate normal patterning is disrupted in *valentino*, as would be expected based on the *kreisler* phenotype.

4.1.2 *dog*, *vgo*, and *cls*, mutants have specific crista and SCC defects

Each of the chosen mutants, *dog-eared* (*dog* (Whitfield et al., 1996)), *van gogh* (*vgo* (Whitfield et al., 1996)), and *colourless* (*cls* (Kelsh et al., 1996; Malicki et al., 1996; Whitfield et al., 1996)) have been described previously. This section summarises their inner ear phenotypes (see also Table 4.1). A more detailed description of the *colourless* phenotype is given in the results and Appendix, as unlike the other mutants, its inner ear phenotype has not been as well described in previous papers.

dog-eared mutants do not form normal canals or cristae.

dog mutants develop normal sized otic vesicles, which form epithelial projections. However, these projections fail to divide the otic vesicle properly. In wild type embryos the projections fuse to form a cross shaped structure, the interconnecting spaces around which will become the SCC (see Fig. 1.2D). In *dog* there appears to be too much projection tissue within the vesicle and the cross structure does not form properly (Fig. 4.1 compare A+C). *dog-eared* mutant vesicles also have small otoliths that can be found in abnormal locations (Fig. 4.1D, arrow). The ear phenotype can be identified molecularly at 48hpf as they fail to express *msxc*, normally found in three ventrolateral domains marking the cristae (Whitfield et al., 1996). *dog-eared* vesicles do not form cristae, although occasionally hair cells are seen in areas where cristae normally form (Fig. 4.1 compare E+G; T. Whitfield pers. comm.). In *dog* mutants the macula patches are smaller than normal, containing fewer hair cells, and become increasingly disrupted with age.

Four alleles of *dog* have been found: *tp85b*, *tm90b*, *to15b* and *tc257e*. No great phenotypic differences between the alleles has been documented, although *to15b* has been reported as having weak delocalised expression of *msxc* (Whitfield et al., 1996). This allele has not been examined in this thesis. *dog* has been shown to disrupt the *eya1* gene, a transcriptional cofactor (see 4.4.1 and Table 4.1 (Kozlowski et al., 2001a)).

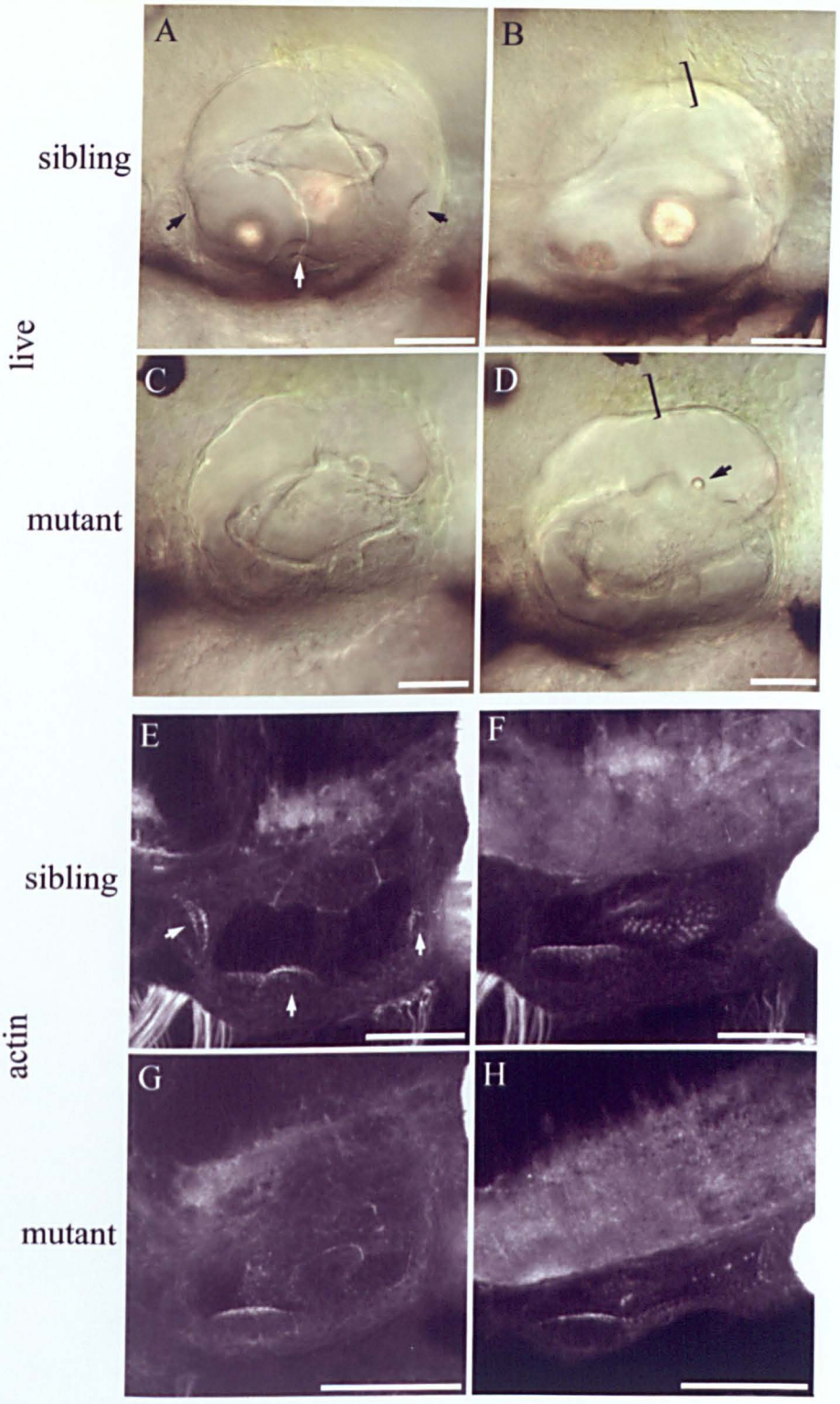

Figure 4.1 *dog* mutant and sibling 72hpf otic vesicles.
(A-D) DIC live (E-H) FITC-phalloidin stains of mutant and sibling *dog tm90b* embryos. All are lateral views of 72hpf embryos, anterior to left. Scale bar = 50 μm.
(A) In siblings the three cristae are visible as thickened regions of epithelium and groups of hair cells (E, arrows). (C+G) These structures are not seen in the mutant. (A) In the sibling the epithelial projections form a regular cross structure. (C+D) In the mutant the projections are disorganised and the normal cross structure does not form. (B+D, bracket) In both the sibling and mutant a putative ED is seen (brackets). (A+B) In the sibling the anterior and posterior otoliths have distinctive different shapes and positions. (D) In the mutants the otoliths are small and can be found in random locations (arrow).

vgo mutants do not form projections or cristae.

vgo mutants have very small otic vesicles, and can be identified at earlier stages than *dog*. Their otic vesicle is visibly smaller by 24hpf. Epithelial projections, which are normally visible at 48hpf, are not seen (Fig. 4.2 compare A+C). Two otoliths of normal size form and, although the volume of the otic vesicle is much reduced, they do not fuse. *msxc* is not expressed and cristae do not develop. These mutants form one single sensory patch along the medial and ventral floor of the vesicle (Fig. 4.2 compare E+F with G and see Chapter 5, 5.4.1)(Whitfield et al., 1996). A large dorsally projecting structure is clearly visible in the mutant, which appears larger than a similar structure seen in the sibling (Fig. 4.2C, D+B bracket). This structure is thought to be an enlarged ED, which has not been described previously and is reported in more detail in the results section (4.1.4). Two alleles are known, *tu85b*, and *tm208*. No differences between them have yet been described. *vgo* has very recently been discovered to be a mutation in *tbx1*, a T box transcription factor (see 4.4.1 and Table 4.1, T. Piotrowski pers. comm.).

cls mutants express *msxc* in an abnormal pattern.

cls mutants are easily identified from 27hpf due to a lack of pigment cells (Kelsh et al., 1996). They also have small otic vesicles and small otoliths. *cls* mutants express *msxc*, although in two ventrolateral domains rather than the three seen in wild type (Whitfield et al., 1996). This change in the normal *msxc* expression pattern indicates there may be further defects in sensory patch patterning. Further characterisation of *cls* patterning defects can be found in the Appendix. Other aspects of its development relating to its cristae and SCC development are explored in the results section of this chapter (Fig. 4.11-15). The *cls* mutation disrupts the *sox10* gene, a transcription factor (see Table 4.1, Dutton et al., 2001). Four alleles have been described: *t3*, *tw2*, and *tw11* (Kelsh et al., 1996; Whitfield et al., 1996) and *m618* (Malicki et al., 1996).

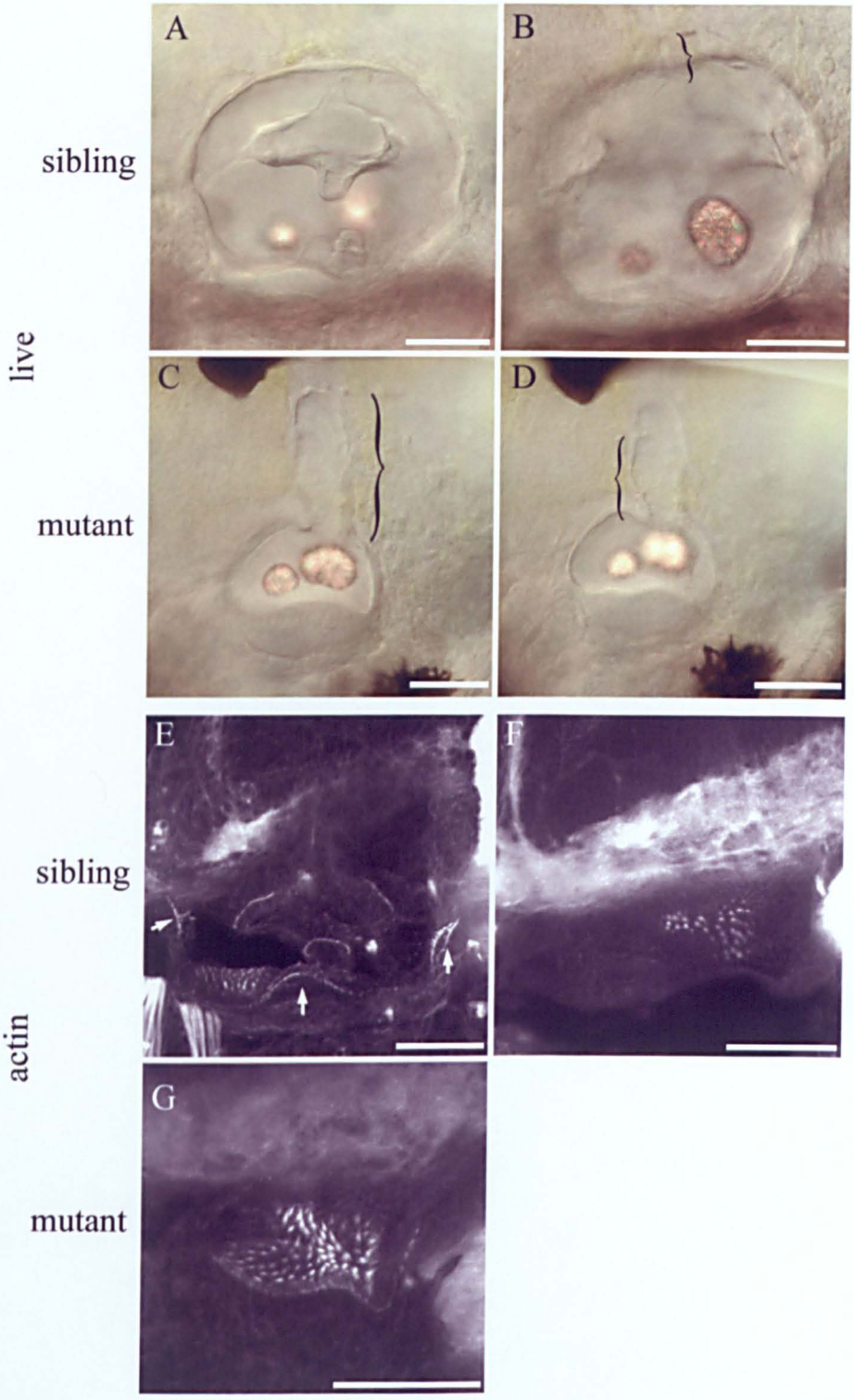

Figure 4.2 *vgo* mutant and sibling 72hpf otic vesicles.
(A-D) DIC live (E-G) FITC-phalloidin stains of mutant and sibling *vgo tu285* embryos. All are lateral views of 72hpf embryos, anterior to the left. Scale bars =50 μm.
(A) In the sibling the epithelial projections have not completely fused to form the cross shaped structure. (C) No projections are visible in the mutant embryo. The mutant vesicle is dramatically smaller than that of the sibling (anterior-posterior length = 90 μm (C) compared to 150 μm (A)). The putative ED is larger in mutants than in siblings (Dorsoventral length = 77 μm (D) compared to 27 μm (B)). (C+D) In mutants this projection may consist of two dorsal extensions (brackets), which is shown more clearly in *bmp4* in situ hybridisations (see Fig. 4.9). (E, arrows) The cristae are shown in the sibling actin stains (arrows) but no cristae are seen in the mutants. (G) The mutant contains one sensory patch, which stretches along the ventral floor and up the medial wall of the otic vesicle.

4.1.3 The inner ear phenotype of *valentino* mutants is not well characterised.

val mutants fail to form a properly segmented hindbrain, and rhombomeres 5 and 6 (R5, R6), which the inner ear develops adjacent to, are not properly specified (Moens et al., 1996). In the mouse, *kreisler* mutants have similar, but not identical, hindbrain patterning defects resulting in cystic malformed ears, which do not form normal SCC, and have a rudimentary or absent ED (Deol, 1964; McKay et al., 1996). The ED will be described in more detail below (4.1.4). If a similar patterning mechanism were at work in zebrafish, the dorsal patterning of the otic vesicle would be disrupted in *val*. This could be tested by analysing the expression of a dorsal marker, *bmp4*.

By 18hpf the *val* otic vesicle is smaller than that of wild type. However, at later stages it these become swollen (5dpf see Fig. 4.23). The epithelial projections fuse to varying extents amongst mutants (B. Riley pers. comm.) and the larvae exhibit circling behaviour that is associated with vestibular defects (Moens et al., 1998). These SCC and behavioural defects are also seen in the mouse mutant (Deol, 1964). There is no information on the formation of sensory patches, or the development of otoliths within these mutants.

Table 4.1 Summary of phenotypes of mutants chosen for study.

mutant (alleles)	**gene**	**cristae**	**epithelial projections**	**maculae**	***msxc* expression**
dog *tm90b, to15b tp85b, tc257e*	transcriptional coactivator *eya1*	none	disorganised	2 that are not maintained	none*
vgo *tu285, tm208*	T box transcription factor, *tbx1*	none	none	1	none
cls *t3, tw2, tw11, m618*	SOX transcription factor, *sox10*	abnormal	disorganised (reduced)	1 posterior	2 domains
val *b337, b361, b475*	bzip transcription factor, *krml1*	?	disorganised	?	?

Summary table describing relevant aspects of the inner ear phenotype for each mutant and the alleles known. * *to15b* has been shown to have weak delocalised *msxc* expression. Information summarised from references given in text and this work.

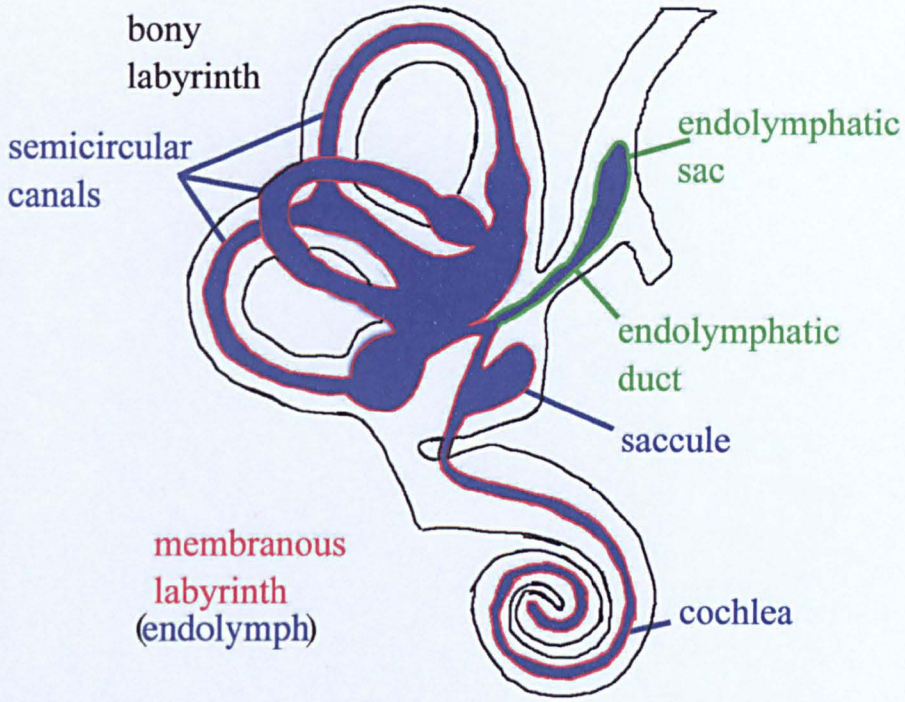

Figure 4.3 Sketch of human inner ear.

Transverse view (not proper section) through bony labyrinth, lateral to left, dorsal to top. The inner ear is an interconnected series of chambers, which can be divided into two layers, the external bony labyrinth (black) which encases the membranous labyrinth (red). These layers are filled with fluids with different properties. The bony labyrinth surrounds the membranous labyrinth with perilymph, and the membranous labyrinth is filled with endolymph (blue). There are not thought to be any open connections between the two fluids. The Endolymphatic duct (green) is part of the membranous labyrinth that projects medially from the saccule. It ends in the endolymphatic sac (green).
Drawing adapted from A.N. Salt (http://oto.wustl.edu/cochlea/intro1.html).

4.1.4 The function of the endolymphatic system is not fully understood.

The ED is a mediodorsal structure, projecting from the saccule, ending in the endolymphatic sac (Fig. 4.3). It has been recently described in zebrafish after 8dpf in both histological plastic sections and paint-fills (Bever and Fekete, in press). The ED is thought to be required to maintain the correct composition and/or volume of endolymph fluid in the inner ear (Rask-Andersen et al., 1999; Thalmann, 1999). This fluid fills the membranous labyrinth of the inner ear i.e. it is found within the lumen of the SCC and all the chambers (unlike perilymph, which is found between the membranous labyrinth and the outer bony labyrinth). The paint fill technique shows the membranous labyrinth, as the paint fills it in a similar manner to endolymph (Fig. 4.4)

The endolymphatic fluid contains a high concentration of K^+, as well as the macromolecules that contribute to the formation of various structures found within the membranous labyrinth (e.g. the cupula). In mammals the high K^+ concentration is thought to be generated and maintained by cells in the stria vascularis in the cochlea (shown in guinea pigs) and possibly by dark cells in the vestibular apparatus (Wangemann, 1995). In the mouse these cell types both express *IsK*, a protein that works with K^+ channels to mediate K^+ secretion (Vetter et al., 1996). This cation concentration is important for maintaining the electric potential across specific areas of the inner ear, such as the cochlea.

There are two human syndromes whose symptoms include deafness that are thought to be due to a malfunctioning ED. Menière's disease is thought to be due to excess endolymph (Salt, 1995), while Pendred's syndrome is due to defective chloride ion resorption (Everett et al., 1999). A third syndrome, DiGeorge syndrome (DGS) can also include hearing defects (Botta et al., 2001). The defects that result in this sensorineural deafness are not understood, but the mouse DGS model has an enlarged ED (see 4.4.2, B.E. Morrow pers. comm.).

4.2 RESULTS

This section describes the mRNA in situ hybridisation expression patterns of *bmp2b* and *bmp4* for each mutant in turn. It then describes the studies of the dorsal domain of *bmp4* expression, and the development of the putative ED.

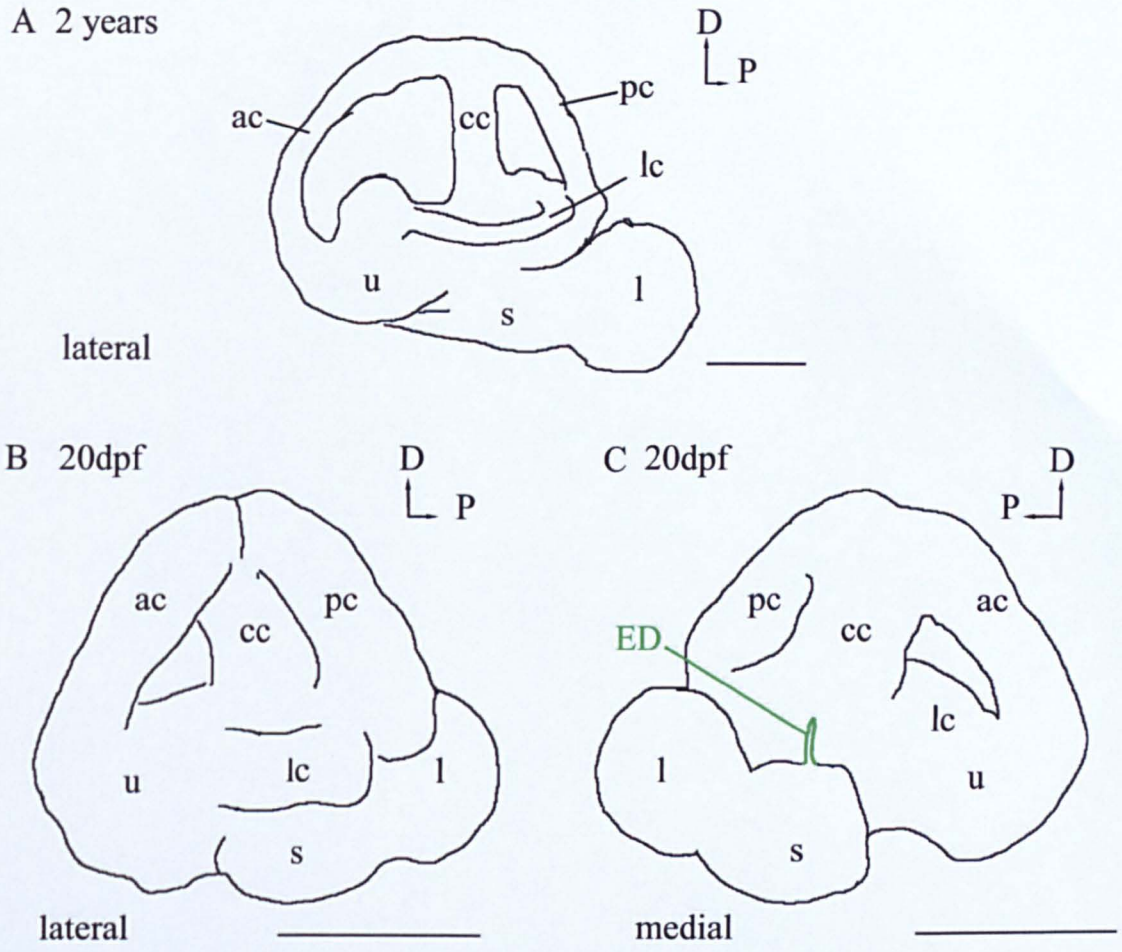

Figure 4.4 Trace of paint filled figure adapted from Bever and Fekete, (in press) showing the position of the ED in 20dpf zebrafish embryos.
A+B lateral views with anterior to left. C is a medial view with anterior to right.
Scale bars = 500 μm (A), 250 μm (B+C).
(A) Trace of a 2 year old paint-filled zebrafish inner ear. The three SCC have projected away from the other chambers of the inner ear and are narrower (B+C). At 20 days the SCC are thicker and the inner ear is much more compact. The lateral view shows the SCC (B) while the medial view shows the lagena and saccule more clearly (C). The ED projects dorsally from the saccule (C, green projection).
Abbreviations: ac, anterior canal; cc, crus commune; ED, endolymphatic duct; l, lagena; lc, lateral SCC; pc posterior SCC; s, saccule; u, utricle.

4.2.1 *bmp4* expression domains are not maintained in *dog* mutants.

Two alleles of *dog* were analysed, *tm90b* (Fig. 4.5) and *tp85b* (Fig. 4.6). At 24hpf in *tm90b*, *bmp4* mRNA expression appears normal, with no difference seen in a clutch of embryos from a mating of an identified pair of heterozygotes (Fig. 4.5A+B). However, at later stages in this allele the four domains seen in wild type and sibling embryos are much reduced. The ventrolateral stain at the anterior or posterior end of the vesicle is much weaker in the mutants (Fig. 4.5C+D). This reduced level of expression is shown at slightly earlier stages in *tp85b* (26hpf, Fig. 4.6A-D, 30hpf, Fig. 4.5C+D). The disorganised projections are evident from 48hpf (Fig. 4.5F). The ventrolateral area of staining fades by 48hpf and has gone by 55hpf (Fig. 4.6F, I +N arrows). By contrast, the dorsal domain of *bmp4* expression in the *dog* mutant vesicles appears normal (Fig. 4.5I-L brackets). The epithelial projections that will form the SCC appear larger, projecting further medially into the otic vesicle than in the siblings (Fig. 4.6 compare P+Q).

4.2.2 *bmp2b* expression levels and domains of expression are reduced in *dog* mutants.

In *dog* mutants, the level of *bmp2b* expression at the anterior and posterior of the otic vesicle is much reduced at 24hpf, although it is expressed in the correct regions (Fig. 4.7 compare A+B with C+D). It is also expressed at normal levels in other areas of the mutant embryos such as the eye and caudal fin (Fig. 4.7E+F and Fig. 4.8B+D). At 30hpf the third ventrolateral domain of expression is not seen in mutants (Fig. 4.8E-G). At 48hpf mutants fail to express *bmp2b* in the epithelium around the cristae (compare Fig. 4.8H with I+J). At 48hpf in the siblings there is faint staining in the epithelial projections (Fig. 4.8H, bracket). However, in the mutants there is strong stain in discrete areas of the epithelial projections (Fig. 4.7I+J). In sibling embryos at 72hpf the epithelial walls of the SCC express *bmp2b* (Fig. 4.7M and Fig. 4.8K+L). Discrete areas of *bmp2b* expression are still seen in the epithelial projections at 72hpf in mutant embryos. The staining appears stronger in *tp85b* (Fig. 4.7N+O) than in *tm90b* mutant embryos (Fig. 4.8N, arrow). This may reflect a difference in stages of development rather than variation between alleles. These areas of stain in mutants, at both 48hpf and 72hpf, appear to coincide with where the projections fuse (Fig. 4.8J, Fig. 4.7K, L, N, +O) (Waterman and Bell, 1984).

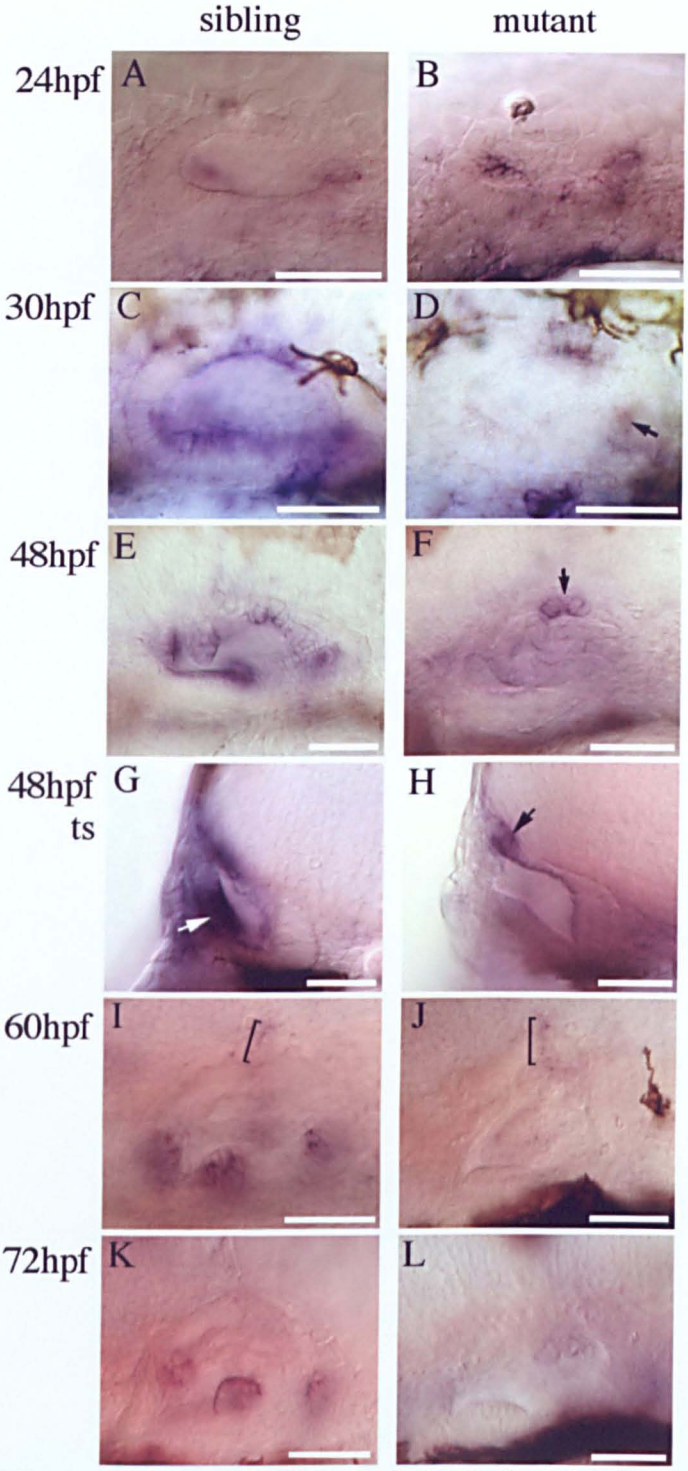

Figure 4.5 *bmp4* mRNA in situ hybridisations in *dog tm90b* mutants and siblings. All are lateral views with anterior to left except H+I, which are transverse sections (ts) with lateral to left. Scale bar = 50 μm

(A+B) In both siblings and mutants *bmp4* is expressed laterally at the anterior and posterior ends of the vesicle at 24hpf. (C) At 30hpf in the sibling *bmp4* is expressed along the dorsal roof of the vesicle and in a broad anterior and a posterior ventrolateral domain. (D) In the mutant the dorsal domain appears unaffected but the anterior ventrolateral domain is not present. There is a small domain of posterior ventrolateral stain (arrow). (E) At 48hpf the sibling has three distinct ventrolateral domains and a dorsal domain. (F) In the mutant the dorsal stain appears as normal (arrows) but the ventrolateral domains are missing. The lack of crista staining in the mutant is clear in the transverse sections cut through the middle of the vesicle (compare G white arrow +H). (H) The dorsal stain is still present in the mutant (black arrow). (I+J) By 60hpf the levels of the dorsal *bmp4* stain are reduced (bracket). (K+L) By 72hpf there is no dorsal *bmp4* stain in either sibling or mutant, although the three ventrolateral domains are still found in the sibling.

Figure 4.6 *bmp4* mRNA in *dog tp85b* mutant and sibling embryos.

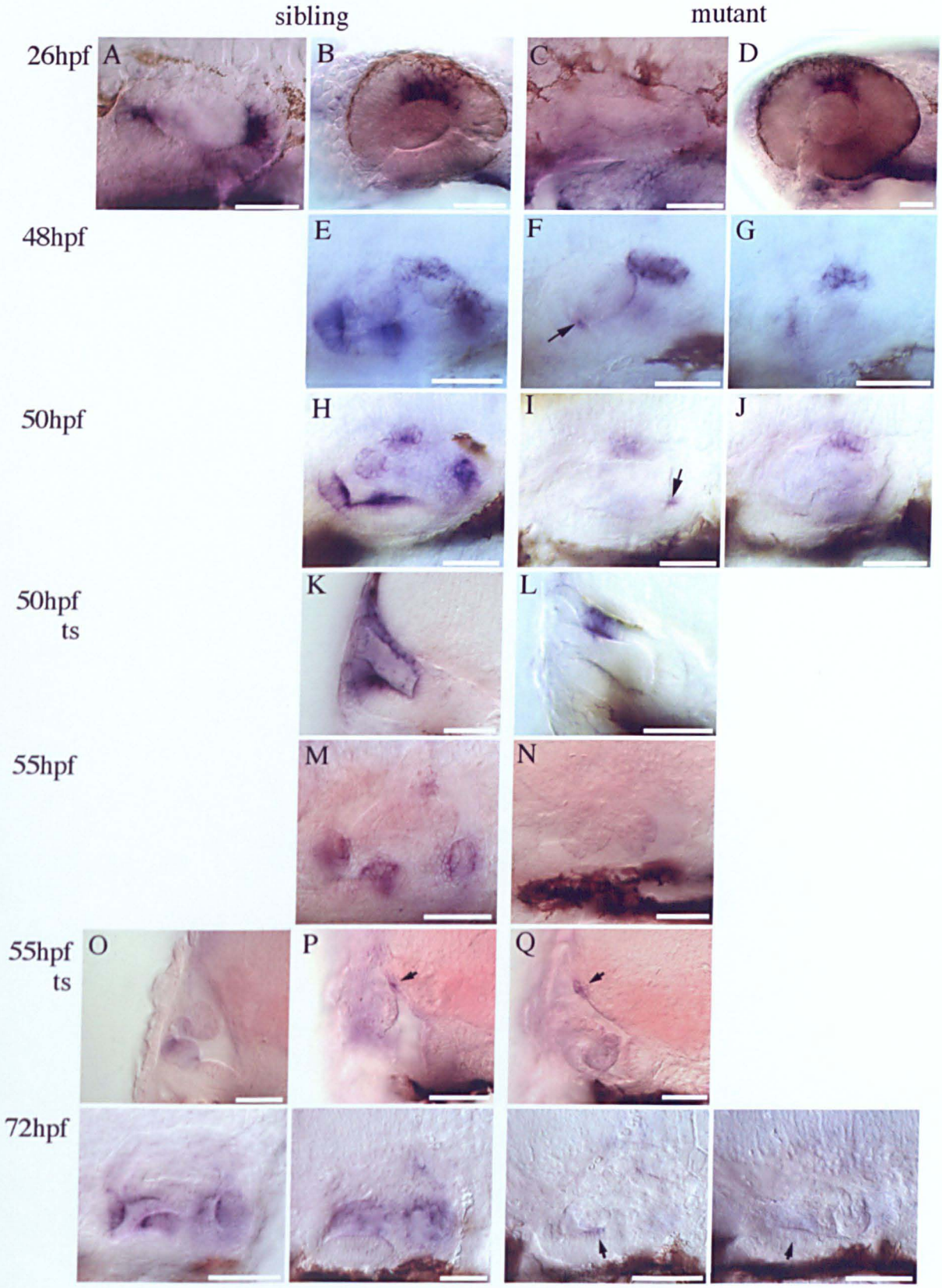

Figure 4.6 *bmp4* mRNA in *dog*^{tp85b} mutant and sibling embryos

All are lateral views with anterior to left, except K+L, O-Q, which are transverse sections with lateral to left. Scale bar=50μm

(A+B) At 26hpf *bmp4* is expressed at the anterior and posterior end of the otic vesicle in siblings and dorsally in the eye. (C+D) In mutant embryos the eye expression is similar but the levels of *bmp4* in the otic vesicle are much reduced. (E) At 48hpf the siblings express four domains of *bmp4*. (F+G) In the mutants the dorsal domain is as normal but the three ventrolateral areas are not seen. (F+I, arrow) There is a small domain of expression in the posterior or anterior (arrow). (N) At 55hpf the dorsal stain is hard to see laterally in the mutant but is still expressed, as shown in a transverse section (Q, arrow). (R+S) At 72hpf only the cristae express *bmp4*; the staining of the rest of the vesicle in S is trapping (inconsistent, granular, staining only the surface). (T+U, arrow) In mutants there appears to be a distinct area of stain ventrally. This is not in the remnant of the anterior macula.

4.2.3 Ventrolateral *bmp4* expression levels are reduced in *vgo* mutants.

bmp4 is expressed very weakly at 24hpf in *vgo* mutants although it appears to be in the correct regions (Fig. 4.9A-D). The three ventrolateral areas of *bmp4* expression, normally seen at later stages, are not seen in the mutants (Fig. 4.9H+I). Piotrowski and Nüsslein-Volhard, (2000) reported this lack of ventral staining at the time of these experiments.

4.2.4 Dorsal *bmp4* expression is expanded in *vgo* mutants.

At 37hpf the levels of *bmp4* expression in the dorsal domain appears stronger in the mutant than in the sibling at a similar stage (Fig. 4.9 compare E+G). The length of the dorsal expression domain (Anterior-Posterior) is similar between mutant and sibling, even though the mutant vesicle is slightly smaller. By 60hpf the dorsal stripe of expression has extended further dorsally labelling a hairpin-like structure two cells thick in both sibling and mutant (Fig 4.9J-L dotted line). This area of staining is positioned medially in both mutants and siblings, shown in transverse sections through the middle of the otic vesicle (Fig. 4.9M+N). The hairpin extends further dorsally in mutant embryos (dorsoventral length 35μm compared to 22μm, Fig 4.9 compare J+K) and appears to be forked. One fork is more obvious, and is lateral to the other, which projects slightly medial to the former one (Fig. 4.9K+L). This forking was seen to some extent in all mutants analysed at that stage. As in sibling embryos the strong dorsal expression persists until 72hpf in mutants, then starts to fade (Fig. 4.9O+Q).

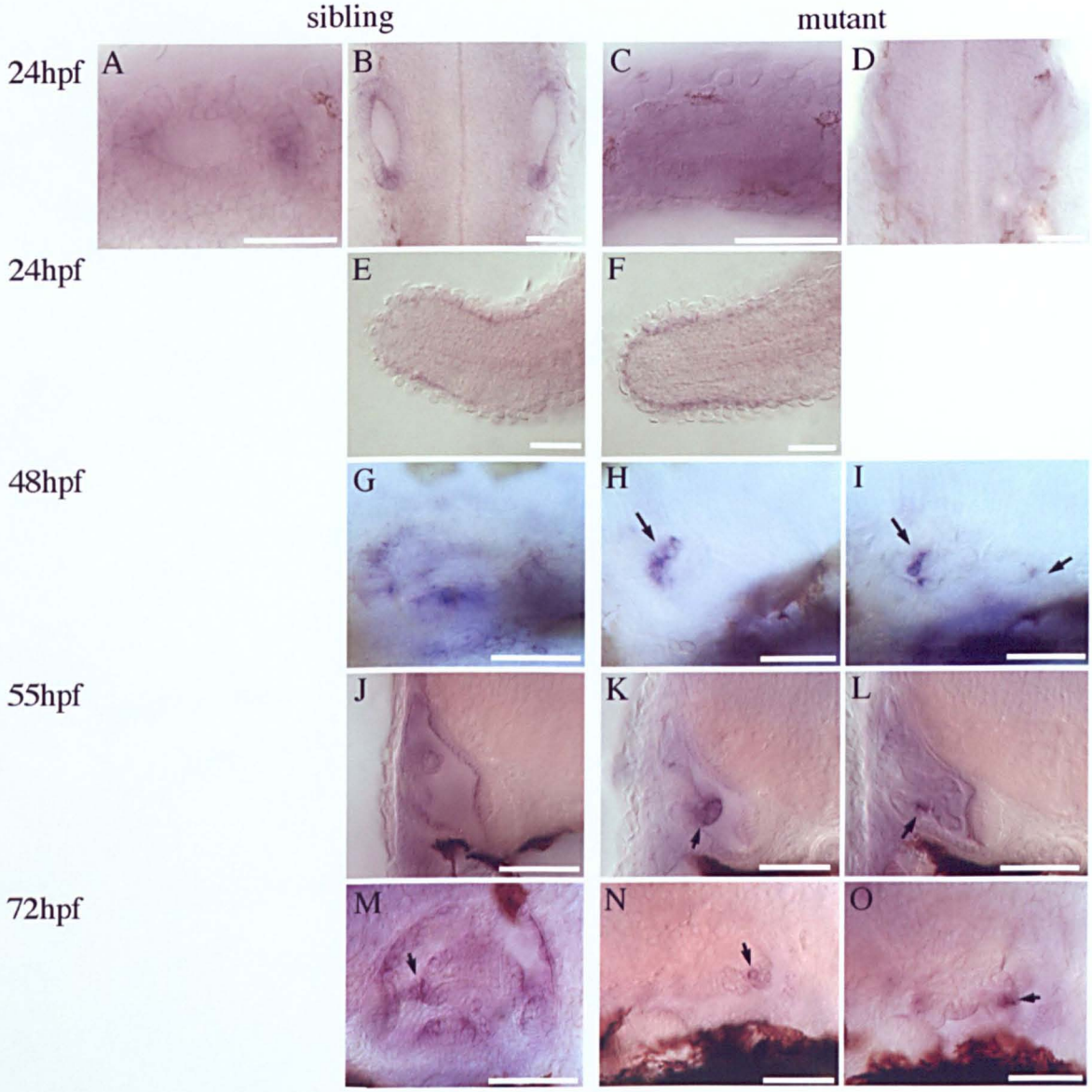

Figure 4.7 *bmp2b* mRNA in *dog tp85b* mutant and sibling embryos.
All are lateral views with anterior to left except J-L, which are transverse sections with lateral to left. Scale bar=50 μm.
(A+B) At 24hpf *bmp2b* is expressed at the anterior and posterior ends of the vesicle. (C+D) In the mutant there is no or very reduced levels of *bmp2b* expression in the otic vesicle although expression elsewhere such as the tail is unaffected (compare E+F). (G) At 48hpf *bmp2b* is expressed in three ventrolateral domains including the three crista thickenings and surrounding epithelium. (H+I, arrows) In the mutant there is strong expression in discrete areas of the epithelial projections. (J) At 55hpf weak *bmp2b* stain can be seen laterally in the epithelial projections. (K+L) In the mutant the discrete areas of strong expression are maintained. (M) At 72hpf *bmp2b* labels the SCC epithelium in siblings. (N+O) However, in mutants there remain only two very discrete areas of stain (arrows).

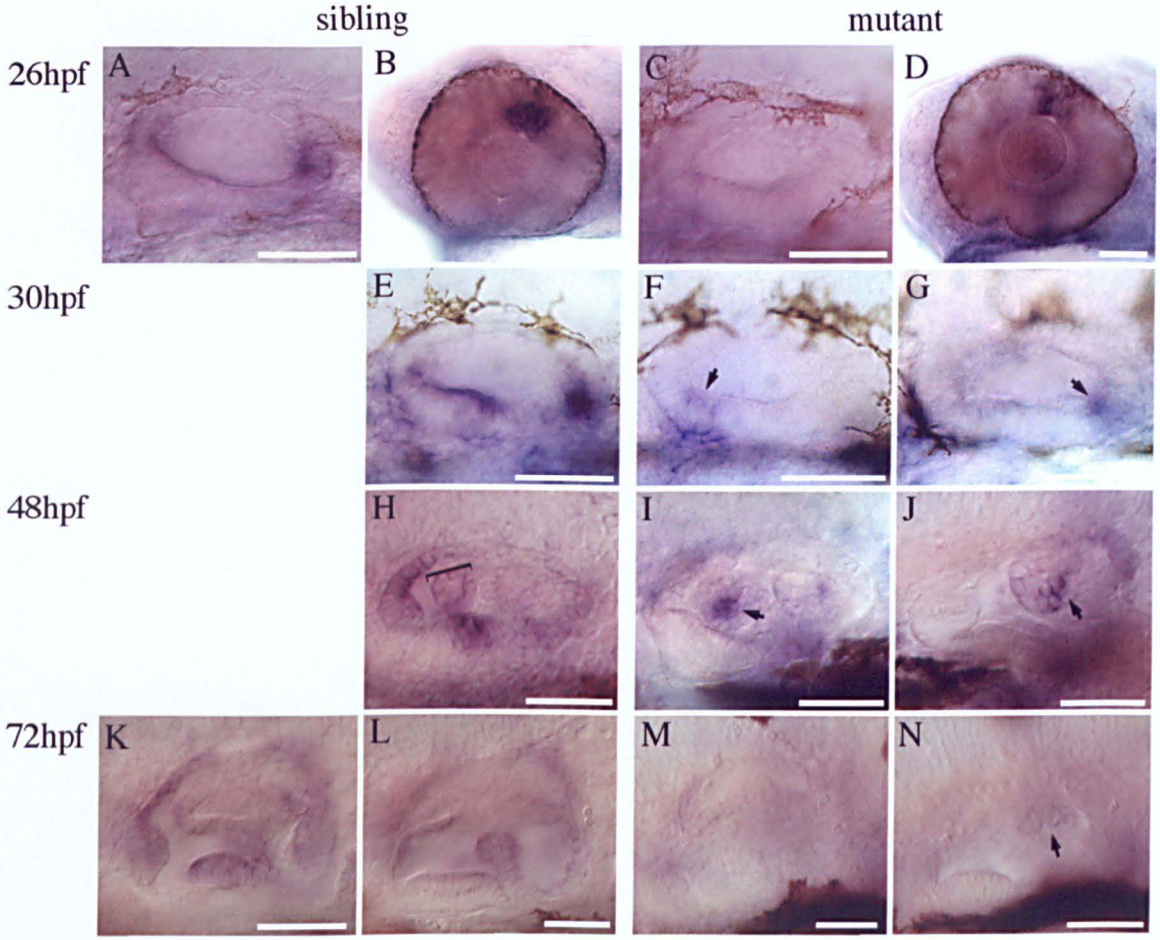

Figure 4.8 *bmp2b* mRNA expression in *dog tm90b* mutant and sibling embryos.
All are lateral with anterior to the left except J, which is a transverse section with lateral to right. Scale bar=50 μm
(A) At 26hpf *bmp2b* is expressed in two domains at the anterior and posterior ends of the vesicle and dorsally in the eye (B). (C) In mutants the levels of expression in the otic vesicle are much reduced, but expression in the eye is unaffected (D). (E) At 30hpf siblings express *bmp2b* in three ventrolateral domains. (F+G) In mutants these levels are reduced and the third ventrolateral domain does not appear. (H) At 48hpf the cristae and a small area of adjacent epithelium express *bmp2b*. There is also low level staining in the epithelial projections (bracket). (I+J) In the mutants there is no ventral stain but there are areas of stain within the projections (arrows). (K+L) At 72hpf the SCC express *bmp2b*. (M+N) In the mutant there are very faint areas of discrete expression in the epithelial projections (arrow).

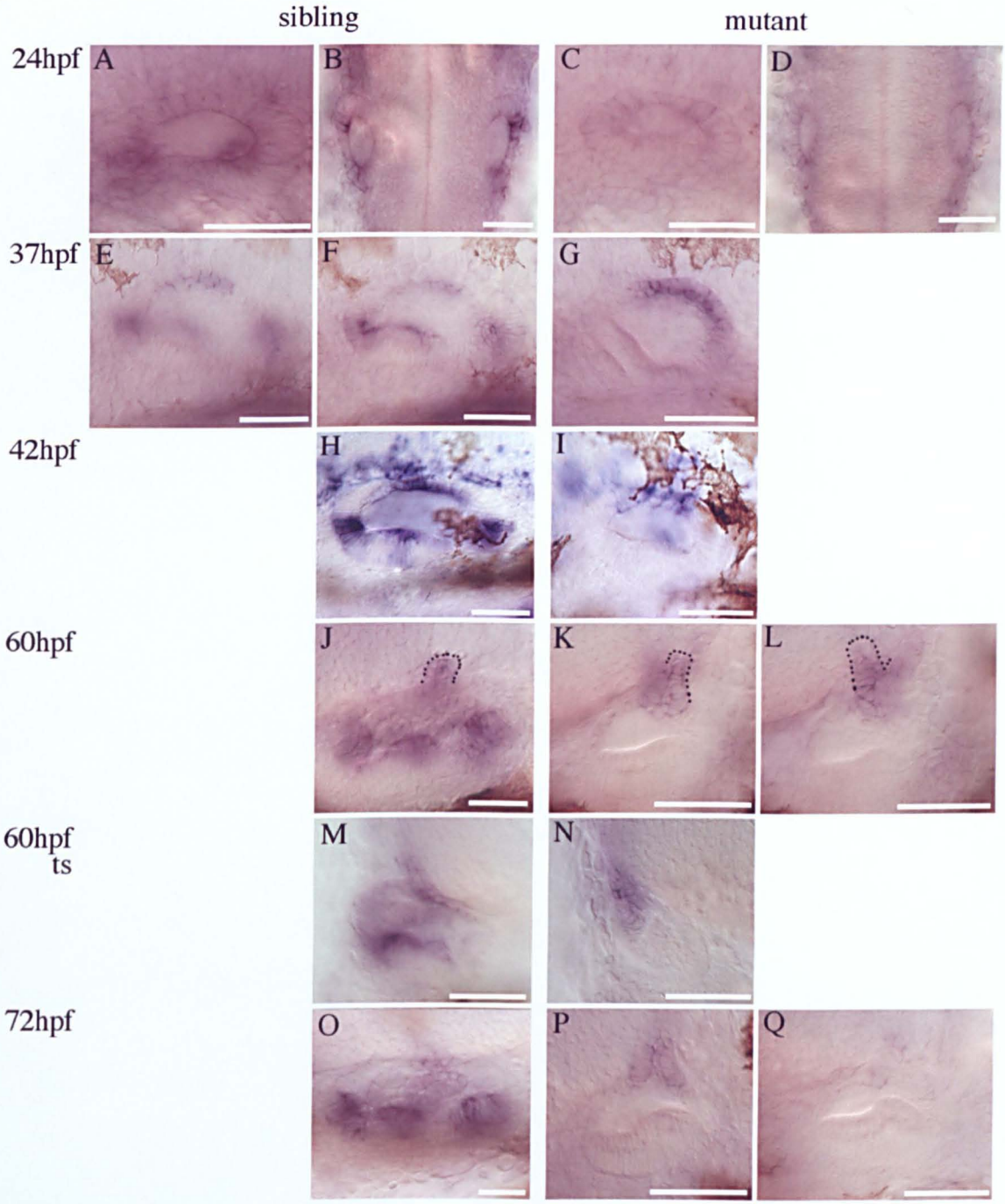

Figure 4.9 *bmp4* mRNA expression in *vgo tu285* mutant and sibling embryos.
All are lateral views with anterior to left except B+D which are dorsal views with anterior to the top, and M+N which are transverse sections with lateral to left. Scale bar=50 μm.

(A+B) At 24hpf *bmp4* is expressed at the anterior and posterior ends of the otic vesicle in the sibling. (C+D) In the mutant it is expressed at very low levels in the right areas. (E+F) At 37hpf in siblings there are 3 ventrolateral domains of expression and a broad dorsal domain. (G) In the mutants the dorsal domain is the same size as the sibling, but appear to be expressed more strongly. The ventrolateral staining is missing. This pattern persists at 42hpf (H+I). (J-L) At 60hpf the hairpin dorsal structure has formed and is labelled with *bmp4* in both the mutant and sibling. (K+L) The mutant hairpin appears forked; (K) is a more lateral view. (N) Transverse sections at 60hpf show the lack of lateral stain in the mutant embryos and the extent of the dorsal staining. (O) At 72hpf the dorsal stain is fading in siblings and mutants. (P) and (Q) are different embryos and the different levels of staining may reflect slight variation in staging.

4.2.5 *bmp2b* expression domains are reduced in *vgo* mutants.

bmp2b expression is much reduced by 24hpf in mutant embryos, although it is expressed at normal levels in the migrating lateral line primordium (Fig. 4.10B+C arrow). At 27hpf staining is present in the correct regions of the otic vesicle; however, it is much fainter than in siblings (Fig. 4.10 compare E+G arrows). Normal levels of expression are seen in other areas of the mutant embryo, such as the eye (data not shown). By 37hpf there is only faint expression in the posterior of the vesicle (Fig. 4.10I arrow). This posterior area is still present at 44hpf (Fig. 4.10K) but has faded by 48hpf and no stain is seen in the developing inner ear at later stages.

4.2.6 *cls* mutants do express *bmp4* and *bmp2b* although abnormally.

Both *bmp2b* and *bmp4* are expressed in the ears of *cls* mutants. However, both *bmps* are found in only two ventrolateral domains from 48 to 72hpf (Fig. 4.11J, M and Fig. 4.12F). These domains initially appear normal, positioned ventrolaterally at the anterior and posterior ends of the vesicle. However, the mutants do not go on to express the third ventrolateral domain of either *bmp2b* or *bmp4* (Fig. 4.12F and Fig. 4.11J, respectively). The dorsal *bmp4* domain is also missing (Fig. 4.11J). *bmp4* appears to be expressed at higher levels at all stages examined (Fig. 4.11). *bmp2b* levels do not appear to be altered (Fig. 4.12). *cls* mutants have more lateral line organs along the trunk and tail than are found in siblings (see Appendix Fig. A7). These organs stain weakly for *bmp4* as in wild type and appear the normal size (Fig. 4.11L+N, arrows). As has been described previously, *msxc* is also expressed in two ventrolateral domains in the otic vesicle, at a similar position to the *bmp2b* and *bmp4* ventrolateral domains (Fig. 4.12G+H and Whitfield et al., (1996)).

4.2.7 In *cls bmp* expression domains coincide with abnormal ventrolateral sensory patches.

The ventrolateral *bmp* expression domains also appear to coincide with regions of *brn3.1* expression. This POU domain transcription factor specifically marks differentiated hair cells (Mowbray et al., 2001). It is expressed in the maculae at 48hpf (earlier stages were not examined) and in the cristae and neuromasts at 72hpf (Fig. 4.13). The two lateral areas

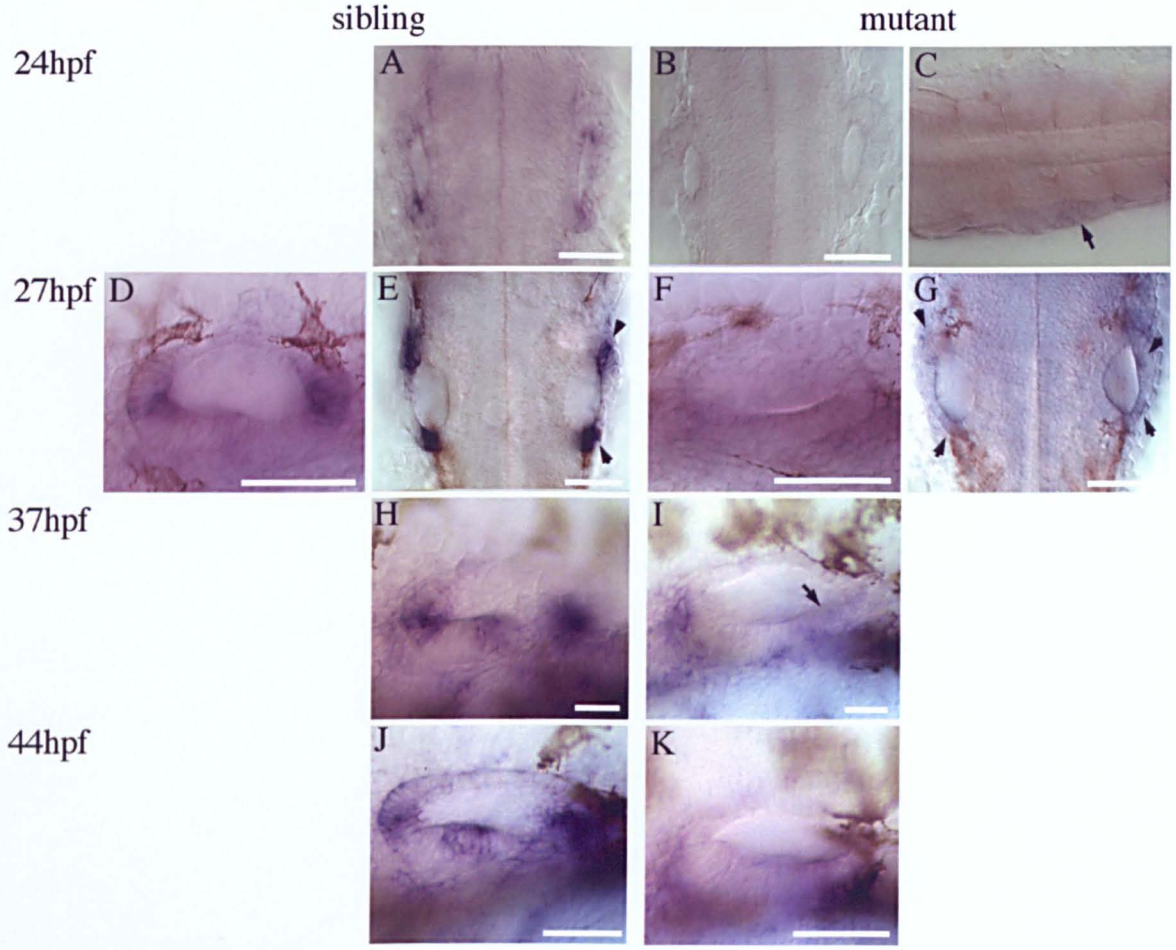

Figure 4.10 *bmp2b* mRNA in *vgo tu285* mutant and sibling embryos.
All are lateral with anterior to left except A-C, E, and G which are dorsal with anterior to the top except C in which anterior is to the left. Scale bar = 50 μm.

(A) In siblings *bmp2b* is expressed at the anterior and posterior ends of the vesicle. (B) This pattern is not detectable in the otic vesicles of the mutant embryos. (C) However, the lateral line expresses normal levels at this stage. (D+E) At 27hpf expression at the anterior and posterior ends is strong in the siblings. (F+G) Staining is weakly detectable in similar positions in the mutant. (H) At 37hpf three ventrolateral domains are visible in the sibling while only a faint posterior domain is seen in the mutant (I). (J+K) A similar pattern is seen at 44hpf.

of *bmp* expression appear to coincide with two strong areas of *brn3.1* expression in *cls* (compare Fig. 4.13C and Fig. 4.11J). Strong *brn3.1* staining is also seen medially in both mutants and siblings (Fig. 4.13E+F, dorsal view). This pattern of lateral and medial staining is also seen at 72hpf (Fig. 4.13O, ts). *cls* therefore expresses crista-specific markers (*bmp4*, *bmp2b* and *msxc*) but in only two domains rather than three. However, the appearance of differentiated hair cells (expressing *brn3.1*) in these "cristae-like" patches is earlier than normal. The presence of hair cells in these areas was confirmed through actin stains.

FITC-phalloidin labels actin found in the stereocilia of hair cells. At 34hpf there are no obvious differences between the developing sensory patches of the *cls* sibling and mutant vesicle. Small collections of hair cells, the maculae, are visible on the anteroventral floor (~7 hair cells) and the posteromedial wall (~3 hair cells) of the vesicle (Fig. 4.14A-D).

However, by 48hpf differences are apparent. In the sibling both the anterior and posterior maculae have grown in size and the ventrolateral epithelial thickenings that will go on to form the cristae are visible (Fig. 4.14E-F, arrow to thickening). In the mutant the two crista-like ventrolateral sensory patches already contain differentiated hair cells (Fig 4.14G, arrows). The posterior macula has enlarged in the mutant as well, but it has not assumed its characteristic frying-pan shape (Fig. 4.14H). The anterior macula, which is normally found on the ventral floor of the vesicle, is not seen in *cls* mutants at this stage or at later stages (Fig. 4.14 compare F+G, and Appendix A4). It is not clear what happens to the anterior tether cells, this is discussed in more detail with markers in the Appendix (A3).

In mutants at 72hpf the "crista-like" lateral collections of hair cells are not as organised as wild type cristae, and now contain fewer hair cells than wild type (~4 hair cells compared to ~15 in wild type crista) (Fig. 4.14 compare J+O with L+N, arrows). The posterior macula continues to expand, spreading around the medial wall of the otic vesicle (Fig. 4.14 compare L+M). Actin stains have been analysed up to 6dpf (see Appendix Fig. A4). The posterior macula continues to stretch across the medial wall of the vesicle. The ventrolateral collections of hair cells do grow larger, but do not assume the shape of cristae or maculae. The lack of organised SCC structure is also apparent in these in situs but is more clearly seen in live pictures (see below).

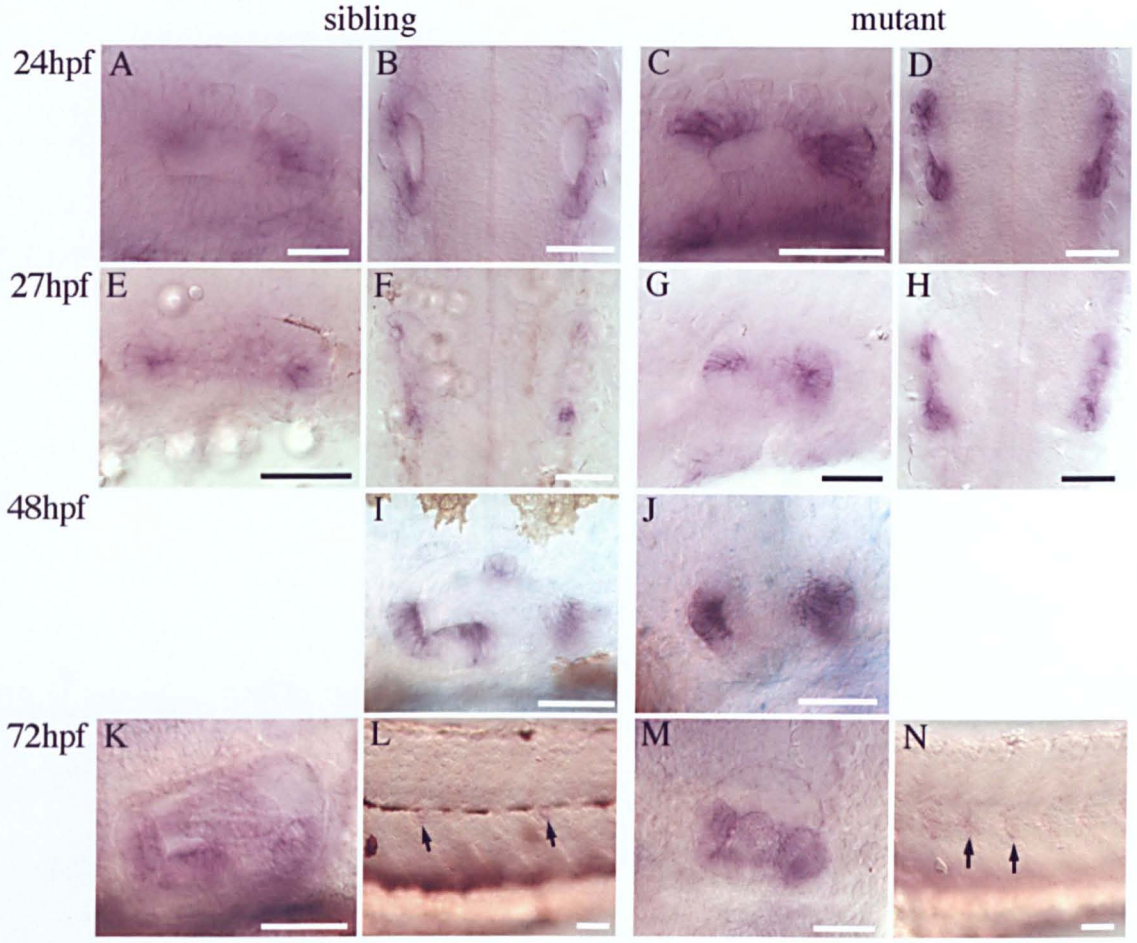

Figure 4.11 *bmp4* mRNA expression in *cls t3* mutant and sibling embryos.
All are lateral views anterior to left, except B, D, F, and H, which are dorsal with anterior to the top. Scale bar =50 μm.
(A-D) At 24hpf *bmp4* is expressed at the anterior and posterior of the vesicle in both sibling and mutant. (C+D) It appears to be expressed at higher levels in mutant embryos. At 27hpf the sibling otic vesicle is larger than the mutant (compare E+G). (I) At 48hpf there are four domains of *bmp4* expression in the sibling. (J) The mutant has only two strong ventrolateral areas of expression. (K+M) This pattern persists at 72hpf. (L+N) *bmp4* is also expressed in the lateral line system in both sibling and mutant. Although there are more organs they each express *bmp4* in *cls* mutants as in siblings.

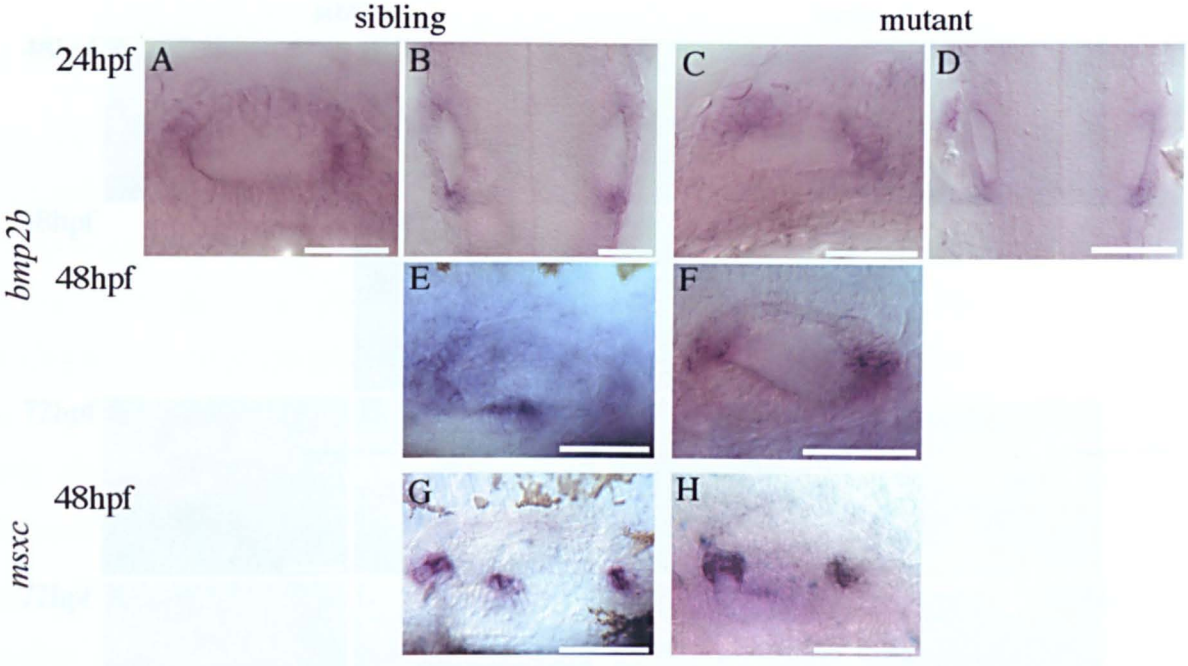

Figure 4.12 *bmp2b* and *msxc* expression in *cls t3* mutant and sibling embryos.
All are lateral views with anterior to the left except B and D, which are dorsal views with anterior to the top. Scale bar = 50 μm.
(A-D) At 24hpf the expression of *bmp2b* is the same in mutant and sibling embryos. (E) At 48hpf *bmp2b* is expressed in three ventrolateral domains. (F) In mutants it is expressed in two ventrolateral domains. (G) *msxc*,which marks the developing cristae in siblings (3 ventrolateral domains), is expressed in two similar ventrolateral domains in the mutant (H).

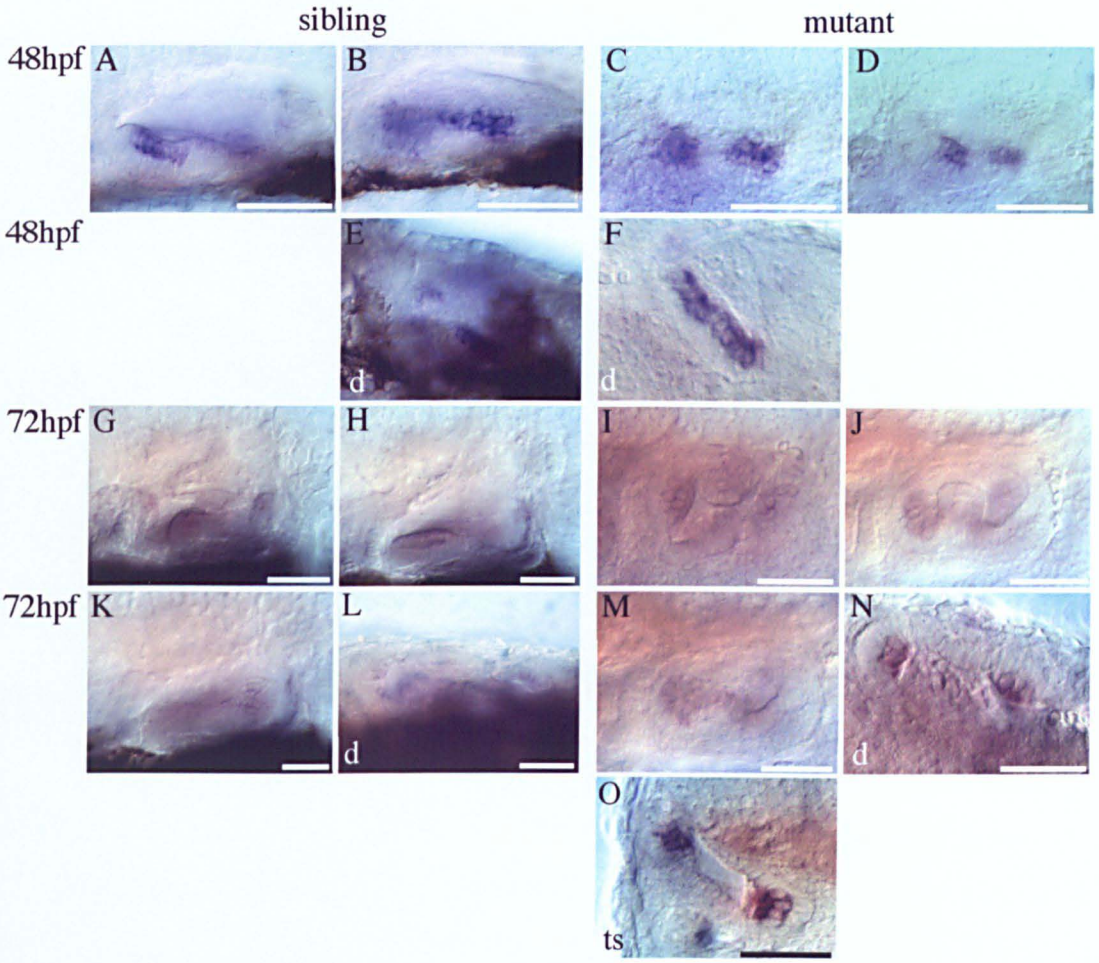

Figure 4.13 *brn3.1* mRNA expression in *cls t3* mutant and sibling embryos.
All are lateral views with anterior to the left except E, F, L and N, which are dorsal views (d) with lateral to the top and O which is a transverse section (ts) with lateral to the left. Scale bar = 50 μm.
(A, B+E) In siblings at 48hpf all the differentiated hair cells are labelled in the anterior macula and the posterior macula. (C, D+F) In mutants there are two ventrolateral positive areas and a more medial domain. (G, H, K, L) At 72hpf in the sibling the hair cells in the three cristae and the two maculae are expressing *brn3.1*. (I, J, M-O) In the mutant there are two ventrolateral domains of expression (N) and a medial domain (M+O).

4.2.8 *cls* mutants do not form normal epithelial projections or otoliths.

cls otic vesicles appear normal at 27.5hpf or possibly slightly smaller (Fig. 4.15A-D). In sibling embryos the epithelial projections are forming by 48hpf; however, they are not seen in the mutant until 72hpf (Fig. 4.15 compare E+K). These projections then do not fuse properly and the cross shaped structure (including dorsal and ventral projections) that normally divides up the otic vesicle is not seen. After 72hpf there is variety in vesicle size amongst the mutants and even between vesicles in the same head (Fig. 4.15 compare J+K with N+O). This becomes more apparent as development progresses with some vesicles becoming greatly expanded (See Appendix Fig. A2).

Otolith development is also abnormal. Normally in sibling embryos by 48hpf the posterior otolith is positioned more medially and is slightly larger than the anterior (Fig. 4.15E, posterior otolith slightly out of focus). In the mutant, both otoliths appear the same size (Fig. 4.15G). As development proceeds the distinction between the lateral, smaller, anterior otolith and the larger, medial, posterior otolith increases in the sibling, whereas they both remain small and in the same focal plane in the mutant (Fig. 4.15 compare L with M+O).

4.3 Development of the dorsal domain of *bmp4* expression.

This part of the results section investigates the dorsal area of *bmp4* expression. *bmp4* and *dachA* in situ hybridisations have been compared with images of live embryos to follow the early development of the putative ED. *dachA* is the zebrafish homologue of *Drosophila dachshund*. Its expression has been reported in the SCC and maculae and it was suggested that a dorsal domain of expression included the ED (K. Hammond, in press).

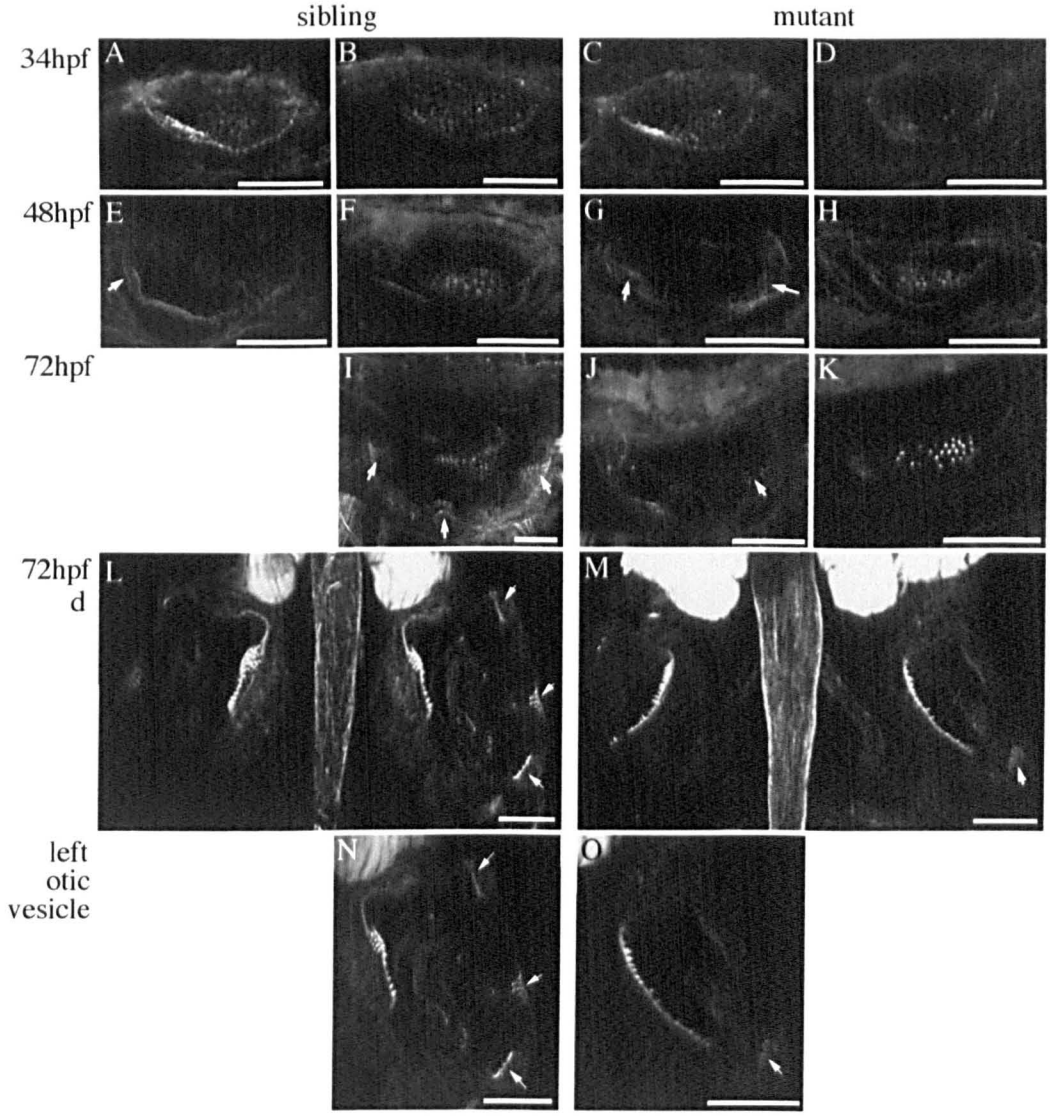

Figure 4.14 Development of sibling and *cls t3* mutant sensory patches.
FITC-phalloidin labelled actin stains showing the position of differentiated hair cells within the otic epithelium. All are lateral views with anterior to the right, except L-O, which are dorsal views with anterior to the bottom. Scale bar = 50 μm.

(A-D) At 34hpf both the sibling and mutant embryos have very few hair cells arranged in similar patterns. (E+F) At 48hpf the sibling has two macula patches: the anterior on the ventral floor of the vesicle, the posterior on the medial wall and the thickenings that will form the cristae (arrows to crista thickenings). (G+H) The mutants have two large, lateral sensory patches (arrows), no anterior macula and an abnormally shaped posterior macula (H). (I, L+N) At 72hpf the sibling has three cristae containing hair cells (arrows), a ventral anterior macula, and a medial frying pan shaped posterior macula. (J, K, M+O) The mutants have some lateral collections of hair cells (arrow) and an abnormal medial sensory patch (K).

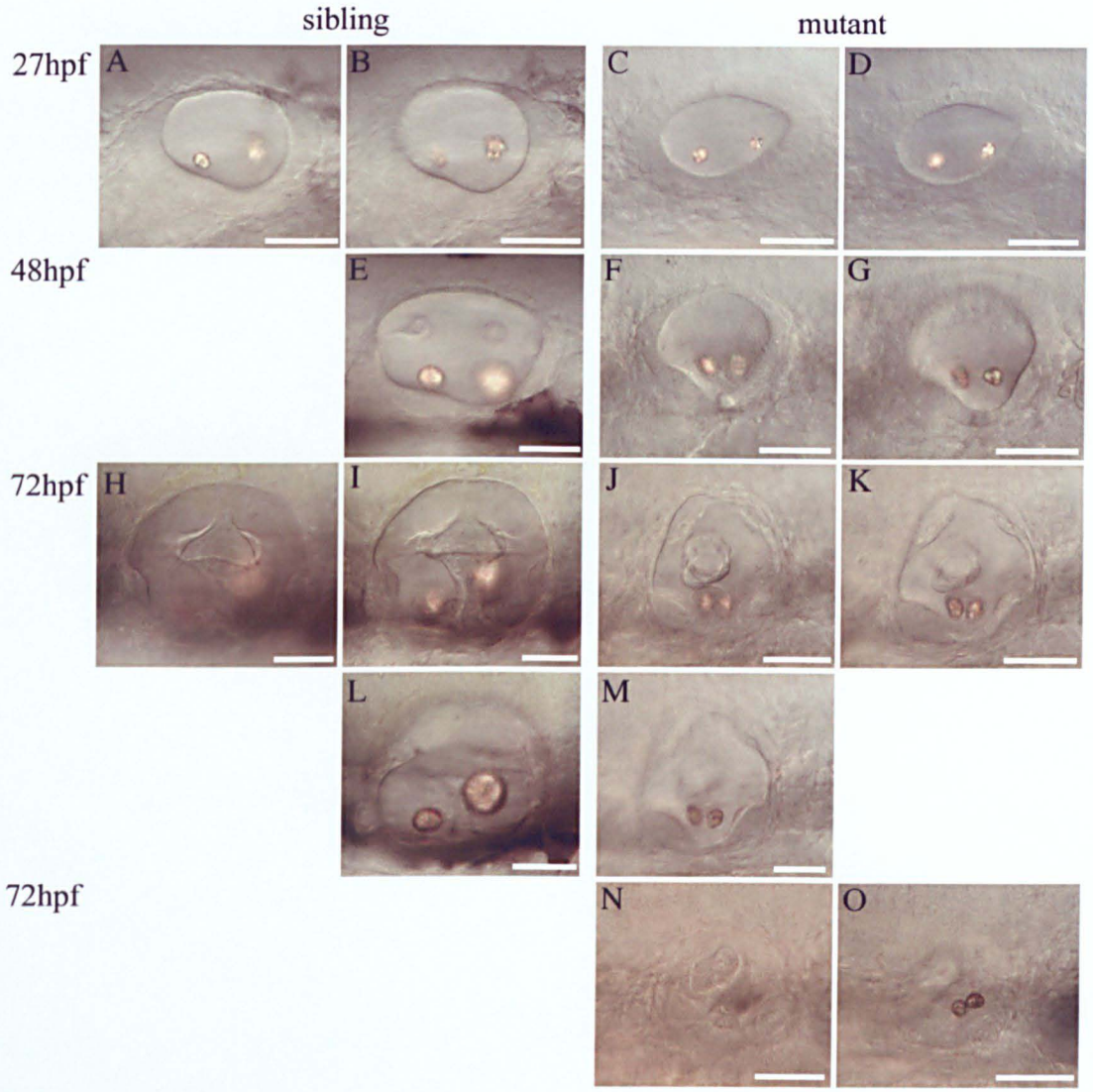

Figure 4.15 Early vesicle development in *cls t3* mutant and sibling embryos.
DIC live images of *cls t3* mutants and siblings. All are lateral views with anterior to the left. Scale bar = 50 μm.
(A-D) At 27hpf the otic vesicles of siblings and mutant embryos are of a similar size both with two otoliths. (E) At 48hpf epithelial projections are visible, pushing into the lumen of the vesicle of the sibling embryos. (J+K) They are not apparent in the mutant until later stages (shown at 72hpf). The expansion of the vesicle is not normal in mutant embryos, which are smaller than the sibling at 48hpf (anterior-posterior length 113 μm compared to 157 μm). At 72hpf there is variation in the size of vesicles (anterior-posterior length varying from 114 μm to 65 μm). The projections do form but are abnormal (see lateral projection in J).

4.3.1 Live images show a dorsomedial extension from the otic vesicle.

As mentioned in Chapter 1 the early zebrafish embryo is transparent. It is therefore possible, using anaesthetised live zebrafish embryos mounted in methyl cellulose, to follow the development of the ED. At 48hpf a dorsomedial thickening of cells is visible (Fig. 4.16A). This thickening is highlighted in blue, in a tracing of the live image (Fig. 4.16B). At 60hpf the cells in this area project dorsally to form a thin protrusion, two cell layers thick (Fig. 4.16C+D). There are numerous blood vessels in its vicinity, through which it possible to watch blood flow. However, no cell flow is seen in this projection. Adjusting the focal plane of the microscope it is possible to trace the projection to its connection to the vesicle. At 72hpf this projection has extended further dorsally (Fig. 4.16E+F) and is still visible at 5dpf (Fig. 4.16G+H).

Another dorsal structure described in zebrafish inner ear development is the dorsal septum. At 72hpf this septum projects down from the dorsolateral wall of the otic vesicle, to divide the prospective anterior and posterior SCC (Fig. 1.2D). This septum forms much later than the dorsal projection and divides the otic vesicle rather than projecting from it. It is therefore unlikely that Figure 4.16 describes the dorsal septum.

4.3.2 *bmp4* and *dachA* are markers of the early stages of ED development.

The live images describe the morphological development of the ED. The dorsal domains of *bmp4* and *dachA* expression provide molecular markers.

At 30hpf *bmp4* is expressed in a broad dorsal area (Fig. 4.17A, bracket). At 48hpf the *bmp4* domain is restricted and in the same position as the thickening in live images (compare Fig. 4.16A and Fig. 4.17B, bracket). At 60hpf the *bmp4* domain has extended dorsally (Fig 4.17C, bracket). At 72hpf the dorsal stain has faded (Fig. 4.17D).

At 48hpf the dorsal *dachA* expression domain is slightly broader. It is not restricted to just the thickening (Fig. 4.17E). At 72hpf *dachA* is expressed medially in the dorsal extension (Fig. 4.17F, bracket). It is also expressed throughout the cross structure laterally where the epithelial projections fuse (Fig. 4.19C and shadows in 4.17F). Therefore *bmp4* and *dachA* expression marks the developing ED from 30hpf to 72hpf.

4.3.3 The dorsal domain of *bmp4* expression is missing in *val* mutants.

The mouse mutant related to *valentino*, *kreisler*, does not form a normal ED. Therefore *val* mutants were analysed to see if the dorsal domain of *bmp4* was affected. Reflecting the disruption to the dorsomedial patterning of the inner ear seen in *kreisler* mutants, *val* mutants examined at 48 and 60hpf did not express *bmp4* dorsally in the vesicle (Fig. 4.18B+D). They did express *bmp4* ventrolaterally in three domains. However, by 60hpf, the anterior and posterior ventrolateral domains appeared larger than in the sibling, extending dorsally (Fig. 4.18D).

It is therefore assumed that the phenotype is similar between *valentino* and *kreisler*, both lacking an ED. These data together with the live images of the dorsal extension suggest the dorsal *bmp4* domain is marking the ED. It may also suggest that similar signalling mechanisms are involved in patterning mouse and zebrafish inner ears.

4.3.4 Dorsal *dachA* and *bmp4* expression is abnormal in *vgo* and *cls* but is unaffected in *dog* mutants.

Live images have shown that *vgo* mutants have an enlarged dorsal projection that expresses *bmp4* (Fig. 4.9 L+P). This mutant also continues to express *dachA* dorsally at 48 and 72hpf (Fig. 4.19B, E, F+H brackets). At 48hpf this *dachA* domain appears to extend further anteriorly than in the sibling (Fig. 4.19 compare B+A). The dorsal thickening is clearly visible in the mutants but is the normal size. At 72hpf the projection has extended dorsally, to a greater extent than seen in the sibling (Fig. 4.19 compare D+E brackets). It is not clear if the same forking evident in the *bmp4* expression pattern is detectable with *dachA*. However, this enlarged projection expresses the same markers and develops in a similar manner as the putative ED in wild type embryos. Therefore, it is assumed this projection is an enlarged putative ED.

In *cls* neither *bmp4* nor *dachA* are expressed dorsally. Unlike *vgo*, *cls* mutants do form epithelial projections and these continue to express *dacha* but there is no dorsomedial staining (Appendix Fig. A3) or putative ED seen in live images. *dog* mutants have a roughly normal sized otic vesicle and their SCC fuse although not normally. Unlike the other mutants described above the dorsal expression of *bmp4* labels a dorsal extension that

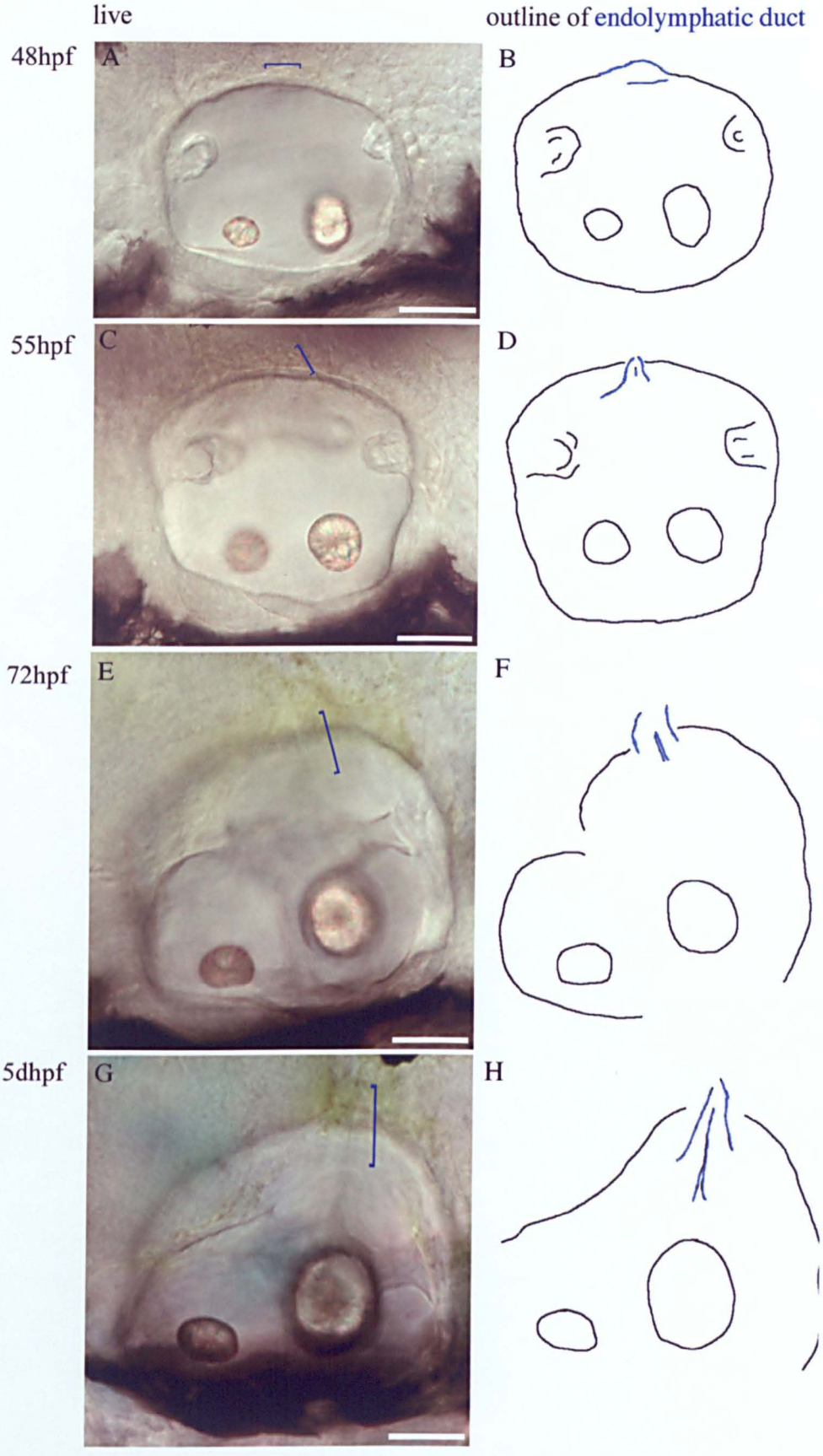

Figure 4.16 Development of the endolymphatic duct in live images.
DIC live images and tracings of major internal structures. All are lateral views with anterior to left. Scale bars = 50 μm.
(A+B) At 48hpf a dorsomedial thickening of epithelial cells is apparent, highlighted in blue in tracing and by bracket on live images. (C+D) At 55hpf this thickening has extended dorsally forming a two-layer projection with a lumen. (E+F) At 72hpf the projection has extended beyond the dorsal extent of the vesicle. (G+H) It is still visible in this type of preparation at 5dpf.

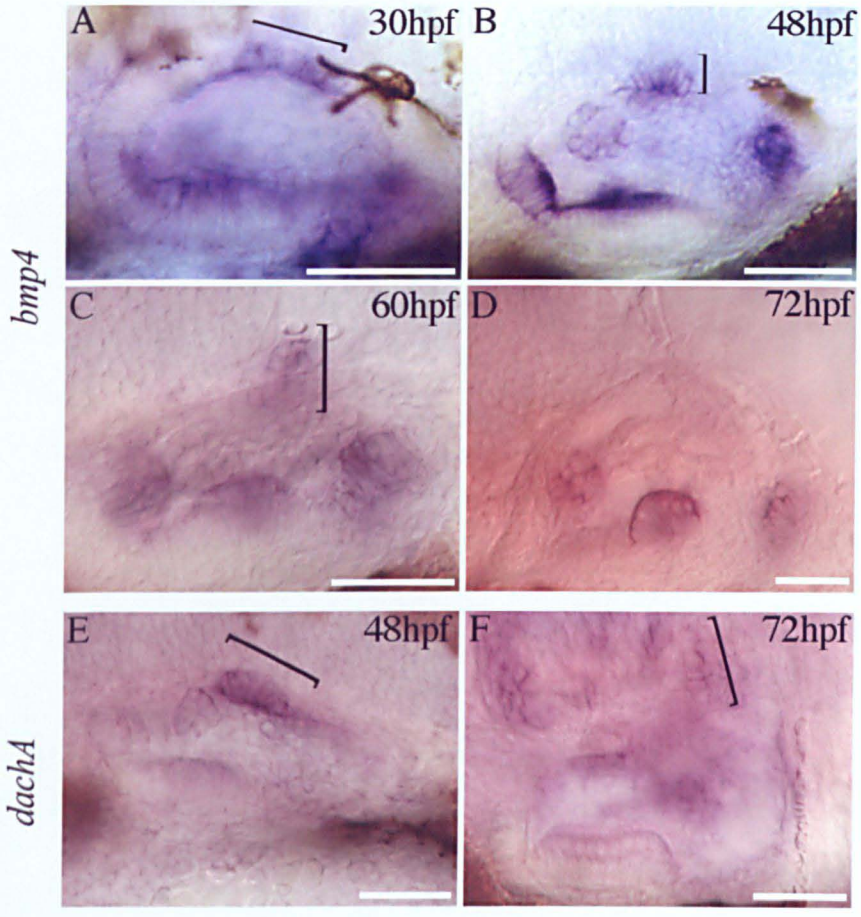

Figure 4.17 Developing ED labelled with *bmp4* and *dachA*.
Wholemount in situ hybridisations of *bmp4* and *dachA* expression in wild type embryos. All are lateral views with anterior to left. Scale bar = 50 μm.
(A) At 30hpf *bmp4* is expressed dorsally (bracket). (B) At 48hpf the dorsal stain is restricted and resembles the thickening described in live embryos above (bracket). (C) At 60hpf the dorsal extension expresses *bmp4*. (D) By 72hpf this dorsal stain has faded. (E) *dachA* is expressed in a broad dorsal domain at 48hpf including the epithelial thickening (bracket). (F) At 72hpf it is expressed dorsomedially in the dorsal projection.

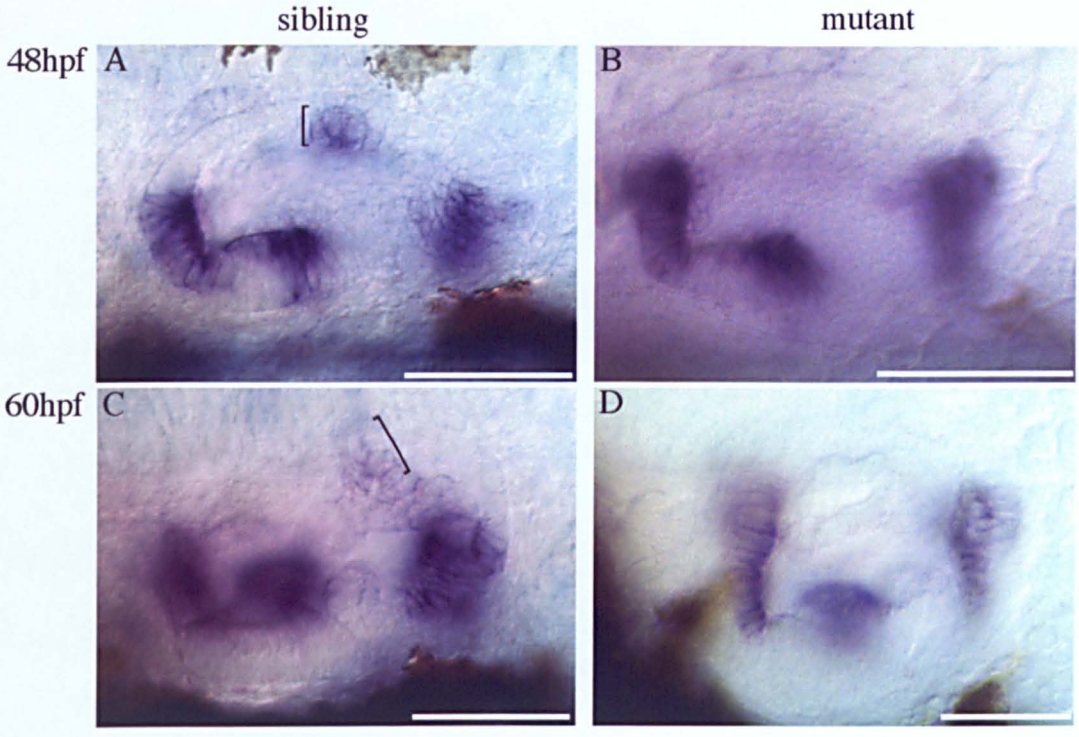

Figure 4.18 *bmp4* in *val* mutant and sibling embryos.
All are lateral views with anterior to the left. Scale bar=50 μm
(A) *bmp4* is expressed in four domains at 48hpf in siblings including a dorsal domain (bracket). (B) In the mutants there is no dorsal expression. (C) At 60hpf there is dorsal stain in the sibling (bracket) but not in the mutant (D).

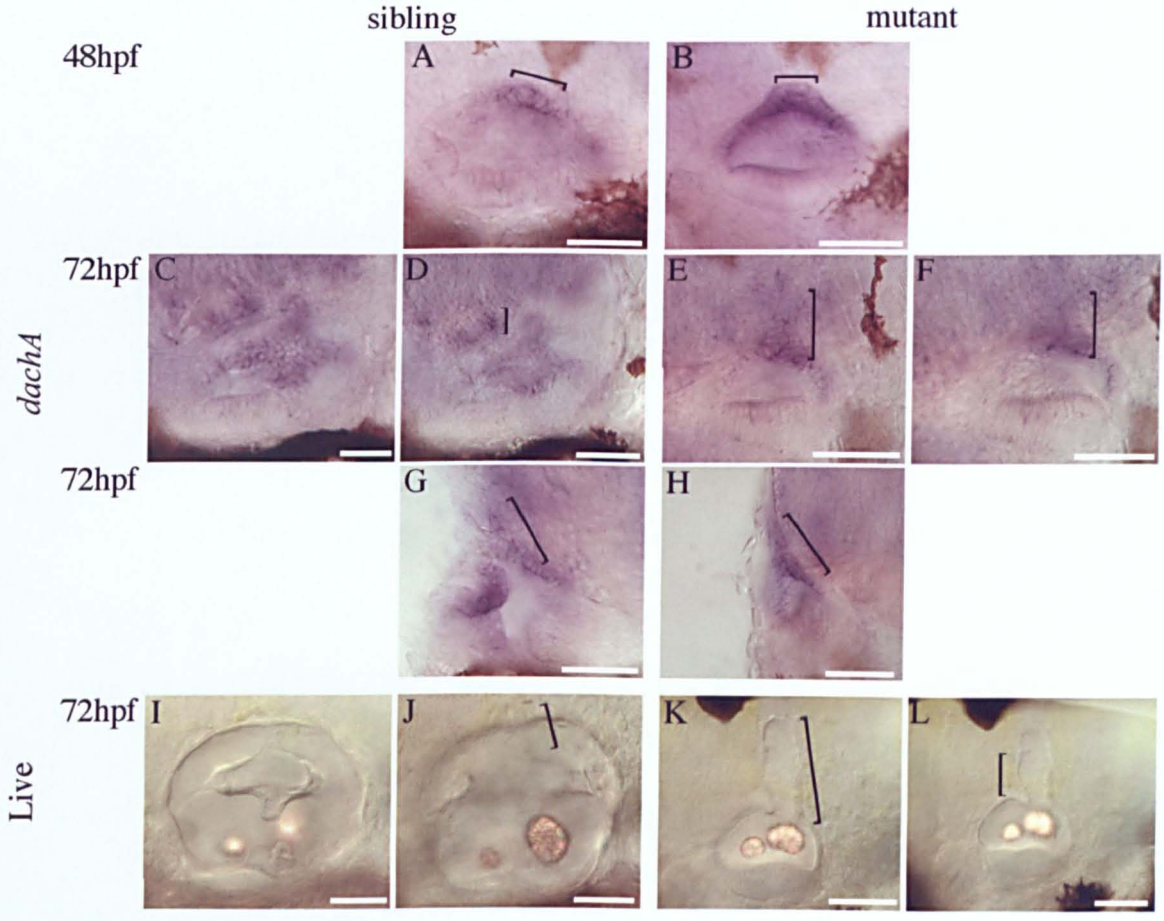

Figure 4.19 *dachA* and DIC images of live *vgo tu285* embryos.
All are lateral views with anterior to right except G+H, which are transverse sections lateral to left and dorsal to top. Scale bar = 50 μm.
(A) At 48hpf *dachA* is expressed dorsally. (B) It extends further anteriorly in the mutant than in the sibling. Its dorsal domain includes the thickening of the putative ED (A+B brackets). (C-H) At 72hpf it is expressed in the epithelial projections and in the putative ED in both siblings and mutants. (E) In the mutant the dorsomedial domain is broader and extends further dorsally than in the sibling (brackets). This extension of the dorsal domain of expression is in the same position as the large dorsal extension seen in live embryos (compare E+F with K+L).

appears to be the normal size and shape (Fig. 4.5+4.6). Putative EDs are visible in live images of *dog* mutants (Fig. 4.1D bracket).

4.4 DISCUSSION

These experiments have shown that the initiation of *bmp2b* and *bmp4* expression is different in different mutants and that the dorsal and ventrolateral domains of *bmp4* are separately regulated. They also show that *msxc* expression correlates with that of *bmp2b*, *bmp4* and the presence of cristae.

4.4.1 The initiation and maintenance of ventrolateral *bmp4* expression in the otic vesicle.

In *dog* mutant embryos the initiation of *bmp4* expression appears normal; however, the levels of expression quickly drop. This suggests *dog* has a role in maintaining *bmp4* expression and is not required for its initiation.

The *dog* gene encodes a transcription factor, Eya1 (Kozlowski et al., 2001a) and so could co-operate with other transcription factors to regulate the transcription of *bmp4* directly. Alternatively *eya1* could have a less direct role, regulating the specification, or survival of cells that will go on to express *bmp4*. At the moment there is evidence for both possibilities.

eya1 is required to regulate *bmp4* expression in the otic vesicle.

eya1 is a homologue of the *Drosophila* gene *eyes absent*. *eyes absent* is required for the development of the adult *Drosophila* eye. In *Drosophila* the eye forms as a wave of differentiation (the morphogenetic furrow) moves across an epithelial sheet of cells (the eye imaginal disc), generating multiple cell types, including sensory cells and neurons in its wake. Eyes absent is one of a collection of proteins that initiate and regulate this process. The others include members of the Pax (Eyeless and Twin of eyeless), Six (Sine oculis), and Dach family (Dac). These proteins are involved in a complicated web of interactions, with feedback loops and protein-protein interactions, which are not fully understood (see Fig. 4.20). However, this web is important in regulating the expression of its constituent genes, and the relative levels of each protein (Curtiss and Mlodzik, 2000). There is thought

to be a feedback loop between *decapentaplegic*, the *Drosophila* BMP homologue, and *eyes absent*. However, it is not clear which protein initiates the loop; *eyes absent* has been shown to be required for the initiation of *decapentaplegic* (Pignoni, 1997; Hazelett et al., 1998), while *decapentaplegic* has been shown to be required to initiate *eyes absent* (Curtiss and Mlodzik, 2000).

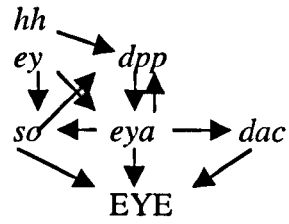

Figure 4.20 Sketch of the web of interactions required to pattern the *Drosophila* eye disc.

This is the current model of the web of interactions between the genes involved in the initiation of the Morphogenetic Furrow (MF) during *Drosophila* eye development (adapted from Curtiss and Mlodzik, (2000). *eya* is thought to be both downstream and upstream of *dpp* at different times during eye development but it is required for the maintenance of *dpp* during the initiation of the MF.
Abbreviations: *dac, dachshund*; *dpp, decapentaplegic*; *ey, eyeless*; *eya, eyes absent*; *hh, hedgehog*; *so, sine oculis.*

A similar Pax-Eya-Six-Dach pathway is involved in patterning chick somites, Medaka eye development (Heanue et al., 1999; Lagutin, 2001) and in the developing mouse inner ear (Xu et al., 1999). In the mouse as in the fly eye the expression of *Six1* (homologue of *so*) but not *Pax2* or *8* (*ey* homologues) is dependent on *Eya1* (Xu et al., 1999). It is possible that a similar Pax-Eya-Six-Dach pathway is used during zebrafish otic vesicle development.

Members of the homologous families are expressed in or adjacent to the zebrafish ear (Table 4.2). *eya1* is expressed from preplacodal stages, well before *bmp* expression in the otic vesicle (Sahly et al., 1999). The *so* homologue *six4.1* is expressed in a similar pattern to *eya*, marking the placode, the ventral vesicle and the epithelial projections (*six 4.2* + *six4.3* are also expressed weakly in otic vesicle (Kobayashi et al., 2000)). Members of the Pax family are also expressed from placodal stages (*pax2.1*, *pax2.2*, *pax5*, and *pax8* (Pfeffer et al., 1998)). *dac* family members are expressed at similar stages to *bmp4*. *dachA*, *B*, and *C* are expressed in distinct areas of the otic vesicle (Hammond et al., (in press)+Table 4.2).

If a similar pathway were at work in zebrafish we would expect the *dog* mutants not to express the *dpp, dac,* and *so* homologues, *bmp*, *dach* and *six*. So far only the *bmps* have

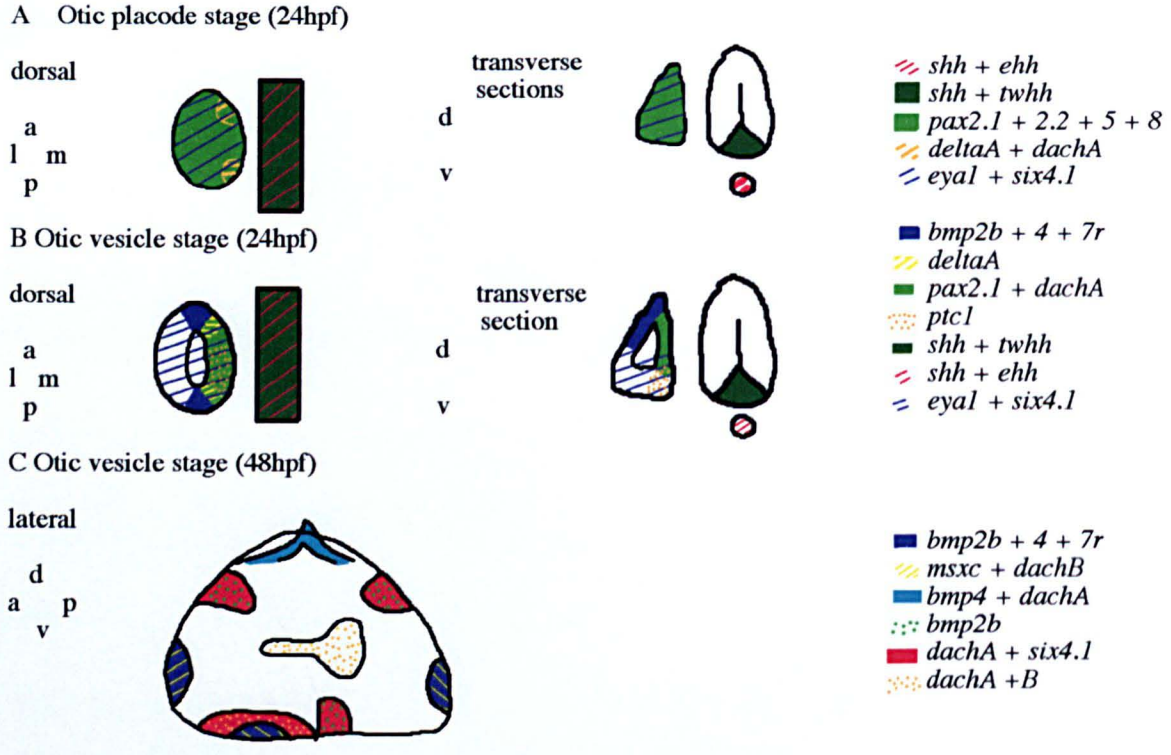

Figure 4.20b The expression patterns of key genes from the *pax*, *hh*, *delta*, *bmp*, *dach*, and *six* families during inner ear development.

This figure illustrates the data in table 4.2 which describe the structures labelled by these genes in more detail and provides the relevant references. The boundaries of expression patterns are unconfirmed as double in situs have not been done.
A + B show a dorsal view of both the otic placode and vesicle respectively and the notochord and floor plate.

Abbreviations: *ehh*, *echidna hedgehog*; *shh*, *sonic hedgehog*; *twhh*, *tiggywinkle hedgehog*

been analysed. These data suggest that *eya1* is required to maintain but not initiate *bmp4* expression. However, these data can not tell us if this is a direct relationship. That would require mapping Eya binding sites at the Bmp promoter amongst other experiments. It is difficult to see how the broad domain of *eya1* alone could directly regulate the expression of the *bmps* in their discrete ventrolateral pattern. Therefore other factors (possibly *six*) may be required.

Table 4.2 The inner ear expression patterns of zebrafish homologues of the *Drosophila* eye patterning genes.

Gene homologues (*Drosophila*) zebrafish	Expression pattern in zebrafish inner ear	
(*hh*) *hh*	*shh*[a], *twhh*[b], + *ehh*[c]	Tissue adjacent to otic vesicle, the notochord and floor plate.
	patched (Hh receptor)[d]	Early otic vesicle.
(ey) *pax*	*pax8* [e]	Early otic primordium, preplacode, placode.
	pax2.1[f]+*2.2*[e]	Preplacode, placode, hair cells in macula + crista.
	pax5 [e]	Placode, anterior macula.
(*eya*) *eya*	*eya1*[i]	Preplacode, ventral otic vesicle, lateral line.
(*so*) *six*	*six4.1*[h]	Preplacode, placode, epithelial projections, lateral line.
(*dpp*) *bmp*	*bmp2b*[g]	Cristae, lateral line, epithelial projections.
	bmp4[g]	Cristae, lateral line, ED.
	bmp7r[g]	Cristae, lateral line.
	bmp7[g]	Discrete area of posterior otic vesicle.
(*dac*) *dach*	*dachA*[j]	Epithelial projections, ED, maculae, lateral line.
	dachB[j]	Anterior macula, lateral line.
	dachC[j]	Ventrolateral region of vesicle

References: a, (Krauss et al., 1993); b, (Ekker et al., 1995); c, (Currie and Ingham, 1996); d, Hammond, in preparation; e, (Pfeffer et al., 1998); f, (Riley et al., 1999); g, (Mowbray et al., 2001); h, (Kobayashi et al., 2000); i, (Sahly et al., 1999); j, (Hammond et al., in press).
Abbreviations: *dac, dachshund*; *dpp, decapentaplegic*; ED, endolymphatic duct; *ehh, echidna hedgehog*; *eya, eyes absent*; *ey, eyeless*; *hh, hedgehog*; *shh, sonic hedgehog*; *so, sine oculis*; *twhh, tiggywinkle hedgehog*.

eya1 may be required as a cell survival factor.

As the ventrolateral areas of *bmp* expression are not being maintained, the cells that normally express them could be switching fate or dying.

The *eya* mutants in *Drosophila*, mouse and zebrafish all show an increase in cell death (Bonini et al., 1993; Xu et al., 1999; Kozlowski et al., 2001a+b). Therefore the cells may be dying before they express *bmp4*. In zebrafish this domain of cell death is restricted to a dorsolateral domain in the *dog* mutant that is not seen in the sibling, and includes the *bmp* expression domain (Fig. 4.21). As the increase in cell death has only been reported at a stage after *bmp4* expression has been initiated (28hpf and 24hpf respectively) it would be that the initial expression of *bmp4* is normal in *dog* mutants, but fades as cells die due to lack of *eya1*.

eya1 is expressed from preplacodal stages (10hpf) in all the cranial placodes. It is expressed throughout the otic placode until 20hpf, when it is restricted to the ventral half of the vesicle and is expressed within the otic vesicle at least until 72hpf (Sahly et al., 1999). Its expression domain includes that of the *bmps* at 24hpf but does not include the region of excessive cell death (Fig. 4.21). As a nuclear protein it is unlikely that Eya1 directly signals to these dorsolateral cells to ensure their survival. In zebrafish all the cells which will make up the inner ear are believed to come from the otic placode (Haddon, 1997) and so their ancestors all expressed *eya1*. Exposure to *eya1* at this early stage may be important in ensuring cell survival, rather than a trophic signal coming from *eya1* expressing ventral cells at a later stage. The mouse *Eya1* homologue is reported to have a similar expression pattern to the zebrafish (Kalatzis et al., 1998). The murine knockout also shows an increase in apoptosis in the inner ear of homozygous mutants, although it is not clear whether this is localised to any specific area (Xu et al., 1999).

If the cells that are not maintaining *bmp* expression are not dying they could be changing fate. Fate maps from 17hpf zebrafish otic placode have revealed some organisation of cell fate at this stage. Cells from one area could contribute to the anterior cristae/SCC/macula (Haddon, 1997) and so fates are probably beginning to be specified at the time and in the area of *eya1* expression. *dog* mutants do not form cristae and may have enlarged projections; therefore, one interpretation is that cells switch fate from cristae to SCC. Cell labelling studies have shown that cells from the *bmp4*-expressing domains can form cristae, but it is not known if they can also form SCC in wild type or mutants (Kozlowski et al., 2001b).

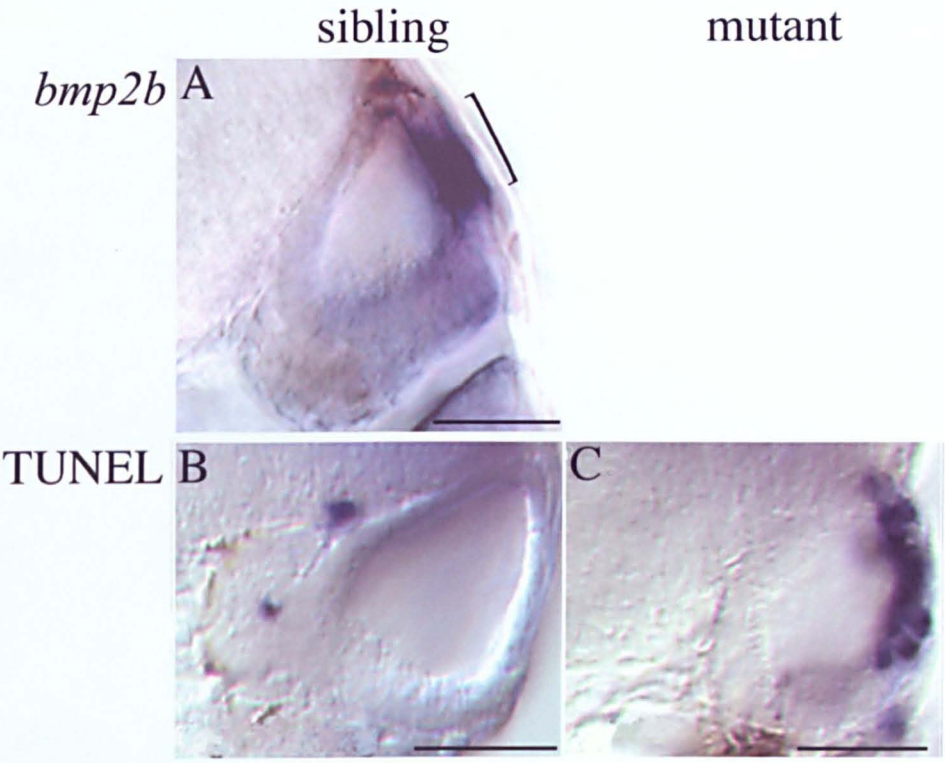

Figure 4.21 Comparison of *bmp2b* wholemount in situ hybridisations and TUNEL-labelled cell death in 28hpf *dog tm90b* mutant and sibling embryos. All are transverse sections with lateral to the right dorsal to top. Scale bar=50 μm.
(A) At 28hpf *bmp2b* is strongly expressed laterally. (B+C) TUNEL labelling of cell death has shown *dog* mutant embryos to have an increase in levels of cell death laterally compared to the few medial cells seen in the sibling (B).

4.4.2 *eya1* is also required to regulate *bmp2b* expression.

bmp2b is normally expressed in domains very similar to *bmp4* (24-72hpf) and these domains are not maintained in *dog*. It is therefore possible that similar regulatory mechanisms are maintaining *bmp2b* expression as well as *bmp4*. However, it is not clear if *bmp2b* expression is initiated normally in *dog*. *bmp2b* is expressed earlier than *bmp4* (20hpf compared to 24hpf) in a broad dorsal domain. Its initiation mechanism is therefore different to that of *bmp4*.

Conclusion

From these data and the discussion above it is concluded that *eya1* is required to maintain the expression of both *bmp4* and *bmp2b* in the inner ear and that there are differences in the initiation of the expression of these two Bmps. As mentioned above vertebrates have multiple homologues of the *Drosophila* genes that make up the *eya* pathway. The expression of multiple members of the same families may overlap at some stages and be independently regulated at others, providing extra levels of control and increasing their possible functions.

It is hypothesised that the cells that go on to express *bmp2b* and *bmp4* require the *eya1* signal at an early stage as a survival factor.

4.4.3 *vgo* fails to initiate the proper expression of *bmp4*.

In *vgo* (a *tbx1* mutant) *bmp4* is not initiated properly, with only very faint levels of expression visible at early stages and no ventrolateral stain seen subsequently. This suggests *vgo* is required for the initiation of *bmp4* expression.

The *vgo* phenotype is morphologically obvious at an earlier stage than that of *dog*. The otic vesicle is induced, cavitates and increases in size up to 42hpf but it then does not continue to increase in size. The early marker *pax2.1* has been analysed and appears normal (Whitfield, pers. comm.). However, inner ear patterning is defective by 24hpf as the vesicle is smaller than normal. The early expression of both *bmp2b* and *bmp4* is abnormal in *vgo* mutants; their normal ventrolateral expression pattern is absent. Another ventral floor marker, *otx1*, is also not expressed (Whitfield et al., 1996). However, *bmp4* is expressed at the normal stage and level dorsally, although the domain is subsequently larger

than normal. The dorsal aspects of this mutant will be discussed in the ED section of the discussion.

These data suggest that:

- *vgo* is required for the early patterning of the inner ear but not for its induction.
- The dorsal domain of *bmp4* expression is regulated independently of ventrolateral expression.
- The dorsal structure labelled by *bmp4* is normally repressed by *vgo*.

In other systems members of the Tbx family have been implicated as downstream targets of *bmp* signalling, e.g. in chick heart and limb development and in *Drosophila* wing development (Nellen et al., 1996; Rodriguez-Esteban et al., 1999; Yamada et al., 2000). Members of the Tbx family are expressed in the mouse (*tbx1*, (Chapman et al., 1996) and chick otic vesicle (*Tbx2, Tbx3* (Gibson-Brown et al., 1998). The *Tbx1* locus is within an area normally deleted in DiGeorge syndrome in humans (Chieffo et al., 1997). This syndrome includes defects in ear function due to inflammation but there are no data on any developmental problems with the inner ear. However, the mouse *tbx1* knock-out recapitulates some of the phenotype of DGS, showing similar late ear defects, but also allowing examination of early developmental problems (B.E. Morrow, pers. comm.). During development these knock-outs show a reduction in the size of the cochlea, vestibule and SCC which appears very similar to the *vgo* phenotype.

Given the expression of the *bmps* and *Tbx2* (Chapter 2+3) and the early phenotype of *vgo* the Tbx family are probably involved at an early stage of inner ear patterning than the Bmps.

Conclusion

From these studies into the *vgo* mutant it is concluded that *tbx1* is required for normal *bmp* expression in the otic vesicle. *tbx1* is clearly required early in inner ear development. However, it remains to be seen where and when *tbx1* is expressed in zebrafish.

4.4.4 Are the *bmps* required for SCC development?

This study does not provide a conclusive answer to whether or not the *bmps* are involved in SCC development. In both *cls* and *dog* mutants there is abnormal SCC development and abnormal *bmp* expression. In *vgo* there is no SCC development and severely reduced levels of *bmp* expression from the earliest stages of otic development. Therefore normal *bmp* expression was not seen in mutants with abnormal SCC development; however, the variety in the phenotypes (of both *bmp* expression and SCC development) seen have not allowed a clear suggestion for the role of Bmp signalling in SCC development (see Chapter 5, 6+7).

In the chick, *bmp4* and *bmp7* are expressed in the mesenchyme around the developing SCC, the SCC epithelium and the walls of the ampulla (chamber containing the cristae) (Wu and Oh, 1996; Chang et al., 1999). Adding ectopic Noggin protein, a BMP antagonist, affected the initial outpocketing and continued growth of the SCC (Chang et al., 1999; Gerlach et al., 2000). These experiments suggest that BMP4 is required for the correct regulation of cell division and apoptosis required to form SCC. It is not known whether the BMP4 signal comes from the mesenchyme or the SCC.

It is possible that the *bmps* are involved in a similar mechanism in the zebrafish. Both *bmprIB* and *smad5* are expressed throughout the epithelial projections (see Fig. 3.1+3.5) and so a Bmp signal could be transduced in those cells. *bmp2b*, *bmp4*, *bmp7r*, and *bmp7* are all expressed strongly within the otic vesicle and could act in a paracrine fashion on the projections (see Chapter 5, 5.3.5). *bmp2b* is also expressed within the developing projections and so could act in an autocrine manner.

bmp2b expression in the projections of *dog* mutants could provide a link between the Bmps and cell division in the projections. *dog* mutants have enlarged epithelial projections and despite reduced levels of *bmp2b* expression elsewhere in the otic vesicle the mutants retain strong discrete areas of *bmp2b* expression within the projections. These areas could mark areas of abnormal cell division producing the enlarged projections. The levels of cell division have not yet been assessed in *dog* mutants. However, wild type otic vesicles staining with BrdU and anti-phosphorylated histone H3 have not revealed any hot spots of cell division. The increase in otic vesicle size is thought to be due to an increase in cell volume rather than cell number (Haddon, 1997). *bmp2b* may therefore be required to

specify cells that enable increases in cell volume in wild type embryos rather than upregulating cell division.

The early loss of *bmp* expression in *vgo* mutants as discussed above suggests an early defect in inner ear development upstream of both *bmp* expression and SCC development.

Conclusion

These expression data together with studies of the rescued *bmp2b* mutant *swirl* (see Chapter 6) suggest *bmp2b* is required to form normal SCC. The role of *bmp4* is less clear although antagonist bead studies in chick suggest it could act as a paracrine signal as it is not expressed in the epithelial projections. Further evidence of *bmp* involvement in SCC development is discussed in Chapter 5 when ectopic BMP4 coated beads applied to zebrafish otic vesicles affected SCC development (see 5.6.5).

4.4.5 *msxc* expression is associated with *bmp2b* and *bmp4* expression domains.

In wild type embryos and all the mutants studied so far *msxc* expression correlates with that of *bmps* in the cristae. It is expressed after the *bmp2b* and *bmp4* in three ventrolateral domains that become the cristae. In mutants where *bmp2b* and *bmp4* expression is reduced (*dog* and *vgo*) *msxc* expression is lost; in mutants where *bmp2b* and *bmp4* are expressed in an abnormal pattern (*cls*) *msxc* shows a similar defect. In no case was *msxc* present in the absence of *bmp2b* and *bmp4* expression or normal *bmp2b* and *bmp4* expression present in the absence of *msxc*. These data strongly suggest that *msxc* is a direct target of the BMP signalling in the cristae.

There is some precedent for this sort of relationship in other systems, although in these cases paracrine signalling between different cells is involved, rather than the autocrine signals that appear to function in the cristae. For example in mice BMP4 and MSX1 establish a feedback loop between the epithelium and mesenchyme to initiate early stages of tooth development (Jernvall and Thesleff, 2000). This sort of relationship may be at work dorsally and is discussed in Chapter 3 (3.7.4). To test whether *msxc* is a target of BMP in the cristae, exogenous BMP4 protein was added using protein coated beads to see

if ectopic *msxc* expression could be induced. These experiments are described in Chapter 5.

4.4.6 High levels of *bmp4* are associated with precocious ventrolateral sensory patches.

The *colourless* mutant provides a further link between *bmp*, *msxc*, and crista development. In the *cls* mutant *bmp4* appears to be expressed at higher levels in two ventrolateral domains. These domains also express *msxc* and differentiated hair cells are present in the same region. Although these domains are expressing the same markers as are found in wild type cristae, in *cls* mutants they contain differentiated hair cells earlier than in wild type and are not the characteristic shape of cristae. The upregulation in the level of *bmp4* expression seen in *cls* could indicate that levels of Bmp4 protein are higher. Perhaps these protein levels have to reach a certain threshold level before cristae development can proceed and in *cls* this level is reached at an earlier stage, enabling the development of precocious patches.

4.5 The dorsal area of *bmp4* staining marks an endolymphatic duct.

4.5.1 Zebrafish have an endolymphatic duct.

This chapter provides a description of the early development of the ED. The live images show a thickening, which goes on to form a mediodorsal projection that is labelled by *dachA* and *bmp4*. *dachA* is also expressed in the SCC including the dorsal septum. However, in transverse sections it is possible to see the more specific medial *bmp4* stain compared to the lateral and medial stain of *dachA* (Fig. 4.22B+C). This resembles an invaginated structure reported by M. Bever in plastic transverse sections of later stages (Fig. 4.22A (Bever and Fekete, in press)).

The study of *vgo* and *val* mutants provides supportive evidence that this dorsal structure is an ED, given the similarity to the phenotype seen in related mutants in other organisms. In the mouse *tbx1* mutant the ED is enlarged (B.E. Morrow, pers. comm.) as it is in *vgo* and in *kreisler* it is absent or reduced (Deol, 1964) as it is in *val*. There may be a connection between the cystic state of some of these mutant otic vesicles and the absence of an ED (see 4.5.4).

4.5.2 *bmp4* is an early marker of the zebrafish endolymphatic duct.

bmp4 is expressed dorsally from around 27hpf, along the dorsal roof of the otic vesicle. It also labels a dorsal projection that is visible from 48hpf and appears to be a pinching of the dorsal roof. The cells may divide in a certain way to push themselves dorsally or undergo cytoskeletal rearrangements.

Different members of the BMP family may be involved in ED development in chick, as although *Bmp4, Bmp5,* and *Bmp7* are expressed dorsally in the otic cup of the chick (Oh et al., 1996) only *Bmp7* is reported to be expressed in the formed ED (Wu et al., 1998).

4.5.3 *vgo* develops an enlarged endolymphatic duct.

Live images show that *vgo* develops an enlarged dorsal projection. This structure expresses *bmp4* and *dachA* and is thought to be an enlarged ED (Fig 4.19). In other species the expression of members of the Tbx family is associated with the ED. The *Tbx1* mouse knock-out phenotype is very similar to *vgo*. The ear remains a simple otocyst, with no SCC and an enlarged ED (B.E. Morrow pers. comm.). In the chick *Tbx2* is expressed in the external auditory meatus, SCC and the ED (Gibson-Brown et al., 1998). It is not known when and where *tbx1* is expressed in the zebrafish otic vesicle, or if the inner ear defects are due to earlier patterning defects elsewhere in the embryo e.g. the hindbrain. *tbx2* is not expressed in the developing zebrafish ED (see Fig. 3.13).

4.5.4 Is the ED required to regulate vesicle size?

Normal otic vesicle size appears to correlate with normal development of the ED, as assessed in live pictures and by the presence of the dorsal *bmp4* expression domain. *dog* mutants have a normal ED and a roughly normal sized vesicle. However, *cls* and *val*, which both lack an ED, can develop cystic vesicles (Fig. 4.23C+D) and *vgo* mutants, which have an enlarged ED, form small vesicles. As described earlier the ED may be required to regulate the volume of endolymph within the inner ear (4.1.4) and this could be important in regulating the size of the vesicle. Therefore, in *vgo* it may be functioning abnormally, failing to allow fluids to transfer across its surface or draining too much fluid resulting in a small vesicle. However, in *cls* and *val* the vesicle appears to accumulate fluid through an

unknown mechanism (osmosis/diffusion), which cannot be regulated, as the ED is not present.

There are several other zebrafish mutants in which otic vesicle size is affected. *big ears*, *headphones*, *lauscher* (Whitfield et al., 1996) and *helter skelter* (Malicki et al., 1996) form large otic vesicles while *microtic*, *little ears* (Whitfield et al., 1996) and *antytalent* (Malicki et al., 1996) form small vesicles. These mutants may have abnormalities in ED development or function. Analysis of these mutants, together with identifying specific markers for the ED such as channel proteins (e.g. Pendrin and aquaporin (Everett et al., 1999; Merves et al., 2000)), may help explain the function of this structure. It is also possible that zebrafish could provide simpler models of complex human diseases that are proving hard to generate in mouse with phenotype-genotype variations due to strain (e.g. DiGeorge syndrome, reviewed in Botta et al., (2001)).

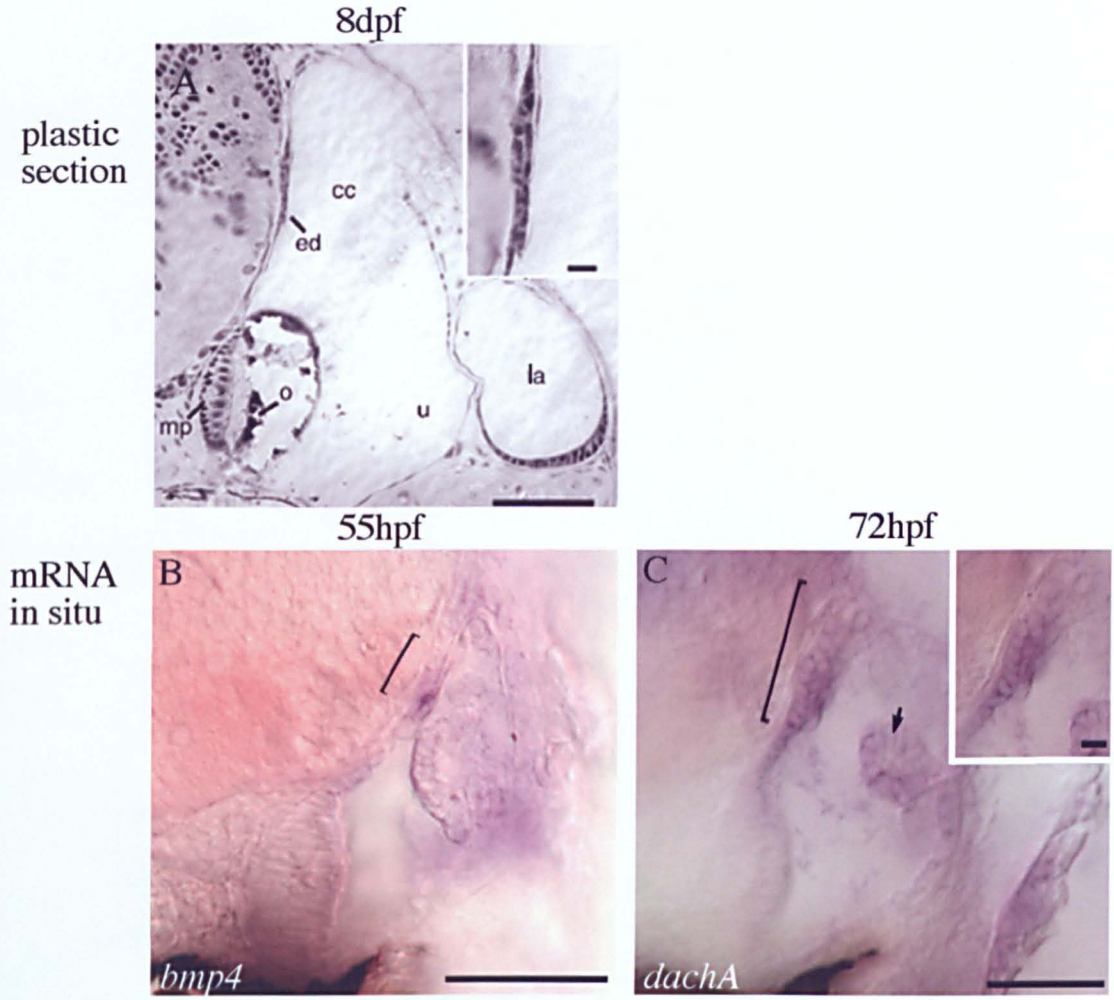

Figure 4.22 Comparison of 8dpf plastic transverse section with thicker hand cut sections of whole mount in situ hybridisations of *bmp4* and *dachA* at earlier stages. All are transverse sections with lateral to the right. Scale bars=50 μm and 10 μm in insets. Plastic section reproduced from Bever and Fekete, (in press).

(A) The plastic section shows a 2-cell thick layer of cells positioned dorsomedially; at higher magnification this is shown to be a single cell layer evagination (inset). (B) At an earlier stage a similar thickening, in a similar position, expresses *bmp4* (55hpf, bracket). (C) At 72hpf this thickening also expresses *dachA* (bracket+ inset). *dachA* also labels the more lateral epithelial projections.

Abbreviations: cc, common crus; ed, endolymphatic duct, la, lateral ampullae (chamber containing lateral crista); mp, posterior macula; o, otolith; u, utricle.

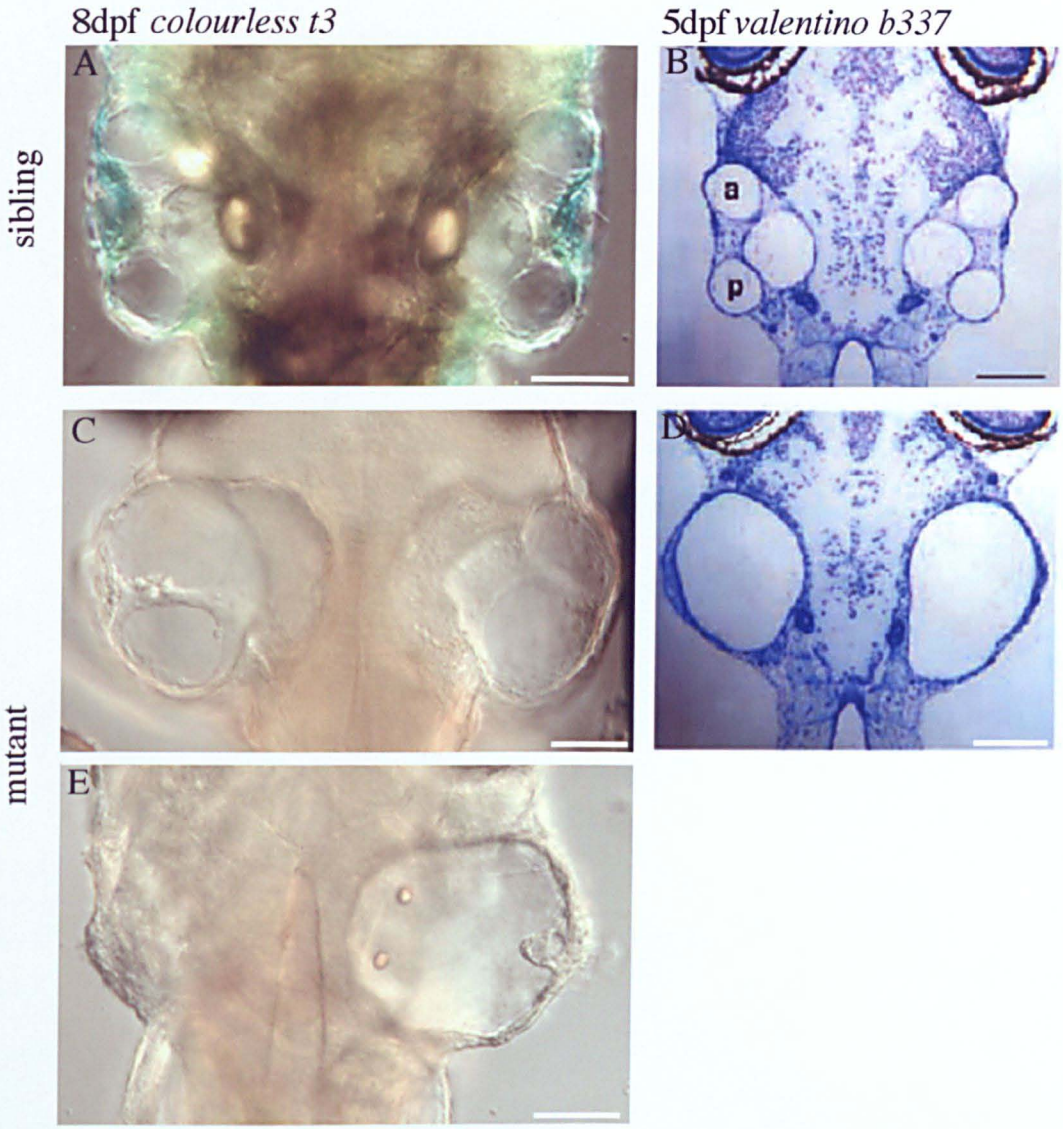

Figure 4.23 Comparison of DIC live images of *cls t3* mutant and sibling embryos and histological sections of stained *val b337* embryos.
All are dorsal views with anterior to the top. Scale bar = 100 μm
(A+B) In sibling embryos the otic vesicle is divided up laterally into the SCC by the fusion of epithelial projections (shown at 8dpf in A and 5dpf in B). (C+E) In *cls* mutants the otic vesicle is greatly expanded and not all the epithelial projections form so the vesicle is not divided. (D) This is also seen in *val* shown at a slightly earlier stage (5dpf). *val* also develops expanded otic vesicles that are not divided. (E) The size of the otic vesicles in *cls* mutants can vary greatly in size. Here the right hand ear is swollen while the left hand ear remains small. (B+D reproduced with permission from Moens et al., 1998)

Chapter 4 Appendix

Initial characterisation of the inner ear and lateral line phenotype of the *colourless* mutant.

A.1 INTRODUCTION

The *sox10* gene is disrupted in *Colourless*. *sox10* is normally expressed in the inner ear from placode stages (18hpf). It is also expressed in migrating and premigratory neural crest cells (ncc) (Dutton et al., 2001). In *cls* mutants, ncc form, but then a sub-population, those with non-ectomesenchymal fates, die (Kelsh and Eisen, 2000). It is thought that *sox10*, together with other genes, is required to specify the fate of this ncc sub-population.

It is not clear whether the otic defects documented here are a direct consequence of the lack of functional *sox10* in the otic vesicle, or a secondary effect due to the loss of signals or cellular contribution from the ncc. However, given the strong and conserved expression of *sox10* in the inner ear, a direct role is likely.

This appendix describes the inner ear phenotype in *cls* ^{t3}. This includes live images, actin stains and in situ hybridisations.

A.2 *cls* otic vesicles do not develop normal epithelial projections.

The early stages of *cls* development have been described within Chapter 4 (see Fig. 4.15). This appendix describes its development at later stages. At 5dpf sibling inner ears have expanded. However, the basic plan resembles that seen at 72hpf. The lateral part of the otic vesicle is divided into three SCC by a cross shaped structure of epithelial projections and there are two otoliths, a smaller, anteroventral one and a larger, posteromedial one (Fig. A1A-C). In the mutant, however, the defects apparent at early stages are still present. There continues to be variation in the size of the vesicle (Fig. A1 compare I+M) and in the extent of epithelial projection development.

The small otic vesicles in *cls* mutants can produce epithelial projections (Fig. A1L+M). However, these do not fuse normally. The lateral projection can fuse with the anterior and posterior projections but the normal cross shaped structure is not formed (Fig. A1I-K). When the vesicles become swollen this lack of fusion could be due to the distances between

When the vesicles become swollen this lack of fusion could be due to the distances between projections being too great. At 6dpf some vesicles do not appear to have projections (Fig. A1P-R). This could be due to earlier small projections not developing further, as all embryos examined at earlier stages appear to have at least small projection-like protrusions.

The SCC defect can also be described using *dachA* expression. This gene marks the SCC, the putative ED, and is faintly expressed in the maculae. At 48hpf siblings express *dachA* in a broad dorsal domain including the putative ED (A3A+B bracket), the epithelial projections (Fig. A3A arrows), and faint expression in the developing anterior macula (A3B arrowhead). The mutants do not express *dachA* dorsally in either the ED or the SCC, although it is expressed in the maculae, possibly at higher levels than in the sibling (Fig. A3B+C arrowhead). At 72hpf in the sibling, the cross structure formed by the fusion of the epithelial projections (Fig. A3E) and the putative ED (Fig. A3F bracket) strongly express *dachA*. This cross structure is not seen in *cls*. However, the projections that do form do express *dachA* (Fig. A3G arrow).

The lack of dorsal *bmp4* expression (Fig. 4.11J) suggests the lack of an ED. It was thought possible that the variable otic vesicle size phenotype could be due to the presence or absence of an ED. Of the ten mutants examined, only one appeared to develop an ED and none of the mutants examined expressed *bmp4* dorsally. In the one case where an ED formed this appeared to be abnormal (Fig. A1R). Therefore there may be a correlation between vesicle size and the presence of a functioning ED. The lack of an ED may inhibit the ability of the otic vesicle to regulate its volume, which is then influenced by other factors.

Abnormal otolith development described at earlier stages is still obvious. In *cls* the otoliths remain small and in the same plane (Fig. A2 compare B+C). The otolith phenotype suggests problems in macula development.

A.3 *cls* develop abnormal sensory patches

Two assays were used to analyse the development of the sensory patches in *cls*: actin stains and *brn3.1* in situ hybridisations. Both these techniques mark differentiated hair cells in the sensory patches. However, the actin stains provided clearer information on the actual state of sensory patch development in *cls*.

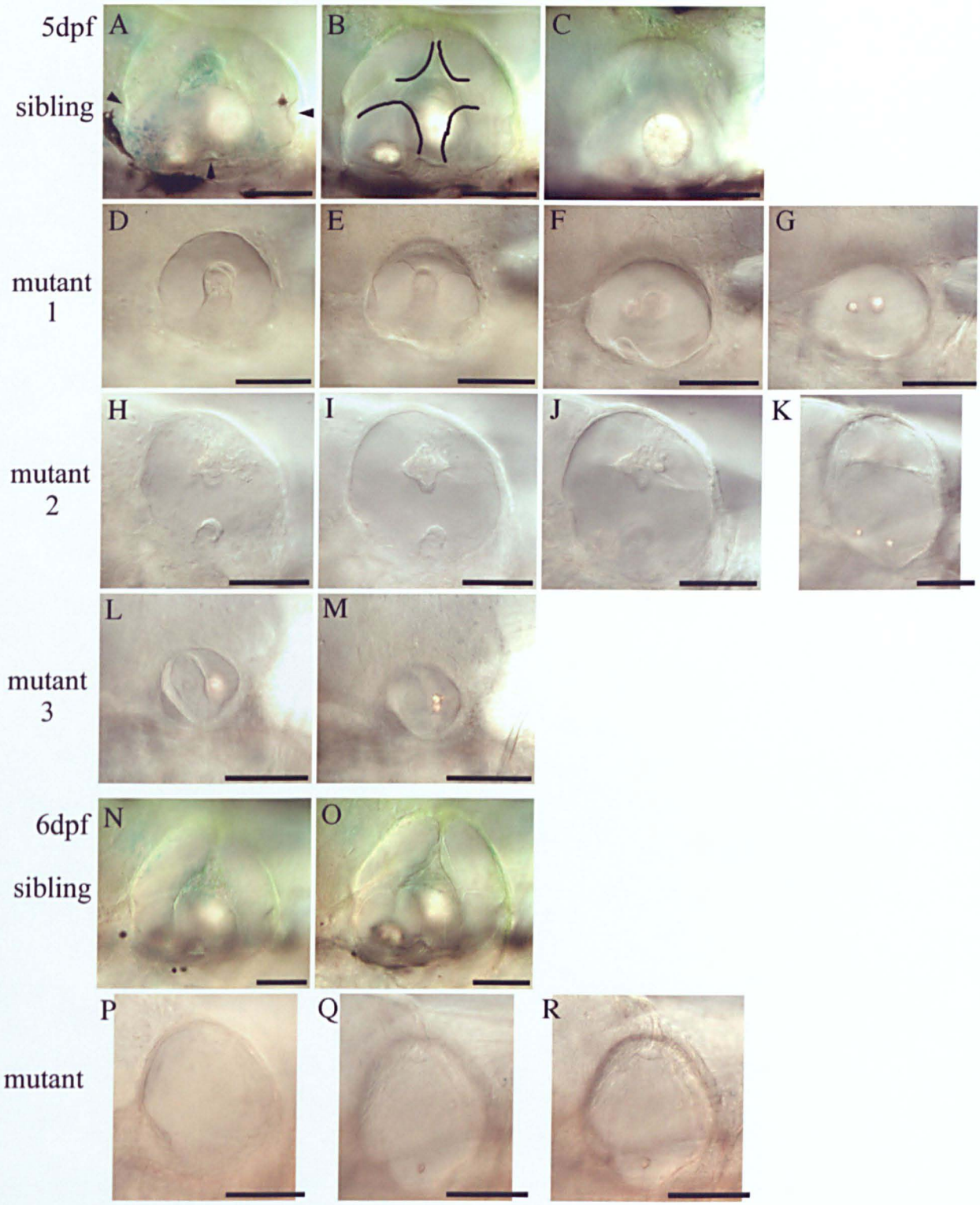

Figure A1 DIC live images of 5+6dpf *cls t3* mutant and sibling embryos.
All are lateral views with anterior to the left. Scale bars=50 μm
(A-C, N+O) At 5dpf in siblings the epithelial projections have fused (outline), crista thickenings are visible (arrows) and two differently sized otoliths are positioned laterally and medially in siblings. (D-M, P-R) In the mutants, vesicle size is still variable (compare L+J), projections have not fused (H+I) and otoliths do not grow (G+M). Some vesicles do not have projections at 6dpf (P-R). The putative ED is not normally seen in *cls* mutants. However, in one case (P+R bracket), an abnormal ED appeared to form.

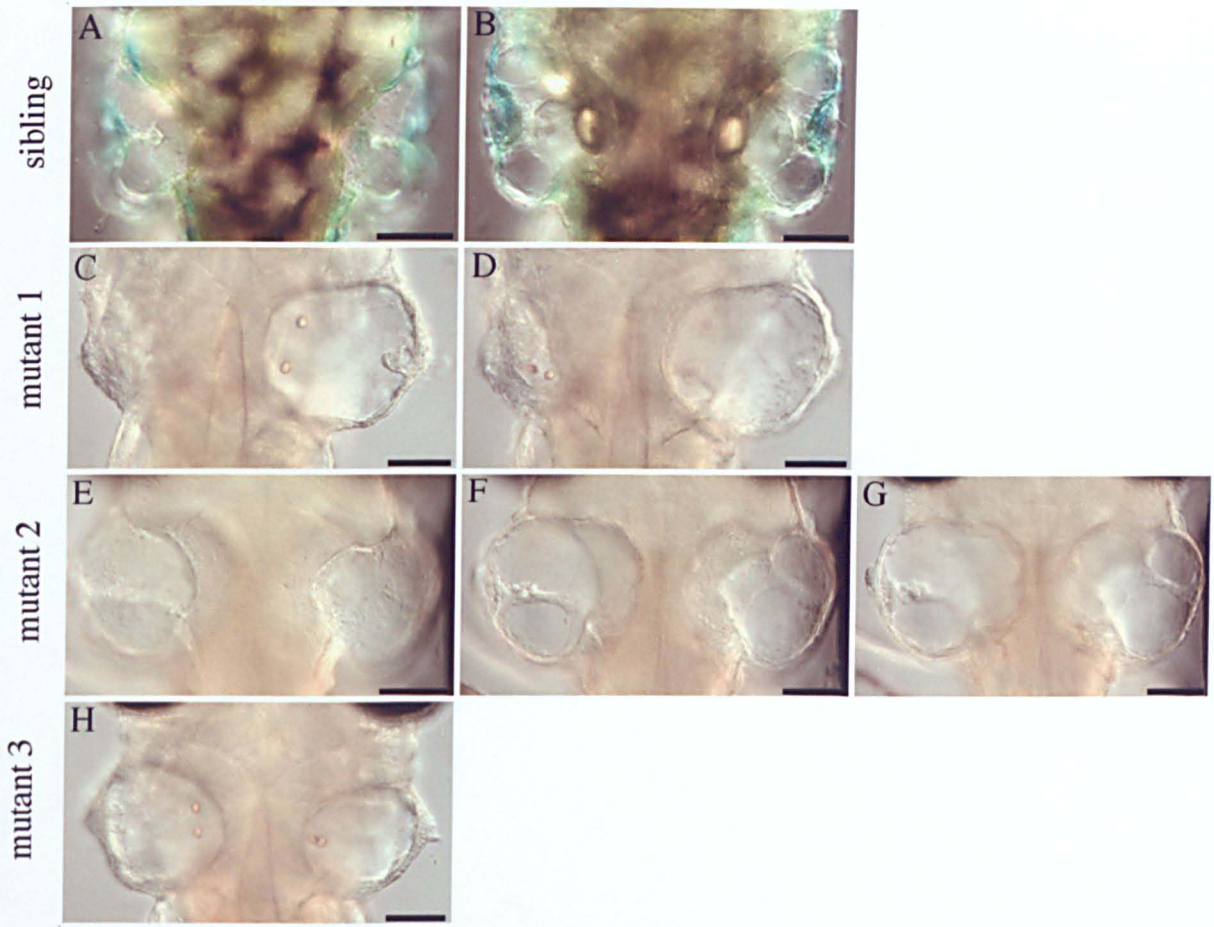

Figure A2 DIC live images of 8dpf *cls t3* sibling and mutant embryos.
All are dorsal views with anterior to the top. Scale bars =50 μm.
(A+B) In the sibling the large posterior otolith is clearly visible (B) and two SCC can be seen in cross section. (C+D) There is still variety in the size of vesicles in the same head of some mutants. Abnormal epithelial projections are visible. (E-H) Even mutants that produce fused epithelial projections fail to form normal SCC. (C+H) Note the different range of vesicle size seen in *cls* mutants.

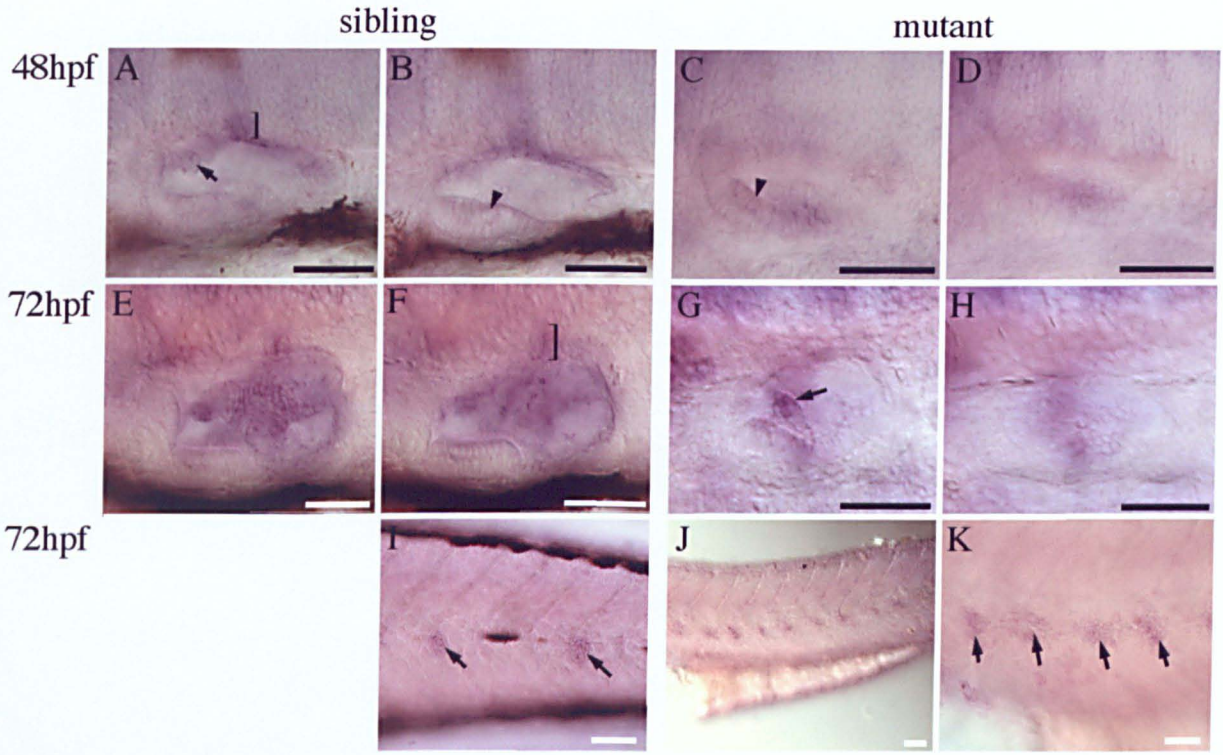

Figure A3 *dachA* mRNA expression in *cls t3* sibling and mutant embryos.
All are lateral views with anterior to the left. Scale bar=50 μm.
(A+B) At 48hpf in the sibling *dachA* is expressed in a broad dorsal domain including the ED (bracket), the epithelial projections (arrow) and faintly in the anterior macula (arrowhead). (C+D) In the mutants, only the macula staining (arrowhead) persists. (E+F) At 72hpf *dachA* is still expressed in the epithelial projections, which have now fused, and in the ED (bracket). (G+H) In this mutant the projection that formed expresses *dachA* (arrow) but it has not fused and there is no dorsal staining. (I) *dachA* is also expressed in the neuromasts (arrows) of the lateral line system. (J+K) *cls* mutants have more neuromasts than their siblings do at the same stage (arrows).

Initially the anterior and posterior tether cells appear to be normal in *cls* mutants (see Fig. 4.14). However, at later stages the anterior macula is not seen to develop on the ventral floor of the vesicle. It is not clear what happens to the primary anterior tether cells. *cls* mutants do form abnormal ventrolateral and posteromedial sensory patches but these patches are in the wrong position to be an anterior macula (see Fig. 4.14). The anterior tether cells may join the abnormal anteroventral or posteromedial patch, or they may die. The expression of *fgf8,* which is normally expressed in the anterior macula at 48hpf, is displaced medially (see below), suggesting that the large posterior macula is actually both a posterior and anterior macula or a misplaced anterior macula. Specific markers or hair cell polarity patterns could be used to distinguish these possibilities. Unfortunately, the lack of a marker specific to the posterior macula, coupled with the disorder of the sensory patches (making examination of hair cell planar polarity difficult), prevents confirmation of this.

In *cls* mutant ears, the posteromedial patch stretches around the medial wall of the otic vesicle in samples up to 6dpf (Fig. A4 compare C+J (+K not to same scale)). It is longer than that of the sibling at 104hpf. The number of hair cells within the posterior maculae of wild type and mutant vesicles have not been compared to see if there is an overproduction. Abnormal ventrolateral sensory patches are still seen at 6dpf (Fig. A4D+M arrowheads). They do not have the distinctive shape of cristae or contain as many hair cells as are found in wild type (Fig. A4 compare A+D arrowheads).

A.4 *cls* otic vesicles have early patterning defects.

Although at early stages morphology and actin stains suggest that *cls* development is proceeding normally, molecular markers show that there are already some patterning defects. At 24hpf, *fgf8,* an anterior marker, is expressed in both the anterior and posterior in *cls* mutants (A5 compare A+C). This could suggest a duplication of anterior fate or as *fgf8* is also expressed transiently at the posterior at earlier stages (20hpf), a delay in specifying posterior fate. However, *follistatin,* a posterior marker, remains expressed in the posterior, suggesting some posterior character is retained (Fig. A5 compare G+I). This misexpression of both anterior and posterior markers rules out a simple anterior or posterior duplication. The early normal expression of *pax2.1,* a medial marker, suggests early mediolateral patterning is correct (Fig. A6A-D). However, the later medial shift of *fgf8* and *follistatin* expression suggests the correct pattern is not maintained (Fig. A5F+L).

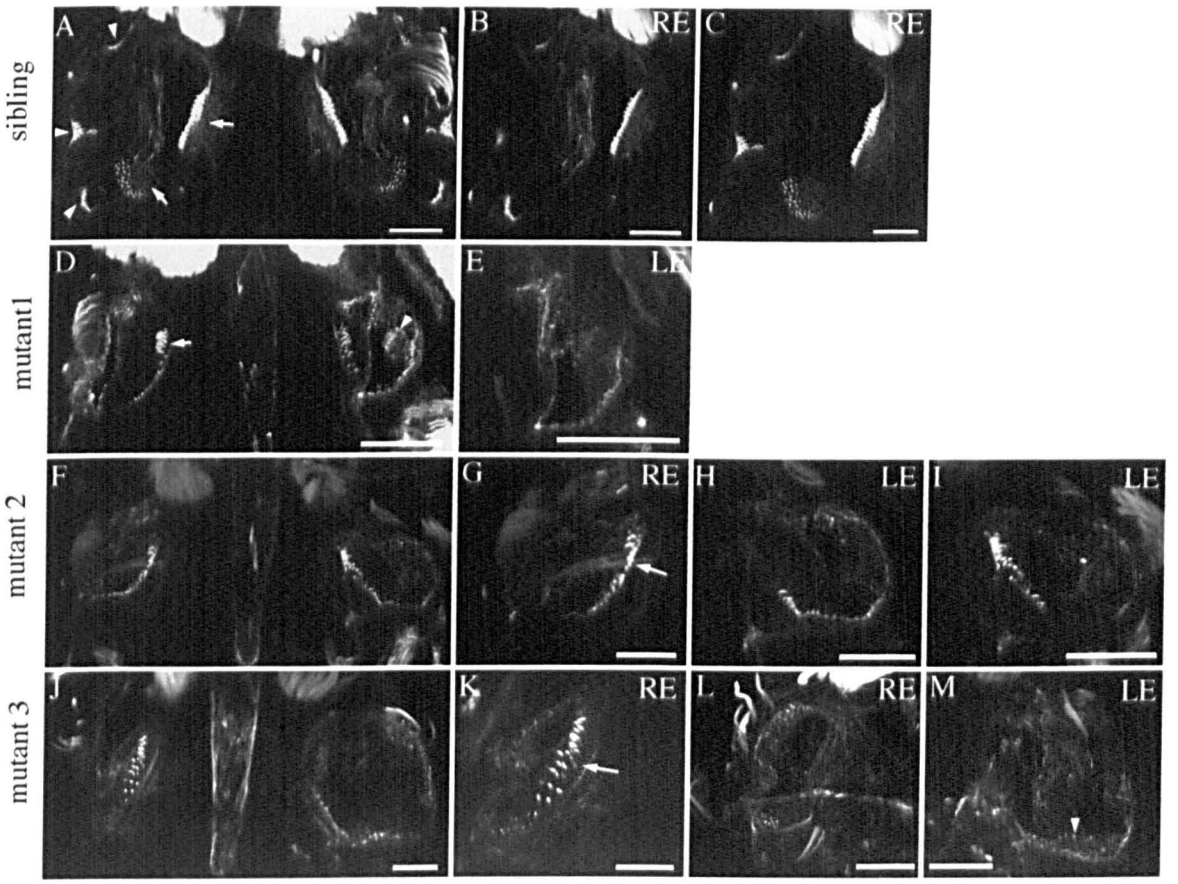

Figure A4 Actin stains in *cls t3* mutant and sibling embryos.
All are dorsal views with anterior down. Scale bars=50 μm
(A-C) At 6dpf the three cristae (arrowheads) and two maculae are clearly distinguishable in siblings. In the *cls* mutants the sensory patches are all disrupted. There are some lateral collections of hair cells (D, E+M arrowheads). However, these do not resemble the wild type cristae. The posterior macula in the mutants has expanded further along the medial wall of the otic vesicle (D, F-K arrows) and its hair cells appear more spread out (compare A+J).

Figure A5 *cls t3* sibling and mutant embryos analysed with different mRNA probes.

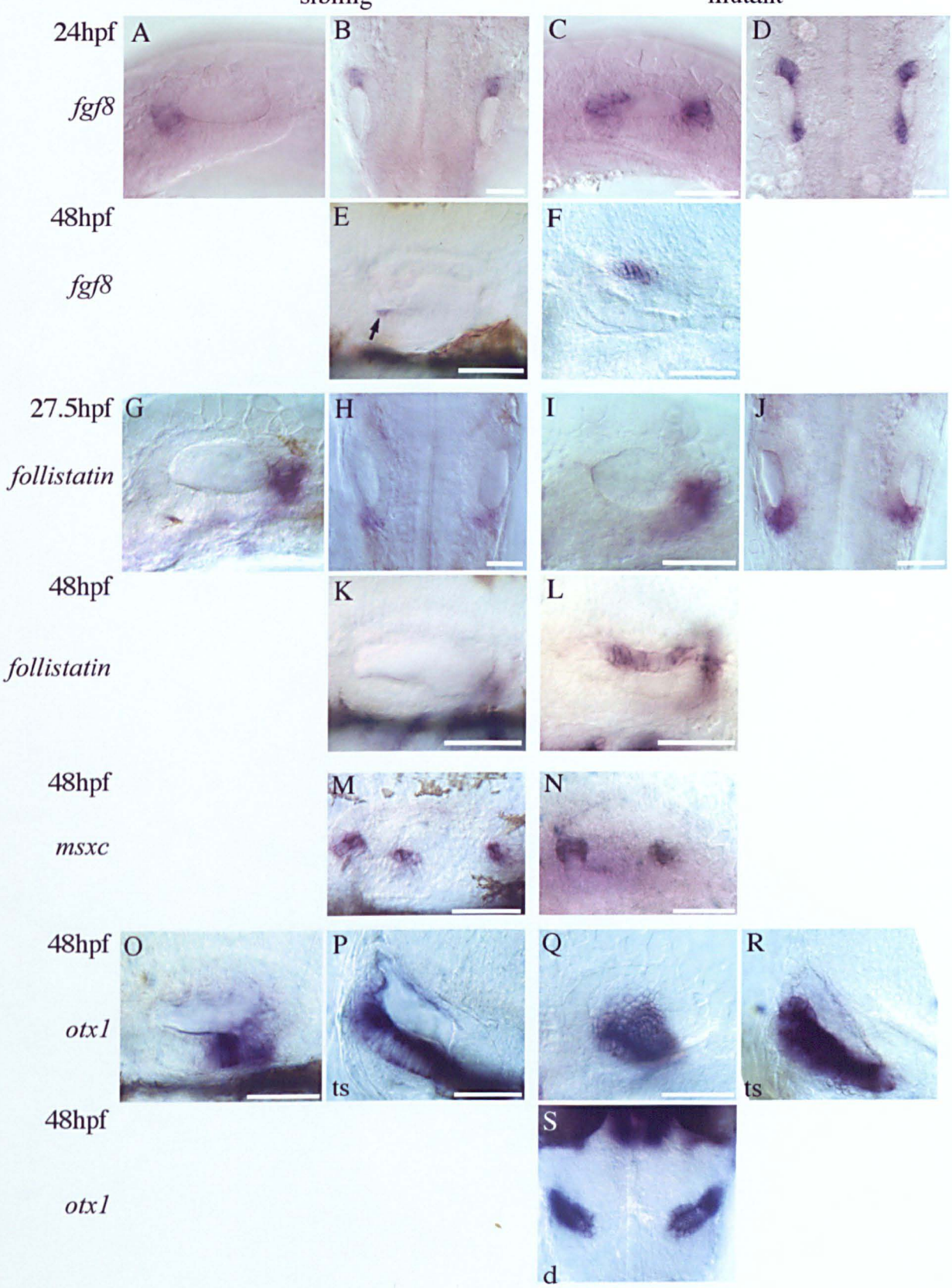

Figure A5 *cls* ^{t3} sibling and mutant embryos analysed with different mRNA probes.

All are lateral views with anterior to the left, except B, C, H, J, and R which are dorsal views with anterior to the top and S+T which are transverse sections with lateral to the left. Scale bars=50μm.

(A+B) *fgf8* is expressed in the anterior of the otic vesicle at 24hpf. (C+D) In *cls* mutants, *fgf8* is expressed at both the anterior and posterior ends of the vesicle. (E) At 48hpf *fgf8* is expressed in a restricted lateral domain in the anterior macula (arrow). (F) In *cls* mutants *fgf8* is expressed more medially. (G, H+J) At 27.5hpf and 48hpf *follistatin* is expressed in the posterior of the otic vesicle. (I+J) At 27.5hpf *follistatin* expression is in the correct domain in *cls* mutants but is possibly expressed at higher levels. (K) At 48hpf *follistatin* is expressed in an expanded posteromedial domain. (L+M) *msxc* is expressed in two rather than three ventrolateral domains. (N+O) *otx1* is expressed at the posterior end of the anterior macula, extending medially across the ventral floor of the vesicle. (P-R) In the mutant this domain may be slightly expanded laterally.

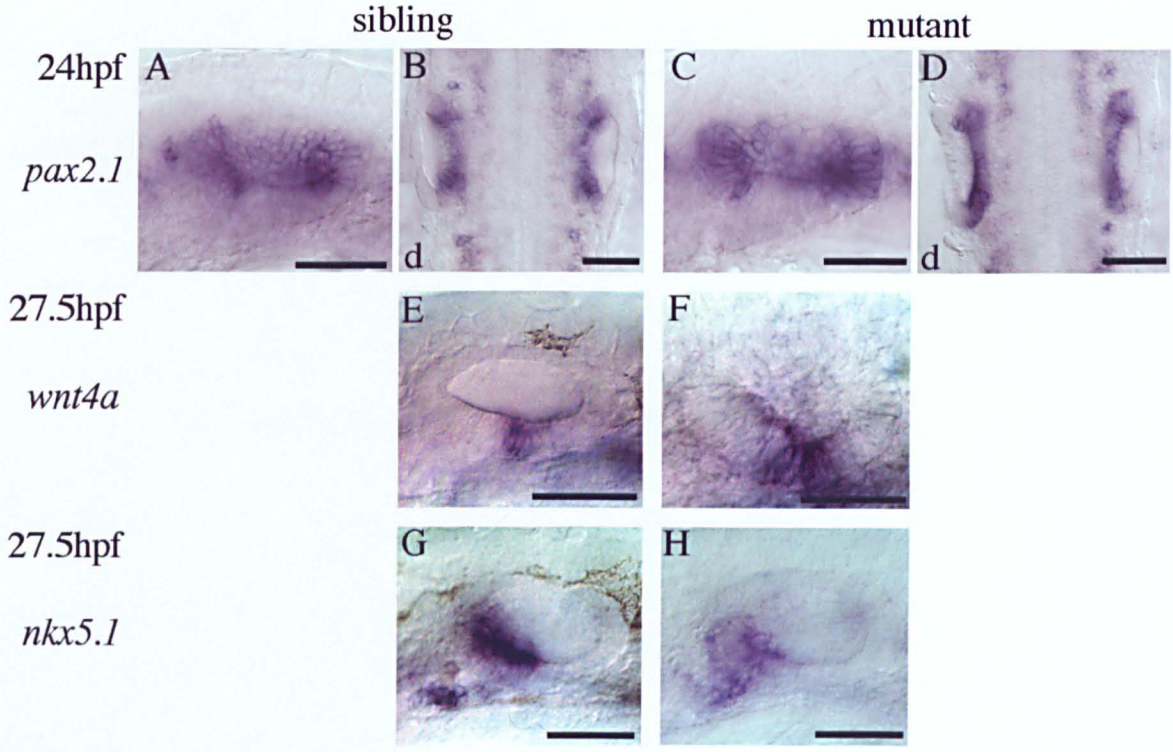

Figure A6 *cls t3* sibling and mutant embryos analysed with different mRNA probes. All are lateral views with anterior to the left, except B+D, which are dorsal views with anterior to the top. Scale bars=50 μm
(A-D) *pax2.1* is expressed medially at 24hpf in both siblings and mutants. It is concentrated at the anterior and posterior of the vesicle. (E+F) *wnt4a* is expressed in a restricted ventromedial domain in both siblings and mutants. (G+H) *nkx5.1* is expressed in the anterior of the otic vesicle and delaminating neurons in both siblings and mutants.

Dorsal patterning is also affected, as the dorsal area of *bmp4* and *dachA* expression is not seen (Fig. 4.11J+M, Fig. A3D+G). However, *nkx5.1* and *wnt4a*, both ventral markers, are unaffected, although they are expressed at the same time as the dorsal area of *bmp4* and *dachA* should normally be induced (Fig. A6E-H). The third ventrolateral area of *bmp4* expression, normally expressed by 30hpf, is in an area slightly lateral to the *wnt4a* expression domain. This domain of *bmp* expression is not expressed in *cls* (see Fig.4.11J+M). Another ventral marker, *otx1*, is normally expressed in few cells at the posterior edge of the anterior macula and medially along the ventral floor of the vesicle. In *cls* this domain appears broader, even taking into account the slightly smaller *cls* vesicle. Interestingly, in the mouse this gene is required for normal SCC development. Lack of *Otx1* function results in the loss of the lateral SCC (Morsli et al., 1999). However, in *cls* mutants each of the SCC is disrupted, it is not clear if the lateral SCC in particular is expanded.

So in summary:

- an anterior marker is also expressed in the posterior (*fgf8*)
- an early medial marker is unaffected (*pax2.1*)
- lateral markers are expressed medially (*follistatin* + *fgf8*)
- ventral markers :- some missing domains (*bmps* + *msxc*)

  -some expressed correctly (*nkx5.1* + *wnt4a* both not very lateral +*eya1*)

  -some expressed at higher levels (*bmp4* + *otx1*)
- dorsal markers are missing (*bmp4* + *dachA*)
- neurogenesis appears relatively normal (*nkx5.1*)

The *pax2.1* expression supports evidence from actin stains and the early development of the otoliths that initial hair cell development (tether cells) is normal. However, the abnormal *fgf8* expression at 24hpf suggests that there are defects in *cls* ear development prior to this stage.

A.5 *cls* have ectopic posterior neuromasts.

Neuromasts (nm) develop, as the otic vesicle does, from cranial placodal ectoderm. This placodal ectoderm forms the lateral line primordia. Between 20 and 42hpf the primordia migrate from the pre and post-otic region posteriorly along the tail and anteriorly over the head, depositing groups of cells that will develop into nm (prenm)(Metcalfe et al., 1985). The nm are regularly spaced, dependent on the position of the last nm, but not through inhibitory signals (Gompel, 2001). In wild type fish more nm eventually form than are initially seen to have been deposited. It is not clear how these later nm develop, but they may bud off the initial prenm (see Fig. A7N arrow). Each nm contains support cells and hair cells, similar to those in the otic vesicle. Neuromasts are used to detect water motion around the fish (Coombs et al., 1989).

cls produces extra posterior prenms (Piotrowski et al., 1999), which express *eya1* and *dachA* (Fig. A7 + Fig. A3I-K). This excess is visible at 55hpf: *cls* mutants have 15 groups of cells expressing the markers, compared to 8 in the sibling (Fig. A7L+N). The anterior lateral line system appears normal. Earlier stains show that the posterior migrating primordium is the normal size and shape (Fig. A7A-J). It is possible that these extra nm are part of the normal complement of the lateral line and the defect lies in the timing of their differentiation. Alternatively they could be truly extra nm, and are either the product of abnormal cell division within the neuromast system, or due to a group of cells abnormally adopting a nm fate.

In situ studies using *fkd6* as a marker of putative Schwann cells have shown that *cls* lacks glial cells along the posterior lateral line nerve (Kelsh et al., 2000). It has been suggested that cells which would normally form glia are misspecified, and that the absent glial cells are normally responsible for inhibiting nm proliferation (Piotrowski et al., 2001). In *Drosophila*, glia have been shown to regulate the proliferation of neurons (reviewed in Jones, (2001)). In support of this, a recent report has shown in vitro that murine postmigratory neural crest cells require *sox10* to survive and to follow a glial fate (Paratore et al., 2001)

The anterior lateral line appears to develop normally in *cls*. Another mutant, *hypersensitive*, appears to have defects that affect only the anterior lateral line (Whitfield et al., 1996). These data suggest that the anterior and posterior lateral lines develop

differently. In other species the anterior lateral line has been shown to develop by the placode extending over the head and then fragmenting, rather than depositing clusters of cells as the posterior lateral line does (*Xenopus laevis*, Winklebauer and Hausen, 1983; reviewed in Lewis, 1986).

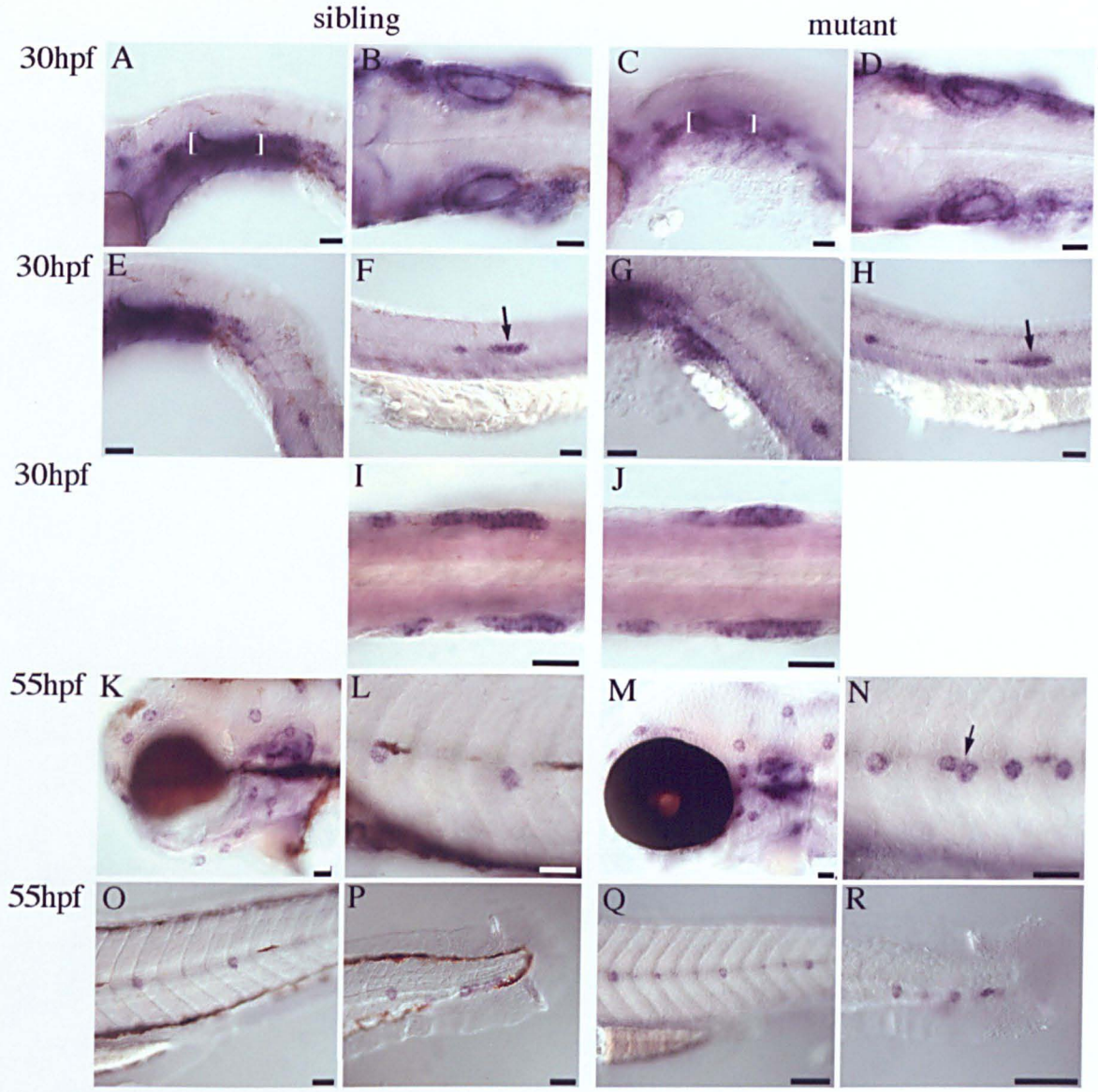

Figure A7 Analysis of lateral line development in *cls t3* sibling and mutant embryos. All are lateral views with anterior to the left except B, D, I, and J, which are dorsal views with anterior to the left. Scale bar =50 μm.
(A-H) Both sibling and mutant embryos express eya1 in the ventral half of the otic vesicle (A-D brackets) and the posterior migrating lateral line primordia (E-H arrows). (I+J) The relative size of the migrating posterior primordia in siblings and mutants appears the same. (K-R) At 55hpf all the preneuromasts have been deposited by the migrating primordia and they all express *eya1* in both siblings and mutants. The number of head (anterior) preneuromasts appears the same in sibling and mutant embryos (compare K+M). However, in the tail there are more in the mutant (compare L+N, and O+P with Q+R). These extra neuromasts may bud off normal preneuromasts (N arrow).

Chapter 5

Implanting protein coated beads to disrupt Bmp signalling within the developing inner ear.

5.1 INTRODUCTION

5.1.1 Aims

This chapter investigates the effect of adding ectopic BMP4 and BMP antagonist proteins via beads to the inner ear. Data from Chapter 3 suggest that controlling the levels of BMP signal is important during zebrafish inner ear development, e.g. BMP antagonists (*follistatin* and *ismads*) are expressed within the vesicle (Fig 3.10, 6+7). Data from Chapter 2 and 3 also suggest the cristae and the medial wall of the otic vesicle are sites of BMP action. Chapter 4 strengthened the association between cristae and the Bmps. It showed that mutants that lacked normal *bmp* expression failed to develop cristae or express *msxc*. This chapter builds upon these results and tests whether BMP4 protein is sufficient to induce ectopic cristae or rescue crista development in one of these mutants (*vgo*). This induction was assessed by analysis of hair cell stereocilia differentiation and *msxc* expression.

Previous work in the chick, described in more detail below (1.5.1), has shown that BMP signals are required for SCC development (Chang et al., 1999; Gerlach et al., 2000). The characterisation of the rescued *swr* mutants (Chapter 6) also supports a role for *bmp2b* in the formation of SCC. Therefore, SCC development was also assessed in otic vesicles treated with ectopic BMP4 or antagonist protein in vivo.

The levels of *bmp4* and *msxc* expression were also analysed in beaded otic vesicles. As discussed previously (see 3.6.4) *Msx1* is thought to be a target of BMP4 signalling in other systems (murine tooth) and so *msxc* expression was analysed to see if it was a direct target of BMP4. There is also evidence of a regulatory feedback loop between BMP4 signalling and *BMP4* expression in the chick limb (Capdevila and Johnson, 1998) and inner ear (see 5.1.5 and Chang et al., (1999)).

5.1.2 Beads as useful biological tools.

Beads have been employed to investigate diverse biological problems. They have been used in vivo to trace the paths used by migrating cells (Bronner-Fraser, 1986), and within cells to trace particles along microtubules (Jesuthasan and Strähle, 1997). Beads have also been used extensively in chick limb development research, where they were used to provide local sources of signals e.g. (Eichele et al., 1984; Tickle et al., 1985). These chick experiments investigated the signals that are required to pattern the developing limb. Candidate signalling molecules (e.g. Retinoic Acid, Shh, and BMPs) were applied to beads, which were then inserted into specific areas of the developing limb bud (reviewed in Tickle, (1999)). These beads resulted in pattern alterations that have provided clues as to the roles of these signals in limb outgrowth and patterning (e.g. the involvement of Shh in the anterior-posterior patterning of chick limb digits, possibly via *bmps* (Yang et al.,1997)). Protein coated beads have also been used in other organisms, such as *Xenopus* (e.g. Activin beads used to investigate how cells interpret morphogen gradients (Gurdon et al., 1996)), and mouse (e.g. FGF and BMP in lung development (Weaver et al., 2000)).

5.1.3 What are beads?

The beads used in these protein studies are made of sepharose with either Cibracon blue or heparin as covalently attached ligands. Sepharose is agarose (a polysaccharide purified from seaweed) that has been crosslinked. This crosslinking gives agarose a defined pore size and improved strength. The beads are macroporous, with large surface areas (J. Baker, Amersham pers. comm.). When they are soaked in the protein of interest, it permeates the bead and becomes attached to the ligand.

The beads can come in many different sizes. Those used in this study range between 24-44μm in diameter. Other studies discussed below used slightly larger beads (Affi-gel 75-100μm, Biorad) which also consist of sepahrose and the Cibracon blue ligand, to investigate the effect of inhibiting BMP signalling during chick inner ear development.

5.1.4 hBMP4 protein has a specific effect on zebrafish development.

Previous work has demonstrated that beads coated in human recombinant BMP4 (hBMP4) can have specific effects in zebrafish and replicate endogenous Bmp4 signalling. Grinblat et al., used hBMP4 soaked beads to investigate whether signals

from the organiser are required to maintain the expression of a neural fate marker. This marker, *odd-paired-like*, is required for the proper patterning of the forebrain (Grinblat et al., 1998).

Early in development the BMPs are important in the patterning of mesoderm, acting against inhibitory signals (the BMP antagonists, e.g. Chordin) from the zebrafish organiser, the shield ((Nikaido et al., 1997) see 1.4.1). The patterning of the mesoderm is important in the patterning of the neuroectoderm. As mentioned above, in order to investigate the establishment of neural fates, Grinblat et al., implanted hBMP4 soaked beads at the time when the shield is being established (6hpf), close to where it will form. The hypothesis was that hBMP4 would ectopically stimulate the same response as endogenous zebrafish Bmp4 would, inhibiting neural fate. The ectopic hBMP4 protein did inhibit the expression of a neural marker (*odd-paired-like*). This effect was not seen with the implantation of control beads (Grinblat et al., 1998).

5.1.5 The use of beads in studies of inner ear development.

There have been three studies using beads to investigate chick inner ear development. The first used Retinoic Acid (RA) soaked beads to investigate with more precision previously reported inner ear defects associated with RA (Choo et al., 1998;Frenz et al., 1996). The second two used ectopic doses of a BMP antagonist, Noggin, to investigate the role of BMP4 in chick inner ear development (Chang et al., 1999; Gerlach et al., 2000). This section briefly describes the RA experiments, then concentrates on the two Noggin papers.

Retinoic acid study

Choo et al., (1998) implanted beads (resin exchange beads, 85-100μm, Biorad) coated in RA into the otocyst of developing chick inner ear (stage 16, E2.5). This technique allows the direct, in vivo, response in the local area to be analysed, without the systemic effects seen in mice where the mother is fed RA (Frenz et al., 1996). These beads had a dose-related effect on SCC, and cochlea duct development.

At the stage when the beads were inserted the otic cup is closing. At this stage *BMP4* and *Msx1* still mark broad domains suggesting individual sensory patches have not yet differentiated (Oh et al., 1996; Wu and Oh, 1996). There is also no morphological SCC development obvious at this stage. In this paper the sensory patches were more resistant to RA treatment than the SCC. Even the most severe phenotype, which lacked

SCC, still produced cristae, macula-like collections of hair cells and otoliths. The ED was only rarely affected (not dose related). The authors also documented a time window when the developing inner ear was most sensitive to the RA beads (stage 16-19, analysed stages from 16-21, (Choo et al., 1998)).

This study showed that the bead technique could work in chick inner ears. However, there were some unanswered questions. Implanting into the otocyst restricted the stages for study to those of stage 16 and later, when the otic cup is closing. The results of control beads (-RA) implantation were not reported. It is therefore possible that the process of implantation was physically disrupting the development of the SCC and cochlea.

Ectopic NOGGIN studies

Chang et al., (1999)

Chang et al., (1999) implanted beads (Affi-blue, 75-150μm, Biorad) coated in *Xenopus* Noggin protein around E3.5-4 (*X*Noggin, also E7 for one experiment) into periotic mesenchyme. They also injected a virus containing chick *Noggin* cDNA into the lumen of the otocyst or surrounding mesenchyme. However, they found that the efficiency of viral infection in the otic epithelium was variable. They also report that implanting beads into the lumen of the otocyst was not as potent in eliciting the phenotype as beads implanted in the mesenchyme around the otocyst.

Both the viral and bead techniques produced the same range of phenotypes, affecting both nonsensory and sensory structures, depending on the dose of *X*Noggin. The developing SCC were the least resistant, affected with the implantation of one *X*Noggin bead. However, the implantation of multiple beads was required to affect the development of sensory patches. The SCC defect was explained as a failure of the pouch that forms the SCC to outpocket properly and the subsequent failure of the SCC to grow. This was shown to be due to a reduction in cell proliferation in the outpocket, and at later stages an increase in apoptosis (Fig. 5.1).

*X*Noggin beads also affected the levels of *BMP4* and *Msx1* expression. The expression of *BMP4* was greatly increased in mesenchyme around the bead, with only a slight increase in *BMP4* expression in adjacent SCC epithelium. *Msx1* expression in the SCC, which is in a region distinct to that of *BMP4*, was greatly reduced. *X*Noggin beads did not affect the ED, which does not express *BMP4*, but does express *Msx1*. These expression data suggest that the *X*Noggin is indirectly inhibiting *Msx1* expression in the

SCC by reducing BMP4 function in the mesenchyme. It also suggests that BMP7, which is expressed in the ED (Oh et al., 1996), is not regulating *Msx1* expression in the ED, or is not inhibited by *X*Noggin. These data also indicate a feedback loop in which the levels of BMP4 protein regulate the levels of *BMP4* expressed in the mesenchyme.

To test the effect of *X*Noggin beads on sensory structures, multiple beads were implanted close to the anterior ampulla and utricle. These beads affected the morphology of the anterior ampulla, anterior crista and the utricular macula. The sensory patches were smaller and their shape disrupted. In the anterior crista the expression of four crista markers was differentially affected. *Msx1* and *p75NGFR* expression was reduced; however, *BMP4* and *Fng* were not affected. No details were given on the macula phenotype. It was suggested that the *X*Noggin beads were therefore having a direct effect on sensory patch development, rather than the abnormal patterning being a secondary effect due to the malformed ampulla.

In these experiments two types of control beads were used (BSA and *X*Noggin+hBMP4), neither of which reportedly produced a phenotype. The BSA soaked beads tested the effect of both the physical disruption and the presence of foreign proteins around the developing otocyst. The *X*Noggin coated beads that were also soaked in hBMP4 suggest that the ectopic *X*Noggin protein was acting by inhibiting endogenous BMP4. Noggin has also been reported to bind in vitro to BMP2 and, at much lower affinity, BMP7 (Zimmerman et al., 1996). BMP2 is not expressed in the chick inner ear but BMP7 is widely expressed through the chick otocyst, in domains including those of BMP4 (Oh et al., 1996). Therefore there is the possibility that these beads could also affect BMP7 signalling or heterodimers, involving BMP4 and BMP7. BMP5 is also expressed in the developing chick otocyst in a pattern similar to BMP4. There are no data on whether BMP5 binds to Noggin.

The analysis of cell death and division by Chang et al., (1999) allowed them to hypothesise the following: they suggest that *X*Noggin is repressing normal endogenous BMP4 activity and that this BMP4 activity is required at two different stages in SCC development (see Fig. 5.1).

1. To promote the outgrowth of the SCC outpocket (*X*Noggin inhibits cell proliferation)
2. For the continued growth of formed SCC (*X*Noggin increases apoptosis).

BMP4 has been implicated in regulating cell division and death in other systems (e.g. during chick limb development (Merino et al., 1998).

Gerlach et al., (2000).

Gerlach et al., (2000) used *X*noggin-secreting cells attached to beads (Cibracon blue agarose, Sigma). The number of cells on each bead was counted and the quantity of protein produced by the cell line calculated using ELISA (Enzyme linked immunosorbant assay). These figures were used to give an estimate of how much protein was being secreted by each bead (14 cells per bead secreting 0.84+/-0.11pg per 24h). Multiple beads were implanted around the developing inner ear from stage 13-20. This paper documented a similar range of phenotypes to those described in Chang et al., (1999), with the SCC being most susceptible to ectopic *X*Noggin. Gerlach et al., (2000) documented the loss of sensory structures if the relevant chamber did not form, although they did not describe this phenotype in detail.

Gerlach et al., (2000) did not analyse the rates of cell death or division. They suggest *X*Noggin is inhibiting the resorption process or the mesenchymal-epithelial interactions required to form the SCC.

The Gerlach group also experimented with beads coated in hBMP4-producing cells. They did not quantitate the amount of protein secreted from these beads but they could show that the hBMP4 beads titrated the effect of the *X*Noggin beads. In these experiments a hBMP4 bead was positioned next to a *X*Noggin bead. By increasing the distance between the beads they could increase the strength of phenotype seen due to the *X*Noggin bead. They suggest this as proof that the extra *X*Noggin is inhibiting the normal role of endogenous BMP4; however, this is not necessarily true given the expression of other BMPs within the developing inner ear (BMP5 and BMP7 (Oh et al., 1996) see above).

Gerlach et al., (2000) provided information on the effect of varying the timing of implantation and the duration of implantation. They describe a time window of sensitivity between stage 13-20 with stage 15 producing the most abnormalities. This stage is before the otic cup closes (stage 16) and before *BMP4* expression is restricted to the anterior and posterior focus. *BMP4* is expressed in a broad domain in the otic cup from stage11 (Wu and Oh, 1996). Gerlach et al., (2000) also showed that 7-12 hours of Noggin exposure at stage 17 was enough to provoke abnormalities similar in severity to those seen if the beads were left in for several days.

Results of the Noggin bead experiments

Both papers suggested that the primary defect is in SCC development (Fig. 5.1 below). Chang et al., (1999) did show that the resorption process occurred normally in vesicles treated with *X*noggin beads. However, it is not clear from this paper or Gerlach et al., (2000) where the endogenous BMP signal comes from, the epithelium or surrounding mesenchyme.

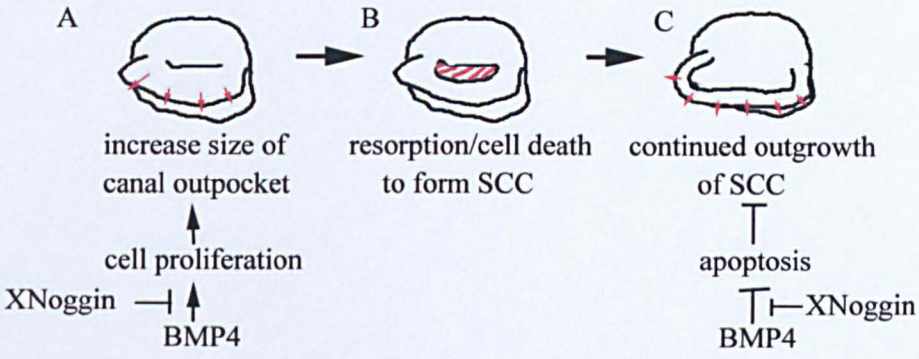

Figure 5.1 Sketch of chick SCC development highlighting the stages where BMP4 signals are thought to be required. Only the lateral canal is shown for simplicity.

(A) Initially the wall of the otic vesicle bulges out to form an outpocket. BMP4 signals are required to promote cell proliferation and growth of this pocket. (B) A region of this outpocket then undergoes a period of cell rearrangements and programmed cell death (resorption) to form the SCC. (C) The SCC then continues to grow away from the vesicle until its adult size is reached. BMP4 signals are required to inhibit apoptosis to allow this outgrowth to continue (see 6.3.3).

These two papers also saw effects on the sensory tissues of the inner ear. Gerlach et al., (2000) suggest early inhibition of BMP4 can prevent development of the cristae, while Chang et al., (1999) showed later modification of BMP4 signalling could manipulate the levels of expression of markers within the cristae. Fine tuning the timing of implantation could be important for establishing when sensory patches are patterned as *BMP4* is still expressed in a broad domain when the early beads were implanted i.e. it is not marking individual sensory patches. It is interesting that Chang et al., (1999) saw an increase in *BMP4* expression around the SCC but no effect on its expression in the cristae, even though ectopic *X*Noggin affected the expression of other crista markers. This suggests that there is no feedback mechanism in the cristae to regulate *BMP4* expression.

Both groups experimented with ectopic BMP4 beads. Chang et al., (1999) used human BMP4 (Genetics Institute) and reported that there was a phenotype but did not provide

details. Gerlach et al., (2000) used beads coated in murine BMP4-expressing cells, which "failed to generate any morphological abnormalities", but unlike their *X*Noggin work they did not quantify how much protein was released from the beads. The difference in response may therefore be dose related or due to the fact that the BMP4 used was from a different species.

Neither of these studies, nor any of the other reports using BMP4 beads, document the quantity of BMP4 protein released into the surrounding tissue, or its range of action.

5.1.6 Adding BMP/antagonist coated beads to manipulate BMP signalling in zebrafish.

Sepharose beads were soaked in hBMP4 protein and implanted around the developing inner ear (see Materials and Methods Fig. 8.2). This surgical manipulation should result in increased BMP signalling within the otic vesicle and provides an interesting comparison to the *swirl* (*bmp2b*, Chapter 6), and other mutant analysis (Chapter 4), which investigated the effect of the lack of BMP signal. Beads coated in the BMP antagonists *X*Noggin or Chordin were also implanted to investigate the effect of reduced BMP signal. These experiments were intended to confirm and extend the mutant analysis. The work in this chapter was carried out with Dr K. Hammond, who helped with establishing the protocol, and Dr D. Biram, who generated the protein from cell lines from Dr R. Harland (*Xenopus* Noggin) and Prof. M. Placzek (chick Chordin).

5.2 Results

5.2.1 Choice of protein.

Initially control experiments were carried out to investigate if the process of implanting the beads affected inner ear development. Beads coated in BSA (Bovine serum albumin) were implanted between 22hpf to 27hpf. The concentrations used reflected the concentration of the recombinant hBMP4 (0.258µg/µl) and an excess (5µg/µl). BSA was used as it provided a source of foreign protein , which could possibly induce a non-specific reaction.

The hBMP4 protein was obtained from the Genetics Institute, Massachusetts. This protein has been used by others to replicate BMP4 signalling in different organisms (e.g. mouse tooth development (St Amand et al., 2000), and zebrafish forebrain

patterning (Grinblat et al. 1998)). It is very similar to the zebrafish Bmp4 protein (the inactive peptide is 90% identical/95% similar to zebrafish Bmp4 (accession number U82231))

In the *X*Noggin experiments a Chinese hamster (CHO) cell line transfected with a *X*Noggin construct (a gift from R. Harland) was used to generate the *X*Noggin protein. In this cell line *XNoggin* is linked to an enzyme that allows infected cells to survive under certain conditions (Lamb et al., 1993). As a control, serum from the untransfected parental cell line was collected.

In the Chordin experiments, samples of chick Chordin were kindly given by M. Placzek, and as a control, beads were soaked in the OPTI-MEM medium in which the Chordin-producing CHO cells grew. The concentration of protein produced was not quantified.

Ideally, Follistatin protein would have been used, as this is the only BMP antagonist found to be expressed in the zebrafish inner ear (Fig. 3.10). Unfortunately this protein was not available. However, *Xenopus* Noggin has been shown to bind both human BMP4 and BMP2 (Zimmerman et al., 1996) and *Xenopus* Chordin has been shown to bind human BMP4 (Piccolo et al., 1996) in immunoprecipitation studies. Therefore it was assumed that these antagonists would reduce the levels of endogenous Bmp signalling within the zebrafish inner ear.

5.2.2 Timing of implantation (22-27hpf) did not affect results.

Beads were implanted between 22 and 27hpf. This stage was chosen for four reasons:

- Expression patterns showed that the *bmps* are expressed after otic induction. The time period chosen correlates with the expression of *bmps* and their receptors.

From 24hpf *bmp4*, *bmp2b*, and *bmp7r* are expressed in similar domains at the anterior and posterior ends of the vesicle (Fig. 2.1, 2.2 +2.4) as are other parts of the signalling pathway (see Chapter 3).

- No morphological or molecular differentiation specific to the tissues of interest are visible at this stage, i.e. it is prior to the differentiation of the SCC and crista, although the hair cells in the maculae have just begun to differentiate.

The otic placode begins to cavitate at 18hpf to form the otic vesicle. By 24hpf it has an expanded lumen which contains two otoliths (see Fig. 1.2L).

- Slightly younger embryos proved difficult to manipulate.
- Embryos at older stages were less tolerant of the surgery.

Embryos around 24hpf proved to be more robust than those at 18hpf. The periderm around the otic vesicle of the slightly older embryo is easier to pierce. However, attempts to implant beads into 48hpf embryos resulted in the death of all the beaded embryos. Therefore the 22-27hpf time period was chosen.

Another study investigating otic placode induction implanted Fgf8 soaked beads at a much earlier stage (6hpf). This work relied on many initial implantations (~100's), to generate a few embryos (n=4) with the bead adjacent to the otic vesicle (Léger and Brand, 2001). It was thought a more targeted approach at later stages would generate more data relevant to the patterning of the otic vesicle after it is induced. For future experiments it may be interesting to try early implantations to investigate if the BMPs have a role in the induction or early patterning of the inner ear. Although the relatively late expression of *bmp4* suggests it may not be important, *bmp2b* and *bmp7r* have broad early expression domains (20hpf) which could suggest an earlier role (See discussion, 3.6.4). However, BMPs are required for the correct dorsoventral patterning of the mesoderm at early stages of development (see 1.4.1). Ectopic protein may therefore affect the viability of the embryo or the beads could affect the development of other structures and hence development of the inner ear as a secondary effect.

5.2.3 Beads could move away from otic vesicle during development.

The position of the bead was noted at the time of insertion and fixation (1-2 days later). The placement of the bead around the otic vesicle was important. If not positioned close to the otic vesicle initially, after 2 days it could be found at some distance from the ear. Beads positioned laterally to the vesicle tended to be found around the yolk sac, or in the cardiovascular sac, whereas beads positioned medial to the vesicle tended to be found in more dorsal positions e.g. in the brain, on fixation (Fig. 5.2). However, provided the bead was close to the otic vesicle, variation in position did not affect the response seen.

5.2.4 The effect of the beads was assessed via live, in situ hybridisation, and antibody analysis.

In order to establish what, if anything, had been affected by beading, the treated zebrafish were analysed live, together with in situ and antibody stains. After beading the embryos were allowed to develop for 48-72 hours. They were then anaesthetised and mounted in methyl cellulose, as described in Chapter 8 (8.6.3), for live photographs to be taken. These pictures allowed the development of the SCC and otoliths to be assessed. The final position of the bead was also recorded. The embryos were then fixed and processed for either in situ or antibody staining.

FITC-phalloidin binds to the actin found in cell boundaries and the stereocilia (the hair cell's apical projections). Therefore this actin stain shows up the position of the hair cells, revealing the size and shape of the sensory patches within the inner ear and reveals the general shape of the otic vesicle. The confocal microscope was used to take optical sections through the otic vesicle, which were then reassembled generating one picture that shows the staining through the whole vesicle. Some embryos were also processed for in situ hybridisation with *msxc*, a marker of crista development (Ekker et al., 1992). This probe was selected as a potential target of Bmp signalling to test the activity of the protein. *bmp4* expression was also analysed. The homologues of *bmp4* and *msxc* have been shown to regulate each other's expression in other systems including the chick inner ear (see 3.6.4 and above). As the zebrafish homologues of BMP4 and MSX1, *bmp4* and *msxc*, are normally expressed in the same regions of the developing zebrafish inner ear it would be interesting to see if there is a regulatory relationship between them in zebrafish.

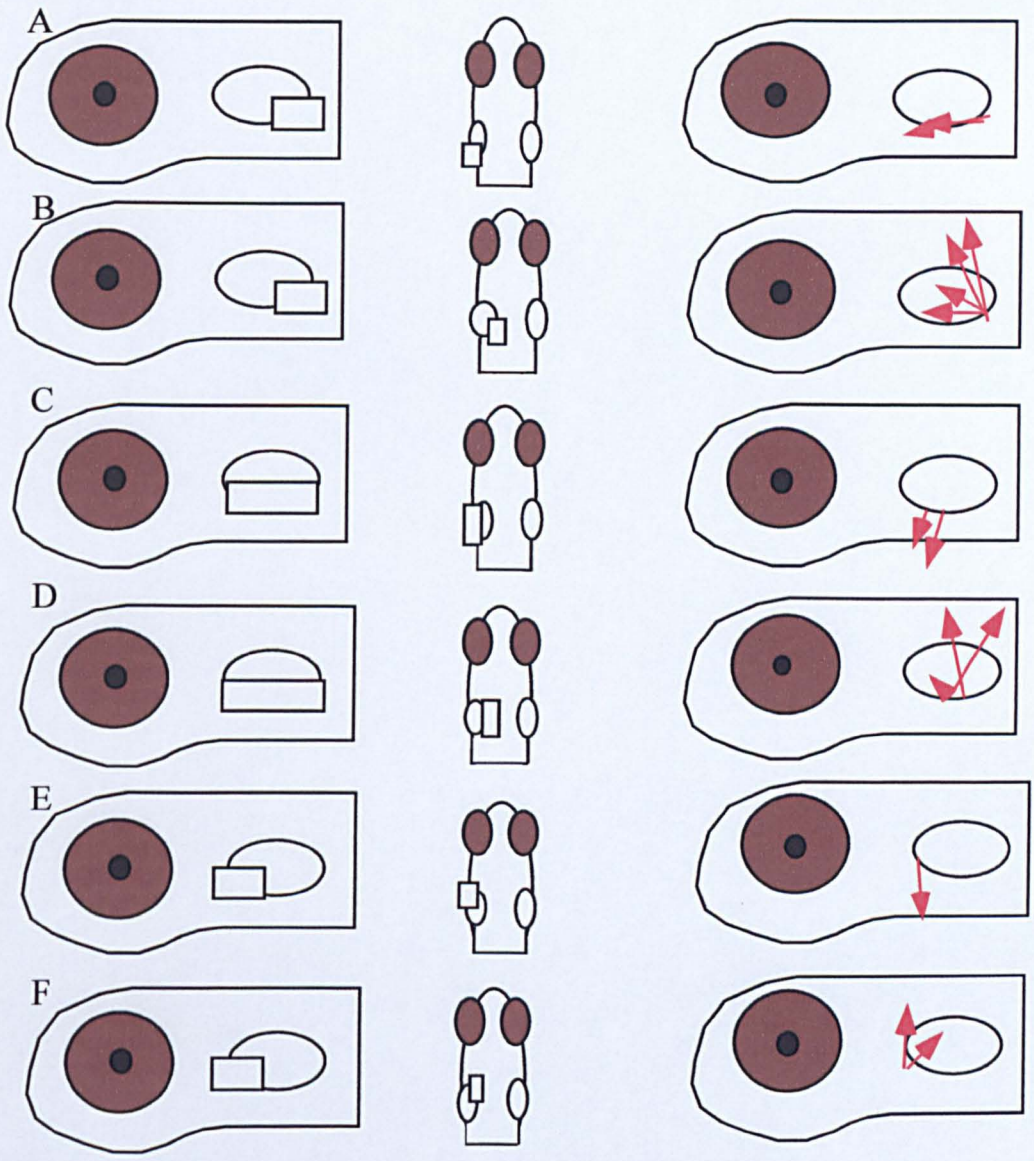

Figure 5.2 Implanted beads can move away from the otic vesicle during development.
These cartoons show lateral and dorsal views of the zebrafish at the time of implantation with a box showing the area of initial bead position, then a lateral view showing (via arrows) the movement of the bead.
(A) Posterolateral beads move anteriorly. (B) Posteromedial beads move dorsally into the brain. (C) Ventrolateral beads under the vesicle moved further ventrally in the yolk or cardiac sac. (D) Ventromedial beads moved dorsally. (E) Anterior lateral beads moved ventrally to heart sac. (F) Anterior medial beads moved dorsally.

5.2.5 Control beads did not affect the development of the otic vesicle.

The implantation of beads coated in BSA or the other relevant controls did not affect the development of the adjacent inner ear (n=80). The SCC formed and fused normally (Fig. 5.3 compare E+I with A). The otoliths also formed normally. The sensory patches were all present, containing both hair cells and support cells and appeared normal (Fig. 5.3; compare G+H with K+L and C+D). After showing that the process of bead implantation itself did not perturb inner ear development, beads coated in hBMP4 and the other proteins were used in similar locations around the otic vesicle under similar conditions. In all cases including control or experimental beads the otic vesicle on the contralateral side to the beaded one was not affected and developed normally. This provides a stage matched internal control for the beaded otic vesicle.

5.3 BMP4 beads in wild type zebrafish.

5.3.1 hBMP4 inhibits the development of the posterior macula.

Implanting hBMP4 coated beads in wild type zebrafish resulted in a reduction in the number of hair cells in the posterior macula, as assessed by the absence of stereocilia using the FITC-phalloidin actin stain. Variety in the timing of implantation (22-27hpf) and placement of the bead along the anteroposterior axis did not seem to alter this phenotype, as long as the bead was in close contact with the developing otic vesicle (Fig. 5.4, compare D+E, Graph and Table 5.1).

At the time of implantation the posterior macula has started to form. Therefore, it is possible that the hBMP4 is arresting posterior macula development at the stage of implantation. However, fixing the beaded zebrafish at an earlier stage (50hpf) after implantation showed that posterior macula development did progress after implantation. The posterior macula did not contain as many hair cells as its contralateral counterpart (Fig. 5.5 compare B+D, F+H); however, it did contain more hair cells than would be found at the time of implantation. This suggests a slowing of posterior macula development rather than a complete arrest (Graph and Table 5.1 p154).

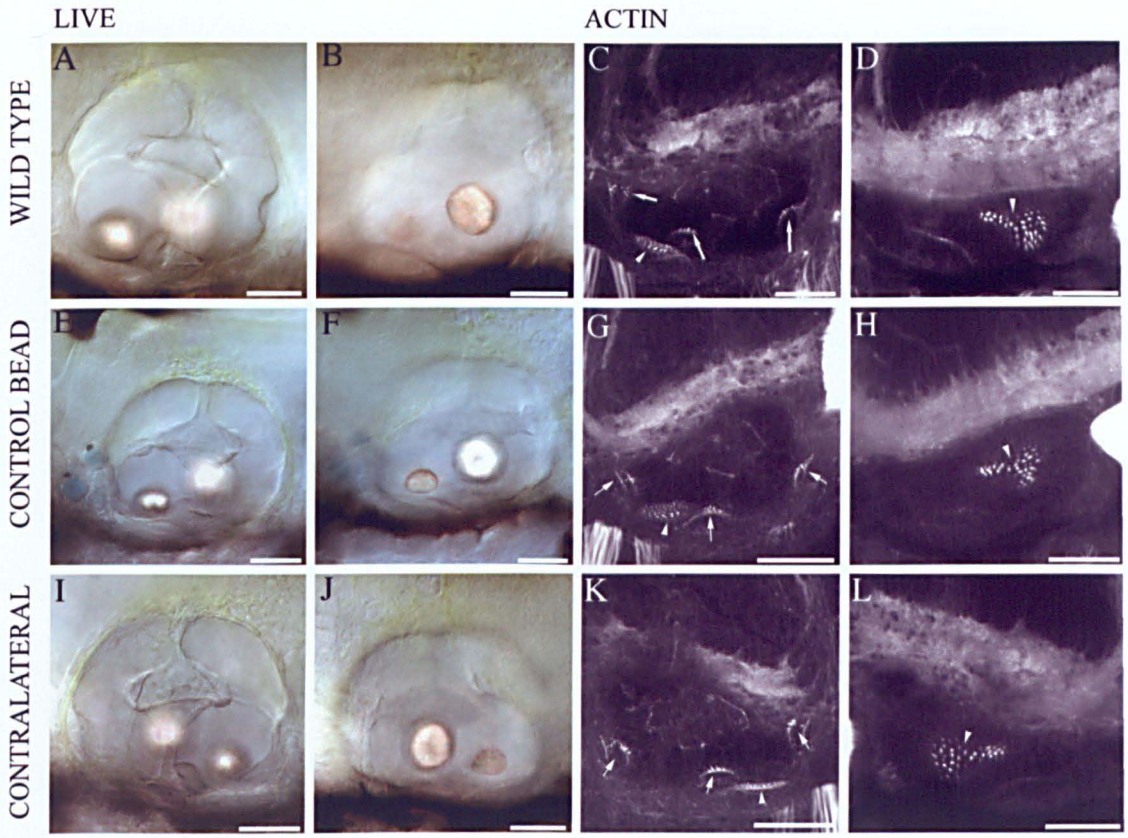

Figure 5.3 Implanting control beads does not affect inner ear development.
Live photographs and FITC-phalloidin labelled actin stains showing different optical sections through whole mount embryos. All are lateral views with anterior to the left except in I-L, which show the contralateral side and have been left with anterior to the right. Scale bar = 50μm.

(A-D) Wild type unbeaded ears showing normal development; the epithelial projections form a cross shape while two otoliths, a smaller more lateral anterior one and a more medial posterior one, also form (A, B). (C) The three cristae are positioned laterally (arrows). The anterior macula is on the ventral floor (C, arrowhead) while the posterior macula is on the medial wall of the inner ear (D, arrowhead).

(E) Multiple beads coated in control proteins (blue spheres, coated in OPT IMEM in this case) were implanted around the anterior of the inner ear. The SCC appear normal with projections fused giving the cross shape (E). (E+F) The otoliths also form normally. (G+H) The three cristae and maculae are in the right position and of the correct size and shape. The contralateral side also shows normal development of the SCC, otoliths (I+J) and sensory patches (K+L).

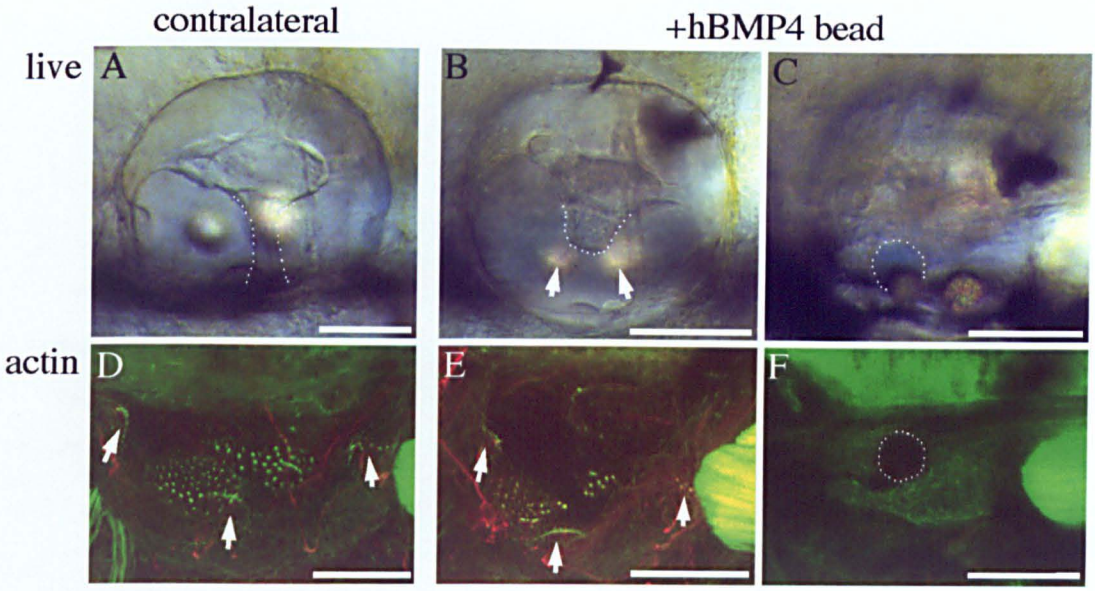

Figure 5.4 Implanting hBMP4 affects the development of wild type otic vesicles. (A-C) are DIC images of the contralateral and beaded sides of the embryo. (D-F) are compressed confocal images showing the sensory patches within these otic vesicles. All are lateral views; anterior is to the left. Scale bar = 50 μm.

(A) Contralateral side showing normal development of the SCC (cross-shaped structure) and position of the otoliths. (B) Epithelial projections have not fused normally on the bead side (outline). (C) The two otoliths are positioned ventrally. The bead is also visible in this picture (outline). (D) On the contralateral side all the sensory patches are visible; the three cristae (arrows), and the two maculae. (E) On the beaded side, the three cristae are present (arrows) as is the anterior macula. There are some hair cells on the medial wall of the vesicle. However, there are many fewer than are found in the contralateral posterior macula. (F) The position of the bead. It appears to be in a slightly different position than in the live image due to mounting.

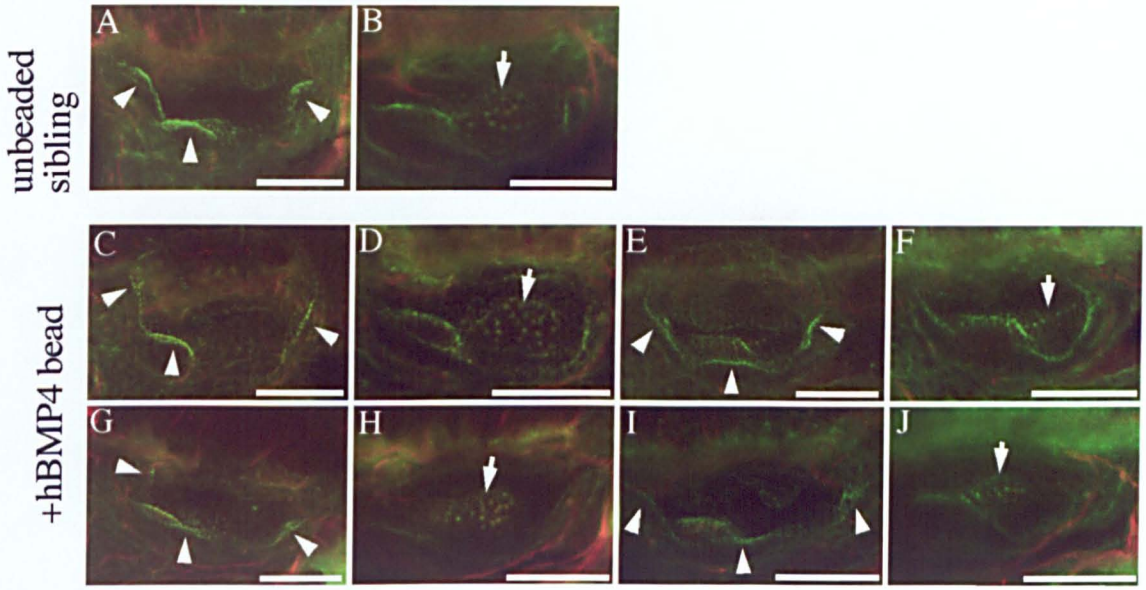

Figure 5.5 hBMP4 affects posterior macula development prior to 50hpf. Compressed confocal images of beaded, contralateral and sibling control vesicles. All are lateral views; anterior is to the left, dorsal to the top. Scale bar=50 μm. (A, B, E, F, I+J) Normally at 50hpf the otic vesicle contains the anterior and posterior macula on the ventral floor and medial wall respectively (arrows). The posterior macula is round and contains around 10 hair cells. The thickenings that will form the cristae are also visible (arrowheads). (C, D, G, H) On the beaded side the posterior macula is abnormally shaped and contains very few hair cells. The anterior macula and crista thickenings appear normal (arrow and arrowheads respectively).

Graph 5.1

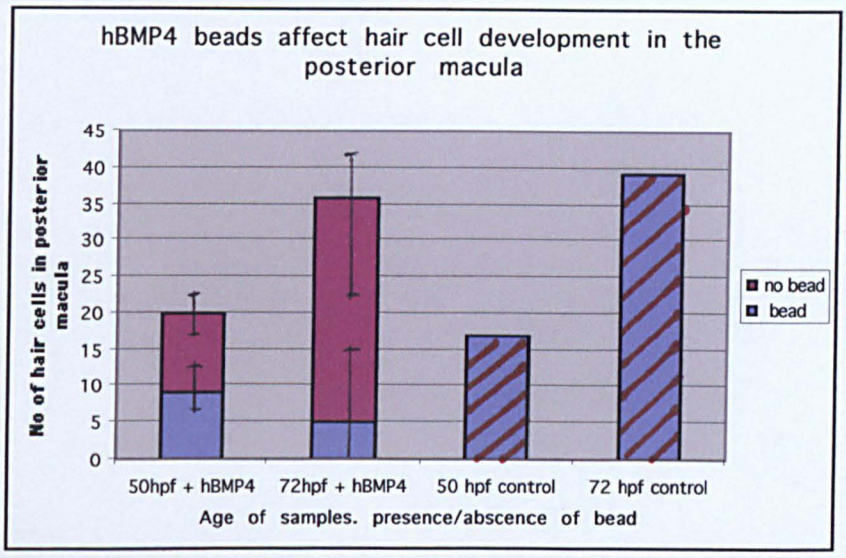

Graph 5.1 shows the mean number of hair cells in the posterior maculae of beaded and contralateral vesicles from Table 5.1. Error bars describe the range of hair cells about this mean (Table 5.1). The control beads were soaked in BSA, serum or Optimen media.
The hBMP4 beads do cause a significant reduction in hair cell number ($P \leq 0.05$, two-tailed Wilcoxon signed rank test). There is no significant difference in control beaded hair cell number ($P \geq 0.05$). See appendix at end of chapter for details.

Table 5.1 The effect of hBMP4 beads on hair cell number in the developing posterior macula at two stages (around 48hpf and 72hpf).

	Beaded side +hBMP4		Contralateral		+ Control bead		Contralateral
Exp	bead	No of pm hc	No of pm hc	Exp	bead	No of pm hc	No of pm hc
24-48hpf							
VII 1	a	6	19	QQ3	a	19	20
VII 2	p *	12	18	QQ7	p	17	17
VII 10	a	7	23	QQ14	nb	16	17
VII 11	p	5	19	QQ16	a	16	16
VII 12	p	11	23				
VII 13	m	13	19				
24-72hpf							
C 1	a	7	22	OO5	a	44	46
C 7	a	0	45	OO10	m	44	42
C 8	a+p	0	35	II 4	p	39	41
D 9	p	0	35	KK 2	a	38	38
E 1	a	8	39	KK3	p	31	29
E 3	m	15	40				

* Bead was not initially touching vesicle; could account for weaker bead phenotype. All beads medial. Control beads were soaked in BSA (QQ), Optimen (KK, OO) Serum (II). Abbreviations: Exp, experiment; hc, hair cells; No, number; pm, posterior macula

Adding exogenous hBMP4 protein has a specific effect on the development of the posterior macula. There are three possible explanations for the reduction in hair cell number in the posterior macula: hBMP4 could be reducing macula size by increasing cell death, decreasing the rate of cell division, or by shifting cells to another fate.

5.3.2 hBMP4 beads do not increase cell death.

Previous studies using TUNEL labelling have shown there to be no great foci of cell death during the development of the zebrafish inner ear (Bever and Fekete, 1999;Haddon, 1997), although more recent work has documented a higher level of cell death than previously thought (Cole and Ross, 2001). The limited study in this thesis showed there was no obvious recurring collections of TUNEL positive cells in particular areas of wild type otic vesicles at 50 or 72hpf (Fig. 5.6 Table 5.2). As a positive control, the level of cell death in *dog* ^{tm90b} mutant and sibling embryos at 27hpf was also assessed using the same technique. As mentioned in Chapter 4, *dog*^{tm90b} have a dorsolateral domain of cell death not seen in the sibling otic vesicle, and an increased level of cell death in the lateral line organ (Kozlowski et al., 2001a). This pattern of cell death was reproduced, indicating that the TUNEL technique worked correctly (Fig 5.6 A-D).

No increase in cell death following the implantation of hBMP4 beads at either 50hpf or 72hpf was seen (Fig 5.6 L-S). A limited number of *X*Noggin implanted beads were also analysed. These embryos did not show any dramatic alteration of levels of cell death (Fig. 5.6 T+U).

There have been reports suggesting that TUNEL may also label necrotic cells or cells damaged after death by fixation (Nishizaki et al., 1999). Therefore any errors in attributing a positive TUNEL signal are likely to overestimate rather than underestimate the number of positive signals.

5.3.3 hBMP4 beads may not affect rate of cell division.

No dramatic areas or time points of cell proliferation have been described in extensive studies of zebrafish otic vesicle development (Haddon, 1997). Work in this thesis using anti-phospho-histone H3 is in agreement with this. Anti-phospho-histone H3 is a marker of cells in late G2 interphase (Hendzel et al., 1997), which is a smaller proportion of the

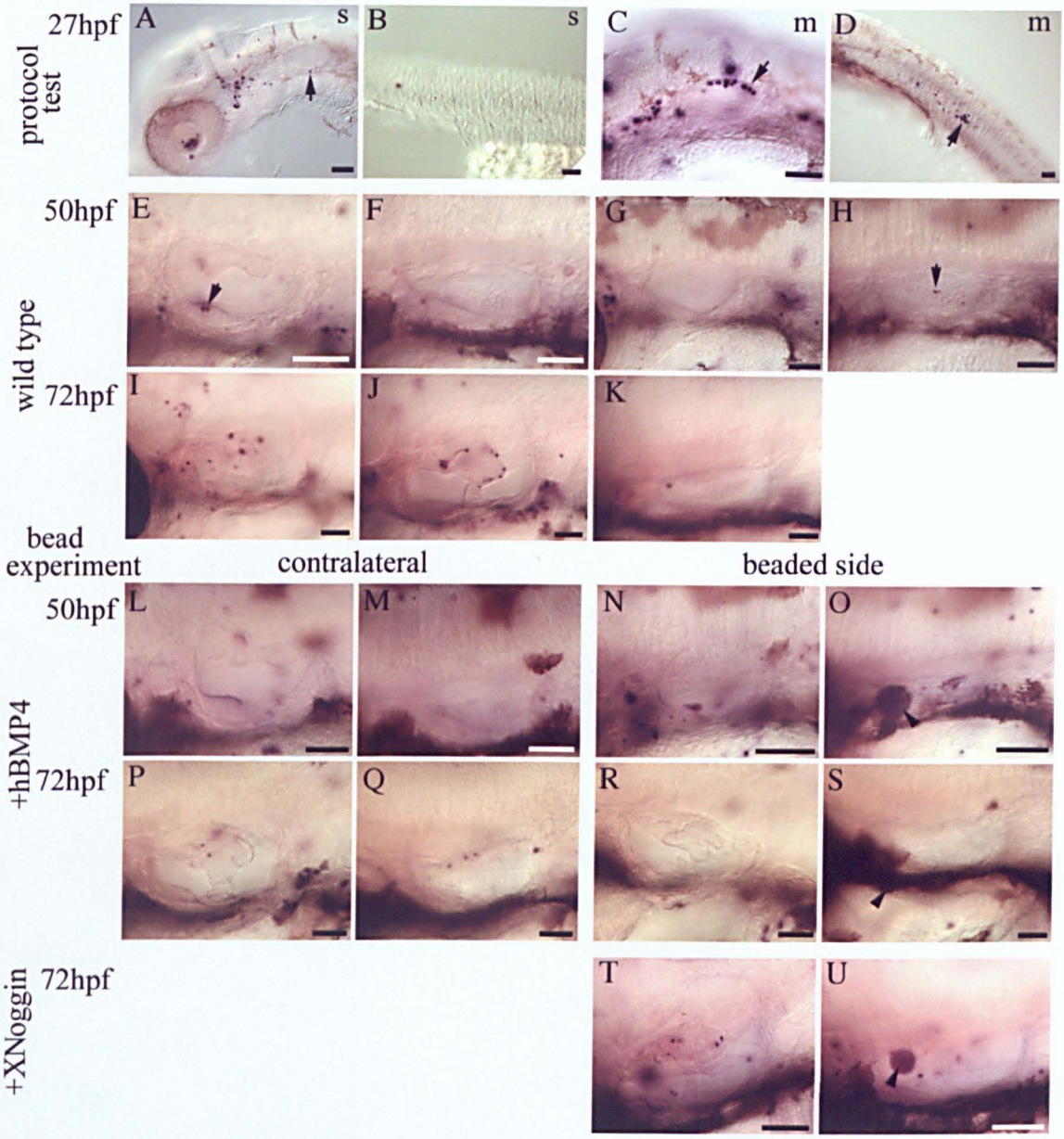

Figure 5.6 hBMP4 beads do not affect rate of cell death.
Whole mount in situ hybridisations of Apoptag labelled apoptotic cells. All are lateral views: anterior is to the left, dorsal to the top. Scale bar=50 μm.

(A-D) To test the protocol a previously reported result was checked (Kozlowski et al., 2001a). At 27hpf *dog* mutants (m) show an increase in cell death in their otic vesicle (C) and lateral line primordium (D). This is not seen in siblings (s, A+B). (E-H) In wild type embryos at 50hpf there are few positive cells within the inner ear (arrows). Positive cells are found in the anterior macula (E) and posterior macula (H) but are not concentrated in a specific area. (I-K) In wild type embryos at 72hpf a few more positive cells are seen in the fusion plate (J). (L, M and P, Q) The contralateral side of hBMP4 beaded ears at similar stages, each with a few positive cells. (N, O and R, S) The beaded side shows a comparable number of positive cells. (T+U) The addition of *X*Noggin coated beads did not affect the pattern of cell death seen.

Table 5.2 hBMP4 beads do not increase rates of cell death

Figures in the table indicate the number of TUNEL positive nuclei seen in different regions of the ear.

Exp	age hpf	bead	posterior macula	anterior macula	cristae	fusion plate	other	total
control								
VII5	50	No	3				1A/M 3 V 1 PL	8
VII4	50	No	-	-	-	-	2 D	2
VII3	50	No	1					1
VII2	50	No	3					3
VII1	50	No		2			1 M	3
beaded embryos								
VII 14	50	Yes		1	3 (P) 2 (A)		1 P	7
VII 14	50	No		1	1 (P) 1 (A)			3
VII 17	50	Yes		1		1	1 P	3
VII 17	50	No			1 (P)			1
VII 18	50	Yes					1	1
VII 18	50	No					1	1
VII 15	50	Yes		2	1 (A)			3
				2	1 (P)	7		11
control								
control	72hpf	no			1(A)	9	5 NM 1 A/M	15
beaded embryos								
X19	72hpf	Yes						0
X19	72hpf	No				2	3 D	5
*VIII 6	72hpf	Yes (N)	1	2		7		11

*VIII 6 was implanted with a *X*Noggin bead. Abbreviations: A, anterior; D, dorsal; M, medial; N, *X*Noggin; NM, neuromast; P, posterior; PL, posterolateral.

cell cycle compared to S phase, which is marked by BrdU. It was therefore difficult to assess if there had been a subtle decrease in the rate of cell division in the posterior macula (Graph and Table 5.3). Alternatively, if cells that normally form posterior macula hair cells were failing to differentiate, and instead were continuing to divide, there would have been an increase in the number of positive cells in the medial wall of the otic vesicle. No such increase was seen.

5.3.4 Implanting hBMP4 beads around wild type otic vesicles did not affect cristae.

hBMP4 beads did not affect the development of the endogenous cristae. They contain differentiated hair cells, which are normally spaced and develop at the right time, and to the right size, compared to the contralateral (nonbeaded) vesicles in the same fish (Fig. 5.4 compare D+E). No ectopic sensory patches were seen to develop adjacent to the bead (assessed via a FITC-phalloidin stain). There was no ectopic expression of *msxc* around the bead (see section 5.3.7 below).

5.3.5 hBMP4 beads did affect the development of the semicircular canals.

The implantation of hBMP4 beads did affect the development of the SCC to slightly varying extents (Fig. 5.7). However, this was not apparent until 72hpf. The earliest stages of SCC development are morphologically visible around 45hpf, when the epithelial projections first push into the lumen of the otic vesicle (Fig. 1.2C (Waterman and Bell 1984)). The implantation of hBMP4 beads did not affect these early stages (Fig. 5.7 1-6). However, at 72hpf the SCC on the hBMP4 beaded side of the embryo were not as well developed as those on the contralateral side. The projections from the anterior and posterior walls of the vesicle do form and fuse but in the majority of cases the ventral projection, which normally develops after these lateral projections, does not project properly or fuse on the beaded side. In some cases the ventral projection is not formed, although projections on the contralateral side have fused to form the cross shaped structure which normally divides up the lumen of the otic vesicle (Fig. 5.7 7-17). This failure of the ventral projection to fuse can still be seen at 5dpf (Fig. 5.7 18-29).

Graph 5.3

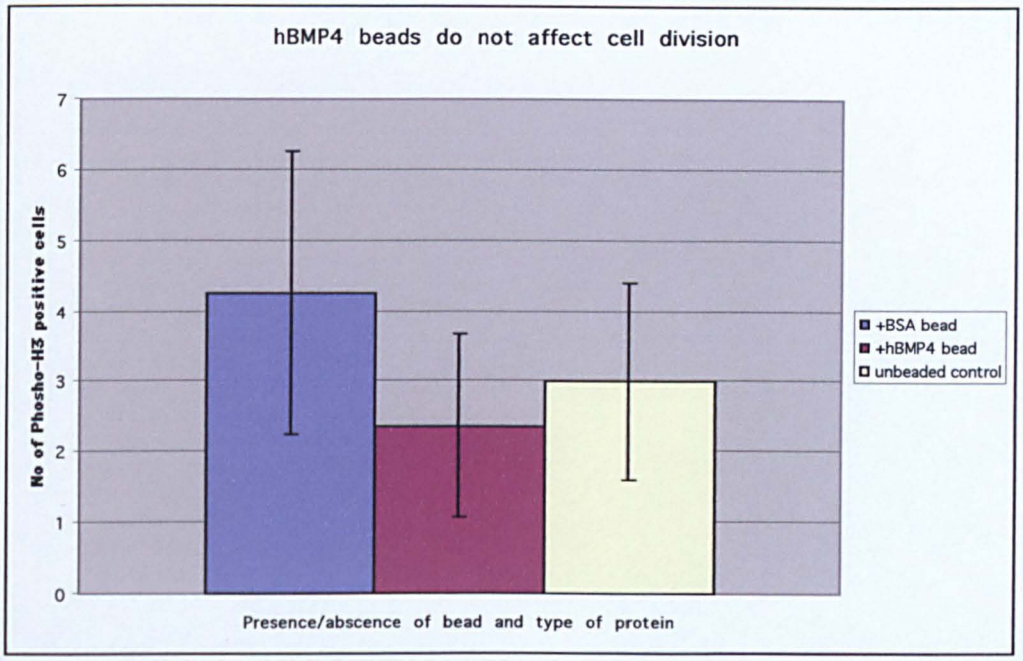

There is no difference in cell division between BSA beaded and unbeaded vesicles. Each bar represents data from four ears (BSA, hBMP4 samples) or two ears (unbeaded control). Error bars represent standard deviation.

Table 5.3 hBMP4 beads do not affect the rate of cell division in the developing otic vesicle.

Experiment	Protein on bead	No of positive cells (No of hc in pmac)	
		+ bead	contralateral
QQ14	BSA	4 (23)	4 (22)
QQ16	BSA	3 (20)	3 (24)
QQ3	BSA	2 (21)	6 (24)
QQ7	BSA	5 (21)	8 (20)
PP11	hBMP4	3 (9)	2 (14*)
PP12	hBMP4	3 (14)	5 (24)
PP17	hBMP4	1 (12)	1 (24)
PP9	hBMP4	2 (8)	2 (24)
Control			
PP4	no bead	4 (24)	
PP3	no bead	2 (20)	

*Inadequate actin staining (bleaching) prevented counting of all hair cells on this side of embryo.

Abbreviations: BSA, bovine serum albumin; hc, hair cells; hBMP4, human Bone Morphogenetic Protein; No, number; pmac, posterior macula.

5.3.6 hBMP4 beads affect the development of otoliths.

hBMP4 beads also affect the development of the otoliths. Normally these structures overlie their respective maculae. When a hBMP4 bead is implanted, the posterior otolith is smaller and positioned more ventrally, closer to the anterior otolith than normal. This is indicative of defects in the underlying macula (see 5.3.1). At later stages the two otoliths can fuse, presumably due to their close association (5dpf Fig. 5.7 23 + 27).

5.3.7 hBMP4 beads did not affect the expression of *bmp4* or *msxc*.

In order to investigate the possibility of feedback loops in which hBMP4 induces the expression of *bmp4* and/or *msxc*, in situ hybridisations were carried out on beaded zebrafish. There was the possibility of affecting the endogenous expression patterns of these genes and/or inducing their ectopic expression. However, no effect was seen on the endogenous *bmp4* or *msxc* expression pattern at 28hpf or 72hpf in hBMP4 beaded embryos (Fig. 5.8). There was no ectopic expression of these genes either.

5.3 CONCLUSIONS

hBMP4 beads have an effect on the development of both sensory and nonsensory tissues in the developing otic vesicle. These effects are specific to hBMP4 i.e. they are not a consequence of bead insertion. These experiments also demonstrated that ectopic BMP4 signalling is not sufficient to generate ectopic cristae. These results will be explored in more detail in the discussion (5.6).

5.4 hBMP4 beads in mutant zebrafish.

The inner ears of *vgo* mutants do not express the *bmps* or *msxc* ventrolaterally. They do not form SCC, cristae or develop normal maculae. They develop a single sensory patch (see Chapter 4).

hBMP4 coated beads were implanted adjacent to the otic vesicles of *vgo* embryos in an attempt to rescue aspects of the *vgo* phenotype. Implantations were carried out before the mutants could be identified by eye and so roughly a quarter of the embryos implanted were mutant in each experiment. These embryos were then processed as the wild type embryos were, using live pictures, actin stains and in situ hybridisations.

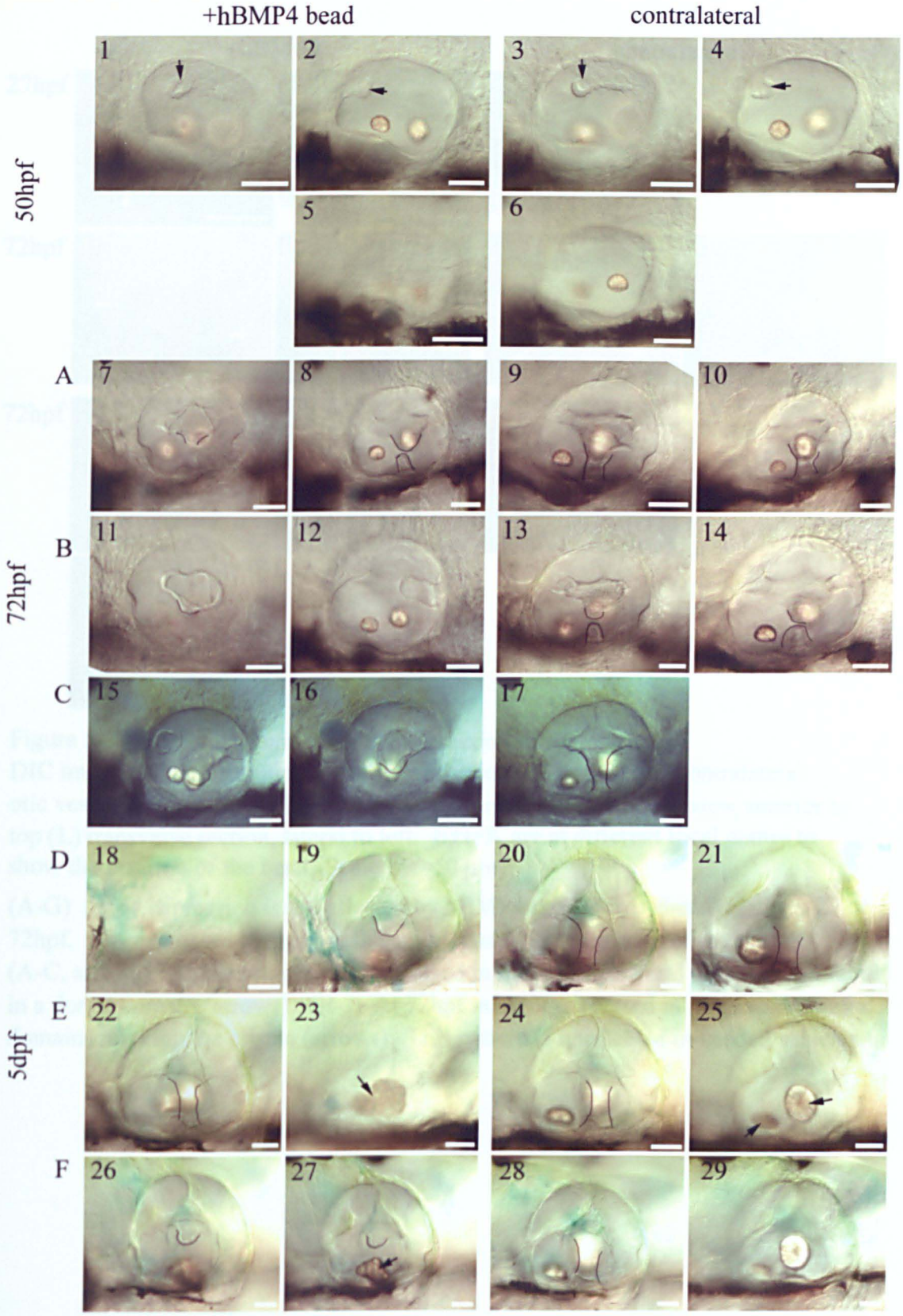

Figure 5.7 hBMP4 affects SCC development.
DIC images of live zebrafish embryos showing beaded and contralateral sides. All are lateral views; anterior to the left and dorsal to the top. Scale bar= 50 µm.
(1-6) At 50hpf normal SCC development is initiated on both beaded and contralateral sides. Anterior, posterior and lateral projections are visible (arrows). (7-17) At 72hpf there is an obvious difference between the two sides. On the beaded side the fusion plate is not the normal shape and the ventral projection is retarded compared to the contralateral side (outline). (18-29) By 5dpf the ventral projection has still not fused on the bead side (outline). In some cases the otoliths which are normally displaced ventrally on beaded vesicle sides have fused (arrows).

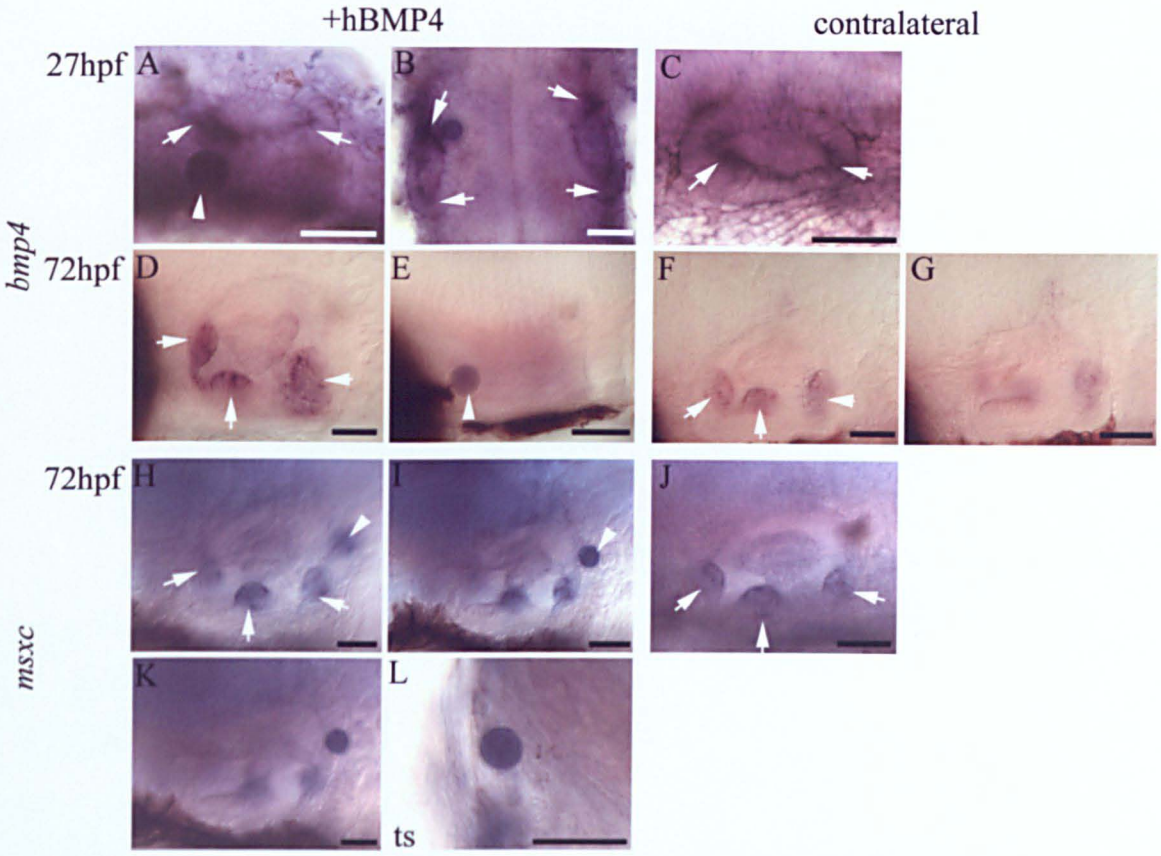

Figure 5.8 hBMP4 does not affect the expression of *bmp4* or *msxc*.
DIC images of whole mount in situ hybridisations of beaded and contralateral otic vesicles. (A, C, D-K) lateral views, anterior to left (B) dorsal view, anterior to top (L) transverse section, lateral to left. E+I+K are at different focal planes to show the position of the bead. Scale bar=50 μm

(A-G) *bmp4* expression is not affected by hBMP4 beads (arrowhead) at either 27 or 72hpf. It is expressed strongly at the anterior and posterior ends of the vesicle (A-C, arrows). At later stages it is expressed in three ventrolateral domains and faintly in a dorsal domain (arrows). (H-J) At 72hpf *msxc* is expressed in three ventrolateral domains marking the cristae (arrows). This pattern is unaffected in beaded vesicles.

5.4.1 hBMP4 beads affect development of part of the single macula in *vgo* vesicles.

Actin stains revealed that, as in hBMP4 beaded wild type zebrafish, the macula of the *vgo* mutant is affected. Specifically, the posterior medial domain of the single macula found in the *vgo* mutants is missing (Fig. 5.9D+E). This suggests that the single sensory patch in *vgo* consists of an abnormal posterior macula, possibly fused to an anterior macula.

5.4.2 hBMP4 beads do not rescue any aspect of the *vgo* phenotype.

There is no rescue of *msxc* expression following implantation of hBMP4 beads (Fig 5.9F-H). Using FITC-phalloidin to label actin, no ectopic patches of hair cells were seen to develop (Fig. 5.9D+E). Live pictures also show that there is no rescue of epithelial projection development, although this was not expected given that in wild type hBMP4 beads inhibit SCC development. The example shown has only 1 otolith (Fig. 5.9A-C). This is not found in all mutants with an affected sensory patch, and is due to the vesicle being punctured when that bead was implanted allowing the otolith to escape.

5.4 Conclusions

There is a defect in the development of the *vgo* sensory patch following implantation of hBMP4 beads. This appears to be identical to the defect seen in wild type beaded embryos. There is no rescue of cristae or SCC development.

5.5 BMP antagonist-coated beads.

5.5.1 NOGGIN beads did not affect development of zebrafish inner ears.

Noggin is a Bmp antagonist, which acts by binding to BMP dimers and preventing them binding to their receptor (Holley et al., 1996; Zimmerman et al., 1996). In the zebrafish, given the results of hBMP4 bead implantation and the chick work it was expected that the development of the SCC, cristae and posterior macula would be affected. However, in zebrafish, *X*Noggin coated beads, at two different concentrations,

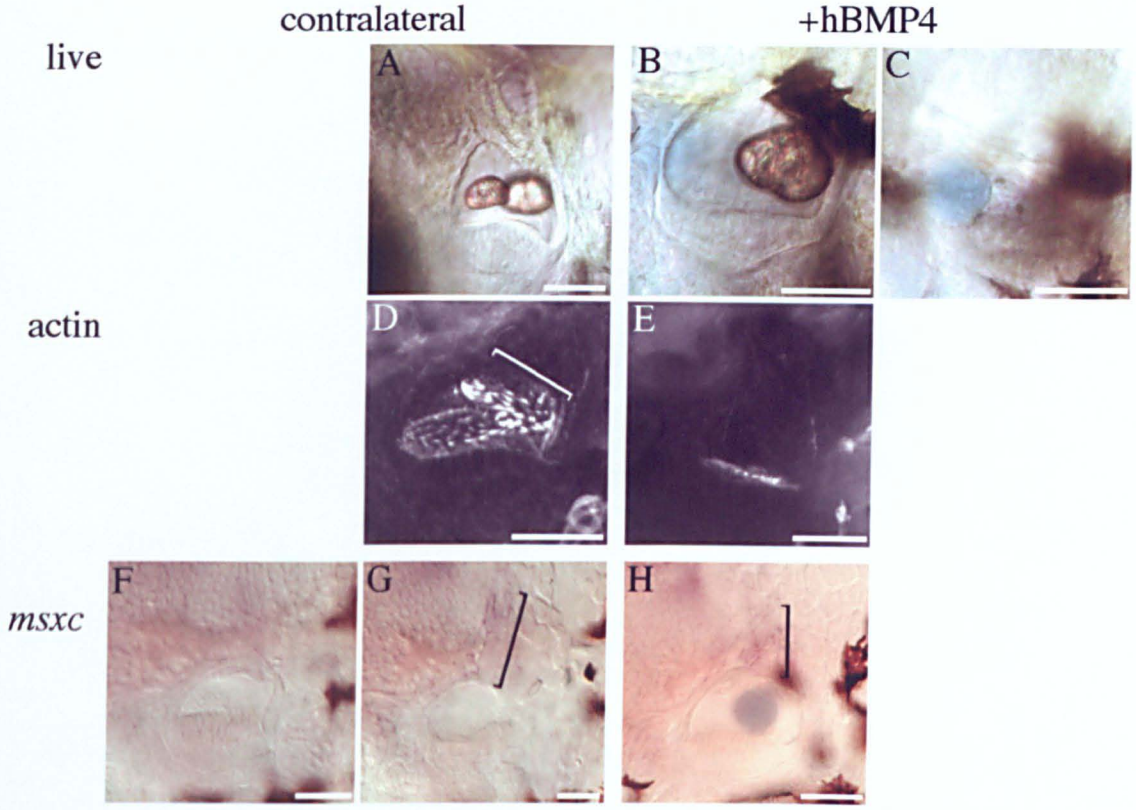

Figure 5.9 hBMP4 beads affect sensory patch development in *vgo* mutants.
DIC images of live (A-C) and whole mount in situ hybridisations (F-H) of beaded and contralateral otic vesicles. (D+E) compressed confocal images of sensory patch in beaded and contralateral sides. All are lateral views with anterior to left and dorsal to the top. Scale bar = 50 μm.
(A) In *vgo* mutants the vesicle is much smaller and has a large dorsal protrusion, but still contains two otoliths. (C+B) The beaded side is usually the same, a small vesicle with a large dorsal extension and two otoliths. However, in this case the anterior otolith was liberated when the bead was implanted. (D) Normally *vgo* mutants have a single sensory patch at this stage which covers the ventral floor and extends up the medial wall of the vesicle. (E) In beaded vesicles the sensory patch does not extend up the medial wall. (F-G) *msxc* is only expressed dorsally in these mutants (brackets). (H) hBMP4 beads do not alter *msxc* expression in *vgo* mutants.

did not affect the development of the SCC or the cristae. They also had no effect on the development of the posterior macula (*Fig 5.10A-H, Graph 5.4 p168*).

Two experiments were used to test the activity of the *X*Noggin protein. In the first, beads were coated in hBMP4 and then soaked in concentrated *X*Noggin. If active, the *X*Noggin would bind to the hBMP4 and titre its activity. A similar experiment in the chick has shown that *X*Noggin from the same cell line could inhibit the action of hBMP4 (Chang et al., 1999). However, this 'double dip' experiment did not modify the hBMP4 bead phenotype seen in zebrafish; the inhibition of posterior macula development was still seen (data not shown).

The second experiment implanted *X*Noggin beads at an earlier stage to try and modify early BMP signalling. As described in Chapter 1, the zebrafish BMP mutants are described as a dorsalised class of mutants, due to defects in the early patterning of the dorsoventral axis. This class contains a range of phenotype from severe embryonic lethal forms (e.g. *swirl*) to milder phenotypes lacking the ventral tail fin (e.g. *piggy tail*) and viable phenotypes (*mini fin*) (Mullins et al., 1996). These phenotypes have been replicated in overexpression experiments using *XNoggin* mRNA (2-5pg) to reduce Bmp signalling. The mRNA was injected into wild type zebrafish at the one cell stage resulting in dorsalised embryos, with disrupted body axes and the misexpression of markers e.g. expansion of expression of the neuroectoderm marker *forkhead3* (Hammerschmidt et al., 1996b).

To test the function of the *X*Noggin coated beads, they were implanted into the ventral side of a gastrula stage embryo (5hpf) i.e. opposite where *noggin* is normally expressed, in an attempt to recreate this dorsalised phenotype. The beading technique did not result in such a dramatic phenotype as that seen following RNA injection. However, *X*Noggin beads did result in a *piggytail*-like phenotype, with embryos losing their ventral tail fin (Fig. 5.11E+F). These results suggest that the *X*Noggin protein is capable of inhibiting endogenous BMP signalling when added to the embryo via beads. The lack of phenotype in the otic vesicles may be due to the relatively low concentration of protein, the efficiency of release from the bead or redundancy among the Bmps. Current experiments are underway to produce a more concentrated form of *X*Noggin, which may affect inner ear development.

5.5.2 Chordin beads did not affect development of zebrafish inner ears.

Chordin is another antagonist of BMP signalling. Implanting chick Chordin coated beads did not affect the development of the otic vesicle in the majority of cases (Fig. 5.10I-P, Graph 5.4). Implantating Chordin beads into the ventral side of the early zebrafish embryo also results in a *piggytail*-like phenotype (expansion of notochord and protruding tailbud (Mullins et al., 1996) (Fig. 5.11A-D)). This suggests that the protein is active and the lack of a more severe phenotype may be similar to the reasons described above for *X*Noggin.

5.5 Conclusions

Antagonist-coated beads can replicate phenotypes seen in previously characterised dorsalised zebrafish mutants, but have no effect on the development of the otic vesicle. The lack of phenotype in otic vesicles may be a consequence of concentration, efficiency of protein release from beads or redundancy amongst the BMPs (see below).

5.6 DISCUSSION

The experiments described in this chapter have shown:

- that beads can be used as local sources of protein in the otic epithelium.
- that exogenous hBMP4 inhibits the differentiation of the posterior macula but has no effect on the other sensory patches of the inner ear.
- that exogenous hBMP4 inhibits the formation and fusion of the epithelial projections that form the SCC, particularly the ventral projection.
- that an exogenous source of hBMP4 is not sufficient to induce ectopic *msxc* or *bmp4* expression or the development of cristae.
- that the results of adding BMP antagonist coated beads are inconclusive.

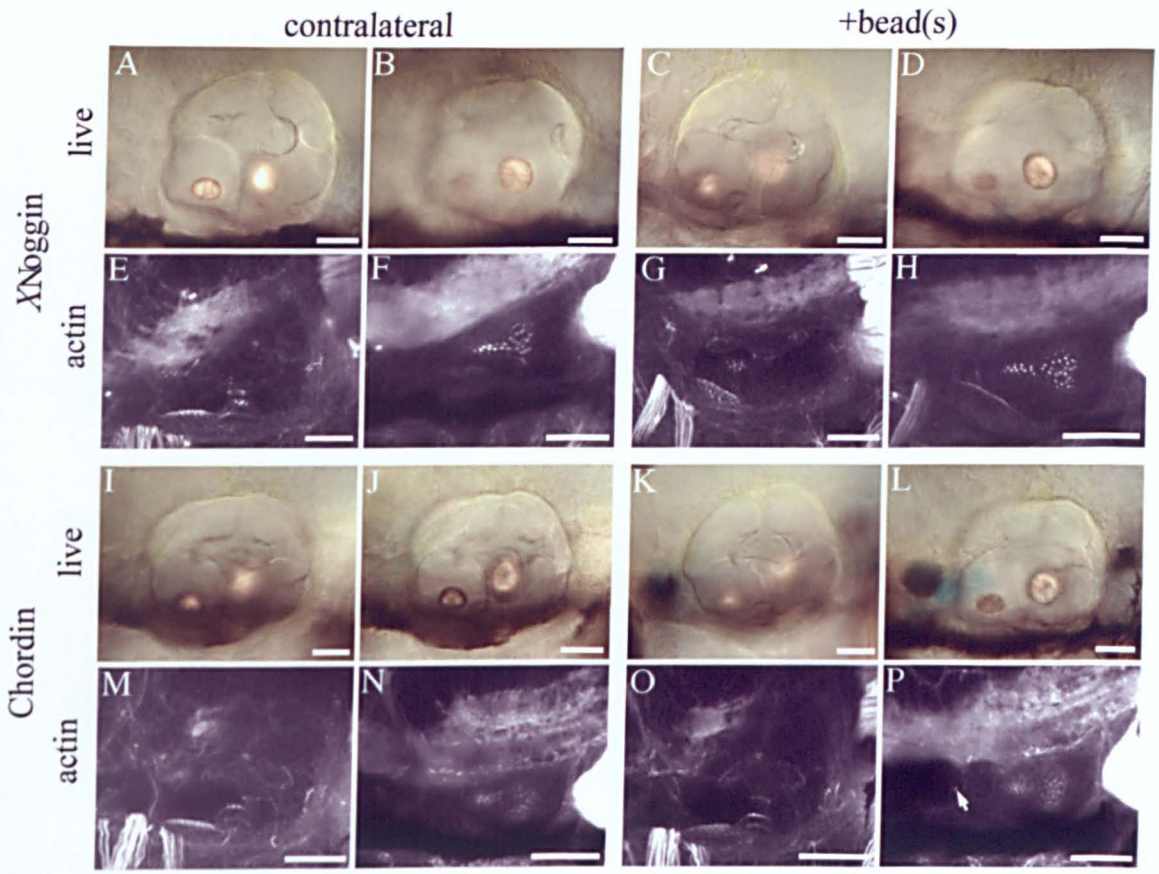

Figure 5.10 Antagonist beads did not affect otic vesicle development.
DIC images of live embryo's otic vesicles beaded and contralateral sides (A-D, I-L). (E-H, M-P) Compressed confocal images of the actin stains of the same otic vesicles. All are lateral views; anterior to left, dorsal top. Scale bars=50 μm.

SCC and otolith development was not affected by the implantation of *X*Noggin (compare A+B to C+D) or Chordin (compare I+J to K+L) soaked beads. Neither *X*Noggin (compare E+F to G+H) or Chordin (compare M+N to O+P) beads affected the development of the sensory patches. Arrow in P shows the position of the bead.

Graph 5.4

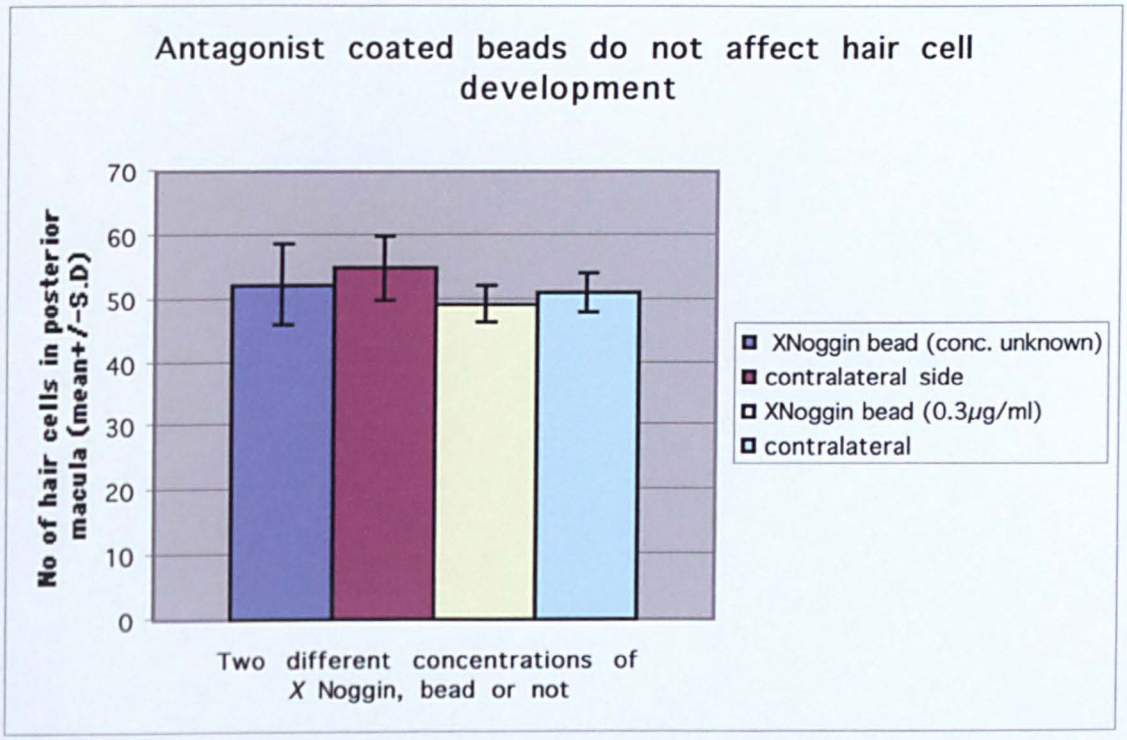

(n=13 for unknown concentration, n=10 for 0.3μg/ml)

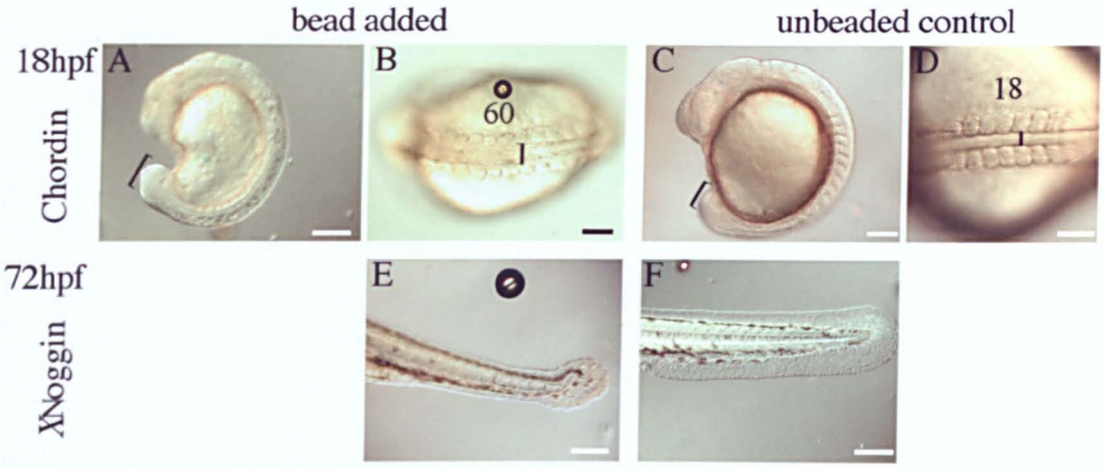

Figure 5.11 Adding antagonist-coated beads to shield stage embryos generates a mild dorsalised phenotype.

DIC images of live embryos either implanted with antagonist coated beads at shield stages or unimplanted controls. (A, C, E+F) lateral views; anterior to left, dorsal to top. (B+D) dorsal views; anterior to left. Scale bar: A, C, E+F= 200, B=100, D=50 μm.

The addition of Chordin soaked beads resulted in an enlarged notochord and tailbud (compare A+B to C+D, brackets, numbers detail width of notochord in μm). The addition of *X*Noggin coated beads resulted in the loss of the ventral tail fin (Compare E+F). No phenotype was seen with control beads (data not shown).

5.6.1 Ectopic hBMP4 has a surprising effect on posterior macula development.

The implantation of hBMP4 beads inhibited the development of the posterior macula. Although none of the *bmps* are expressed in the posterior macula, the discrete domain of one of its receptors does include it (*bmprIB*, Fig. 3.1) and so part of the signalling pathway is present. However, it is not clear if the endogenous BMPs do signal to these cells (see discussion 3.6.3).

The expression of *follistatin* could indicate the need to control the medial signalling of BMPs. This BMP antagonist is expressed in the posterior epithelium of the vesicle from 24hpf (Fig. 3.10). This expression pattern suggests that the level of BMP signalling in that region needs to be inhibited to produce a normal otic vesicle. This could be turned into the simple model below.

Fig. 5.12 Control of medial cell fate

Follistatin ⊣ BMP ⊣ posterior macula

If this model is correct one way to test it would be to inhibit the BMPs and see if that expanded the posterior macula. However, as discussed above, the experiments, using Chordin or *X*Noggin-coated beads have not yet proved conclusive.

5.6.2 What is happening to posterior macula cells?

Following implantation of the hBMP4 beads there are four possible fates for cells that would normally form the posterior macula. They can carry on as normal and differentiate into hair cells, die, keep dividing and fail to differentiate, or differentiate into another kind of cell.

Death and division

Comparing the posterior maculae of hBMP4 beaded vesicles at 50hpf and 72hpf shows that hair cells continue to differentiate after the bead has been implanted. However, compared to the contralateral side, there are fewer hair cells, the macula is not patterned normally and differentiation does not continue beyond 72hpf; although hair cells are present on the medial wall of the vesicle at the earlier time point, they are much reduced or completely absent by 72hpf. However, there are more hair cells present at 50hpf than

have differentiated at the time of implantation and therefore some differentiation occurs in the presence of the beads.

The hair cells that do differentiate following bead implantation could have been committed to their fate at the time of implantation and so are not affected by the ectopic protein. This suggests that the ectopic hBMP4 is inhibiting hair cell development at an earlier precursor stage. It would be interesting to follow the development of the hair cells, as markers for the different stages of hair cell differentiation are discovered, to see how far, if at all, this differentiation progresses.

BMPs have been implicated in regulating cell death and division (see 1.4.3). Pushing the cell into either of these fates would prevent it forming a hair cell. However, no increase was seen in studies into cell death and proliferation after beading. Cell death was examined at two time points: 50 and 72hpf. Hair cells were still present in the posterior macula of beaded vesicle examined at 50hpf and therefore they had not all died at an earlier stage. No great increase was seen in cell death or division between these stages, when the hair cells are failing to differentiate. If the cell proliferation experiments were to be repeated BrdU would be used. BrdU labels cells in a part of the cell cycle which is longer than that labelled by phospho-H3 (S, and late G2 respectively). Therefore, a short pulse of BrdU will label a higher proportion of cells in the vesicle making it easier to see any subtle changes in cell division rates.

Cell fate switch

After hBMP4 bead implantation, actin stains, in situ hybridisations and live images suggest the otic vesicle is normal apart from the posterior macula and the SCC. The lack of suitable in situ hybridisation markers for the different structures of the inner ear makes investigating the possibility of a change of fate difficult. To confirm a change in fate, fate maps would have to be performed. However, using the confocal microscope and actin stains, the medial wall of the vesicle appears normal apart from the lack of hair cells.

It has been suggested that there is a gradual specification of cell fates within the inner ear. In a recent model otic cells are designated as being sensory or nonsensory (dependent on positional cues) before being specified as a particular cell type within that sensory patch (Fekete, 1996 and see Fig. 7.1). The hBMP4 beads could be acting at two levels in this differentiation pathway. The ectopic hBMP4 could act after the cell has been specified to become sensory, biasing it towards a support cell rather than a hair

cell fate (see below). Alternatively the hBMP4 signal could inhibit the cells from becoming sensory, so instead they form the epithelium that lines the otic vesicle. The timing of this sensory or nonsensory fate decision is not clear, however, by 24hpf the expression patterns of initially widely expressed genes have become restricted to particular domains (e.g. *pax2.1*, *eya1*, *dlx3* Whitfield et al., in press) suggesting cell fates are also being restricted. At this time point the restricted domains of *bmp* expression appear (see Chapter2).

In the *mindbomb* zebrafish mutant defects in Notch-Delta signalling lead to the differentiation of ectopic hair cells. These cells are thought to arise from normal macula domains in which support cells are never specified, becoming hair cells instead (Haddon et al., 1999). The opposite cell fate switch may be happening following the implantation of hBMP4 beads. The ectopic protein may bias cells towards a support cell fate. However, in chick, *BMP4* is expressed in the support cells of the differentiating maculae and so it would have to be acting in an autocrine manner if it were required to form support cells (Oh et al., 1996). In zebrafish, it is not clear if *bmp4* is segregated to hair or support cells in the cristae and there are no known markers of support cells yet identified to check this hypothesis.

Normally, the otoliths sit in a gelatinous layer on top of each macula, remaining in contact with the hair cells (Riley and Grunwald, 1996). In beaded vesicles the posterior otolith is normally positioned more ventrally than the contralateral side and is smaller. This otolith may require the missing hair cells as an anchor for itself or its gelatinous layer.

Support cells are thought to be required for the synthesis of macromolecules required for otolith formation (see 1.2.4). If the posterior macula hair cells in beaded vesicles are forming ectopic support cells perhaps enlarged otoliths would be expected. This was not seen. Alternatively, the smaller posterior otolith could suggest a decrease in the number of support cells in the posterior patch inhibiting the growth of the otolith. However, without markers this lack of support cells is hard to confirm.

5.6.3 Ectopic hBMP4 also affects *vgo* mutant's medial macula.

hBMP4 beads inhibit the development of the medial portion of the large sensory patch in *vgo*. This is supporting evidence that this large sensory patch found in the mutant is a fusion of the anterior and posterior maculae. There are no posterior macula specific markers as yet. The lack of *msxc* expression and very reduced expression of *bmps*

suggests that the collections of hair cells in *vgo* inner ears are not like those of the cristae in nature. The expression of the anterior macula marker *fgf8* has not been analysed. The hair cells of each macula have different polarity patterns (see 1.2.6). Analysing the polarity of the hair cells within *vgo*'s sensory patch as well as looking at a stage series of actin stains could confirm if the patch is actually two closely positioned maculae and could possibly distinguish them as being anterior and posterior.

hBMP4 beads were added to test whether any aspects of the *vgo* phenotype could be rescued. These beads were not sufficient to induce expression of *bmp4* or *msxc* or the differentiation of hair cells in *vgo* vesicles. It is possible that *vgo* is required early in inner ear development and in the mutant, cells which normally respond to the BMP signal may not be specified, i.e. there is a defect earlier in vesicle development, which inhibits the production of cells competent to form cristae (see Fig. 8.1). *vgo* mutant vesicles are obviously smaller than normal by 27hpf, so defects in vesicle development are morphologically visible just after the beads have been implanted. Further characterisation of the *vgo* mutant will demonstrate when its patterning is disrupted.

It would be interesting to examine the expression of the BMP receptors in these mutants to check if they could be responsible for transducing the BMP signal in the posteromedial area. The lack of certain members of the signalling pathway may explain why the hBMP4 beads could not induce ectopic *msxc* expression.

5.6.4 Ectopic hBMP4 is not sufficient to form cristae.

The implantation of hBMP4 coated beads did not lead to the generation of ectopic hair cells or induce the expression of *msxc*. This does not rule out a role for endogenous BMP4 in the development of the cristae; however, it does demonstrate that hBMP4 is not sufficient to induce crista development.

Timing and range of protein action

It is not clear when the ectopic protein is acting, although the experiments in which the embryos were analysed at 50hpf showed that the hBMP4 beads were already affecting development of the posterior macula. The ventrolateral thickenings, which are the first morphological signs of crista development, are visible by 50hpf. However, the first molecular signs of crista development are visible at an earlier stage (3 ventrolateral domains of *msxc* expression first seen at 38hpf, Fig. 3.11). Therefore cells that are competent to express *msxc* do so after the time of bead implantation. In the chick

experiments, the addition of *X*Noggin beads resulted in a decrease in *Msx1* expression levels (Chang et al., 1999). In mice limb bud and dental mesenchyme culture experiments, the addition hBMP4 beads induced the expression of *Msx1* (Vainio et al., 1993;Wang and Sassoon, 1995 respectively); therefore an expansion of *msxc* was expected in hBMP4 treated zebrafish.

In the chick experiments, 12 hours of *X*Noggin exposure was sufficient to generate the same SCC phenotypes seen if the beads were left in for 7 days (Gerlach et al., 2000). If a similar diffusion of hBMP4 is happening in zebrafish the protein may be acting during the 12 hours after bead implantation (24-36hpf). The smaller size of the zebrafish otic placode suggests that the protein would diffuse more quickly and travel further than in the chick. It would then be more likely to affect the posterior macula, as it is forming at the time of implantation, rather than the later forming cristae. However, the SCC phenotype does show that the hBMP4 beads can have an effect on later lateral aspects of otic vesicle development. Without antibody studies it is not possible to say how fast or far the protein spreads.

Location of bead

There were no differences seen in response to differently positioned hBMP4 beads, provided they were in contact with the developing vesicle. They could be implanted around the anterior edge of the otic vesicle and still affect the development of the posterior but not the anterior macula. Implanting beads adjacent to the anterior and posterior cristae did not affect their development. However, this was not expected, as the cristae are such strong sources of endogenous *bmp*. It was expected that reducing the level of BMP signals would inhibit the development of endogenous cristae. However, as discussed below, the antagonist bead experiments require further work.

5.6.5 Ectopic hBMP4 affects SCC development.

hBMP4 beads inhibit the development of the epithelial projections and their fusion to form the SCC. This effect was not due to the implantation of beads, as control beads did not generate the same response. As described in the first chapter, the SCC develop from epithelial fusions that push into the otic vesicle and fuse to form the cross structure that divides the lumen of the vesicle into the SCC. These SCC then increase in size projecting out from the lumen as elegantly shown in paint fill experiments carried out by Michele Bever (see Fig. 1.1 (Bever and Fekete, in press)).

This is slightly different to how SCC form in the chick and mouse. In the chick ear, pockets of vesicle epithelium project out from the vesicle (the dorsal and lateral pockets) rather than the vesicle becoming divided up by ingressing projections. However, the processes are thought to be very similar (Haddon and Lewis, 1991). As in zebrafish projections push into the outpockets in the chick ear. The area where these projections meet (the "fusion plate") then undergoes cellular rearrangements and programmed cell death to form the SCC. In the chick experiments, ectopic *X*Noggin inhibited the cell division and increased cell death at distinct stages during the development of the outpockets and SCC (Fig. 5.1). The limited studies described above (5.3.2+5.3.3) suggest that there was no significant reduction in cell death or an increase in cell division following addition of ectopic hBMP4 in zebrafish.

In hBMP4 beaded otic vesicles the last projection to form, the ventral projection, is the one most commonly affected; this could reflect the timing of action of the hBMP4 protein. In zebrafish the epithelial projections are elongated, not due to dividing cells but to the increasing volume of the acellular matrix within them (see 1.2.1). Ectopic hBMP4 may result in fewer cells being available to form the ventral projection, not due to cell death or reduced cell division but due to a change in cell fate. These cells may not be able to produce the hyaluronan-rich matrix required to push the ventral projection into the middle of the vesicle.

5.6.6 Why were antagonist experiments inconclusive?

The antagonist work was disappointing, with no specific effects seen following treatment of inner ears with antagonist-coated beads. The problem may be that too low a concentration of Chordin or *X*Noggin was used. The shield stage implantations showed that both proteins could weakly inhibit BMP signalling in the mesoderm, but their effects were not dramatic. In the developing vesicle there is strong expression of *bmp2b*, *bmp4*, and *bmp7r* in similar domains at similar stages. Both *X*Noggin and Chordin will bind BMP2b and BMP4 (it is unknown whether they also bind BMP7r). Therefore the endogenous BMP proteins may titre out the ectopic antagonist. The different Bmps similar proteins may also be able to replace each other functionally and so a higher concentration of antagonist is required to remove all possible Bmp signals.

The chick experiments did not have the same problem. BMP2 is not expressed in the chick; therefore the only competitors for the *X*Noggin are BMP7 and BMP5. BMP5 is expressed transiently and there are no data on its affinity for *X*Noggin. However, it is in

the same family of BMPs as BMP7, which has a lower affinity for *X*Noggin than BMP4. Therefore, *X*Noggin beads in chick are likely to reduce all BMP4 signalling without too much competition from the other BMPs.

Follistatin may provide a more efficient inhibition of BMP signalling, as this is the only antagonist expressed in the zebrafish otic vesicle. It is believed to inhibit BMP signalling in a slightly different manner to the two readily available antagonists. It has been shown to bind both Bmp4 and Bmp2b in vitro, although at slightly lower affinity than Chordin and Noggin. However, in vivo it binds to the Bmp dimer and the receptor, rather than preventing the dimer binding to the receptor as the other antagonists do. However, it does inhibit the activation of the type I-type II receptor complex (Iemura et al., 1998). This distinction means that both the receptor and dimers are blocked which reduces the possibility of signalling by other Bmps.

While this chapter provided data on the effects of ectopic BMP signalling the next chapter investigates the results of losing Bmp2b signalling during inner ear development.

Appendix

Wilcoxon Signed Rank Test

Table 5.1 The effect of hBMP4 beads on hair cell number in the developing posterior macula at two stages (around 48hpf and 72hpf).

	+bmp4 bead	no bead				Contralateral			
Exp	No of pm hc	No of pm hc	d	rank	Exp	No of pm hc	No of pm hc	d	rank (pooled)
24-50hpf									
VII 1	6	19	13	+4	QQ3	19	20	1	0.5
VII 2	12	18	6	+1.5	QQ7	17	17	0	
VII 10	7	23	16	+6	QQ14	16	17	1	0.5
VII 11	5	19	14	+5	QQ16	16	16	0	
VII 12	11	23	12	+3					
VII 13	13	19	6	+1.5					
t				21					1
24-72hpf									
C 1	7	22	15	+1	OO5	44	46	2	+2.5
C 7	0	45	45	+6	OO10	44	42	-2	-2.5
C 8	0	35	35	+4.5	II 4	39	41	2	+2.5
D 9	0	35	35	+4.5	KK 2	38	38	0	
E 1	8	39	31	+3	KK3	31	29	-2	-2.5
E 3	15	40	25	+2					
t				21					5

t = the sum of the ranks. The degree of freedom is equal to the number of sample-1. Zero values are disregarded.

As this is a two-tailed Wilcoxon signed rank test (as it is not clear if numbers are expected to go up or down) the P value as given in table is doubled. The 50hpf control group is too small.

Chapter 6

Inner ear development in rescued zebrafish mutant *swirl* embryos.

6.1 INTRODUCTION

swirl disrupts the zebrafish *bmp2b* gene. As mentioned in Chapter 1, *swirl* is one of a class of dorsalised mutants in which dorsal structures are expanded at the expense of ventral structures (Mullins et al., 1996; Martinez-Barbera et al., 1997; Mullins et al., 1998; Nguyen et al., 1998)(See section 1.3.6+1.4.1). These dorsalised mutants show a range of phenotypes depending on their place in the BMP pathway. *swirl* (*swr*) has the most severe phenotype, lysing at around 13 somites (14hpf). *swr* mutants have an expanded notochord and somites (dorsal structures) and are missing blood and tail tissue (ventral structures). The somites extend around the entire embryo fusing on the ventral side, extending much further than normal somites. The yolk is squeezed anteriorly as more somites form and the embryos lyse, due to the increase in hydrostatic pressure. These embryos do not express the otic placode marker *dlx3*, normally expressed at 14hpf (Nguyen et al., 1998).

6.1.2 Injection of mRNA rescues *swirl* mutants.

swirl mutants therefore die at the stage when the otic placode normally forms. However, it is possible to investigate inner ear development in a *swirl* mutant embryo by injecting mRNA, which rescues *swirl* mutants to adulthood. In vitro synthesised, capped sense mRNA, coding for wild-type *bmp2b*, can be injected into the yolk of a 1-4 cell embryo. This mRNA is taken up into the cells and is distributed throughout the embryo. The wild type mRNA provides the Bmp2b signal required during early dorsoventral patterning, rescuing this part of the *swirl* phenotype. These rescue experiments were one of the ways used to show that *swirl* is a *bmp2b* mutant (Kishimoto et al., 1997; Nguyen et al., 1998). Rescued *swirl* mutants become fertile adults, although the rescuing mRNA is not thought to last longer than 24hpf. Studies into the stability and longevity of injected mRNA have shown that by the 20 somite stage the level of undegraded mRNAs has dropped to around

20% of its initial concentration (Hammerschmidt et al., 1999). These rescue experiments therefore suggest that *bmp2b* has no other unique role during embryogenesis after this time (Kishimoto et al., 1997; Nguyen et al., 1998). However, as is discussed below, the longevity of the resultant protein is not known and there may be a later role for Bmp2b.

6.1.3 Adult rescued *swirl* mutants have a balance defect.

There is evidence of a later, unique role for Bmp2b in zebrafish inner ear development. Two laboratories have independently observed the same behavioural defect in rescued *swirl* adults (M. Mullins and M. Hammerschmidt, pers. comm.). The rescued adults swim normally except when making sudden changes in direction. When turning the rescued adults "swirl", meaning they lose their dorsoventral orientation momentarily and perform a messy somersault instead of a neat turn. This behaviour suggests a vestibular defect- the zebrafish are not sure which way is up.

The zebrafish circler mutants have defects in the reception or transmission of vestibular stimuli that are manifested in abnormal swimming behaviour, circling and swimming at an acute angle (Nicolson et al., 1998). The adult *swirl* phenotype is not as severe as those described for the circler mutants, suggesting *swirl* is a more subtle defect.

As well as detecting gravity via their vestibular system, zebrafish use visual cues to orientate themselves. The dorsal light reflex is the tendency of fish to orientate their dorsal side towards light. Adjusting the light source to give a "false" dorsal signal can affect the orientation of wild type embryos over an extended period of time. In the rescued *swirl* adults this reflex could allow the zebrafish to orientate themselves normally most of the time. However, when they turn, the adults may receive abnormal impulses from the vestibular system, which temporarily override the dorsal light reflex. Once turned the dorsal light reflex then becomes the dominant signal allowing the zebrafish to swim normally. This reflex has not yet been tested in rescued *swirl* adults.

6.1.4 mRNAs from different organisms and levels of the BMP signal pathway can be used to rescue *swirl* mutants.

Injecting mRNA from different levels of the BMP pathway (e.g. *smads* and *receptors*), either from zebrafish or another species' homologue has helped in understanding the role of

Bmps in dorsoventral patterning (Blader et al., 1997; Fürthauer et al., 1997; Neave et al., 1997). Injecting zebrafish *bmp2b*, *bmp4* and *Xenopus BMP7* and *BMP4* mRNA rescues *swr* and other dorsalised mutants with different levels of efficiency (Nguyen et al., 1998). These results demonstrated that an early dorsoventral patterning mechanism similar to that described in *Xenopus* is working in zebrafish (Chapter 1.4.1).

There is some debate on the requirement for *smad5* (Bmp rSMAD) during dorsoventral patterning and whether *smad5* can rescue *swr* mutant embryos (Hild et al., 1999 and Prof. Mullins, pers. comm.). The *smad5* mutant, *somitabun*, is one of the dorsalised class of mutants and its phenotype is as severe as *swirl* (Mullins et al., 1996). The Mullins lab (and this work) has used *smad5* mRNA to rescue *swirl*. However, it has also been reported that *smad5* does not rescue *swirl* whereas *smad1* mRNA will (Dick et al., 1999; Hild et al., 1999). It has also been shown that injecting full length *smad1*, but not *smad5* mRNA results in *chordino* and *mercedes* like, i.e. ventralised, phenotypes (Müller et al., 1999). It is not yet clear why the Hammerschmidt and Mullins labs have different results; both are using the same alleles of *swirl* and injected zebrafish *smad5*.

The work in this chapter uses zebrafish rescued by both types of mRNA. Our lab rescued *swirl* mutants using zebrafish *smad5*, and these were checked using a genotyping protocol from the Hammerschmidt lab (see Fig. 8.1 and Hild et al., 1999). Embryos rescued with *bmp2b* mRNA from homozygous mutant parents were also analysed (a gift from G. Runke in Prof. Mullins lab).

6.2 RESULTS

6.2.1 *smad5* injections rescue *swirl* mutant embryos.

During the initial setting up of this project Dr K. Hammond injected a variety of concentrations of *smad5* mRNA to attempt to rescue the *swirl* phenotype. Four different concentrations were examined (500ng/µl, 300ng/µl, 100ng/µl and 20ng/µl). Of these, 300ng/µl resulted in the highest percentage of normal looking zebrafish rather than dorsalised (extended somites, expanded notochord, loss of ventral tail fin) or ventralised (reduced eyes, reduced/absent notochord, enlarged blood islands), which resulted when too little or too much mRNA was injected. This is more than the concentration of *bmp2b*

mRNA previously used to rescue *swirl* mutants, suggesting *smad5* is not as efficient as *bmp2b* (40pg (Nguyen et al. 1998) 1-2pg (Kishimoto et al., 1997)). I carried out the rest of the work described here.

The rescuing mRNA was coinjected with GFP (green fluorescent protein), which has been shown not to perturb normal development (Dick et al., 1999). This coinjection technique allows the injected mRNA to be tracked and gives an idea of how long it is active. The injected embryos fluoresced when illuminated with light at 488nm up until 24hpf (although very weakly). As GFP protein is still present at this time, it is assumed the Smad5 protein is being synthesised over the same period, although this depends on the relative translation and degradation rates of the two proteins.

These injected embryos were allowed to grow until 5 or 7dpf and then their tails were clipped and genotyped using a nested PCR protocol ((Hild et al., 1999) and see Materials and Methods 8.5+Fig. 8.1).

Rescued embryos were also provided by Greg Runke, from Prof. Mullins' laboratory in Philadelphia. These swr^{dc24} embryos are the progeny of two rescued homozygous *swirl* mutants and so the entire clutch is *swirl* mutant. This makes the rescuing experiments easier.

6.2.2 Sensory patches appear normal in rescued embryos.

FITC-phalloidin was used to analyse the development of the sensory patches and the SCC in the rescued embryos. Rescued embryos from 48hpf to 7dpf were analysed. By 48hpf the anterior and posterior maculae have formed, on the ventral floor and the medial wall of the vesicle respectively, and SCC development has started with the ingression of the epithelial projections. During the time period examined these maculae increase in size, the cristae develop and the SCC form as the epithelial projections fuse.

In all the stages examined the correct sensory patches had formed and SCC development appeared to be progressing normally (Table 6.1). In Table 6.1 the sizes and general shape of the sensory patches were assessed. One out of five 5dpf rescued embryos examined did not show a wild type phenotype. This vesicle did develop all its sensory patches and SCC; however, its posterior macula was not the normal shape or size. It consisted of a few scattered hair cells on the medial wall (data not shown). However, all the other rescued

zebrafish examined displayed normal development (n=13, Fig. 6.1). The structure and shape of the stereocilia in the hair cell bundles did not seem abnormal. As all the rescued adults are reported to display the balance defect (M. Mullins+M. Hammerschmidt pers. comm.) this one odd case may represent a secondary defect due to incomplete rescue of the earlier phenotype, an anomaly during injection or a non-specific developmental anomaly.

6.2.3 Selected in situ hybridisation markers are expressed normally.

The expression of *bmp4* is normal at 48hpf in these otic vesicles. It is expressed in a single dorsal and three ventrolateral domains (Fig. 6.2A-C). Early in development Bmp2b is required for the expression of *bmp4* (Hammerschmidt et al., 1996b). A similar relationship was not found in rescued *swirl* inner ears. Other putative targets of Bmp signalling discussed in previous chapters were also examined (Chapters 3+4). *msxc*, a marker of cristae is expressed normally in the cristae of rescued mutants (Fig. 6.2D+E) in agreement with the actin stains discussed above. *dachA* marks the SCC, it is expressed dorsally and in the epithelial projections as they form. At 48hpf *dachA* is expressed in a broad dorsal domain, which may mark a region competent to form SCC (Hammond et al., in press). This domain of expression was normal in rescued embryos (Fig. 6.2F+G).

Table 6.1 Comparison of the dimensions of structures in rescued *swirl* otic vesicles and wild type controls at four different time points.

Exp/ wt	Side A				Side B				
	vesicle size (μm)	p.m.	a.m.	cristae /SCC.	vesicle size (μm)	p.m.	a.m	cristae /SCC	Age
1	150	18	20	-	100	20	18	-	48h
2	140	40	25	-	-	-	-	-	48h
3	130	30	20	-	130	25	20	-	48h
4	110	25	20	-	140	30	20	-	48h
wt	120	35	20		130	40	35		48h
wt	130	30	25		140	30	30		48h
1	170	55	30	ok	170	55	30	ok	72h
2	170	55	30	ok	170	50	30	ok	72h
wt	180	60	35	ok	170	55	35	ok	72h
wt	170	55	40		180	50	40	ok	72h
1	250	70	60	ok	250	72	60	ok	5d
2	240	70	55	ok	250	60	55	ok	5d
3	250?	?	50	ok	?	20?	50	ok	5d
4	240	65	55	ok	250	68	50	ok	5d
5	250	55	50	ok	260	55	48	ok	5d
wt	250	55	50	ok	250	40	40	ok	5d
1	260	65	50	ok	260	75	45	ok	7d
2	250	65	45	ok	250	72	45	ok	7d
wt	280	75	50	ok	280	75	50	ok	7d
wt	260	70	50	ok	250	75	50	ok	7d

The long anteroposterior axis of the vesicle and posterior macula and the mediolateral axis of the anterior macula were measured. The cristae +SSC were assessed in live and actin stains. They were marked as ok if they were in the normal position and of the correct size and shape.

Fish 1 from the 48hpf set has a smaller anterior and posterior macula, this embryo appears slightly younger than the others. Data from only one side of Fish 2 from 48hpf set was collected.

Fish 3 of the 5dpf set has a disrupted posterior macula and vesicle.

Abbreviations; a.m., anterior macula; d, days post fertilisation; Exp, experimental; h, hours post fertilisation; p.m., posterior macula; SCC, semicircular canal; wt, wild-type; - data not available.

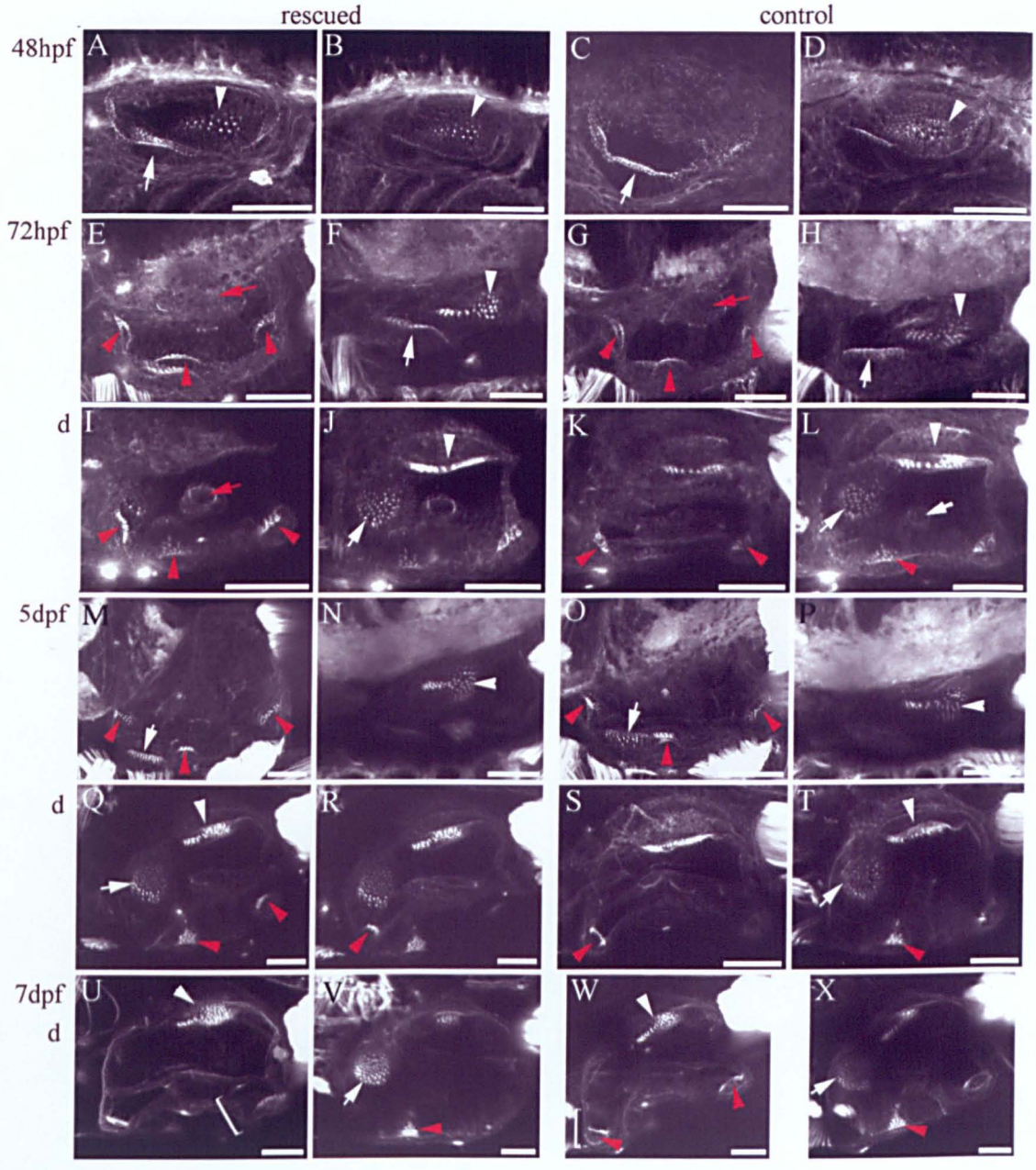

Figure 6.1 FITC-phalloidin labels of actin in hair cells and cell boundaries. Compressed confocal images. A-H, M-P lateral views anterior to left, dorsal to the top. I-L, Q-X dorsal views, anterior to left medial to top. 1 control and 1 experimental fish is shown for each age and orientation at different focal planes. Scale bars = 50 μm. (A-D) The anterior (arrow) and posterior maculae (arrowhead) are present in both the rescued and control embryos at 48hpf. (E-L) At 72hpf the cristae (red arrowhead) have developed and the maculae have increased in size. The fusion plate of the SCC is visible in both the rescued mutant and wild type (E+G red arrows). The ventral projection is also visible in dorsal views (I+L, red arrows). (M-T) At 5dpf the general pattern of the sensory patches is the same although they have all increased in size. (U-X) At 7dpf the sensory patches have increased in size and all appear normal in rescued mutants. The SCC have matured such that the cristae are within their ampullae (U+W, bracket).

The *eya1* mutant *dog* has abnormal *bmp* expression and a possible feedback relationship between *eya1* and the *bmps* was discussed in Chapter 4. However, *eya1* expression appears normal in rescued embryos (Fig. 6.2H+I) suggesting *bmp2b* is not required for *eya1* expression (see 4.4.1).

6.3 DISCUSSION

This chapter has characterised the early development of rescued *swirl* embryos up to 7dpf. Actin stains show that the sensory patches and SCC develop normally and mRNA markers also show that certain cell fates are properly specified in rescued embryos.

6.3.1 Inner ear development progresses normally in rescued *swirl* embryos.

The work documented in this chapter shows that the rescued *swirl* embryos appear to develop normal inner ears during the period examined. All the sensory patches form in the correct places at the correct time and normal SCC development is initiated and proceeds until at least until 7dpf. No behavioural defects were noted in rescued embryos (data not shown). No difference was seen between embryos rescued with *smad5* or *bmp2b* mRNA.

All these results suggests that *bmp2b* does not have a unique role in the early stages of inner ear development or that it is required at very early stages when rescuing mRNA or its protein product may still be present. As mentioned in the introduction M. Hammerschmidt has studied the degradation of injected mRNA and found that the mRNA he analysed, *indian hedgehog*, was very greatly reduced by 20 somite stage (~19hpf, (Hammerschmidt et al., 1999)). It is therefore likely that some mRNA is still present during the early stages of otic placode and vesicle development. Northern blots could be used to address this possibility. Protein synthesised from the injected *bmp2b* mRNA may also still be present at 24hpf as weak GFP fluorescence is still visible at this stage.

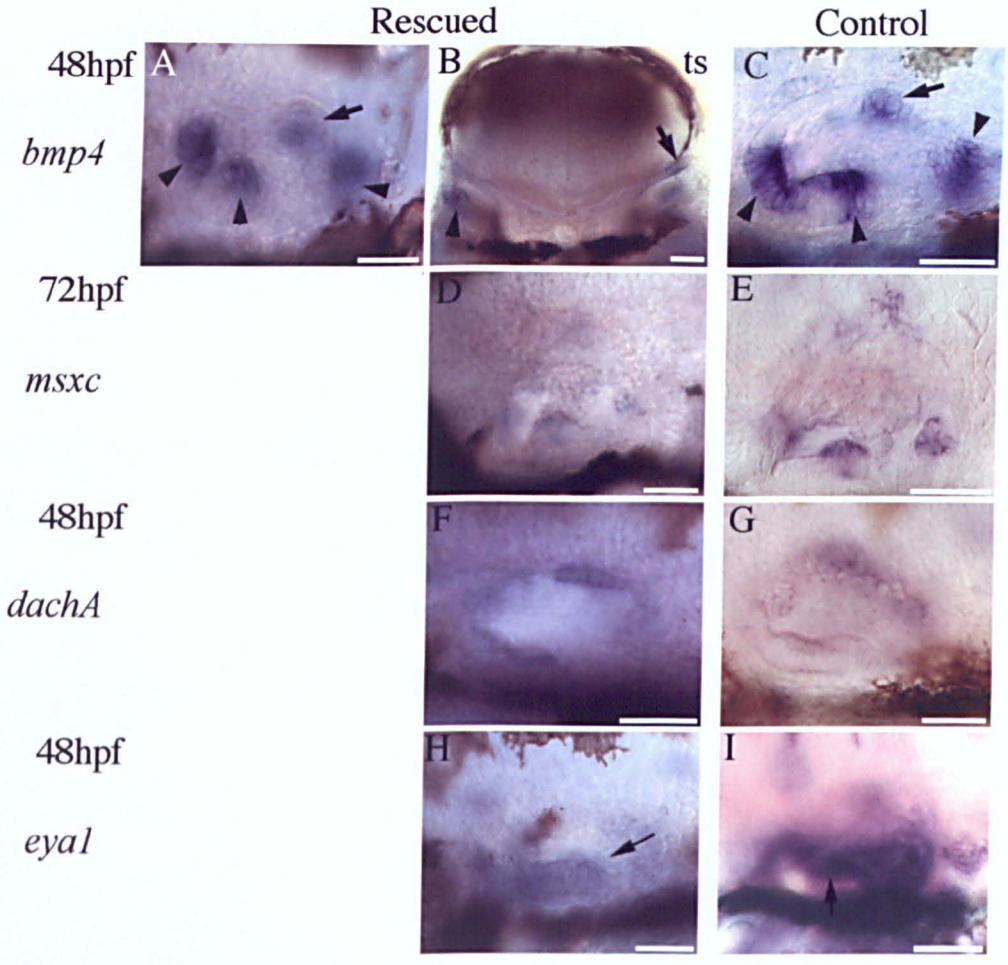

Figure 6.2 Expression of *bmp4*, *msxc*, *dachA*, and *eya1* in rescued *swirl* embryos. DIC images of whole mount in situ hybridisations. All are lateral views, anterior to left, dorsal to top, except B, which is a transverse section dorsal to top. Scale bar = 50 μm. (A-C) *bmp4* is expressed in a single dorsal domain (arrow) and three ventrolateral domains (arrowheads) at 48hpf in both wild type and rescued embryos. (D+E) *msxc* is expressed in three ventrolateral domains in both the rescued and wild type 72hpf embryo. (F+G) *dachA* is expressed in the dorsal roof of the otic vesicle at 48hpf in both rescued and wild type. (H+I) *eya1* is expressed in the anterior maculae in both rescued and control otic vesicles (arrows).

bmp2b is one of the earliest *bmps* expressed, in the otic vesicle from 20hpf in a broad dorsolateral domain, which at 17hpf includes regions fated to form the cristae and SCC (Haddon, 1997). This early domain of expression is unique to *bmp2b* amongst the *bmps* and so it will be important to establish whether there is any residual rescuing mRNA or protein at this time, before conclusions can be drawn about the importance of this early expression domain.

bmp2b is also expressed continually within the otic vesicle until at least 3dpf in the cristae and after this stage in the SCC epithelium. *bmp2b* is coexpressed with other *bmps* in three ventrolateral domains that mark the cristae. The loss of one *bmp* may therefore not be as crucial in the development of cristae. However, as is explained below, the SCC, which do not express any other *bmps*, are affected at some unknown later stage. It is also important therefore to investigate *bmp* expression within the developed inner ear at later stages. Performing in situ hybridisations on sections would provide clearer information on when and where *bmp2b* is expressed in or around the SCC epithelium of older zebrafish.

6.3.2 Studies on the adult rescued *swirl* mutants.

Work done by Helen Loynes in the Whitfield lab has revealed that adult *swirl* mutants (n=6) lack SCC; however, the ampullae and the cristae are present. Each of the other chambers and their associated sensory patches are present within sectioned inner ears (Fig. 6.3B). Therefore the "swirling" vestibular defect could be due to the lack of correct stimuli to the cristae when turning.

Normally endolymph (fluid within the membranous labyrinth) fills the SCC. The relative movement of fluid with respect to the SCC is thought to provide information on the orientation of the head. This displacement is detected through the movement of hair cells in the cristae. As rescued *swirl* mutants do not have canals, the displacement of this fluid will not truly represent the acceleration in any given vector, resulting in the confusion seen during turning, when orientation rapidly changes.

Once our rescued stocks have grown up it will be possible to do more detailed behavioural studies. As described in the introduction there is a visual aspect to vestibular

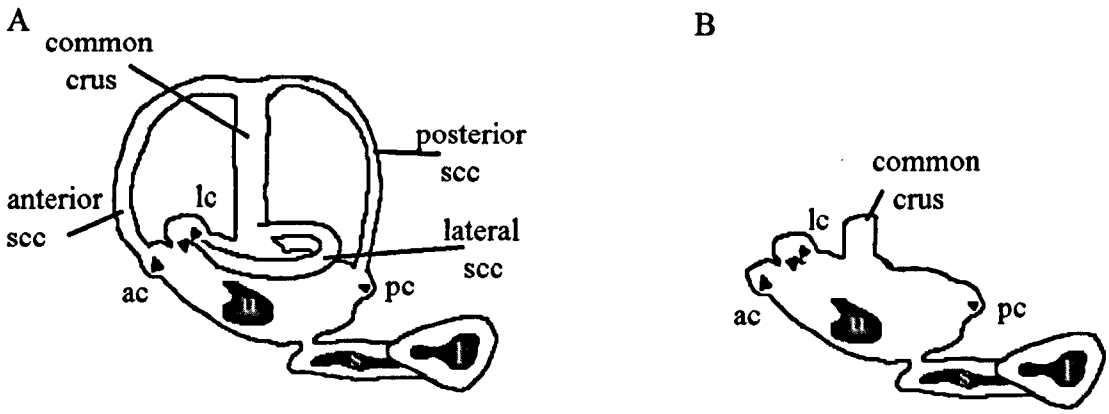

Figure. 6.3 Sketch comparing adult inner ears of wild type (A) and rescued *swirl* (B) fish. This diagram is adapted from information generated by H. Loynes' thin sections of adult rescued *swirl* and wild-type heads (n=6, two ages examined, 3 months +2 years old). The sections were cut in three orientations. Rescued *swirl* adults do not have any SCC, although they do have ampullae and cristae. The other chambers of the inner ear also form normally.
Abbreviations; ac, anterior crista; l, lagenar macula; lc, lateral crista; pc, posterior crista; s, saccular macula; u, utricular macula.

function, the dorsal light reflex. This can be tested using a lamp to manipulate where the light, or dorsal signal, comes from. This test could be used to check the contribution of the vestibular part of the inner ear to dorsoventral orientation. The hypothesis is that rescued *swirl* adults would orientate to a new dorsal signal provided by the lamp, unlike wild type zebrafish, which would still receive gravitational cues from their SCC. Examining the behaviour of rescued *swirl* zebrafish as they matured will provide clues as to when vestibular function is being impaired which will help narrow down stages for more detailed study (see *lost-a-fin* below).

It would also be interesting to examine the sensory patches of the adults in more detail. Members of the circler class of zebrafish mutants, which also displayed a balance defect, develop abnormal hair bundles (*mariner* and *sputnik* (Nicolson et al., 1998)). The appearance of the stereocilia in rescued *swirl* adults could be checked using actin stains of dissected adult inner ears, a technique being perfected by Dr K. Hammond in the Whitfield lab.

6.3.3 Role for *bmp2b* in semicircular canal development.

In functional studies in chick, the SCC were the most sensitive structures in the ear to a reduction in BMP signalling (due to the application of antagonist-coated beads) which correlates with the results described above.

As discussed in Chapter 5, the addition of BMP antagonist-coated beads affected two stages of SCC development (Fig. 5.1) in the chick. They inhibit both the initial out-pocketing and the continued growth of the SCC (Chang et al., 1999; Gerlach et al., 2000). In zebrafish, however, the initial stages of SCC development appear normal in rescued *swirl* embryos. Defects only become evident at a later stage, possibly when the SCC grow to adult proportions. The SCC epithelial cells probably divide and undergo rearrangements to form the long thin SCC seen in the adult. It will be interesting to see if there is an increase in apoptosis at these later stages in the rescued *swirl* zebrafish, as seen in the chick. This would suggest that BMP signals are required as a survival signal.

bmp2b is the only *bmp* to be expressed in the SCC in zebrafish. In the chick, *Bmp4* is expressed in the SCC epithelium and the surrounding mesenchyme. The addition of the antagonist beads affected *Bmp4* expression in both these areas. It is therefore not clear

where the Bmp4 signal that is required for normal SCC development comes from. Unlike the expression in chick inner ears, no mesenchymal expression of *bmps* has been detected in zebrafish (Chapter 2).

6.3.4 Bmp signalling may be required at semi-metamorphosis stage to form normal semicircular canals.

Prof. Mullins has also recently noted that another rescued member of the dorsalised class of mutants, *lost-a-fin*, has similar 'swirling" behaviour after 3-4 weeks, to that seen in the rescued *swirls* (M. Mullins pers, comm.). *lost-a-fin* is a mutant in a novel type I Bmp receptor, *alk8* (Bauer et al., 2001;Mintzer et al., 2001). It is not clear where this gene is expressed during inner ear development.

Assuming this is a similar phenotype to that seen in the rescued *swirls*, this suggests an age range when the *swirl* defect is likely to occur. It has been suggested that this 3-4 week time point reveals a semi-metamorphosis, when the young fish becomes an adult generating its scales and stripes (see Johnson et al., (1995) and references therein). These processes and the final maturation of structures like the heart and the inner ear may require another burst of signals including Bmps (M. Mullins pers. comm.).

The next chapter summarises the finding of this thesis while Chapter 8 describes the methods used during this work.

Chapter 7

Conclusions and future prospects.

7.1 Four possible sites of Bmp action identified.

The results described in this thesis suggest four possible sites of Bmp action during the development of the otic vesicle: the cristae, the posterior macula, the semicircular canals (SCC) and the endolymphatic duct (ED). The evidence for each of these is summarised below.

The loss of function work using antagonist coated beads was inconclusive. It is thought the concentrations used were not sufficient to inhibit endogenous Bmp signalling. Therefore these results are not considered here but remain as a caveat to the rest.

The expression analysis revealed distinct sites of receptor and putative target gene expression, which did not overlap with other members of the signal pathway. It is assumed that further analysis of already known and new members of this pathway (as they are discovered) will provide the missing parts of the pathway.

7.1.1 The cristae.

The wild type expression data showed that three out of four Bmps are expressed in the presumptive cristae, up to and including their differentiation to form hair cells and support cells. This is similar to the Bmp expression patterns seen in chick, mouse, and *Xenopus*.

The putative Bmp target, *msxc*, is coexpressed with *bmp2b*, *bmp4* and *bmp7r* in the cristae. This correlation of *bmp* with *msxc* expression and the formation of cristae together with the failure to express these markers and form cristae in inner ear mutants suggest these genes are required to form cristae. Neither *dog* nor *vgo* mutants express the *bmps* ventrolaterally or form cristae while *cls* has two out of three ventrolateral *bmp* domains and does develop precocious crista patches.

In the chick, reducing endogenous Bmp signals led to a reduction in the expression of crista markers and affected the size and shape of the cristae (Chang et al., 1999). However, functional studies in zebrafish have shown that adding ectopic hBMP4 is not sufficient to

induce ectopic *msxc* or cristae. This could be due to the saturation of endogenous receptors, or the timing of implantation not being correct. It is also possible that hBMP4 is not as efficient as zebrafish Bmp4 (mature protein sequences are 90% identical) or that Bmp4 is just not able to induce *msxc* or form cristae.

Loss of function studies in rescued *swirl* embryos suggest that *bmp2b* is not required to form cristae or maintain them through life. The rescued embryos all formed cristae and later studies of adult rescued *swirls* have shown that cristae are still present (H. Loynes, unpublished data). It is not clear when the rescuing Bmp2b protein or mRNA is degraded; however, even if there is an overlap of rescuing signal and the early stages of crista development, these data indicate that Bmp2b is not required for the development of cristae at later stages (unlike SCC, see below).

7.1.2 The posterior macula

The medial wall of the vesicle, where the posterior macula develops, expresses *bmprIB* (type I receptor), *smad5* (rSmad) and at later stages a putative target of Bmp signalling *spalt*. There is also evidence from the hBMP4 bead experiments that Bmp signals can act on the medial wall, resulting in the inhibition of posterior macula development. This inhibition is not due to a dramatic increase in cell death or decrease in cell division.

Chick studies, in which the use of Bmp antagonist coated beads reduced the size of sensory patches (Chang et al., 1999) suggested adding exogenous protein would result in an expansion of the sensory patches in zebrafish and so the inhibition of posterior macula development was unexpected. However, in zebrafish, the Bmp antagonist (*follistatin*) is expressed within the otic vesicle at the same time that *bmp4* is expressed. The presence of this antagonist may be required to moderate levels of Bmp signalling to ensure the correct development of the posterior macula. Therefore, low levels of Bmp signalling may be required to form a posterior macula.

The addition of ectopic hBMP4 to *vgo* mutant inner ears suggests that the medial portion of the mutant's single sensory patch is similar to the posterior macula found in wild type. The mutant macula showed a very similar response to that of wild type with a reduction of its medial part.

The loss of function rescued *swirl* studies suggest Bmp2b signalling is not required to form the posterior macula. Given the results discussed above, an increase in the size of the posterior macula would be expected in the rescued *swirl* embryos. This was not seen. It could be that other members of the Bmp family compensate for the loss of Bmp2b.

7.1.3 The semicircular canals (SCC)

bmp2b is expressed in epithelia lining the SCC in zebrafish as are *bmprIB* , the *iSmads* and *smad5*. In *dog* mutants, which develop abnormal, possibly overgrown epithelial projections, there are unusual discrete areas of *bmp2b* expression within the projections. This is unlike the more general expression seen in the projection epithelia of wild type embryos. The overgrown projections seen in *dog* mutants could be the result of cells changing fate from cristae to SCC (see below); alternatively, these *bmp2b* cells may label abnormal sites of cell division. This role in cell division has not been examined in *dog* mutants.

In the chick, the addition of BMP antagonist-coated beads affected the development of the SCC at two stages, during their initial outgrowth (outpockets) and later during their continued growth. This lack of BMP signal reduced proliferation and induced apoptosis respectively. However, the ingression of epithelial projections into these outpockets (the beginning of the resorption process) is apparently normal (see Fig. 5.1) (Chang et al., 1999). In zebrafish, the addition of extra hBMP4 inhibited the formation of these epithelial projections. The analysis of cell death and division carried out here did not reveal any dramatic change in the beaded embryos, although as this was only slightly affected in chick, it may require closer analysis. Therefore, in chick, the removal of Bmp signalling inhibited the initial outgrowth of the SCC outpocket, while in zebrafish, adding ectopic Bmp signal inhibited the initial ingression of projections required to form SCC.

The rescued *swirl* mutants also suggest that Bmp2b is required for the correct formation of adult SCC (H. Loynes, unpublished data). It remains to be tested when the rescuing Bmp2b protein is degraded to rule out any earlier requirement. Another rescued member of the Bmp pathway, *lost-a-fin* (alk8 mutant), may also have defective SCC development, as it has been reported to have a similar balance defect to that seen in the adult rescued *swirls*.

The other *bmps* may also have a role. The cristae are strong sources of Bmp signal. It is not clear if these ventrolateral *bmp*-expressing cells can form SCC or if they just provide a Bmp signal. Intriguingly *dog* and *vgo* mutants both lack these sources of Bmp but show opposite SCC phenotypes. *dog* mutants develop overgrown projections while *vgo* mutants have no projections. *vgo* (Tbx1) may act further upstream than *dog* (Eya1) in the SCC development pathway. Therefore in *dog* mutants, cells that were going to form cristae may form SCC, while in *vgo* mutants these crista/SCC bipotent cells or cells which provide the SCC Bmp signal may not be specified (see Fig. 7.1).

There is a strong case for the requirement for Bmps (especially Bmp2b) in the development of the SCC. This may require low levels of Bmp signal at early stages and a Bmp2b signal via the Alk8 type I receptor at later stages.

7.1.4 The endolymphatic duct (ED)

bmp4 marks the dorsal roof of the otic vesicle before the thickening that is the first morphological sign of ED development is visible. This is reminiscent of the expression pattern seen in the chick, where *bmp4* and *bmp7* are expressed dorsally, in domains which may include the early ED, while at later stages *bmp7* and *Msx1* are reported to be expressed in the formed ED (Oh et al., 1996; Wu and Oh, 1996). In zebrafish, at later stages *msxc* is expressed in the mesenchyme around the ED. This pattern of Bmp4 in the epithelium inducing *msx* expression in the mesenchyme is found in other systems (e.g. tooth development (Jernvall and Thesleff, 2000)).

The correlation of ED development and the expression of *bmp4* and *dachA* found in the analysis of inner ear mutants suggest that *dachA* and *bmp4* are markers of ED development. However, it is not clear if they are either necessary or sufficient for its development. It is not known if the ED is present in adult rescued *swirl* mutants but the vesicles examined were of the normal size suggesting the ED is normal.

It was reported at a recent meeting that the addition of beads coated in a weak Bmp antagonist, DAN, could redirect the outgrowth of the ED in chick (Gerlach-Bank and Barald, 2001). Therefore, *bmp4* is a marker of the early stages of ED development and may have a role in directing the projection growth.

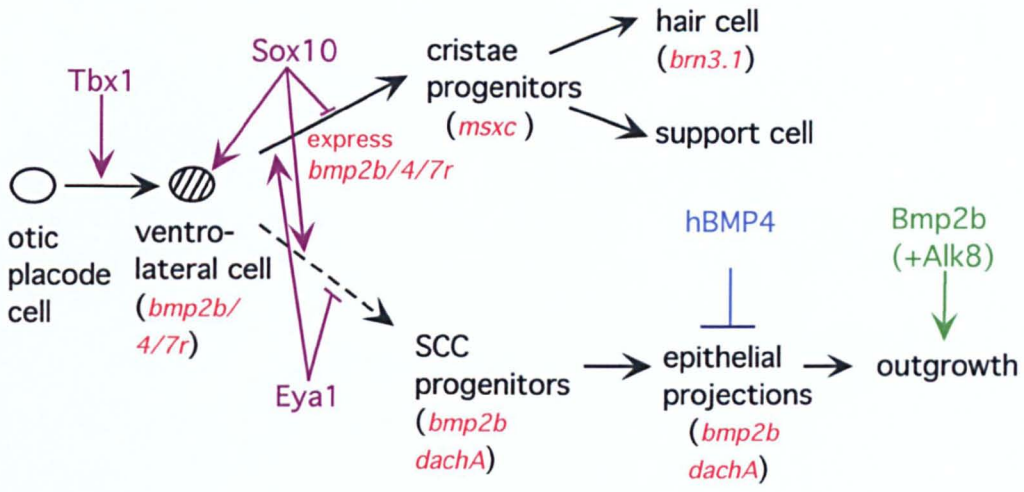

Figure 7.1 Simplified model of cristae and SCC development.

Flow diagram detailing the different stages of differentiation between the otic placode and the cristae or SCC. It is not clear if the ventrolateral *bmp* expressing cells form SCC or if the Bmps act as a signal on neighbouring cells (dotted line). Fate mapping studies carried out by C. Haddon have shown that cells in the same area can give rise to both SCC and cristae cells, although it was not clear if both can arise from a common precursor (Haddon, 1997).

mRNA markers are in red; possible sites of protein action (inferred from mutant analysis) are shown in purple. Tbx1 may be required for the specification of the ventrolateral *bmp* expressing cells. The *cls* mutation inhibits the development of the correct number of ventrolateral *bmp* domains and Sox10 may be required for the development of the SCC and inhibit crista development. *eya1* may be required to form cristae (either by regulating *bmp* expression or as a survival signal) and inhibit SCC development. hBMP4 inhibits invagination of SCC projections (blue) and Bmp2b is required for outgrowth during SCC development (green).

7.2 Future prospects

Role for endogenous BMPs in crista/posterior macula development.

To establish if the BMPs do have a role in the development of the cristae it would be necessary to eliminate Bmp signalling from the otic vesicle at a stage prior to that when rescuing RNA/protein runs out in the *swirl* mutants. This could be done using the antagonist coated beads at an increased concentration or possibly using electoporation to target specific areas with a dominant negative BMP receptor construct (L. Niswander in press (Kos et al., 2001)) or morpholinos (Nasevicius and Ekker, 2000). There are different ways of targeting the expression of a dominant negative construct.

Caged fluorescein has been used as a marker to create a fate map of early zebrafish placodal tissues. In this technique a laser activates (uncages) an injected label in one or two cells. These cells can then be followed through a certain number of cell divisions (Kozlowski et al., 1997; Gee et al., 2001). It would be useful to have a transgenic line of *bmp4-GFP* zebrafish. In this line cells that express *bmp4* will also produce the GFP protein and fluoresce. These glowing cells will provide a target for uncaging or a similar technique involving an inducible heat shock promoter (hsp70), to express a dominant negative construct. This construct will allow specific inhibition of BMP signalling in parts of the otic vesicle such as the cristae (Halloran et al., 2000; Ando et al., 2001).

Similar techniques could prove useful in analysing the role of BMPs in the development of the posterior macula. It would be expected that there would be an expansion of posterior macula tissue in the case of reduced BMP signalling, if it normally inhibits its development.

Endolymphatic Duct

The work described in this thesis suggests that the zebrafish may be a useful model for the study of the ED. Now that it has been described, other markers and mutants in which its development is disrupted can be analysed. The position of the ED (medial to the otic vesicle) means ablation studies are probably not feasible. However, the early expression of *bmp4* may provide a means of targeting ablation to those specific cells (see above).

The ED may be required to regulate the volume of endolymph (Thalmann, 1999). It would therefore be interesting to analyse the development of the ED in mutants with abnormally

sized vesicles to see if there is a correlation between otic vesicle size and the presence of an ED.

Colourless

The work described here on *colourless* has begun to characterise what is obviously an early acting defect during inner ear development. It is important to establish when otic patterning is disrupted and if the *sox10* is required within the placode and/or is provided by surrounding tissue. *sox10* is expressed in neural crest cells, which do migrate past the developing vesicle (Schilling and Kimmel, 1994; Dutton et al., 2001).

The *colourless* mutations result in the failure to specify a branch of neural crest fate (nonectomesenchymal) (Dutton et al., 2001) and so there is a possibility that the inner ear phenotype is secondary to a neural crest defect. There may be a small neural crest contribution to the zebrafish inner ear (T. Schilling pers. comm.) and transplantation of otic vesicles between healthy and mutant embryos together with neural crest labelling studies may resolve this question. However, the strong expression of *sox10* within the developing otic vesicle suggests that it is directly required in inner ear development (Dutton et al., 2001).

Chapter 8

Materials and methods

All chemicals are from Sigma unless stated.

8.1 Fish Handling

8.1.1 Zebrafish stocks

Three wild-type *Danio rerio* strains were used through this work: AB, TL and WIK. The mutants used are detailed in Table 8.1.

Table 8.1 Mutants used in this study

Mutant	Gene name	Allele	Reference
dog-eared	*eya1*	*tm90b, tp85b*	(Whitfield et al., 1996; Kozlowski et al., in preparation)
van gogh	*tbx1*	*tu285*	(Whitfield et al., 1996) (T. Piotrowski pers. comm.)
colourless	*sox10*	*t3*	(Kelsh et al., 1996; Whitfield et al., 1996; Dutton et al., 2001)
swirl	*bmp2b*	*ta72a*	(Mullins et al., 1996; Mullins et al., 1998; Nguyen et al. 1998))
valentino	*krml1*	*b337*	(Moens et al., 1996;Moens et al., 1998)

All fish were raised at 27°C and staged in hours post fertilisation (hpf), or days post fertilisation (dpf) (Kimmel et al., 1995). For convenience some embryos were moved to the 18°C incubator after completion of epiboly stages to slow down development overnight, allowing collection of early somite stages. Embryos were grown in E3 in petri dishes until 7dpf after which they are put onto the aquarium system. The eggs were collected either by marbling or by separating out a male and a female fish in smaller mating tanks as in Westerfield, (1995).

E3 5mM NaCl, 0.17mM KCl, 0.33mM $CaCl_2.2\ H_2O$, 0.33 mM $MgSO_4.7H_2O$

8.2 *in situ* hybridisation I

Preparing probes.

8.2.1 DNA preparation

Probes were synthesised from templates kindly supplied by G. Begemann (*follistatin*), P. Blader (*wnt4*), A. Chin (*bmp4*), M. Fürthauer (*noggin1-3, bmp7*), M. Hammerschmidt (*smad6, 7, tkv, tgfβR1*), M. Mullins (*bmp2b, bmpr1B*), F. Reifers (*fgf8*), K. Sampath (*brn3.1*), T. Schilling (*bmp7-related*), S. Schulte-Merker (*chordino, nkx5.1*), U. Strühle (*smad1* and *5*), T. Jowett (*pax2.1*), M. Westerfield (*msxc*), and J. Wittbrodt (*spalt*).

Most of these templates were sent as spots on Whatman paper (500ng of plasmid in 1µl of 10mM Tris pH 7.6). On arrival 50µl of 10mMTris pH7.6 were added to the spot. The final concentration of the plasmid was assumed to be around 10ng/µl (Rosman and Miller, 1990).

8.2.2 Transformation

50ng of the plasmid DNA in 10µl of dH_2O plus 25µl of DH5α, Ca^{2+} competent cells (Gibco) were heat shocked at 42°C for 90 seconds and chilled on ice for 1-2 min. 800µl of LB was added and the tubes incubated at 37°C for 45 mins. The cells were spread (200µl/plate) on LB plates plus ampicillin (1ml of 50mg/ml in 1litre) and incubated overnight at 37°C. Plates spread with untransformed competent cells were incubated as a control (Sambrook et al., 1989).

LB medium: 10g bacto-tryptone (Difco), 5g bacto-yeast extract (Difco), 10g NaCl in 950ml dH_2O, pH to 7 with 5M NaOH, make up to 1 litre. Autoclave.

For plates 15g bacto-agar was added before autoclaving. If required 1ml of ampicillin (50mg/ml) was added once cooled (Sambrook et al., 1989).

8.2.3 Midi preps

Qiagen midiprep kits were used. The yield of the DNA preparation was assessed using an UV spectrophotometer, reading at 260nm (nucleic acids) and 280nm (protein). 5µl of the

sample was diluted in 1ml dH_2O (1/200). 1 OD unit = 50ng/ml of double stranded DNA, 40µg/ml for single stranded DNA or RNA, and about 20µg/ml for single stranded oligonucelotides. The ratio OD_{260}/OD_{280} provides an estimate of the purity of nucleic acids, 1.8-2 being pure. Contamination reduces this ratio.

8.2.4 Linearisation of plasmid template

Normally 25µg of DNA was cut in a total reaction volume of 400µl, with 50 units of restriction enzyme at 37°C for 1 hour. The digest was checked on a 0.8% agarose gel with the uncut sample run alongside. Once linearised 20µl of 10%SDS and 2µl of proteinase K was added and the mixture incubated for 20 mins at 37°C. This stops the reaction.

8.2.5 Phenol chloroform extraction

An equal volume of phenol:chloroform:isoamyl alcohol (P:C:I) was added to the sample and the mixture vortexed hard to mix the two layers. After spinning at 14k for 3 mins the top, aqueous layer was kept. A second extraction with chloroform alone removed any remaining phenol. $1/10^{th}$ of the sample volume of 3M NaOAc and 2x the sample volume of EtOH were added and the DNA precipitated at -20°C for 30 mins. After spinning for 5 mins at 13k the pellet was washed with 0.5ml of 70% EtOH and dried using a Speed vac rotating vacuum pump (Savant). Pellets were resuspended in 25µl dH_2O (final concentration ~ 25µg/µl) and stored at -20°C.

8.2.6 Probe preparation

Probes were prepared essentially as in Jowett and Lettice, (1994). Probes were synthesised using Roche DIG or Fluorescein mix kits and instructions. The reagents were incubated at 37°C for 2 hours. 2µl of 0.2M EDTA pH8 were added to stop the reaction. The RNA was precipitated with 2.5µl 4M LiCl and 75µl (-20°C) 100% ethanol at -70°C for 30 mins. The RNA was spun, washed with 70% ethanol and the pellet dried in Speed vac for a couple of minutes. The RNA was resuspended in 27µl dH_2O. 2µl (heated to 70°C) was run on a 0.8% agarose gel (in a tank cleaned with ethanol and dH_2O to remove RNases). This gel checked that the synthesis worked and gave an indication of the concentration of the probe;

the gel showed two bands, a larger one (linearised template DNA) and a smaller RNA one. 25µl of formamide (BDH) was added to probe and it was stored at -20°C.

8.3 *in situ* hybridisation II

8.3.1 Protocol

Embryos were collected at the desired stage, dechorionated removed and fixed overnight at 4°C in fish fix (Westerfield, 1995). They were washed 2x5 mins in PBS and 2x5 mins in 100% methanol at room temperature and stored at -20°C for at least 2 hours before use.

Embryos were rehydrated (5 mins each in 50%, 30% MeOH/PTW, and 4x5 mins in PTW) at room temperature. Embryos older than 48hpf were then acetone cracked. For this they were rinsed in dH_2O and incubated in acetone for 7 mins at –20°C, rinsed in dH_2O then put back into PTW. Cracking improves the penetration of probes into the tissues.

Embryos were then digested with proteinase K 10µg/ml in PTW, 5 mins for 24hpf and older, slightly less for younger stages. They were washed 4x5 mins in PTW at room temperature, fixed for 20 mins in fish fix and washed 5x in PTW. Embryos were rinsed in hyb, which was replaced with fresh hyb, and the samples were incubated at 70°C for at least 1hour. Embryos were then incubated with the probe overnight at 70°C. The probe was usually diluted 1:450µl, probe:hyb mix.

Embryos were washed for 10 mins each with : 75:25 hyb:2xSSC, 50:50, 25:75, 100% 2xSSC at 70°C followed by 2x30 mins with 0.2xSSC at 70°C, and then 5 mins each with 75:25 hyb:PBT, 50:50, 25:75, and 100% PBT at room temperature. Embryos were then blocked for 1 hour at room temperature and incubated overnight at 4°C with 1:2000 dilution of anti-digoxigenin or anti-fluorescein FAB fragments (Roche) in PBT.

The following day the embryos were washed 6x15 mins in PBT and 2x5 mins in staining buffer at room temperature. They were then incubated in staining buffer plus 3.5µl/ml BCIP and 4.5µl/ml NBT (Roche) in the dark. To stop the staining, embryos were washed in PTW (3 changes) and stored at 4°C. Alternatively fix was added for at least an hour before being replaced with PTW.

Fish fix: 4% Paraformaldehyde, 4% sucrose, 0.15mM $CaCl_2$, 0.1M PBS.

PBS:	0.8% NaCl, 0.02% KCl, 0.02M PO4 pH7.3
PTW:	0.1% Tween 20, PBS
PBT:	0.2% Bovine Serum albumin, PTW
Hyb:	50% Formamide, 5xSSC, 500µg/ml tRNA, 50µg/ml Heparin, 0.1% Tween 20, pH to 6 with 1M Citric Acid
Staining buffer;	0.1M TrisHCl pH9.5, 50mM $MgCl_2$, 0.1M NaCl, 0.1% Tween 20, 0.005M Levamisole

8.4 Rescue Injections.

8.4.1 *smad5* mRNA.

This plasmid was a gift from the Mullins lab. Sense *smad5* was provided in a pCS2+ vector. It was linearised with Acc65I and transcribed using SP6, phenol chloroform extracted twice; chloroform purified once and precipitated using ethanol and 3M NaOAc at -20°C overnight. The precipitates were resuspended in dH_2O and checked on a 1% agarose gel. The linearised plasmid was used as the template for the capped sense mRNA.

mRNA synthesis

Template	5µg
10x transcription buffer (Promega)	5
100mM DTT (Promega)	7
rNTPs	2
1mM rGTP	5
Cap (0.5Aunits) (Roche)	5
RNAsin (Promega)	2
Polymerase (Promega)	2.5
H_2O	16.5
total	50

The above reagents were briefly vortexed and spun, to ensure proper mixing. The mixture was incubated at 37°C for 30 mins then 2.5µl 10mM rGTP was added incubating for a further 1 hour then 5µl of RQ1 DNase I (Promega) was added and incubation continued for 30 mins. 1µl was run out on a fresh gel. If there was DNA visible on the gel (high band) more DNase was added and the reaction incubated for another 30 mins. Once completed the sample was P:C:I extracted twice and then precipitated with 3M NaOAc and ethanol. The pellet was washed with 75% ethanol (to remove unincorporated nucleotides) and

resuspended in 50µl of DEPC treated water. The RNA was then quantified using an UV spectrophotometer at 260/280nm, aliquoted and stored at -70°C.

DEPC: 800µl in 800ml of dH_2O gently mix, loosen lid and leave in fume hood for around 2 hours then autoclave.
rNTP mix: 25mM ATP, 25mM CTP, 25mM UTP.

Injection protocol

8.4.2 Injection solution

The *smad5* RNA was quantified at ~1450ng/µl. In initial trials a range of concentrations were examined; 20ng/µl, 100ng/µl, 300ng/µl and 500ng/µl. The injection solution also contained GFP RNA at 75ng/µl, and phenol red (1µl of neat in 10µl) in DEPC water.

Embryos were collected on the morning of injection and mounted in injection trays. These are petri dishes containing 1.5% agarose/10% Hanks in which several grooves have been moulded (Kates' Groove Tool (some slides, a ruler and a bulldog clip) or a plastic mould with multiple square projections). Embryos were aligned in these grooves and surrounded by 10% Hanks P/S solution to prevent infection. Capillaries with filaments were pulled to a diameter narrow enough not to cause too much damage to the embryo, but strong enough to puncture the chorion. Capillaries were back filled and a graticule was used to estimate the volume of RNA injected (5nl).

Embryos were injected into the yolk at the 2-4 cell stage using a pressure-driven microinjector (Narishige IM 300 Microinjector) then transferred to a petri dish containing 10% Hanks P/S and allowed to grow up in incubator at 27.5°C. The next morning embryos were checked for GFP fluorescence; embryos with evenly distributed, high levels of fluorescence were kept.

Hanks solution 1: 8g NaCl, 0.4g KCl in 100ml DEPC dH_2O
Hanks solution 2: 0.358g Na_2HPO_4, 0.6g KH_2PO_4 in 100ml DEPC dH_2O
Hanks solution 4: 0.72g $CaCl_2$ in 50ml DEPC dH_2O
Hanks solution 5: 1.23g $MgSO_4.7H_2O$ in 50ml DEPC dH_2O
Sodium bicarbonate: 0.35g $NaHCO_3$ in 10ml DEPC dH_2O
Hanks Premix: 10ml Hanks 1, 1ml Hanks 2, 1ml Hanks 4, 86ml DEPC dH_2O, 1ml Hanks 5 combined in this order.
Hanks Final: 9.9ml Hanks Premix, 0.1ml fresh sodium bicarbonate solution.

10% Hanks P/S: penicillin and streptomycin (solution kept in 1ml aliquots in –20°C) 1ml in 200ml of 10% Hanks.

Hanks solutions as in (Westerfield, 1995)

8.5 Genotyping injected embryos.

To identify rescued embryos a nested PCR technique was used to amplify around the site of the *ta72* mutation in the *bmp2b* gene (Fig. 8.1). This genotyping protocol was devised by M. Hild et al., and identifies wild type, heterozygous or homozygous mutants, using four primers in a single PCR reaction (Hild et al., 1999). Tails were clipped from fixed embryos and the DNA prepared from them using the Quick and Dirty protocol as in Westerfield (Westerfield, 1995).

8.5.1 DNA preparation

Tail tips were digested in 50µl of extraction buffer at 56°C for 3-4 hours with occasional vortexing. To inactivate the proteinase K in the extraction buffer samples were boiled for 5-10 mins. Samples were then spun for 1 min and stored at –20°C. 10µl of this mixture was used in the PCR reaction. Care was taken not to suck up debris stuck to the side.

Extraction buffer: 10mM Tris pH8, 2mM EDTA, 0.2% Triton X-100, 200µg/ml Proteinase K. (buffer can be stored without PK)

8.5.2 PCR reaction

A 2x buffer was made up and the Taq polymerase (1 unit) and DNA (10µl) were added to this (total volume 21µl). All the PCR reagents came from Promega.

2x buffer	x10 Mg^{2+} free buffer	200µl
	25mM Mg^{2+}	200µl
	50x dNTPs	40µl
	dH_2O	~
	primers (10µg/ml)	~

The programme and primers are as published in Hild et al., (1999).

94°C (3 mins), 10 cycles of 94°C (30 sec), 57.5°C (45 secs), 72°C (1 min), 20 cycles of 94°C (30 sec), 48°C (45 sec), 72°C (1 min), followed by 72°C (10 min).

Outer sense primer;	gctatcatgctttctactg
Outer antisense primer;	gttttgttcattcaacataaat
Wild type sense primer;	tgtgggtgccgatga
Mutant antisense primer;	ttggggagattgttcc

A 1321 ctctatgtgg acttcagtga tgtcggctgg aacgagtgga tcgtggcacc gccaggctat
1381 catgctttct actgccatgg cgagtgtccg ttccctctgc cggaccatct aaactccacc
1441 aaccatgcca ttgtccagac gctggtgaac tcggtcaact ccaacattcc caaagcctgt
1501 tgcatcccga cggagctcag ccctatctca ctgctgtacc tggacgagta cgagaaggtc
1561 attcttaaaa actaccagga catggtggtg gagggctgtg ggtgccgatg (a/g)gaacaatct
1621 ccccaatgaa gacttttatt tatacaaaag agcgagctat ttggaggaag aaaagaaata
1681 tatatgaata tatttatgtt gaatgaacaa aacaaaaaaa aaaaaaaaaa aa

outer forward primer
outer reverse primer
wild type forward primer
mutant reverse primer

B

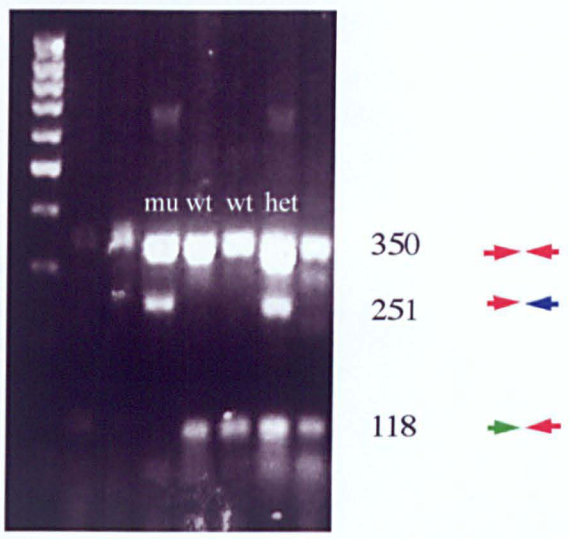

Figure 8.1 *swirl* genotyping protocol
(A) 3' end of wild type *bmp2b* sequence (AF072456) showing position of primers used in this genotyping PCR. Two external primers (red, sense and antisense) and two internal primers were used (green = wild type sense, blue = mutant antisense).
swirl ta72 is a point mutation changing a stop codon (tga) to a tryptophan (tgg) at position 1611 (a/g in figure), resulting in an extra 6 amino acids being added to the predicted mutant protein, inhibiting dimer formation (Kishimoto et al., 1997; Nguyen et al., 1998). The mutant and wild type specific primers were designed so their ends were at the site of the point mutation.
(B) A gel showing the PCR from tail clips of control and suspected rescued fish. All samples show the 350 base pair band amplified between the outer primers (red arrows). Wild type samples also have a smaller band at 118 base pair (green/red arrows), while mutant samples have a larger band at 251 base pairs (red/blue arrows) and heterozygotes have all three bands.

50x dNTPs: 10mM dATP, 10mMdCTP, 10mM dTTP, 1mM dGTP

8.6 Beading

8.6.1 Preparing beads

Beads were obtained from a HiTrap affinity column (Pharmacia). Beads were stored in 20% ethanol at room temperature. Before use the beads were washed: 50µl of PBS was added to 2µl of beads in siliconised tubes and the beads were soaked for 5 mins at room temperature. The beads were then spun at 13k for 5 mins and the supernatant removed. This was repeated 3 times with an extra spin after the last wash to remove all traces of PBS. The beads were then resuspended in 3µl of the control or the protein solution. These solutions were added using siliconised tips and left at room temperature for at least an hour before being stored in the fridge overnight. Siliconised plastics were used to prevent the protein sticking to the plastic instead of the beads. During use the beads were stored on ice. Soaked beads were not kept for longer than two days. For the hBMP4 experiments BSA was used as a control and for the *X*Noggin and Chordin experiments serum from the parental cell line was used. The concentrations used were; hBMP4, 0.258µg/µl; BSA, 0.258µg/µl and 5µg/µl; *X*Noggin, 0.3µg/ml and unquantified.

8.6.2 Mounting embryos

Embryos were collected the day before beading and moved to 18°C after completion of epiboly to increase the time window of implantation (22-27hpf). Embryos were anaesthetised using Tricane as in Westerfield, (1995) and mounted (usually laterally) in 1.5% low melting point agarose (BDH, made up with 10% normal Ringers solution) on a microscope slide. Embryos were arranged laterally before the agarose set. Small rectangles containing the embryos were cut out using a razor blade. Embryos were aligned against a coverslip attached to another slide with agarose and held in place by some more agarose (Fig. 8.2). The slide was then submerged in a petri dish containing 10% normal Ringers P/S.

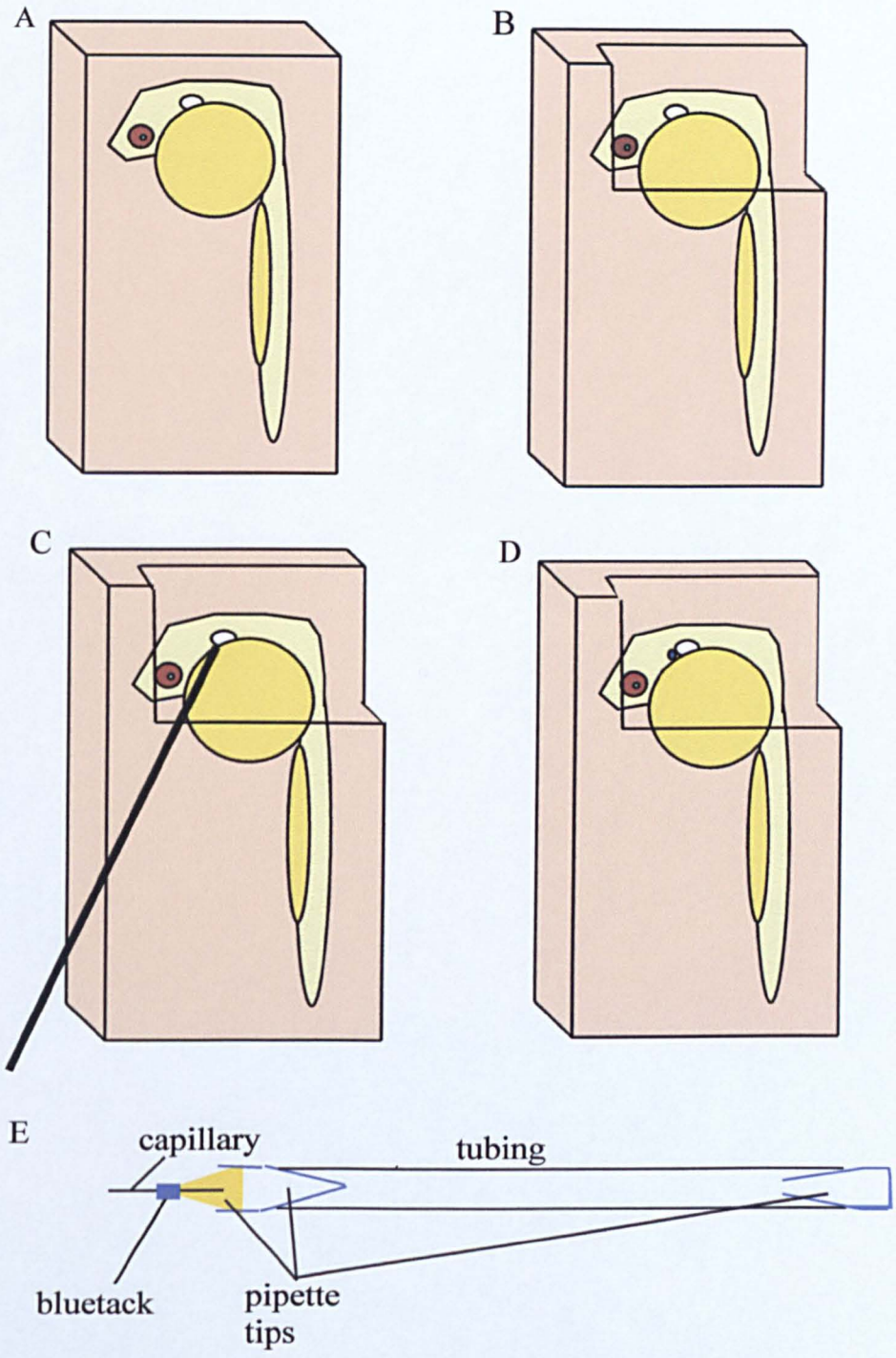

Figure 8.2 Sketch detailing the different stages of bead implantation.

(A) The embryo was mounted, usually laterally, in a rectangle of low melting point agarose. (B) The overlying section of agarose is removed revealing the otic vesicle. (C) A hole was made in the embryo using a glass capillary. (D) The bead was implanted using a capillary adjacent to the otic vesicle. (E) A mouth pipette was constructed out of some tubing, pipette tips and blue tack.

8.6.3 Implantation

Capillaries without filaments were pulled to provide a point just smaller than the beads but still strong enough to puncture embryos and not bend. These were attached to a mouth pipette, which allowed beads to be sucked up and held at the capillary tip.

A window was cut into the agarose using a small syringe with a microlance needle allowing access to the ear (this seemed easiest from a dorsal posterior angle).

A capillary was used to puncture the embryo. Then a bead was sucked up and pushed into the hole. Embryos were then left for a few mins before being carefully released from the agarose and the position of the bead recorded both laterally and dorsally. Embryos were then transferred to a 24 multiwell plate and left in 10%Ringers P/S for around an hour at 27.8°C. The Ringers was then replaced with E3 and the embryos left to grow in the incubator for 3-4 days. After the required time has elapsed, the embryos were anaesthetised with Tricane, mounted with 3% methyl cellulose and a picture taken showing the position of bead and the state of both the beaded and contralateral otic vesicle. Embryos were transferred back into E3 for an hour to remove the methyl cellulose, which seemed to reduce the efficiency of actin stains, possibly affecting the permeability of embryos. Embryos were then fixed and processed as normal for either actin stains or in situ hybridisation.

Tricaine (3-amino benzoic acidethylester): for 1litre 400mg Tricaine, 97.9ml dH_2O and about 2.1ml 1M Tris (pH9) to pH to around 7.
Ringers: 100% = 116mM NaCl, 2.9mM KCl, 1.8mM $CaCl_2$, 5mM HEPES, pH7.2 use 10% and add 1ml of Penicillin/Streptomycin to 200ml.
Agarose: 1.5% low melting point in 10% Ringers (no P/S)

Non-filament capillaries 1mm O.D.x0 .58mm I.D (Harvard apparatus)

8.7 TUNEL in situ assay of apoptosis

This protocol was recommended by Dr D. Kozlowski. It uses the ApopTag Plus in situ Apoptosis Detection Kit (Oncor) and is similar to the version given in the kit.

8.7.1 Protocol.

Embryos were dechorionated and fixed in 4% PFA for 2 hours at room temperature or overnight at 4°C. Embryos were washed in 2 changes of PBS and stored in methanol at

-20°C for at least 1 hour. Embryos were then rehydrated through a methanol series as with normal in situs and incubated for 15 mins in proteinase K (10µg/ml). Embryos were washed in PTW 3x5 mins, fixed for 20 mins with 4% PFA then in EtOH:Glacial Acetic Acid (2:1) for 10 mins at -20°C, then rinsed for 3x5 mins in PBS.

Embryos were incubated in 50µl of equilibrium buffer (in kit) for 1 hour at room temperature, then incubated in TdT enzyme at 37°C for 1.5 hours. This enzyme adds nucleotide triphosphates (including some digoxigenin labelled nucleotides) to the 3'OH end of double and single stranded DNA.

reaction buffer	38µl
TdT enzyme	16µl
Total	54µl

Embryos are then incubated in the stop reaction (in kit) for 3 hours at 37.5°C, washed for 3x5 mins in PTW, and incubated in PBT block for 1hour at room temperature. Embryos were then incubated in antibody (1:2000, antiDIG alkaline phosphatase FAB fragments, Roche) overnight at 4°C, washed 8x15 mins PBST, and rinsed 3x5 mins in stain buffer (as in normal in situ). Staining (BCIP+NBT) was carried out at room temperature (usually staining in ~15 mins)

PBT: 0.2%BSA in PTW
Stain BCIP +NBT as in in situ hybridisation protocol (8.3.1).

8.8 Mitosis marker.

Embryos were fixed for 2 hours at room temperature. Embryos were then washed in PBS 2x10 mins, incubated in dH_2O for 10 mins, acetone cracked in –20°C for 10 mins (over 24hpf) then put back into dH_2O 2x5 mins. Embryos were then rinsed in PBS 4x5 mins and blocked for 1 hour.

Embryos were incubated in anti-phospho Histone H3 antibody (1:2000, Upstate Biotech UK) overnight at 4°C. The next day embryos were washed in block for several changes over 1 hour. The secondary antibody was added (Rabbit IgG (whole molecule), TRITC labelled, 1:100) and incubated for 2 hours at room temperature or overnight at 4°C in dark. For double labelling with phalloidin, FITC-phalloidin was added to this solution (1:20 see below). Samples were then washed for 1 hour in PTW.

Antibodies were diluted in block solution.

Block: 1xPBS, 0.1% BSA, 0.1% Triton X100, 1%DMSO.

8.9 Phalloidin labelled actin stains

Embryos were fixed in fish fix overnight at 4°C and rinsed in PBS:Triton (2% for 72hpf, 24-48hpf 1%, 48-72hpf 1.5%) for 3 hours at room temperature. Embryos were stained overnight at 4°C in working stain solution in the dark. Embryos were then washed at least 2x in PBS for at least 2 hours, in the dark, at room temperature. This wash step is important. See below for mounting and confocal technique.

8.9.1 Actin and tubulin double stains

After fixing and soaking in PBS:Triton embryos were rinsed in BDPF for 1 hour and left overnight at 4°C in 1:100 dilution of anti-acetylated tubulin in BDPF. After rinsing for 2 hours in BDPF at room temperature embryos are incubated overnight at 4°C in the dark in the secondary antibody rhodamine rabbit anti-mouse IgG (1:50) and FITC-phalloidin (2.5µg/ml). Embryos were then washed for 2 hours in PBS at room temperature and mounted in Vectashield.

FITC-phalloidin stock solutions: 0.1mg in sterile PBS stored at -20°C (50µg/ml).

Working solution: 0.1ml stock in 2ml PBS (2.5µg/ml).

BDPF: 1%BSA, 0.1% DMSO, 5% Fetal calf serum in PBS.

8.10 Microscopy

8.10.1 Light microscopy

Fixed samples and live embryos were normally viewed using DIC optics on a Zeiss Axioplan or an Olympus BX51 compound microscope. Images were captured with either a microscope-mounted compact (Zeiss) or digital camera (Olympus Camedia C-3030). The compact camera used T75 Kodak film. A PC using AnalySIS software (Soft Imaging Software) controlled the digital camera.

For fixed samples the yolk sacs were removed and the embryos taken through a glycerol series over about 15-20 mins. Individual embryos were mounted in cavity slides made

from holes cut in layers of electrical insulation tape (24hpf 1 or 2 layers, 72hpf 3) which had been stuck to a microscope slide. Further dissections, such as transverse sections through the ear, were hand cut after mounting on slides, keeping the parts of the embryo together which was useful for staging purposes. To capture live images the embryos were anaesthetised in Tricane and mounted in 3% methyl cellulose.

8.10.2 Confocal microscopy

Confocal images were generated using a Leica SP confocal microscope. This microscope takes optical sections at different levels through a wholemount sample. The accompanying software reassembled this data to stack a series of Z sections, providing an image of the internal structures of the inner ear.

After staining and washing embryos were mounted in Vectashield on taped slides. In order to generate good dorsal views embryos 3 days and older had their skin and brains removed. Coverslips were fixed with nail polish.

Bibliography

Ahn, D. G., I. Ruvinsky, A. C. Oates, L. M. Silver and R. K. Ho (2000). *tbx20*, a new vertebrate T-box gene expressed in the cranial motor neurons and developing cardiovascular structures in zebrafish. Mechanisms of Development **95**: 253-8.

Akimenko, M. A., S. L. Johnson, M. Westerfield and M. Ekker (1995). Differential induction of four *msx* homeobox genes during fin development and regeneration in zebrafish. Development **121**: 347-57.

Amores, A., A. Force, Y. L. Yan, L. Joly, C. Amemiya, A. Fritz, R. K. Ho, J. Langeland, V. Prince, Y. L. Wang, M. Westerfield, M. Ekker and J. H. Postlethwait (1998). Zebrafish hox clusters and vertebrate genome evolution. Science **282**: 1711-4.

Ando, H., T. Furuta, R. Y. Tsien and H. Okamoto (2001). Photo-mediated gene activation using caged RNA/DNA in zebrafish embryos. Nature Genetics **28**: 317-25.

Baker, C., V. and M. Bronner-Fraser (2001). Vertebrate cranial placodes I. Embryonic induction. Developmental Biology **232**: 1-61.

Baker, J. C. and R. M. Harland (1997). From receptor to nucleus: the Smad pathway. Current Opinion in Genetics and Development **7**: 467-73.

Bang, P. I., W. F. Sewell and J. J. Malicki (2001). Morphology and cell type heterogeneities of the inner ear epithelia in adult and juvenile zebrafish (*Danio rerio*). Journal of camparative Neurology **438**(2): 173-90.

Barth, K. A., Y. Kishimoto, K. B. Rohr, C. Seydler, S. Schulte-Merker and S. W. Wilson (1999). Bmp activity establishes a gradient of positional information throughout the entire neural plate. Development **126**:4977-87.

Bauer, H., A. Meier, M. Hild, S. Stachel, A. Economides, D. Hazelett, R. N. Harland and M. Hammerschmidt (1998). Follistatin and Noggin are excluded from the zebrafish organizer. Developmental Biology **204**(2): 488-507.

Bauer, H., Z. Lele, G. J. Rauch, R. Geisler and M. Hammerschmidt (2001). The type I serine/threonine kinase receptor Alk8/*Lost-a-fin* is required for Bmp2b/7 signal transduction during dorsoventral patterning of the zebrafish embryo. Development **128**(6): 849-858.

Begemann, G. and P. W. Ingham, W. (2000). Developmental regulation of *Tbx5* in zebrafish embryogenesis. Mechanisms of Development **90**: 299-304.

Bendall, A. J. and C. Abate-Shen (2000). Roles for Msx and Dlx homeoproteins in vertebrate development. Gene **247**: 17-31.

Bever, M. M. and D. M. Fekete (1999). Ventromedial focus of cell death is absent during development of *Xenopus* and zebrafish inner ears. Journal of Neurocytology **28**(10-11): 781-93.

Bever, M. M. and D. M. Fekete (in press). Atlas of the developing inner ear in zebrafish. Developmental Dynamics.

Bissonnette, J. P. and D. M. Fekete (1996). Standard atlas of the gross anatomy of the developing inner ear of the chicken. Journal Of Comparative Neurology **368**(4): 620-630.

Blader, P., S. Rastegar, N. Fischer and U. Strähle (1997). Cleavage of the BMP-4 antagonist chordin by zebrafish tolloid. Science **278**(5345): 1937-1940.

Bonini, N. M., W. M. Leiserson and S. Benzer (1993). The *eyes absent* gene: genetic control of cell survival and differentiation in the developing *Drosophila* eye. Cell **72**: 379-95.

Botta, A., F. Amati and G. Novelli (2001). Causes of the phenotype-genotype dissociation in DiGeorge syndrome: clues from mouse models. Trends in Genetics **17**(12): 551-4.

Briscoe, J., Y. Chen, T. M. Jessell and G. Struhl (2001). A hedgehog-insensitive formof patched provides evidence for direct long-range morphogen activity of sonic hedgehog in the neural tube. Molecular Cell **7**: 1279-91.

Bronner-Fraser, M. (1986). Guidance of neural crest migration. Latex beads as probes of surface-substratum interactions. Developmental Biology 3:301-337 New York.

Bubnoff, A., and K.W. Y. Cho. (2001). Intracellular BMP Signaling Regulation in Vertebrates: Pathway or Network? Developmental Biology **239**: 1-14.

Campuzano, S., and J. Modolell (1992). Patterning of the Drosophila nervous system: the achaete-scute gene complex. Trends in Genetics **8**: 202-8.

Capdevila, J. and R. L. Johnson (1998). Endogenous and ectopic expression of *noggin* suggests a conserved mechanism for regulation of BMP function during limb and somite patterning. Developmental Biology **197**: 205-17.

Chang, W. S., F. D. Nunes, J. M. De Jesus Escobar, R. Harland and D. K. Wu (1999). Ectopic Noggin blocks sensory and nonsensory organ morphogenesis in the chicken inner ear. Developmental Biology **216**(1): 369-381.

Chapman, D. L., N. Garvey, S. Hancock, M. Alexiou, S. I. Agulnik, J. J. Gibson-Brown, J. Cebra-Thomas, R. J. Bollag, L. M. Silver and V. E. Papaioannou (1996). Expression of the T-box family genes, *Tbx1-Tbx5*, during early mouse development." Developmental Dynamics **206**: 379-90.

Chen, Y., M. Bei, I. Woo, I. Satokata and R. Maas (1996). Msx1 controls inductive signaling in mammalian tooth morphogenesis. Development **122**(10): 3035-44.

Chen, Y., and A.F. Schier (2001). The zebrafish Nodal signal Squint functions as a morphogen. Nature **411**:607-10.

Chieffo, C., N. Garvey, W. Gong, B. Roe, G. Zhang, L. Silver, B. S. Emanuel and M. L. Budarf (1997). Isolation and characterization of a gene from the DiGeorgechromosomal region homologous to the mouse *Tbx1* gene. Genomics **43**: 267-77.

Chin, A. J., J. N. Chen and E. S. Weinberg (1997). *Bone morphogenetic protein-4* expression characterises inductive boundaries in organs of developing zebrafish. Development Genes and Evolution **207**(2): 107-114.

Choo, D., J. L. Sanne and D. K. Wu (1998). The Differential Sensitivities of Inner Ear Structures to Retinoic Acid during Development. Developmental Biology **204**:136-50.

Christian, J. L. (2000). BMP, Wnt and Hedgehog signals: how far can they go? Current Opinion in Cell Biology **12**: 244-9.

Cole, L. L. and L. S. Ross (2001). Apoptosis in the Developing Zebrafish Embryo. Developmental Biology **240**: 123-42.

Connors, S. A., J. Trout, M. Ekker and M. C. Mullins (1999). The role of *tolloid/mini fin* in dorsoventral pattern formation of the zebrafish embryo. Development **126**(14): 3119-3130.

Coombs, S., P. Gorner and H. Munz (eds) (1989). The Mechanosensory Lateral Line:Neurobiology and Evolution. New York:Springer-Verlag.

Cui, Y., R. Hackenmiller, L. Berg, F. Jean, T. Nakayama, G. Thomas and J. L. Christian (2001). The activity and signaling range of mature BMP-4 is regulated by sequential cleavage at two sites within the prodomain of the precursor. Genes and Development **15**: 2797-802.

Currie, P. D. and P. W. Ingham (1996). Induction of a specific muscle cell type by a hedgehog-like protein in zebrafish. Nature **382**: 452-5.

Curtiss, J. and M. Mlodzik (2000). Morphogenetic furrow initiation and progression during eye development in Drosophila: the roles of decapentaplegic, hedgehog and eyes absent. Development **127**(6): 1325-36.

Dahn, R. D. and J. F. Fallon (2000). Interdigital regulation of digit identity and homeotic transformation by modulated BMP signaling. Science **289**: 438-41.

Davidson, D. (1995). The function and evolution of Msx genes: pointers and paradoxes. Trends in Genetics **11**: 405-11.

de Celis, J. F., R. Barrio and F. C. Kafatos (1996). A gene complex acting downstream of *dpp* in *Drosophila* wing morphogenesis. Nature **381**: 421-4.

de Celis, J. F., R. Barrio and F. C. Kafatos (1999). Regulation of the *spalt/spalt-related* gene complex and its function during sensory organ development in the *Drosophila* thorax. Development **126**: 2653-62.

Denk, W., J. R. Holt, G. M. Shepherd and D. P. Corey (1995). Calcium imaging of single stereocilia in hair cells: localization of transduction channels at both ends of tip links. Neuron **16**: 1311-21.

Denman-Johnson, K. and A. Forge (1999). Establishment of hair bundle polarity and orientation in the developing vestibular system of the mouse. Jounal of Neurocytology **28**: 821-35.

Deol, M. S. (1964). The abnormalities of the inner ear in *kreisler* mice. Journal of Embryological and Experimental Morphology **12**: 475-490.

Dewulf, N., K. Verschueren, O. Lonnoy, A. Moren, S. Grimsby, K. Vandespiegle, K. Miyazono, D. Huylebroeck and P. Tendijke (1995). Distinct Spatial and Temporal Expression Patterns Of 2 Type-I Receptors For Bone Morphogenetic Proteins During Mouse Embryogenesis. Endocrinology **136**(6): 2652-2663.

Dheen, T., I. Sleptsova-Friedrich, Y. Xu, M. Clark, H. Lehrach, Z. Gong and V. Korsch. (1999). Zebrafish tbx-c functions during formation of midline structures. Development **126**: 2701-13.

Dick, A., M. Hild, H. Bauer, Y. Imai, H. Maifeld, A. F. Schier, W. S. Talbot, T. Bouwmeester and M. Hammerschmidt (2000). Essential role of Bmp7 (*snailhouse*) and its prodomain in dorsoventral patterning of the zebrafish embryo. Development **127**(2): 343-354.

Dick, A., T. Mayr, H. Bauer, A. Meier and M. Hammerschmidt (2000). Cloning and characterization of zebrafish *smad2*, *smad3* and *smad4*. Gene **246**: 69-80.

Dick, A., A. Meier and M. Hammerschmidt (1999). Smad1 and Smad5 have distinct roles during dorsoventral patterning of the zebrafish embryo. Developmental Dynamics **216**: 285-98.

Dosch, R., V. Gawantka, H. Delius, C. Blumenstock and C. Niehrs (1997). Bmp-4 acts as a morphogen in dorsoventral mesoderm patterning in *Xenopus*. Development **124**(12): 2325-34.

Driever, W., L. Solnica-Krezel, A. F. Schier, S. C. F. Neuhauss, J. Malicki, D. L. Stemple, D. Y. R. Stainier, F. Zwartkruis, S. Abdelilah, Z. Rangini, J. Belak and C. Boggs (1996). A genetic screen for mutations affecting embryogenesis in zebrafish. Development **123**: 37-46.

Drossopoulou, G., K. E. Lewis, J. J. Sanz-Ezquerro, N. Nikbakht, A. P. McMahon, C. Hofmann and C. Tickle (2000). A model for anteroposterior patterning of the vertebrate limb based on sequential long- and short-range Shh signalling and Bmp signalling. Development **127**: 1337-48.

Dutton, K. A., A. Pauliny, S. S. Lopes, S. Elworthy, T. J. Carney, J. Rauch, R. Geisler, P. Haffter and R. N. Kelsh (2001). Zebrafish *colourless* encodes *sox10* and specifies non-ectomesenchymal neural crest fates. Development **128**: 4113-25.

Eichele, G., C. Tickle and B. M. Alberts (1984). Microcontrolled release of biologically active compounds in chick embryos: beads of 200-microns diameter for the local release of retinoids. Anals of Biochemistry **142**:542-55.

Ekker, M., M. A. Akimenko, M. L. Allende, R. Smith, G. Drouin, R. M. Langille, E. S. Weinberg and M. Westerfield (1997). Relationships among *msx* gene structure and function in zebrafish and other vertebrates. Molecular Biology and Evolution **1997**: 1008-22.

Ekker, M., M. A. Akimenko, R. Bremiller and M. Westerfield (1992). Regional Expression Of 3 Homeobox Transcripts In the Inner-Ear Of Zebrafish Embryos. Neuron **9**(1): 27-35.

Ekker, S. C., A. R. Ungar, P. Greenstein, D. P. von Kessler, J. A. Porter, R. T. Moon and P. A. Beachy (1995). Patterning activities of vertebrate hedgehog proteins in the developing eye and brain. Current Biology **5**: 944-55.

Elstob, P. R., V. Brodu and A. P. Gould (2001). spalt-dependent switching between two cell fates that are induced by the *Drosophila* EGF receptor. Development **128**: 723-32.

Erkman, L., R. J. McEvilly, L. Luo, A. K. Ryan, F. Hooshmand, S. M. O'Connell, E. M. Keithley, D. H. Rapaport, A. F. Ryan and M. G.

Rosenfeld (1996). Role of transcription factors Brn-3.1 and Brn-3.2 in auditory and visual system development. Nature **381**: 603-6.

Everett, L. A., Morsli. H., D. K. Wu and E. D. Green (1999). Expression pattern of the mouse ortholog of the Pendred's syndrome gene (*Pds*) suggests a key role for pendrin in the inner ear. Proceedings of the National Acadamy of Sciences U S A **96**(17): 9727-32.

Fekete, D. M. (1996). Cell fate specification in the inner ear. Current Opinion In Neurobiology **6**:533-541.

Fekete, D. M. (1999). Development of the vertebrate ear: insights from knockouts and mutants. Trends in Neuroscience **22**: 263-9.

Fekete, D. M., S. A. Homburger, M. T. Waring, A. E. Riedl and L. F. Garcia (1997). Involvement of programmed cell death in morphogenesis of the vertebrate inner ear. Development **124**(12): 2451-2461.

Fekete, D. M., S. Muthukumar and D. Karagogeos (1998). Hair cells and supporting cells share a common progenitor in the avian inner ear. Journal Of Neuroscience **18**(19): 7811-7821.

Force, A., M. Lynch, F. B. Pickett, A. Amores, Y. L. Yan and J. Postlethwait (1999). Preservation of duplicate genes by complementary, degenerative mutations. Genetics **151**: 1531-45.

Frenz, D. A., W. Liu, V. Galinovic-Schwartz and T. R. Van De Water (1996). Retinoic acid-induced embryopathy of the mouse inner ear. Teratology **53**: 292-303.

Fürthauer, M., B. Thisse and C. Thisse (1999). Three different *noggin* genes antagonize the activity of bone morphogenetic proteins in the zebrafish embryo. Developmental Biology **214**(1): 181-196.

Fürthauer, M., C. Thisse and B. Thisse (1997). A role for FGF-8 in the dorsoventral patterning of the zebrafish gastrula. Development **124**(21): 4253-4264.

Gee, K. R., E. S. Weinberg and D. J. Kozlowski (2001). Caged Q-rhodamine dextran: a new photoactivated fluorescent tracer." Bioorganic & Medicinal Chemistry Letters **11**: 2181-3.

Gerlach-Bank, L. M. and K. F. Barald (2001). Developmental expression and activity of DAN in chick and mouse inner ear development. The Molecular Biology of Hearing and Deafness., Bethesda, USA, with permission.

Gerlach, L. M., M. R. Hutson, J. A. Germiller, D. NguyenLuu, J. C. Victor and K. F. Barald (2000). Addition of the BMP4 antagonist, noggin, disrupts avian inner ear development. Development **127**(1): 45-54.

Gibson-Brown, J. J., S. Agulnik, L. M. Silver and V. E. Papaioannou (1998). Expression of T-box genes *Tbx2-Tbx5* during chick organogenesis. Mechanisms of Development **74**: 165-9.

Gompel, N., Cubedo, N., Thisse, C., Thisse, B., Dambly-Chaudiere, C., and Ghysen, A. (2001). Pattern formation in the lateral line of zebrafish. Mechanisms of Development **105**: 69-77.

Graham, A., P. Francis-West, P. Brickell and A. Lumsden (1994). The signalling molecule BMP4 mediates apoptosis in the rhombencephalic neural crest. Nature **372**: 684-6.

Grinblat, Y., J. Gamse, M. Patel and H. Sive (1998). Determination of the zebrafish forebrain: induction and patterning. Development **125**(22): 4403-16.

Gurdon, J. B., A. Mitchell and K. Ryan (1996). An experimental system for analyzing response to a morphogen gradient. Proceedings of the National Acadamy of Sciences U S A **93**(18): 9334-8.

Haddon, C., Y. J. Jiang, L. Smithers and J. Lewis (1998). Delta-Notch signalling and the patterning of sensory cell differentiation in the zebrafish ear: evidence from the *mind bomb* mutant. Development **125**(23): 4637-4644.

Haddon, C. and J. Lewis (1996). Early ear development in the embryo of the zebrafish, *Danio rerio*. Journal Of Comparative Neurology **365**(1): 113-128.

Haddon, C., C. Mowbray, T. Whitfield, D. Jones, S. Gschmeissner and J. Lewis (1999). Hair cells without supporting cells: further studies in the ear of the zebrafish *mind bomb* mutant. Journal of Neurocytology **28**(10-11): 837-50.

Haddon, C. M. (1997). The development of the zebrafish ear and a quest for genes involved in sensory patterning. Open University, Open University.

Haddon, C. M. and J. H. Lewis (1991). Hyaluronan As a Propellant For Epithelial Movement - the Development Of Semicircular Canals In the Inner-Ear Of *Xenopus*. Development **112**(2): 541-50.

Haffter, P., M. Granato, M. Brand, M. C. Mullins, M. Hammerschmidt, D. A. Kane, J. Odenthal, F. J. M. van Eeden, Y. J. Jiang, C. P. Heisenberg, R. N. Kelsh, M. Furutani Seiki, E. Vogelsang, D. Beuchle, U. Schach, C. Fabian and C. Nüsslein Volhard (1996). The identification of genes with unique and essential functions in the development of the zebrafish, *Danio rerio*. Development **123**: 1- 36.

Halloran, M. C., M. Sato-Maeda, J. T. Warren, F. Su, Z. Lele, P. H. Krone, J. Y. Kuwada and W. Shoji (2000). Laser-induced gene expression in specific cells of transgenic zebrafish. Development **127**: 1953-60.

Hammerschmidt, M., Blader,P., and Strähle, U. (1999). Strategies to perturb zebrafish development. The Zebrafish: Biology. H. W. I. Detrich, Westerfield, M., and L. I. Zon. London: Academic Press. **59:** 87-116.

Hammerschmidt, M., F. Pelegri, M. C. Mullins, D. A. Kane, F. J. M. van Eeden, M. Granato, M. Brand, M. FurutaniSeiki, P. Haffter, C. P. Heisenberg, Y. J. Jiang, R. N. Kelsh, J. Odenthal, R. M. Warga and C. Nüsslein Volhard (1996a). *dino* and *mercedes*, two genes regulating dorsal development in the zebrafish embryo. Development **123**: 95-102.

Hammerschmidt, M., Serbedzija, G.N., and McMahon., A.P. (1996b). Genetic analysis of dorsoventral pattern formation in the zebrafish: requirement of a BMP-like ventralizing activity and its dorsal repressor. Genes and Development **10**: 2452-61.

Hammond, K. L., R. E. Hill, T. T. Whitfield and P. D. Currie (in press). Isolation of three zebrafish *daschund* homologues and their expression in sensory organs, the central nervous system and pectoral fin buds. Mechanisms of Development.

Hata, A., G. Lagna, J. Massague and A. HemmatiBrivanlou (1998). Smad6 inhibits BMP/Smad1 signaling by specifically competing with the Smad4 tumor suppressor. Genes & Development **12**(2): 186-197.

Hata, A., J. Seoane, G. Lagna, E. Montalvo, A. Hemmati-Brivanlou and J. Massague (2000). OAZ uses distinct DNA- and protein-binding zinc fingers in separate BMP-Smad and Olf signaling pathways. Cell **100**: 229-40.

Hazama, M., A. Aono, N. Ueno and Y. Fujisawa (1995). Efficient expression of a heterodimer of bone morphogenetic protein subunits using a baculovirus expression system. Biochemical and Biophysical Research Communications **209**(3): 859-66.

Hazelett, D. J., M. Bourouis, U. Walldorf and J. E. Treisman (1998). *decapentaplegic* and *wingless* are regulated by e*yes absent* and *eyegone* and interact to direct the pattern of retinal differentiation in the eye disc. Development **125**: 3741-51.

Heanue, T. A., R. Reshef, R. J. Davis, G. Mardon, G. Oliver, S. Tomarev, A. B. Lassar and C. J. Tabin (1999). Synergistic regulation of vertebrate muscle development by Dach2, Eya2, and Six1, homologs of genes required for *Drosophila* eye formation. Genes and Development **13**: 3231-43.

Hemmati-Brivanlou, A. and G. H. Thomsen (1995). Ventral Mesodermal Patterning In *Xenopus* Embryos - Expression Patterns and Activities Of Bmp-2 and Bmp-4. Developmental Genetics **17**(1): 78-89.

Hendzel, M. J., Y. Wei, M. A. Mancini, A. Van Hooser, T. Ranalli, B. R. Brinkley, D. P. Bazett-Jones and C. D. Allis (1997). Mitosis-specific phosphorylation of histone H3 initiates primarily within pericentromeric heterochromatin during G2 and spreads in an ordered fashion coincident with mitotic chromosome condensation. Chromosoma **106**(6): 348-60.

Hild, M., A. Dick, G. J. Rauch, A. Meier, T. Bouwmeester, P. Haffter and M. Hammerschmidt (1999). The smad5 mutation somitabun blocks Bmp2b signaling during early dorsoventral patterning of the zebrafish embryo.Development **126**(10): 2149-2159.

Hogan, B. L. M. (1996). Bone morphogenetic proteins: Multifunctional regulators of vertebrate development. Genes & Development **10**(13): 1580-1594.

Holley, S. A., Neul, J.L., Attisano, L., Wrana, J.L., Sasai, Y., O'Connor, M.B., De Robertis, E.M., and Ferguson, E.L. (1996). The *Xenopus* dorsalizing factor noggin ventralizes Drosophila embryos by preventing DPP from activating its receptor. Cell **86**: 607-17.

Hu, G., H. Lee, S. M. Price, M. M. Shen and C. Abate-Shen (2001). Msx homeobox genes inhibit differentiation through upregulation of *cyclin D1*. Development **128**:2373-84.

Huang, E. J., W. Liu, B. Fritzsch, L. M. Bianchi, L. F. Reichardt and M. Xiang (2001). *Brn3a* is a transcriptional regulator of soma size, target field innervation and axon pathfinding of inner ear sensory neurons. Development **128**(13): 2421-32.

Iemura, S., T. S. Yamamoto, C. Takagi, H. Uchiyama, T. Natsume, S. Shimasaki, H. Sugino and N. Ueno (1998). Direct binding of follistatin to a complex of bone-morphogenetic protein and its receptor inhibits ventral and epidermal cell fates in early *Xenopus* embryo. Proceedings of the National Acadamy of Sciences U S A **95**: 9337-42.

Imamura, T., M. Takase, A. Nishihara, E. Oeda, J. Hanai, M. Kawabata and K. Miyazono (1997). Smad6 inhibits signalling by the TGF-beta superfamily. Nature **389**: 622-6.

Ishisaki, A., K. Yamato, S. Hashimoto, A. Nakao, K. Tamaki, K. Nonaka, P. ten Dijke, H. Sugino and T. Nishihara (1999). Differential inhibition of Smad6 and Smad7 on bone morphogenetic protein- and activin-mediated growth arrest and apoptosis in B cells. Journal of Biological Chemistry **274**: 13637-42.

Jernvall, J. and I. Thesleff (2000). Reiterative signaling and patterning during mammalian tooth morphogenesis. Mechanisms of Development **92**(1): 19-29.

Jesuthasan, S., and Stahle, U. (1997). Dynamic microtubules and specification of the zebrafish embryonic axis. Current Biology **7**: 31-42.

Johnson, S. L., D. Africa, C. Walker and J. A. Weston (1995). Genetic control of adult pigment stripe development in zebrafish. Developmental Biology **167**: 27-33.

Jones, B. W. (2001). Glial cell development in the Drosophila embryo. Bioessays **23**: 877-87.

Jones, C. M., K. M. Lyons and B. L. M. Hogan (1991). Involvement Of Bone-Morphogenetic Protein-4 (Bmp-4) and Vgr-1 In Morphogenesis and Neurogenesis In the Mouse. Development **111**(2): 531-42 .

Jowett, T. and L. Lettice (1994). Whole-mount in situ hybridizations on zebrafish embryos using a mixture of digoxigenin- and fluorescein-labelled probes. Trends in Genetics **10**(3): 73-4.

Kalatzis, V., I. Sahly, A. El-Amraoui and C. Petit (1998). *Eya1* expression in the developing ear and kidney: towards the understanding of the pathogenesis of Branchio-Oto-Renal (BOR) syndrome. Developmental Dynamics **213**(4): 486-99.

Kelsh, R. N., M. Brand, Y. J. Jiang, C. P. Heisenberg, S. Lin, P. Haffter, J. Odenthal, M. C. Mullins, F. J. van Eeden, M. Furutani-Seiki, M. Granato, M. Hammerschmidt, D. A. Kane, R. M. Warga, D. Beuchle, L. Vogelsang and C. Nusslein-Volhard (1996). Zebrafish pigmentation mutations and the processes of neural crest development. Development **123**: 369-89.

Kelsh, R. N., K. Dutton, M. J. and J. S. Eisen (2000a). Expression of zebrafish *fkd6* in neural crest-derived glia. Mechanisms of Development **93**(1-2): 161-4.

Kelsh, R. N. and J. S. Eisen (2000b). The zebrafish *colourless* gene regulates development of non-ectomesenchymal neural crest derivatives. Development **127**(3): 515-25.

Kil, S.-H. and A. Collazo (2001). Origins of Inner Ear Sensory Organs Revealed by Fate Map and Time-Lapse Analyses. Developmental Biology **233**: 365-379.

Kimmel, C. B., W. W. Ballard, S. R. Kimmel, B. Ullmann and T. F. Schilling (1995). Stages of embryonic development of the zebrafish." Developmental Dynamics **203**(3): 253-310

King, J. A., P. C. Marker, K. J. Seung and D. M. Kingsley (1994). Bmp5 and the Molecular, Skeletal, and Soft-Tissue Alterations In Short Ear Mice. Developmental Biology **166**(1): 112-122.

Kishimoto, Y., K. H. Lee, L. Zon, M. Hammerschmidt and S. Schulte Merker (1997). The molecular nature of zebrafish *swirl*: BMP2 function is essential during early dorsoventral patterning. Development **124**(22): 4457-4466.

Knochel, S., K. Dillinger, M. Koster and W. Knochel (2001). Structure and expression of *Xenopus tropicalis BMP-2* and *BMP-4* genes. Mechanisms of Development **109**: 79-82.

Kohlhase, J. (2000). SALL1 mutations in Townes-Brocks syndrome and related disorders. Human Mutation **16**: 460-6.

Kopp, A., and Duncan, I. (1997). "Control of cell fate and polarity in the adult abdominal segments of Drosophila by optomotor-blind." Development **124**: 3715- 26.

Kos, R., M. V. Reedy, R. L. Johnson and C. A. Erickson (2001). The winged-helix transcription factor FoxD3 is important for establishing the neural crest lineage and repressing melanogenesis in avian embryos. Development **128**: 1467-79.

Kishimoto, Y., K. H. Lee, L. Zon, M. Hammerschmidt and S. Schulte Merker (1997). The molecular nature of zebrafish *swirl*: BMP2 function is essential during early dorsoventral patterning. Development **124**(22): 4457-4466.

Kobayashi, M., H. Osanai, K. Kawakami and M. Yamamoto (2000). Expression of three zebrafish *Six4* genes in the cranial sensory placodes and the developing somites. Mechanisms of Development **98**(1-2): 151-5.

Kozlowski, D. J., T. Murakami, R. K. Ho and E. S. Weinberg (1997). Regional cell movement and tissue patterning in the zebrafish embryo revealed by fate mapping with caged fluorescein. Biochemistry and Cellular Biology **75**: 551-62.

Kozlowski, D. J., Whitfield. T.T., Hukriede, N.A., and E. S. Weinberg (2001a). *dog-eared* encodes the transcriptional coactivator *eyes absent-1* which is required for the survival of sensory cell precursors in the inner ear and lateral line. Zebrafish Genetics and Development, London, with permission.

Kozlowski, D. J., T. T. Whitfield, N. A. Hukriede and E. S. Weinberg (2001b). *dog-eared* encodes *eyes-absent-1* which is required for survival of sensory cell precursors in the zebrafish inner ear and lateral line. The Molecular Biology of Hearing and Deafness, Bethesda, USA, with permission.

Kozlowski, D. J., T. T. Whitfield, N. A. Hukriede and E. S. Weinberg (in preparation). *dog-eared* encodes *eyes-absent-1* which is required for survival of sensory cell precursors in the zebrafish inner ear and lateral line.

Krauss, S., J. P. Concordet and P. W. Ingham (1993). A functionally conserved homolog of the *Drosophila* segment polarity gene hh is expressed in tissues with polarizing activity in zebrafish embryos. Cell **75**: 1431-44.

Lagutin O, Z., C., Y. Furuta, D. H. Rowitch, A. P. McMahon, G. Oliver (2001). Six3 promotes the formation of ectopic optic vesicle-like structures in mouse embryos. Developmental Dynamics **221**(3): 342-9.

Lamb, T. M., A. K. Knecht, W. C. Smith, S. E. Stachel, A. N. Economides, N. Stahl, G. D. Yancopolous and R. M. Harland (1993). Neural induction by the secreted polypeptide noggin. Science **262**: 713-8.

Lecuit, T., W. J. Brook, M. Ng, M. Calleja, H. Sun and S. M. Cohen (1996). Two distinct mechanisms for long-range patterning by Decapentaplegic in the *Drosophila* wing. Nature **381**: 387-93.

Lee, K. H., J. J. Marden, M. S. Thompson, H. MacLennan, Y. Kishimoto, S. J. Pratt, S. Schulte Merker, M. Hammerschmidt, S. L. Johnson, J. H. Postlethwaite, D.C. Beier and L. I. Zon (1998). Cloning and genetic mapping of zebrafish BMP-2. Developmental Genetics **23**(2): 97-103.

Leger, S. and M. Brand (2001). Identification of ace/FGF8 as a bona-fide inducer of inner ear development. Zebrafish Genetics and Development, London, with permission.

Lewis, J. (1986). Programs of cell division in the lateral line system. Trends in Neuroscience **9**:135-138.

Lewis, J. (1998). Notch signalling and the control of cell fate choices in vertebrates."Seminars in Cell and Developmental Biology **9**: 583-589.

Lu, Z., and A.N. Popper (2001). Neural response directionality correlates of hair cell orientation in a teleost fish. Journal of Comparative Physiology **187**: 453-65.

Ma, C., L. Fan, R. Ganassin, N. Bols and P. Collodi (2001). Production of zebrafish germ-line chimeras from embryo cell cultures. Proceedings of the National Acadamy of Sciences U S A **98**: 2461-6.

Macias, D., Y. Ganan, T. K. Sampath, M. E. Piedra, M. A. Ros and J. M. Hurle (1997). Role of BMP-2 and OP-1 (BMP-7) in programmed cell death and skeletogenesis during chick limb development. Development **124**: 1109-17.

Malicki, J., A. F. Schier, L. Solnica-Krezel, D. L. Stemple, S. C. F. Neuhauss, D. Y. R. Stainier, S. Abdelilah, Z. Rangini, F. Zwartkruis and W. Driever (1996).Mutations affecting development of the zebrafish ear. Development **123**: 275-283.

Marazzi, G., Wang, Y., and Sassoon, D. (1997). Msx2 is a transcriptional regulator in the BMP4-mediated programmed cell death pathway. Developmental Biology **186**: 127-38.

Martin, P. and G. J. Swanson (1993). Descriptive and Experimental-Analysis Of the Epithelial Remodellings That Control Semicircular Canal Formation In the Developing Mouse Inner-Ear. Developmental Biology **159**(2): 549-558.

Martinez-Barbera, J. P., H. Toresson, S. Da Rocha and S. Krauss (1997). Cloning and expression of three members of the zebrafish Bmp family: *Bmp2a*, *Bmp2b* and *Bmp4*. Gene **198**(1-2): 53-59.

Massague, J. (1998). TGF-beta signal transduction. Annual Review Of Biochemistry **67**:753-791.

Massague, J. (2000). How cells read TGF-beta signals. Nature Reviews Molecular Cell Biology **1**: 169-78.

Massague, J. and Y. G. Chen (2000). Controlling TGF-beta signaling. Genes and Development **14**: 627-44.

Masuda, M., S. Usami, K. Yamazaki, Y. Takumi, H. Shinkawa, K. Kurashima, T. Kunihiro and J. Kanzaki (2001). Connexin 26 distribution in gap junctions between melanocytes in the human vestibular dark cell area. Anatomy Record **262**: 237-46.

McKay, I. J., J. Lewis and A. Lumsden (1996). The role of FGF-3 in early inner ear development: an analysis in normal and *kreisler* mutant mice. Developmental Biology **174**(2): 370-8.

Merino, R., Y. Ganan, D. Macias, A. N. Economides, K. T. Sampath and J. M. Hurle (1998). Morphogenesis of digits in the avian limb is controlled by FGFs, TGF betas, and noggin through BMP signaling. Developmental Biology **200**(1): 35- 45.

Merves, M., B. Bobbitt, K. Parker, B. K. Kishore and D. Choo (2000). Developmental expression of aquaporin 2 in the mouse inner ear. Laryngoscope(110): 1925-30.

Metcalfe, W. K., C. B. Kimmel and E. Schabtach (1985). Anatomy of the posterior lateral line system in young larvae of the zebrafish. Journal of comparative Neurology **233**(3): 377-89.

Miller-Bertoglio, V., A. Carmany-Rampey, M. Fürthauer, E. M. Gonzalez, C. Thisse, B. Thisse, M. E. Halpern and L. Solnica-Krezel (1999). Maternal and zygotic activity of the zebrafish *ogon* locus antagonizes BMP signaling. Developmental Biology **214**: 72-86.

Miller-Bertoglio, V. E., S. Fisher, A. Sanchez, M. C. Mullins and M. E. Halpern (1997). Differential regulation of *chordin* expression domains in mutant zebrafish. Developmental Biology **192**(2): 537-550.

Mintzer, K. A., M. A. Lee, G. Runke, J. Trout, M. Whitman and M. C. Mullins (2001). *lost-a-fin* encodes a type I BMP receptor, Alk8, acting maternally and zygotically in dorsoventral pattern formation. Development **128**(6): 859-869.

Moens, C. B., S. P. Cordes, M. W. Giorgianni, G. S. Barsh and C. B. Kimmel (1998). Equivalence in the genetic control of hindbrain segmentation in fish and mouse. Development **125**(3): 381-391.

Moens, C. B., Y. L. Yan, B. Appel, A. G. Force and C. B. Kimmel (1996). *valentino*: a zebrafish gene required for normal hindbrain segmentation. Development **122**(12): 3981-3990.

Morrow, B. E., B. Funke, J. A. Epstein, R. K. Pandita, J. Liao, C. Brown, T. Van De Water and J. Adams (2001). Altered TBX1 dosage causes ear disorders in mouse models of velo-cardio-facial syndrome/DiGeorge syndrome. The Molecular Biology of Hearing and Deafness, with permission.

Morsli, H., F. Tuorto, D. Choo, M. P. Postiglione, A. Simeone and D. K. Wu (1999). *Otx1* and *Otx2* activities are required for the normal development of the mouse inner ear. Development **126**(11): 2335-43.

Morsli, H., D. Choo, A. Ryan, R. Johnson and D. K. Wu (1998). Development of the mouse inner ear and origin of its sensory organs. Journal Of Neuroscience **18**(9): 3327-3335.

Mowbray, C., M. Hammerschmidt and T. T. Whitfield (2001). Expression of BMP signalling pathway members in the developing zebrafish inner ear and lateral line.Mechanisms of Development **108**: 179-184.

Müller, F., P. Blader, S. Rastegar, N. Fischer, W. Knochel and U. Strahle (1999). Characterization of zebrafish *smad1*, *smad2* and *smad5*: the amino-terminus of smad1 and *smad5* is required for specific function in the embryo. Mechanisms of Development **88**(1): 73-88.

Mullins, M. C., M. Hammerschmidt, D. A. Kane, J. Odenthal, M. Brand, F. J. M. van Eeden, M. Furutani Seiki, M. Granato, P. Haffter, C. P. Heisenberg, Y. J. Jiang, R. N. Kelsh and C. Nüsslein Volhard (1996). Genes establishing dorsoventral pattern formation in the zebrafish embryo: The ventral specifying genes. Development **123**: 81-93.

Nellen, D., R. Burke, G. Struhl and K. Basler (1996). Direct and long-range action of a DPP morphogen gradient. Cell **85**: 357-68.

Nagaso, H., A. Suzuki, M. Tada and N. Ueno (1999). Dual specificity of activin type II receptor ActRIIb in dorso-ventral patterning during zebrafish embryogenesis.Development Growth & Differentiation **41**(2): 119-133.

Nasevicius, A. and S. C. Ekker (2000). Effective targeted gene 'knockdown' in zebrafish. Nature Genetics **26**: 216-20.

Neave, B., N. Holder and R. Patient (1997). A graded response to BMP-4 spatially coordinates patterning of the mesoderm and ectoderm in the zebrafish. Mechanisms Of Development **62**(2): 183-195.

Nellen, D., R. Burke, G. Struhl and K. Basler (1996). Direct and long-range action of a DPP morphogen gradient. Cell **85**: 357-68.

Neuhauss, S. C., L. Solnica-Krezel, A. F. Schier, F. Zwartkruis, D. L. Stemple, J. Malicki, S. Abdelilah, D. Y. Stainier and W. Driever (1996). Mutations affecting craniofacial development in zebrafish. Development **123**: 357-367.

Nguyen, V. H., B. Schmid, J. Trout, S. A. Connors, M. Ekker and M. C. Mullins (1998). Ventral and lateral regions of the zebrafish gastrula, including the neural crest progenitors, are established by a *bmp2b/swirl* pathway of genes. Developmental Biology **199**(1): 93-110.

Nicolson, T., A. Rusch, R. W. Friedrich, M. Granato, J. P. Ruppersberg and C. Nüsslein Volhard (1998). Genetic analysis of vertebrate sensory hair cell mechanosensation: the zebrafish circler mutants. Neuron **20**(2): 271-283.

Nieuwkoop, P. D. and J. Fabre, (Eds.) (1994). Normal Table of *Xenopus laevis (Daudin)*. New York & London:Garland Publishing, Inc.

Nikaido, M., M. Tada, T. Saji and N. Ueno (1997). Conservation of BMP signaling in zebrafish mesoderm patterning. Mechanisms Of Development **61**(1-2): 75-88.

Nikaido, M., M. Tada, H. Takeda, A. Kuroiwa and N. Ueno (1999). In vivo analysis using variants of zebrafish BMPR-IA: range of action and involvement of BMP in ectoderm patterning. Development **126**(1): 181-190.

Nikaido, M., M. Tada and N. Ueno (1999). Restricted expression of the receptor serine threonine kinase BMPR-IB in zebrafish. Mechanisms Of Development **82**(1-2):219-222.

Nishimatsu, S. and G. H. Thomsen (1998). Ventral mesoderm induction and patterning by bone morphogenetic protein heterodimers in *Xenopus* embryos. Mechanisms Of Development **74**(1-2): 75-88.

Nishimatsu, S., A. Suzuki, A. Shoda, K. Murakami and N. Ueno (1992). Genes for bone morphogenetic proteins are differentially transcribed in early amphibian embryos. Biochemical and Biophysical Research Communications **186**(3): 1487- 95.

Nishizaki, K., T. Yoshino, Y. Orita, S. Nomiya and Y. Masuda (1999). TUNEL staining of inner ear structures may reflect autolysis, not apoptosis. Hearing Research **130**(1-2): 131-6.

Oh, S. H., R. Johnson and D. K. Wu (1996). Differential expression of bone morphogenetic proteins in the developing vestibular and auditory sensory organs. Journal Of Neuroscience **16**(20): 6463-6475.

Ott, T., K. H. Kaestner, A. P. Monaghan and G. Schutz (1996). The mouse homologue of the region specific homeotic gene *spalt* of *Drosophila* is expressed in the developing nervous system and in mesoderm-derived structures. Mechanisms of Development **56**: 117-28.

Padgett, R. W., J. M. Wozney and W. M. Gelbart (1993). Human BMP sequences can confer normal dorsal-ventral patterning in the Drosophila embryo. Proceedings of the National Acadamy of Sciences U S A **90**: 2905-9.

Paine-Saunders, S., B. L. Viviano, A. N. Economides and S. Saunders (2001). Heparan sulfate proteoglycans retain Noggin at the cell surface: A potential mechanism for shaping BMP gradients. Journal of Biological Chemistry **277**: 2089-96.

Paratore, C., D. E. Goerich, U. Suter, M. Wegner and L. Sommer (2001). Survival and glial fate acquisition of neural crest cells are regulated by an interplay between the transcription factor *Sox10* and extrinsic combinatorial signaling. Development **128**(20): 3949-61.

Pathi, S., J. B. Rutenberg, R. L. Johnson and A. Vortkamp (1999). Interaction of Ihh and BMP Noggin signaling during cartilage differentiation. Developmental Biology **209**(2): 239-253.

Patten, I. and M. Placzek (2002). Opponent activities of Shh and BMP signalling during floor plate induction in vivo. Current Biology **12**: 47-52.

Pfeffer, P. L., T. Gerster, K. Lun, M. Brand and Büsslinger. M. (1998). Characterization of three novel members of the zebrafish *Pax2/5/8* family: dependency of *Pax5* and *Pax8* expression on the Pax2.1 (*noi*) function. Development **125**(16): 3063-74.

Phillips, B. T., K. Bolding and Riley. B.B. (2001). "Zebrafish *fgf3* and *fgf8* Encode Redundant Functions Required for Otic Placode Induction." Developmental Biology **235**: 351-365.

Piccolo, S., Y. Sasai, B. Lu and E. M. De Robertis (1996). Dorsoventral Patterning in *Xenopus*: Inhibition of Ventral Signals by Direct Binding of Chordin to BMP-4. Cell **86**: 589-98.

Pickles, J. O., S. D. Comis and M. P. Osborne (1984). Cross-links between stereocilia in the guinea pig organ of Corti, and their possible relation to sensory transduction. Hearing Research **15**: 103-12.

Pignoni, F., and Zipursky, S.L. (1997). Induction of Drosophila eye development by decapentaplegic. Development **124**: 271-8.

Pingault, V., N. Bondurand, K. Kuhlbrodt, D. E. Goerich, M. O. Prehu, A. Puliti, B. Herbarth, I. Hermans-Borgmeyer, E. Legius, G. Matthijs, J. Amiel, S. Lyonnet, I. Ceccherini, G. Romeo, J. C. Smith, A. P. Read, M. Wegner and M. Goossens (1998). *SOX10* mutations in patients with Waardenburg-Hirschsprung disease. Nature Genetics **18**: 171-3.

Piotrowski, T., C. Nüsslein Volhard and I. B. Dawid (2001). Genetic screen for defects in the development of the lateral line sensory system. Zebrafish Genetics and Development, London, with permission.

Piotrowski, T. and Nüsslein-Volhard, C. (2000). The endoderm plays an important role in patterning the segmented pharyngeal region in zebrafish (*Danio rerio*). Developmental Biology **225**: 339-56

Pizette, S., C. Abate-Shen and L. Niswander (2001). BMP controls proximodistal outgrowth, via induction of the apical ectodermal ridge, and dorsoventral patterning in the vertebrate limb. Development **128**: 4463-74.

Platt, C. (1993). Zebrafish Inner-Ear Sensory Surfaces Are Similar to Those In Goldfish. Hearing Research **65**(1-2): 133-140.

Ramirez-Weber, F. A., and Kornberg, T.B. (1999). Cytonemes: cellular processes that project to the principal signaling center in Drosophila imaginal discs. Cell **97**: 599-607.

Rask-Andersen, H., J. E. DeMott, D. Bagger-Sjoback and A. N. Salt (1999). Morphological changes of the endolymphatic sac induced by microinjection of artificial endolymph into the cochlea. Hearing Research **138**(1-2): 81-90.

Reddi, A. H. (1994). Bone and cartilage differentiation. Current Opinion in Genetics and Development **4**: 737-44.

Riley, B. B., M.-Y. Chiang, L. Farmer and R. Heck (1999). The *deltaA* gene of zebrafish mediates lateral inhibition of hair cells in the inner ear and is regulated by *pax2.1*. Development **126**: 5669-5678.

Riley, B. B. and D. J. Grunwald (1996). A mutation in zebrafish affecting a localized cellular function required for normal ear development. Developmental Biology **179**(2): 427-435.

Riley, B. B., C. W. Zhu, C. Janetopoulos and K. J. Aufderheide (1997). A critical period of ear development controlled by distinct populations of ciliated cells in the zebrafish. Developmental Biology **191**(2): 191-201.

Rodriguez-Esteban, C., T. Tsukui, S. Yonei, J. Magallon, K. Tamura and J. C. Izpisua Belmonte (1999). The T-box genes *Tbx4* and *Tbx5* regulate limb outgrowth and identity. Nature **398**: 814-8.

Rosman, G. J. and A. D. Miller (1990). Improved method for plasmid shipment. Biotechniques **8**: 509.

Ross, J. J., Shimmi, O., Vilmos, P., Petryk, A., Kim, H., Gaudenz, K., Hermanson, S., Ekker, S.C., O'Connor, M.B., and Marsh, J.L. (2001). Twisted gastrulation is a conserved extracellular BMP antagonist. Nature **410**: 479-83.

Ruvinsky, I., A. C. Oates, L. M. Silver and R. K. Ho (2000). The evolution of paired appendages in vertebrates: T-box genes in the zebrafish. Development Genes and Evolution **210**: 82-91.

Sahly, I., P. Andermann and C. Petit (1999). The zebrafish *eya1* gene and its expression pattern during embryogenesis. Development Genes and Evolution **209**(7): 399-410.

Salt, A. N. (1995).http://oto.wustl.edu/cochlea/intro4.htm.updated15 August 2000.

Sambrook, J., E. F. Fritsch and T. Maniatis (1989). Molecular Cloning. A laboratory manual. New York: Cold Spring Harbour Laboratory Press.

Sampath, T. K., K. E. Rashka, J. S. Doctor, R. F. Tucker and F. M. Hoffmann (1993). *Drosophila* transforming growth factor beta superfamily proteins induce endochondral bone formation in mammals. Proceedings of the National Acadamy of Sciences U S A **90**: 6004-8.

Satokata, I. and R. Maas (1994). *Msx1* deficient mice exhibit cleft palate and abnormalities of craniofacial and tooth development. Nature Genetics **6**(4): 348-56.

Schier, A. F. (2001). Axis formation and patterning in zebrafish. Current Opinion in Genetics and Development: 393-404.

Schilling, T. F. and C. B. Kimmel (1994). Segment and cell type lineage restrictions during pharyngeal arch development in the zebrafish embryo. Development **120**:483-94.

Schmid, B., M. Furthauer, S. A. Connors, J. Trout, B. Thisse, C. Thisse and M. C. Mullins (2000). Equivalent genetic roles for *bmp7/snailhouse* and *bmp2b/swirl* in dorsoventral pattern formation. Development **127**(5): 957-967.

Scholtz, A. W., J. H. Fish 3rd, K. Kammen-Jolly, H. Ichiki, B. Hussl, A. Kreczy and A. Schrott-Fischer (2001). Goldenhar's syndrome: congenital hearing deficit of conductive or sensorineural origin? Temporal bone histopathologic study. Otology and Neurotology **22**: 501-5.

Schulte Merker, S., K. J. Lee, A. P. McMahon and M. Hammerschmidt (1997). The zebrafish organizer requires *chordino*. Trends In Genetics **13**(1): 14-21.

Smith, J. (1999). T-box genes: what they do and how they do it. Trends in Genetics **15**:154-8.

Solnica-Krezel, L., and Driever, W. (2001). The role of the homeodomain protein Bozozok in zebrafish axis formation. International Journal of Developmental Biology **45**: 299-310.

St Amand, T. R., Y. Zhang, E. V. Semina, X. Zhao, Y. Hu, L. Nguyen, J. C. Murray and Y. Chen (2000). Antagonistic signals between BMP4 and FGF8 define the expression of Pitx1 and Pitx2 in mouse tooth-forming anlage. Developmental Biology **217**: 323-32.

Steel, K. P. (1998). Progress in progressive hearing loss. Science **279**: 1970-1.

Suzuki, A., E. Kaneko, J. Maeda and N. Ueno (1997). Mesoderm induction by BMP-4 and -7 heterodimers. Biochemical and Biophysical Research Communications **232**(1): 153-156.

Takemura, T., M. Sakagami, K. Takebayashi, M. Umemoto, T. Nakase, K. Takaoka, T. Kubo, Y. Kitamura and S. Nomura (1996). Localization of *bone morphogenetic protein-4* messenger RNA in developing mouse cochlea. Hearing Research **95**((1-2)): 26-32.

Taylor, J. S., Y. Van de Peer and A. Meyer (2001). Genome duplication, divergent resolution and speciation. Trends in Genetics **17**: 299-301.

ten Dijke, P., H. Yamashita, T. K. Sampath, A. H. Reddi, M. Estevez, D. L. Riddle, H. Ichijo, C. H. Heldin and K. Miyazono (1994). Identification of type I receptors for osteogenic protein-1 and bone morphogenetic protein-4. Journal of Biological Chemistry **269**: 16985-8.

Thalmann, R., and Thalmann, I. (1999). Source and role of endolymph macromolecules. Acta Oto-Laryngologica **119**(3): 293-6.

The, I., Y. Bellaiche and N. Perrimon (1999). Hedgehog movement is regulated through tout velu-dependent synthesis of a heparan sulfate proteoglycan. Molecular Cell **4**: 633-9.

Torres, M. and F. Giraldez (1998). The development of the vertebrate inner ear. Mechanisms Of Development **71**(1-2): 5-21.

Tsang, M., R. Kim, M. P. de Caestecker, T. Kudoh, A. B. Roberts and I. B. Dawid (2000). Zebrafish nma is involved in TGFbeta family signaling. Genesis **28**: 47-57.

Tucker, A. S., A. Al Khamis and P. T. Sharpe (1998). Interactions between Bmp-4 and Msx-1 act to restrict gene expression to odontogenic mesenchyme. Developmental Dynamics **212**: 533-9.

Vahava, O., R. Morell, E. D. Lynch, S. Weiss, M. E. Kagan, N. Ahituv, J. E. Morrow, M. K. Lee, A. B. Skvorak, C. C. Morton, A. Blumenfeld, M. Frydman, T. B. Friedman, M. C. King and K. B. Avraham (1998). Mutation in transcription factor *POU4F3* associated with inherited progressive hearing loss in humans. Science **279**: 1950-4.

Vainio, S., I. Karavanova, A. Jowett and I. Thesleff (1993). Identification Of Bmp-4 As a Signal Mediating Secondary Induction Between Epithelial and Mesenchymal Tissues During Early Tooth Development. Cell **75**(1): 45-58.

Verpy, E., M. Leibovici and C. Petit (1999). Characterization of otoconin-95, the major protein of murine otoconia, provides insights into the formation of these inner ear biominerals. Proceedings of the National Acadamy of Sciences U S A **96**: 529-34.

Vetter, D. E., J. R. Mann, P. Wangemann, J. Liu, K. J. McLaughlin, F. Lesage, D. C. Marcus, M. Lazdunski, S. F. Heinemann and J. Barhanin (1996). Inner ear defects induced by null mutation of the *isk* gene. Neuron **17**: 1251-64.

Walsh, E. C., and D.Y. Stainier (2001). UDP-glucose dehydrogenase required for cardiac valve formation in zebrafish. Science **293**: 1670-3.

Wang, Y., and Sassoon, D. (1995). Ectoderm-mesenchyme and mesenchyme-mesenchyme interactions regulate Msx-1 Expression and cellular Differentiation in the murine limb bud. Developmental Biology **168**: 374-382.

Wangemann, P. (1995). Comparison of ion transport mechanisms between vestibular dark cells and strial marginal cells. Hearing Research **90**(1-2): 149-57.

Waterman, R. E. and D. H. Bell (1984). Epithelial Fusion During Early Semicircular Canal Formation In the Embryonic Zebrafish, *Brachydanio-Rerio*. Anatomical Record **210**(1): 101-114.

Westerfield, M. (1995). The Zebrafish Book. Eugene: University of Oregon Press.

Whitfield, T. T., M. Granato, F. J. van Eeden, U. Schach, M. Brand, M. Furutani-Seiki, P. Haffter, M. Hammerschmidt, C. P. Heisenberg, Y. J. Jiang, D. A. Kane, R. N. Kelsh, M. C. Mullins, J. Odenthal and C. Nüsslein-Volhard (1996). Mutations affecting development of the zebrafish inner ear and lateral line. Development **123**: 241-54.

Whitfield, T. T., B. B. Riley, M.-Y. Chiang and B. Phillips (in press). Development of the zebrafish inner ear. Developmental Dynamics.

Willot, V., J. Mathieu, Y. Lu, B. Schmid, S. Sidi, Y.-L. Yan, J. H. Postlethwait, M. Mullins, F. Rosa and N. Peyrie (2002). Cooperative Action of ADMP- and BMP-Mediated Pathways in Regulating Cell Fates in the Zebrafish Gastrula. Developmental Biology. **241**: 59-78

Winklebauer, R., and P. Hausen (1983). Development of the lateral line system in *Xenopus laevis*. Journal of Embryology and Experimental Morphology **76**: 265-81

Wrana, J. L. (2000). Regulation of Smad activity. Cell **100**: 189-92.

Wu, D. K. and S. H. Oh (1996). Sensory organ generation in the chick inner ear. Journal Of Neuroscience **16**(20): 6454-6462.

Wu, D. K., F. D. Nunes and D. Choo (1998). Axial specification for sensory organs versus non-sensory structures of the chicken inner ear. Development **125**(1): 11-20.

Xu, P. X., J. Adams, H. Peters, M. C. Brown, S. Heaney and R. Maas (1999). *Eya1*-deficient mice lack ears and kidneys and show abnormal apoptosis of organ primordia. Nature Genetics **23**(1): 113-7.

Yamada, M., J. P. Revelli, G. Eichele, M. Barron and R. J. Schwartz (2000). Expression of chick *Tbx-2, Tbx-3,* and *Tbx-5* genes during early heart development:evidence for BMP2 induction of *Tbx2*. Developmental Biology **228**:95-105.

Yamashita, H., P. ten Dijke, C. H. Heldin and K. Miyazono (1996). Bone morphogenetic protein receptors. Bone **19**: 569-74.

Yamashita, H., P. ten Dijke, D. Huylebroeck, T. K. Sampath, M. Andries, J. C. Smith, C. H. Heldin and K. Miyazono (1995). Osteogenic Protein-1 Binds to Activin Type-Ii Receptors and Induces Certain Activin-Like Effects. Journal Of Cell Biology **130**(1): 217-226.

Yelick, P. C., T. S. Abduljabbar and P. Stashenko (1998). zALK-8 a novel type I serine/threonine kinase receptor, is expressed throughout early zebrafish development. Developmental Dynamics **211**(4): 352-361.

Zhu, H., P. Kavsak, S. Abdollah, J. L. Wrana and G. H. Thomsen (1999). A SMAD ubiquitin ligase targets the BMP pathway and affects embryonic pattern formation. Nature **400**: 687-93.

Zimmerman, L. B., M. De Jesu´s-Escobar and R. M. Harland (1996). The Spemann Organizer Signal noggin Binds and Inactivates Bone Morphogenetic Protein 4. Cell **86**: 599-606.

Zou, H., and Niswander, L. (1996). Requirement for BMP signaling in interdigital apoptosis and scale formation. Science **272**: 738-41.